

Technology and the Professional Engineer a challenge that must be met!

We are living in an era of rapid and apparently unending advances in technology—so much so that the expression “exciting challenge” has become almost shop worn. Nonetheless, I believe the challenges of new technology in the radar and antenna design areas today are as exciting and stimulating as anything we have seen in this field since the early days of bedspring antennas.

For years some form of the dish antenna was the bread and butter of the radar designer; feed techniques were the chief source of modifying sensor performance, but antenna design remained relatively stable. Communications systems and their antennas showed a similar sameness, remarkable more for the apparent static nature of antenna design than for any other feature.

But no more. For more than ten years now we have been involved with all the problems and attendant opportunities of electronically steered array radars—the flat-faced array has arrived. Further, we’ve seen great antenna fields spreading over acres of land serving as antenna systems for high-frequency radars. Space work has opened up a virtually unlimited new area for imaginative antenna design. Even the staid old broadcast antenna is developing new dimensions and encountering new problems.

The challenges are not limited to antennas alone. Computer control of radars is growing apace, presenting a whole new dimension of problems and—more important—opportunities for building better systems at lower cost. Moreover, refinements in technology now make it possible to obtain so much information that signal processing and data processing systems must be capable of immensely complex real-time performance.

Perhaps the greatest challenge of all has come in the area of designing to cost. All modern major systems are inherently expensive, and Government funding for development effort has been unable to keep up with the capacity of our engineers to evolve more complex (and more costly) equipment. Accordingly, many of the most important technological advances in recent years have come from concerted efforts to provide performance at the lowest possible cost.

These, then, are some of the challenges and opportunities that make the radar and antenna field a very exciting venture and promise even greater challenge as the technology continues to unfold.



Dudley M. Cottler
Chief Engineer
Missile and Surface Radar Division
Moorestown, New Jersey

- Editor
- Associate Editor
- Art Editor
- Editorial Secretary
- Subscriptions
- Composition
- Technical Publications Adm.,
Electronic Components
- Technical Publications Adm.,
Laboratories
- Technical Publications Adm.,
Corporate Engineering Services
- Mgr., Quality and Reliability
Assurance, Solid State Div.
- VP, Engineering, NBC
Television Network
- Mgr., Technical Information
Services, RCA Laboratories
- Manager, Consumer Products
Adm., RCA Service Co.
- Chief Engineer,
Record Division
- Chief Technical Advisor,
Consumer Electronics
- Div. VP, Technical Planning
Electronic Components
- Staff VP, Engineering
- Exec. VP, Leased Facilities
and Engineering,
Global Communications, Inc.
- Manager, Engineering
Professional Development
- Division VP,
Government Engineering

Our cover

... features part of a new broadcast antenna complex being planned for the World Trade Center (New York City) installation. Climbing the antenna are engineer Frank Chwieroth (lower left) and wiremen Richard Carver (top left), Harold James (center), and Harry Crowthers (top right). **Photo credit:** Bill Eisenberg, GCS, Camden.

A technical journal published by
RCA Corporate Engineering Services 2-8,
Camden, N.J.

RCA Engineer articles are indexed
annually in the April-May Issue and
in the "Index to RCA Technical Papers."

• To disseminate to RCA engineers technical information of professional value • To publish in an appropriate manner important technical developments at RCA, and the role of the engineer • To serve as a medium of interchange of technical information between various groups at RCA • To create a community of engineering interest within the company by stressing the interrelated nature of all technical contributions • To help publicize engineering

achievements in a manner that will promote the interests and reputation of RCA in the engineering field • To provide a convenient means by which the RCA engineer may review his professional work before associates and engineering management • To announce outstanding and unusual achievements of RCA engineers in a manner most likely to enhance their prestige and professional status.

Contents

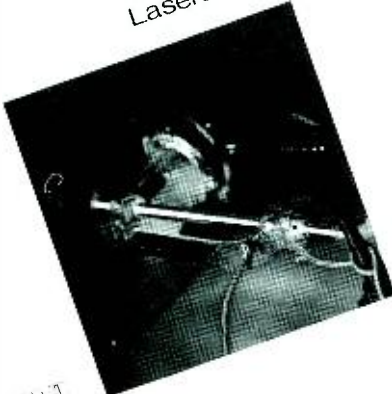
Theme—radar, communication, and antennas

Editorial input	Reprints of RCA Engineer Articles	J. P. Dunn	2
Special	Four RCA men elected IEEE Fellows		4
Engineer and the Corporation	Television receiving antennas in blue and gold.	J. D. Callaghan D. W. Peterson	6
	G&CS antenna range	W. C. Wilkinson	11
Broadcast antennas	New VHF Filterplexer	D. G. Hymas J. J. Matta P. C. Nole A. N. Schmitz	15
	Computer-aided design of vertical patterns for TV antennas	Dr. Krishma Praba	18
Radar	Lunar sounder experiment for Apollo 17	Dr. S. L. Goldman E. J. Nossen	22
	Displays for modern radar systems	G. A. Senior	26
	Phase shifter and driver design for the AN/SPY-1 phased array	N. R. Landry H. C. Goodrich	29
	High-efficiency avalanche diodes (TRAPATT)* for phased-array radar systems	Dr. K. K. N. Chang Dr. H. Kawamoto Dr. V. A. M'kenas H. J. Prager Dr. J. Reynolds A. Rosen	34
	High power latching ferrite phase shifters for AEGIS	L. J. Lavedan, Jr.	40
	High-frequency high-power multi-octave distributed-amplifier transmitter	D. L. Pruitt	44
	Low backlobe antenna for airborne missile-warning system	H. Honda	48
Communication	Ultra-lightweight deployable antennas	W. S. Sepich	53
	Communication antennas for Viking Mars Lander	W. C. Wilkinson W. A. Harmening O. M. Woodward	56
	Decoder for delay-modulation coded data	J. Lewin	60
	Simple analytical model for the envelope distribution for a sinusoidal carrier in atmospheric radio noise	C. V. Greenman	64
Engineer and the Corporation	RCA-MIT Research Conference	W. O. Hadlock	66
General interest	Advanced packaging with thin-film microcircuits	W. J. Grieg R. Brown	74
	Charge-coupled devices and applications	J. E. Carnes W. F. Kosonocky	78
Engineering and Research Notes	Analog to digital (rolling sample) correlator	H. C. Goodrich E. C. Farnett	86
	Self-contained impact detector and reporter	A. J. Lisicky M. G. Staton E. D. Grim	87
Departments	Pen and Podium		88
	Patents Granted		90
	Dates and Deadlines		91
	News and Highlights		93



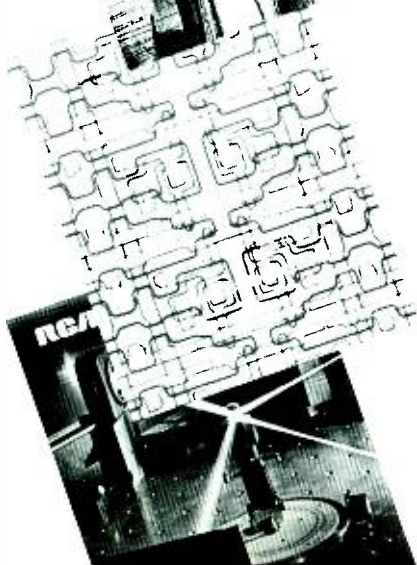
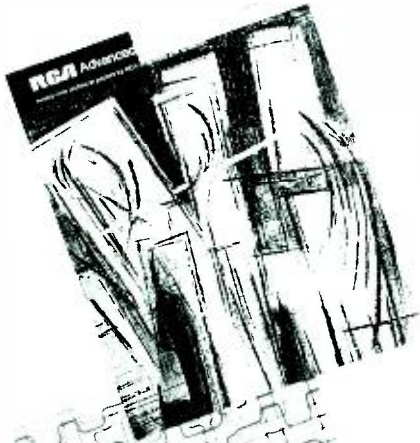
RCA

Lasers



J.P.D.

Holographic information storage and retrieval



Reprints of *RCA Engineer* articles

J. P. Dunn, Art Editor

Although the *RCA Engineer* can be distributed only inside RCA, reprints of articles from any issue can be supplied quickly and economically, and may go to customers, opinion leaders, prospective employees, or students. RCA Technical Publications staff provides these reprints to divisions wishing to promote their products or to provide their clients, prospects, and customers with valuable information.

AS MANY OF OUR READERS KNOW, articles appearing in the *RCA Engineer* can be reprinted on a single article basis or as an anthology of several articles (from several issues) devoted to a single theme, technology, or facility. Covers for reprints may be custom designed to suit a specific purpose. Assistance in cover design, brochure content, and utilization of reprints will be provided by the *RCA Engineer* editorial staff.

Varied uses

Over 100,000 copies per year of reprints of *RCA Engineer* articles are used by the various divisions throughout the company. Orders have varied from simple two-page leaflets to a 200-page brochure with a full-color cover. Reprints are valuable for many purposes:

- as informative brochures or descriptive bulletins;
- to display engineering and technical skills;
- for marketing and sales mailings and handouts;
- for mailings to prospects, customers, and opinion leaders;
- for answering any inquiries that require technical explanations;
- for use with commercial and government proposals; and
- to give to personnel groups for orientation, training and recruiting.

An additional fifty copies of each reprint ordered is kept on file by Staff Technical Publications, and a limited amount of these is available, should a division need backup. Certain other comprehensive booklets become available from time to time

(usually an announcement is made in *Trend*) and limited quantities can be ordered by phoning or writing the *RCA Engineer* editorial office. (See section titled "How to Order".) A catalogue listing all *RCA Engineer* reprints is available from your division TPA or library.

Covers

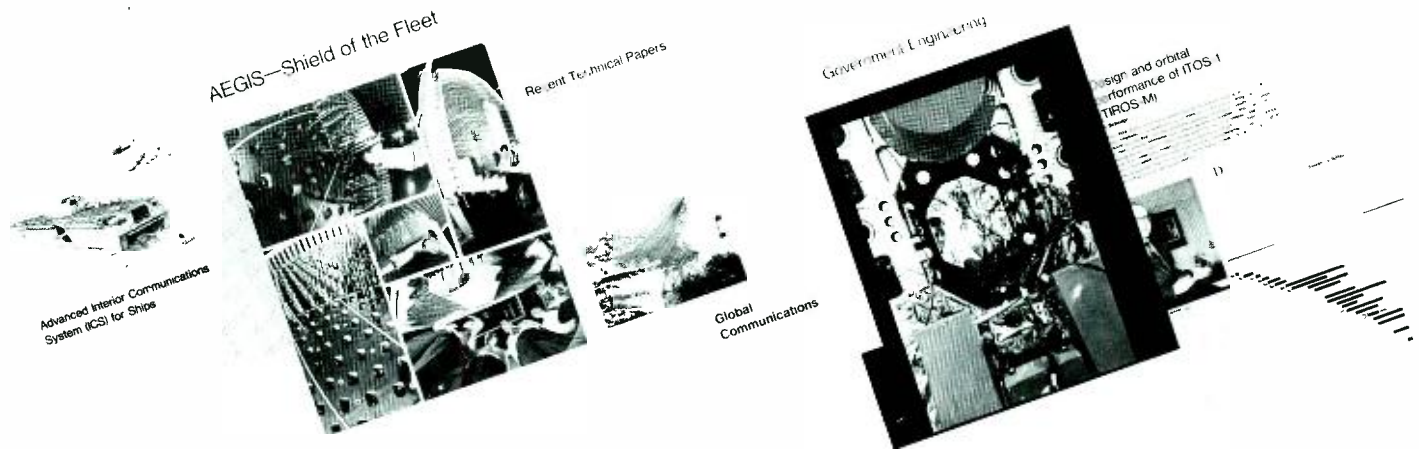
Single articles

On single-article reprints, a simple title page imprint (article title, author, RCA logotype, and division) is included when a blank page is available. For economy, reprints are prepared in increments of four pages each; thus, a three-page article would be printed as a four-page reprint with the extra page used as a cover. In a four-page article, the cover information is placed on the title page of the article unless the separate title page is requested; the four-page article is then handled (and priced) as an eight-page reprint.

Booklets

On booklet reprints, covers are custom-designed to suit the "theme" of the articles, using typography and artwork to suit. These booklets can also utilize previous *RCA Engineer* covers in either full color or in black-and-white. Cover messages, marketing contacts, or other additional information appropriate to the purpose of the booklet may be placed on the inside front and back covers.

Reprint RE-18-5-9



Cost and delivery

Delivery

Four- and eight-page reprints can be supplied within two weeks of the receipt of the order. Reprint booklets are available on a four-to-eight-week time cycle, depending on the complexity of the additional cover material. Rush schedules may affect price and are handled on an individual basis.

Cost

Approximate prices for various reprints are tabulated below.

How to order

All policy on reprint content, availability and utilization is administered by the *RCA Engineer* editorial staff, since additional changes must be made to reprints before they can be distributed. Reprints can be obtained only through the *RCA Engineer* editorial office, RCA Building 2-8, Camden, N.J. For rush orders, phone WO 3-8000, Ext. PC-4018. The following information must be supplied with order:

- 1) Article or articles desired;
- 2) Special instructions on cover requirements or special information to be added;
- 3) Quantity desired;
- 4) Delivery requirements (time and place); and
- 5) Account No. (not a purchase order).

An *RCA Engineer* article reprint is an easy, economical way to promote the work of your division. If you've never availed yourself of this useful service, or just haven't thought about it lately, we'd like to suggest that you try it.

Reprint price list

		<i>Quantity</i>							
		100	500	1000	2500	5000	7500	10,000	<i>Additional</i> 1000's
<i>Self</i>	<i>Size of</i> <i>reprint (pages)</i>								
<i>cover</i>	2	20.00	22.00	27.00	51.00	68.20	84.70	104.50	9.00
	4	38.00	41.00	47.00	99.00	126.50	170.50	198.00	17.00
	8	70.40	88.00	104.50	209.00	302.50	444.40	554.40	50.00
	12	84.70	123.20	171.60	257.40	481.80	664.40	830.50	75.00
	16	89.10	128.70	177.10	268.40	492.80	680.90	869.00	79.00
<i>With 1-</i>	32	237.60	328.90	425.70	630.30	1,150.00	1,570.00	1,910.00	174.00
<i>color</i>	48	382.80	476.30	594.00	976.80	1,578.00	2,151.00	2,695.00	246.00
<i>enamel</i>	64	429.00	616.00	764.50	1,250.00	2,005.00	2,719.00	3,350.00	320.00
<i>cover</i>	72	540.10	715.00	869.00	1,450.00	2,250.00	2,990.00	3,750.00	330.00
	80	600.60	825.00	946.00	1,550.00	2,440.00	3,310.00	4,140.00	360.00
	86	697.40	891.00	1,045.00	1,640.00	2,610.00	3,515.00	4,405.00	390.00
	96	792.00	995.50	1,140.00	1,730.00	2,805.00	3,880.00	4,780.00	455.00

Cost for 4-color cover: add this cost to the price shown above for reprints with 1-color enamel covers (color covers are picked up from an existing *RCA Engineer* cover.)

305.00	380.00	450.00	515.00	590.00	56.00
--------	--------	--------	--------	--------	-------

Extra typesetting is added to the above prices (e.g., for an added table of contents in booklets.)

Four RCA men elected IEEE Fellows



Dr. George M. Heilmeyer ... for fundamental discoveries of electro-optic effects in liquid crystals and basic liquid crystal device defects.

Dr. Heilmeyer (now on leave of absence) was Head of the Device Concepts Research Group at RCA Laboratories before being appointed a White House Fellow, assigned to the Department of Defense, in September, 1970. In September 1971, Secretary of Defense Melvin Laird appointed Dr. Heilmeyer Assistant Director of Defense Research and Engineering (Electronics and Computer Sciences).

Dr. Heilmeyer received the BSEE (with distinguished honors) from the University of Pennsylvania in 1958, and the MSE, MA, and PhD in solid state materials and electronics from Princeton in 1960, 1961, and 1962, respectively. His work at Princeton University was done under the sponsorship of the RCA Laboratories. In 1960 he received the RCA Laboratories Achievement Award for his work in parametric and tunnel diode devices, in 1962 for pioneering work in the field of crystalline organic semiconductors, and in 1965 for research in the area of liquid crystalline phenomena. He has received two IR-100 awards (1968, 1969) for outstanding new product developments in the field of liquid crystal display devices. He was also a co-recipient of the 1969 David Sarnoff Outstanding Team Award in Science for "basic studies of liquid crystals with imaginative ideas for their application to practical display." In March of 1968 he was the recipient of one of the "Outstanding Young Electrical Engineer" awards of Eta Kappa Nu. In March of 1969 he received the Eta Kappa Nu award as the "Outstanding Young Electrical Engineer in the U.S.A."

Dr. Heilmeyer has fifteen U.S. patents issued or pending and has published or presented over 40 papers in the areas of microwave solid state devices, organic semiconductors, adaptive thin film ferroelectric devices, solid state devices, optical modulators and displays.

In 1966 he became the Head of the Solid and Liquid State Device Research Group at RCA Laboratories and Head of the Device Concepts Research Group in 1968.

The four RCA men cited herein have been honored for their professional achievements by being elected Fellows of the Institute of Electrical and Electronics Engineers. This recognition is extended each year by the IEEE to those who have made outstanding contributions to the field of electronics.



Barton Kreuzer ... for contributions in applying electronics to sound motion pictures, satellite meteorology, lunar exploration, and communications.

Barton Kreuzer, Executive Vice President, RCA Corporate Headquarters, New York, N.Y., was appointed Executive Vice President, Consumer Electronics, of RCA in December 1969 and held that post until December 1972.

As Executive Vice President, Consumer Electronics, Mr. Kreuzer was responsible for the world-wide operation of RCA Consumer Electronics, which manufactures television sets, radios and other consumer products, and also includes the RCA Sales Corporation and RCA Distributing Corp. Mr. Kreuzer formerly was Executive Vice President, Commercial Electronics Systems, with headquarters in Camden, N.J. Prior to that he had served since June, 1968 as Vice President and General Manager of the division. Earlier, Mr. Kreuzer was Division Vice President and General Manager, Commercial Electronic Systems Division, a post to which he was named in August, 1967. Before this assignment he served for more than seven years as Division Vice President and General Manager, Astro-Electronics Division. He joined that Division when it was formed in 1958 as Manager of Marketing and became its head in 1960.

Mr. Kreuzer joined RCA in 1928, after receiving the BSEE Electrical Engineering from Brooklyn Polytechnic Institute. As a young engineer, he helped establish RCA's pioneer television station, W2XBS, in New York City, in 1928-29. In 1935, Mr. Kreuzer became head of RCA film-recording equipment sales in the East, and six years later was named national manager. He was appointed Manager of RCA Theater Equipment activities in 1943. His promotion in 1946 to Manager, RCA Industrial Products Department, made him responsible for a wide range of products in the industrial and commercial electronics field. Mr. Kreuzer in 1950 was named General Product Manager of the former Engineering Products Division which produced defense, broadcast, communications, and industrial electronic systems. In 1954, he was appointed Director of Product Planning on the RCA Corporate Staff, a post he held until 1958 when he joined the newly established Astro-Electronics Division.

Mr. Kreuzer is a former President of the SMPTE of which he continues as a Fellow. Mr. Kreuzer is a director of RCA Ltd. (Canada) and of RCA Ltd. (Taiwan).

Editor's note: In addition to these four recipients, three past RCA employees received the grade of Fellow from IEEE: **Julian J. Bussgang**, formerly with Aerospace Systems Division, Burlington, Mass., "for contributions to sequential detection theory, radar techniques, and statistical communications,"; **Dr. Joseph J. Loferski**, formerly with RCA Laboratories, "for contributions to radiation

damage in semiconductors, solar cell technology, and education; and **Arthur W. Vance**, formerly with RCA Laboratories and Astro-Electronics Division, "for pioneering contributions to television, electronic instruments, regulated power supplies, weapons systems, and simulators."



Dr. Harold Sobol ... for contributions in the field of microwave techniques.

Dr. Harry Urkowitz ... for contributions to radar signal processing and to graduate education.

Dr. Sobol, Head, Communications Technology Research, Communications Research Laboratory, RCA Laboratories, Princeton, N.J. presently directs a research group concerned with the development of new microwave devices and technology for communication systems.

Dr. Sobol received the BSEE from the City College of New York in 1952. He then attended the University of Michigan, receiving the MS and PhD in Electrical Engineering in 1955 and 1959, respectively. From 1952 to 1959, he did research in the radar, weapon guidance, and microwave fields at the Willow Run and Electron Physics Laboratories of the University of Michigan.

From 1960 to 1962, Dr. Sobol investigated superconducting films at the IBM Watson Research Center. He joined the Microwave Research Laboratory, RCA Laboratories in 1962. A year later he was named Head of Power Generation Research and in 1965, Head, Microwave Integrated Circuits Research. In the latter position, he directed the research and development of microwave integrated circuits in RCA's corporate-wide Blue Chip Program.

He was Manager, Microwave Microelectronics, at the RCA Solid State Division in Somerville, N.J., from 1968 to 1970. Under his direction, the basic technology for fabricating microwave integrated circuits was advanced from laboratory status to a pilot production. He then served as a Corporate Staff Engineer from 1970 until his present appointment.

Dr. Sobol is a member of the American Physical Society, Eta Kappa Nu, Tau Beta Pi, Sigma Xi and Phi Kappa Phi.

He held a Sperry Fellowship in Electron Physics during 1955-1956 and was the IEEE 1970 National Lecturer in Microwaves. Dr. Sobol is listed in *Who's Who in the East and American Men of Science*. He is author or co-author of 28 papers in technical journals and has presented more than 35 papers at technical meetings.

He was an Adjunct Lecturer in the Graduate School at Drexel University during 1963 and 1964. He has lectured for several University of Michigan Summer Courses.

Dr. Urkowitz, Missile and Surface Radar Division, Moorestown, N.J. received the BSEE from Drexel University in 1948, and the MSEE and PhD from the University of Pennsylvania in 1954 and 1972, respectively. He was employed by the Philco Corporation from 1948 to 1964, and by General Atronics Corporation from 1964 to 1970. He joined the RCA Missile and Surface Radar Division in 1970, where he is on the Scientific Staff of the Systems Engineering Department.

Throughout his industrial career, Dr. Urkowitz has been involved in the analysis and design of signal processing techniques, particularly for signals which have been corrupted by, besides additive noise, unwanted clutter reflection and by passage through random and/or time varying media. His studies have been applied to radar, sonar, scatter communication, and to the processing of seismic signals.

He is the author of more than 30 technical papers and has presented many papers to scientific meetings.

Dr. Urkowitz is a member of the Information Theory and Aerospace and Electronic Systems Groups of the IEEE. He is a past chairman of the Philadelphia Chapter, IEEE Group on Circuit Theory, a founder and the first chairman of the Philadelphia Chapter, IEEE Group on Information Theory. He has served on the IEEE Philadelphia Section Meetings Committee and for several years was an industry representative to the Subcommittee on Ultrasonic Delay Lines of the Electronic Industries Association. He is presently chairman of the Signal Theory Subcommittee, Standards Coordinating Committee, IEEE Group on Information Theory.

Dr. Urkowitz is an adjunct professor of electrical engineering at Drexel University's Graduate School of Engineering, where he presently teaches a course in stochastic processes. He has been associated with the graduate faculty since 1952. He introduced, wrote the texts, and taught the first graduate courses in modern network theory and in stochastic processes as applied to electrical engineering.

Television receiving antennas in blue and gold

J. D. Callaghan | D. W. Peterson

The profitable television receiving antenna product-line, being designed and produced by RCA Parts and Accessories, demonstrates the success that can be obtained by entrepreneurship within divisional boundaries of a large corporation. The necessary elements of such success are the recognition of a viable market, the ability to reach it, and the talent to produce product at a competitive cost. Add a management team with the wisdom and foresight to identify and exploit these elements and the courage to make the necessary investment and the result is a new area of profit where none had previously existed. This paper describes the engineering effort behind the development of the current RCA product line of "blue and gold" TV receiving antennas and how its success has paved the way for the introduction of other product lines into market areas previously untouched by RCA.

RCA PIONEERED in the design and sale of television receiving antennas. However, the antenna business was only an adjunct to the home instrument business and, as such, was isolated from the mainstream of television receiver design and manufacture. Consequently, RCA was an early dropout.

In 1966, the RCA Parts and Accessories Division at Deptford, New Jersey, re-entered the receiving antenna business and, in 1970, introduced a new line of RCA-designed antennas; this new line has proven to be an outstanding success. The "Permacolor" antenna line illustrates how RCA may profitably enter well-established small markets.

The television receiving antenna industry produces a national aggregate gross income of about \$50-million annually and is dominated by several relatively small manufacturers who have been in existence from the early days of TV. For most of the major manufacturers, antennas represent a substantial proportion of their total business. This means that they must organize their manufacturing along quite simple and efficient lines to make their product highly cost competitive. To re-enter this business, RCA had to implement an effective plan which would entail full control of engineering, manufacturing, and marketing—a plan that would equal or exceed the efficiency of major competitors.

This was accomplished through several phases. The first phase involved specifying and procuring a line of antennas from

Reprint RE-18-5-5

Final manuscript received November 29, 1972.

a competitor for exclusive sale by RCA. There are many drawbacks to buying from a competitor; but there was no other practical way since, at the outset, it had been decided that marketing, engineering, and manufacturing organizations were to be established on a pay-as-you-go basis utilizing profits from antenna sales. There are several major drawbacks to this approach:

- 1) A necessary economy in marketing antennas is the drop shipping of finished goods from factory to distributor. Thus, the competitor knows at all times who the RCA customers are; he knows their level of purchases; and can approach the more attractive accounts on the sale of their own "original" brand.
- 2) The antennas are easily recognized in the marketplace as the competitor's product, a decided product identity disadvantage.
- 3) RCA, as an intermediary between manufacturer and distributor, must mark up the cost whereas a merchandising manufacturer can sell directly to distributors without this additional mark up. This cost disadvantage is probably the most serious drawback.

Nevertheless, Parts & Accessories established an aggressive marketing organization which has been able to build sales to an attractive level.

Once the ability to achieve a significant share of this market was established, the next step was to develop a highly distinctive line of antennas that could be produced by a non-competitive manufacturing source or by an RCA production facility. To accomplish this next phase, additional engineering and support personnel were hired and an engineering facility was designed and constructed.

Antenna development facility

Antenna development and design requires a special facility which must include outdoor antenna testing ranges. Such a facility was planned and built at Deptford, N.J., in 1968. Radio-wave reflections from an adjacent building can seriously limit the capabilities of an antenna range, so the antenna building was designed to minimize these reflections. Since television broadcasting employs horizontally polarized radiation, transverse horizontal wiring and plumbing in the building was avoided. Radio-frequency measurements of building materials were made as the basis for choosing non-reflecting materials. The sidewalls of the frame structure made use of vinyl siding with Celotex sheathing and interior walls, materials with far

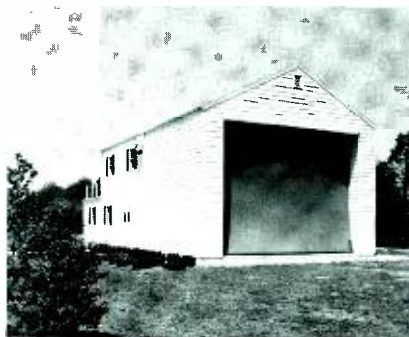


Fig. 1—Antenna development facility at Deptford. The curved radio-transparent wall will be used for "indoor" testing of antennas is at this end of the building.

lower reflection coefficients than most building materials. The roof material was corrugated fiberglass sheet. The net result was a building unusually free of radio-wave reflections.

Special laboratory accommodations were incorporated in the design of the building to enable antenna development and design work to be carried on indoors despite inclement weather which often hinders antenna work on a conventional outdoor range. This "indoor" laboratory is a room 20 ft high by 30 ft wide by 20 ft

Donald W. Peterson, Mgr., Product Development Engineering, RCA Parts and Accessories, Deptford, N.J., joined RCA as an engineering trainee in 1936 and started in the radio receiver Service Department in 1937 as a technical writer. He transferred to the RCA Research Laboratories in Camden, N.J. in 1940, where his activities included development and research in antennas and radio wave propagation. As a member of the original technical staff of the Princeton Laboratories, he received a laboratory award and the IRE Scott Helt award for the development of time domain reflectometry for television transmitting antenna testing. He also received a laboratory award for concepts in UHF broadcasting. In 1961 he transferred to the Missile and Surface Radar Division as an antenna development and design engineer. Projects included development of a circularly polarized feed for the lunar excursion erectable TV antenna. He received a citation for work on the "two pound radar" antenna. In 1967 Mr. Peterson joined Parts and Accessories where he was responsible for the development of the RCA line of TV receiving antennas.

J. D. Callaghan, Mgr., Engineering, RCA Parts and Accessories, Deptford, N.J., was employed by RCA in 1946 as a member of the RCA Service Company Home Instruments Engineering Department. His responsibilities included the development and approval of TV receiving antennas and antenna systems. He also engaged in the development of color TV test equipment, TV technician training and liaison between the TV service activity and Consumer Electronics Engineering. In addition, he received the RCA Award of Merit in 1951. In 1959 he joined the RCA Service Company BMEWS project where he became Engineering Manager with responsibility for on-site installation check-out and test of all BMEWS equipment. Mr. Callaghan came to RCA Parts and Accessories in 1964 and organized the present Engineering group which develops accessory products such as TV antennas, rotators, signal distribution systems, color TV test jigs, and automobile stereo tape players. During the course of his employment with RCA, Mr. Callaghan has been granted nine U. S. patents.

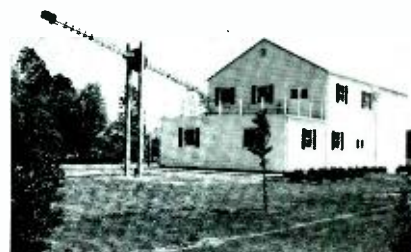


Fig. 2—This end of the antenna development facility shows the tower at one end of the radiation-pattern measurement range.

deep. It is situated at one end of the building and has a 20x30-ft radio-transparent window in one wall facing an outdoor radiating source. The window was designed "in house" and is considered unique. It consists of dacron-reinforced vinyl sheeting stretched across a sturdy wood frame. The vinyl sheet is edge supported with heavy elastic ties to produce a natural tautness. The top and bottom edges curve outward while the side edges curve inward. The resulting compound curvature imparts stability to the sheet, even in high winds (see Appendix A). After four years of service, the radio window shows no deterioration. An outside view of this radio-transparent wall is shown in Fig. 1.

The indoor test room is ideal for gain and VSWR measurements. The room is part of a 100-ft antenna test range and is used for gain measurement at all TV frequencies. An x-y plotter makes it possible to

Authors Peterson (left) and Callaghan.



plot antenna gain over the entire TV spectrum automatically in minutes. Equipment is also available in the room for automatically plotting VSWR measurements vs. frequency. The entire new RCA "Permacolor" outdoor line of antennas was developed and initial tests were performed in this room.

The opposite end of the antenna building houses the operating terminal of a 250-ft antenna test range set up primarily for radiation pattern measurement. The tower for the range is shown in Fig. 2. This tower can be lowered onto the building deck by remote control for access to the antenna mount. The range is instrumented with a polar pattern plotter which operates with a bandwidth of only 5 Hz to eliminate extraneous interference.

The antenna under test is operated as a signal source. The range receiving antenna may thus be situated at the remote end of the Range where its directional characteristics are used for minimizing local TV station interference to the extent that patterns may be measured between picture and sound carrier frequencies of the local TV stations if desired.

Product development and design

Having planned and built the antenna facility, the first activity was development of a complete line of outdoor TV receiving antennas. This meant that new electrical and mechanical design concepts were needed in an art which had been thoroughly worked over for many years by experienced competitors.

It was clear at the outset that the new RCA line would, of necessity, be electrically similar to competitive lines. All competitors were using an end fire array for the VHF portion of the antenna with a 54-to-88-MHz and a 174-to-216-MHz band. Fortunately, most of the basic electrical design ideas came from early RCA work on HF antennas. Common array elements for the low VHF and high VHF bands were obviously desirable for economy. This required creativeness and, similarly, the means of incorporating a UHF antenna for an all-channel line required new concepts.

Existing competitive antenna designs were examined early in the program to

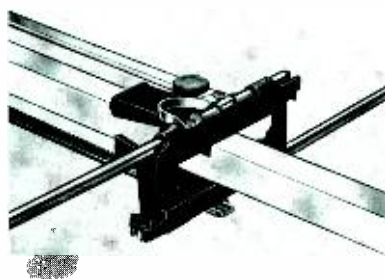


Fig. 3 — Antenna unfolding and interlocking apparatus.

assess both their weaknesses and their strengths. A significant weakness that was common to all of the popular existing designs was soon discovered. In each of these designs, the antennas are packaged in a folded condition to facilitate storage and shipment. This requires them to be unfolded by the installing technician. In the usual design, each dipole element is folded by use of a rivet acting as a hinge pin. The contradiction in concept of setting the rivet loose enough for hinging and at the same time tight enough for reliable electrical conduction makes it almost inevitable that RF noise will develop when weathering causes corrosion at the hinge joint. Here was an opportunity for design improvement. An electrical design was developed which separated the hinge function from the electrical connecting function. This made it possible to accomplish a permanent electrical connection that is immune to atmospheric deterioration. The strap which permanently connects the dipole to the transmission line is solidly riveted and is shown in Fig. 3. Permanent electrical connection is further assured by the use of special, fluted aluminum rivets which cut into the sides of the holes in the material being riveted.

A new feature was to overlap the dipoles at their insulating support. This overlap provided an easy means of transmission line transposition by simply reversing the overlap on successive dipoles. In the final product, the two halves of the insulator were designed to unfold and interlock as shown in Fig. 3, thus providing a noise-free dipole supporting structure of great strength.¹ The overlap also provided a new means for separating low-VHF and high-VHF antenna functions.² The shunt capacity needed to accomplish separation was provided inexpensively by merely lengthening the element overlap at the appropriate place in the array.

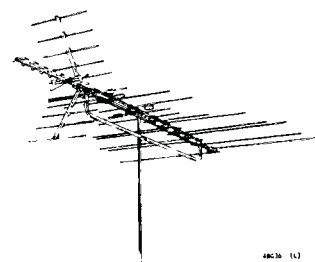


Fig. 4 — Model 4BG36 "Permacolor" antenna.

Another electrical feature introduced in the design provided for a novel means of placing low-VHF directors in front of the high-VHF antenna without degrading high-VHF performance. This feature was accomplished by the bugle-shaped members seen as part of model 4BG36 of the "Permacolor" line illustrated in Fig. 4. The UHF antenna was incorporated into the total configuration by placing a corner reflector type of antenna in front of the VHF antenna and tuning the reflector members to act as directors for the high VHF band.³

Of economic necessity, the antennas are fabricated using the same kinds of parts and material as the competitors use: sheet metal stampings, butt-seam tubing, welded tubing, and plastic moldings. These are all parts that can be fabricated with high-speed automatic machines to make them cost competitive. A kit of about 75 common parts was designed for this project. From this kit, all of the antennas needed for a complete line of six VHF, three UHF, one FM and nine all-channel antennas could be made. There are also seven of these models packaged complete with all installation material and several types of transmission line for the do-it-yourself market.

Colors for the new antenna line, predominately blue with gold support booms, were adopted by merchandising to add "eye appeal." The color choice also represented innovation since all-gold finish had become standard with the industry.

Even the package size of the product is a significant cost factor because warehousing and shipping represent cost just as surely as do materials and labor. The antenna was, therefore, designed to be the ultimate in compactness when folded. All

but four antennas of the 19-antenna product line are packaged in standard long, slender cartons that are only 5/4 inches square. Despite their folded compactness, the antennas unfold with ease and lock positively and permanently into their functioning configuration.

The antennas are marketed by the Parts and Accessories Division located at Deptford, N.J. The salesmen reach RCA Consumer Electronics distributors, as well as many other independent outlets throughout the entire nation. Sales volume has grown to the point where single distributors often order tractor trailer-size deliveries.

The advertising of this product has been both straightforward and effective. The forthright character of the RCA advertising makes it stand out in an industry which has often grossly exaggerated in their advertising copy.

The RCA product has strong and easily recognized sales features which give both the Advertising Department and the salesmen a story for their customers.

All of the RCA antenna laboratory products and components are fully documented within the RCA drawing system. The general excellence of this system has permitted both precision and flexibility in dealing with vendors as well as tight control of the product in the antenna factory.

Antenna factory

Most of the metal parts used in production are fabricated "in-house". The factory employs high-speed stamping machines, rolling mills, piercing machines, swaging machines, and other similar equipment. All aluminum sheet metal is pre-finished before stamping, rolling, or piercing. Even welded tubing, which is purchased, is finished before forming and welding. A tube-bending machine is shown in Fig. 5. Stamped parts are produced with automatic machines at a high rate with progressive dies. Plastic parts are produced from RCA molds by suppliers who specialize in these items.

Antennas are assembled with automatically fed riveters along a 200 ft moving belt as shown in Fig. 6. Quality is assured by inspection of vendor-supplied

parts, and by assembly line inspection. Antenna quality has remained high from the start of production.

Entrepreneurship—Parts and Accessories style

As a business enterprise, RCA engineering, manufacturing, and marketing of antennas is an unqualified success. The product is good, the price is right, the customers are pleased, and RCA shows a respectable profit. The entire undertaking has been carefully tailored to fit the product with no room for frills. Every member of the team plays a vital role and every member knows how he relates to the overall effort. Morale is high among the participants because everyone sees tangible results from his individual efforts. Business success becomes personal success.

The antenna activity is integrated as part of RCA Parts and Accessories. Marketing, Advertising, Sales, Accounting, Purchasing, and Engineering activities are located in Deptford, N.J. The sales organization operates throughout the entire United States.

The RCA investment in a sales organization, an engineering facility, the design effort, tooling, and the manufacturing facility, along with successful production and promotion, has convinced even the most skeptical that RCA is in this business to stay.

RCA's superior position in marketing home instruments has, of course, helped in marketing RCA antennas. The RCA name and reputation have been of significant value in opening customer doors for this new product line. For growth to continue at a healthy rate, however, it has been necessary that the antenna line measure up to the name. Along with the relationship to the Cor-

poration, at large, the new antenna activity has been able to create its own way of life—a way that is highly efficient in the production and sales of a product in an established and competitive market.

After successfully launching the manufacture of the "Permacolor" outdoor line of antennas in the RCA antenna factory, other products were examined for possible addition. Similarly, a highly distinctive line of indoor antennas was also developed; these antennas are now produced in our manufacturing facility. In both cases, the advantages of in-house manufacture proved to be a substantial factor in achieving planned business results.

The future

The RCA antenna laboratory building at Deptford also provides for an engineering activity engaged in investigating a variety of other potential products. There is a complete model shop, a design and drafting room, and general engineering laboratories.

Other product items that have been developed by P. & A. Engineering include a TV-antenna-system accessories line of 45 items. These consist of amplifiers and passive devices required for small home type MATV, (master-antenna TV) systems, a few of which are shown in Fig. 7. There is an antenna rotator line with three models, plus a complete line of antenna-installation hardware. RCA Parts and Accessories also engages in other diversified product design. One of these is car stereo tape players, some items of which are shown in Fig. 8. The RCA engineering contribution to the design of these products varies from complete product design to critical review and modification. Careful factory production control is exercised on all product lines. It



Fig. 5 — Tube-bending machine.



Fig. 6 — Automated riveting operation.

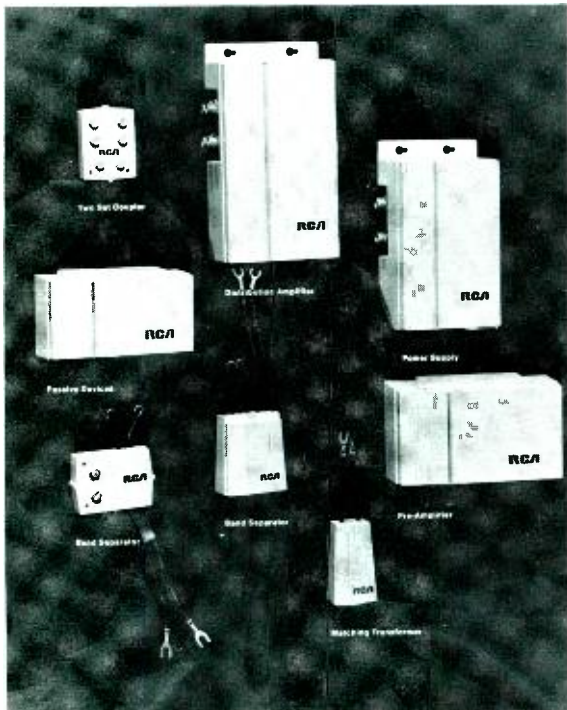


Fig. 7 — Some of the accessories-line for master-antenna TV systems.

is expected that some of these products will eventually go the full way from outside procurement to RCA manufacture along the same lines patterned by the antenna business.

The Deptford engineering group has already had substantial experience with antenna rotator and RF amplifier design. There has also been an advanced development project in cooperation with

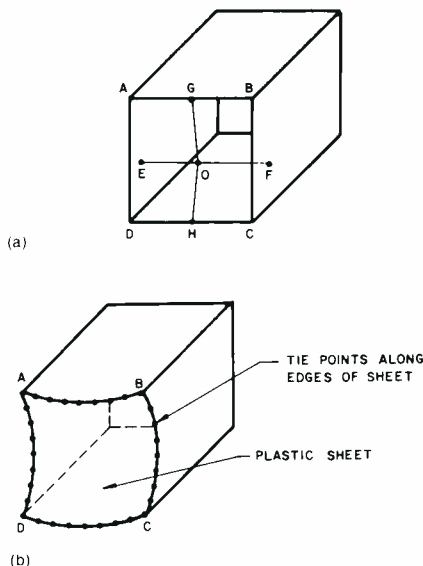


Fig. 9—Sketches of radio transparent window.



Fig. 8 — Some of the car stereo-tape line.

the David Sarnoff Research Center.⁴ This has resulted in the creation of a new concept of a miniature transistorized, rotatable, outdoor antennas which is enclosed in a weatherproof housing. This product will be introduced early in 1973. The development of this antenna will be fully described in a future issue of the *RCA Engineer*.

Acknowledgments

Neil Burwell and Frank DiMeo were responsible for the mechanical design and

the product design of the "Permacolor" antenna line. Mr. Burwell died shortly after conclusion of the mechanical design phase of the antenna line.

References

- 1 DiMeo, F. R. and Burwell, N. W. (RCA). *Collapsible structure to support antenna element*, U.S. Patent 3,263,117 (Nov., 1971)
- 2 Peterson, D. W. (RCA). *Combined VHF-UHF dipole antenna array*, U.S. Patent 3,653,056.
- 3 Callaghan, J. D. (RCA). *Multi-frequency antenna*, U.S. Patent 3,683,391
- 4 The new antenna concept was developed at Deptford under the leadership of Dr. James Gibson of the David Sarnoff Research Center

Appendix A—Design of the radio-transparent window for the antenna development facility at Deptford, N.J.

The radio-transparent window consists of an edge-supported, single plastic sheet 600 ft² in area. A sheet of this size will be exposed to approximately 14,000 lbs of air pressure in a 90 mi/h wind. It is not difficult to design a wood structure for the static load that this imparts to the supporting frame. However, if such a sheet is drawn taut to a flat surface, it tends to oscillate in the wind. It is the oscillation which makes the sheet self-destructive and adds substantially to the stresses imparted to the support members.

A method for minimizing wind-induced oscillation was conveyed by Neil Burwell. If ABCD of Fig. 9a represents the open end of a box, a vertical string attached to top and bottom can be rendered incapable of oscillation in its fundamental mode by pulling it toward the inside of the box at point O at the center. A second string stretched horizontally across the opening can be similarly rendered non-oscillating by pulling its center outward from the box. If the ends

of the horizontal string are moved inward, EOF and GOH become a stable system with neither string capable of fundamental-mode oscillation. A similar balance of forces may be accomplished in a sheet attached to points ABCD by curving the top and bottom outward and the sides inward as shown in Fig. 9b.

The outside wall of the antenna laboratory is such a compound curved sheet, made of polyvinyl chloride reinforced with a dacron fibers. The sheet constitutes the entire end wall of the building shown in Fig. 1. It was drawn taut and permitted to be self-equalizing by use of heavy elastic ties along the edges.

Prior to the erection of the full-scale wall, a scale model of the plastic sheet and the elastic supports was constructed over a vacuum chamber. The behavior to be expected in high winds was studied by partially evacuating the chamber and measuring tension in the elastic ties.

G&CS antenna range

W. C. Wilkinson

The antenna is a major element in most of the systems produced by the various divisions of G&CS. The development and measurement of these antennas requires increasingly sophisticated facilities and controlled conditions. A new RCA antenna test range for this work has been planned and is being implemented. Special attention has been paid to the problems of mutual and external interference from systems both in operation and under test. Management as well as technical design will play an important role in the solution of these everpresent problems.

SINCE THE COMPANY was formed more than 50 years ago, RCA has had a major role in antenna research, design, and manufacture. One of the earliest was the Beverage¹ or wave antenna consisting of two horizontal wires 9 miles long. One of the latest is the AN/SPY-1 antenna,² consisting of 4480 electronically steered elements. The types, sizes, and frequencies have been as varied and as extreme as the electronic communications art itself.

A necessary adjunct to any antenna development is a test or measurement capability. In RCA, these measurement facilities have taken many forms

Reprint RE-18-5-16
Final manuscript received October 25, 1972

William C. Wilkinson, Ldr.
Space and Airborne Antennas
Radiation Equipment Engineering
Missile and Surface Radar Division
Moorestown, N.J.

graduated from Purdue University in 1941, with the BSEE. Since then, he has been employed by RCA; in 1941-1942, at the Manufacturing Co., Camden, N. J.; in 1942-1961 at the RCA Laboratories, Princeton, N.J.; and since March 1961 at the Missile and Surface Radar Division, Moorestown, N.J. His experience has been in applied research and advanced systems development, RF transmission and components, and in antennas. Particular areas of experience are: narrow-beam rapid-scanning antennas at microwave and millimeter waves; airborne high-resolution radar; and ground-space communication antennas. At present, he is engaged in developmental programs on antenna systems. Mr. Wilkinson is a member of Sigma Ki, Eta Kappa Nu, and a Senior Member of the IRE.



in numerous locations: building roofs, vacant lots, unused baseball fields, specially designed buildings, and elaborately graded terrain. In the past (and to some extent even at present), the test locations and facilities represented the narrow needs of a single division or product line. Although such parochialism limited the resources that could be used for capital equipment, a competitive position could generally be maintained.

However, the great strides made in electronics during and since the World War II, and the pressing requirements for communication by the world's increasing population have enormously increased the complexity and necessary capability of antennas. In addition, labor costs and schedule needs make high-data-rate test equipment mandatory. The result is that test facilities have increased manyfold in sophistication and cost. Hand-turned positioners and point-by-point hand-plotted data points exist only in the reminiscences of not-so-old engineers.

History

Somewhat over ten years ago, the defense group of RCA divisions consolidated the antenna personnel at Moorestown in the Missile and Surface Radar Division for the purpose of enhancing the development and design capability. The commonality of antenna experience would improve and cross-feed designs for the various divisions; the DEP Antenna Skill Center came into being. In the years since its formation, the grouped antenna skills have served all five divisions in many programs, and have contributed materially to the needs of the commercial divisions. (An antenna range is operated by CSD at

The
Engineer
and the
Corporation

Gibbsboro, N.J. for development and production test of FM and TV broadcast transmission antennas.³ Another range for TV receiver antennas is operated at Deptford.⁴

At about the same time that the Antenna Skill Center was instituted, the range facilities at Moorestown were seriously affected by operation of the prototype of the BMEWS tracker, the AN/FPS-49, a nearby very high power radar. A number of the antenna test programs were moved to the just previously relinquished Home Instruments receiver test site at Medford, N.J., approximately nine miles from the M&SR plant. This small site has been in continuous use since, for programs which could not tolerate the ambient electrical noise level at Moorestown. However, the site was only an expedient and never became a complete permanent range.

The need for a consolidated permanent range has been recognized, but the apparent requirement for more suitable land became a stumbling block. As noted, the pressing needs for better facilities triggered an evaluation of previous range plans in light of existing constraints. The difficulties of obtaining land located sufficiently close and situated such that it would be in a noise-free environment for the reasonable future, forced a re-examination of the potential usefulness of the Moorestown property itself. Two conclusions were reached:

- 1) This property could be used if a full program of noise control were carried out; and
- 2) No other location would be markedly better.

The particular and general range needs were assessed and a master plan developed for an orderly implemen-

tation over a 4- to 5-year period. This plan has been approved, and periodic reviews and assessments will modify the plan details, if necessary, as time goes on.

Requirements

As noted, the types and sizes of antennas developed at MSRD have spread over a large span. It is expected that this will continue. Thus a broad general capability must be met, recognizing of course that there will always be sizes and types so extreme that special techniques and facilities will be required. The general requirements for a range site are:

Size	adequate for developmental tests
Interference	minimal or within control
Accuracy	permanent calibrated ranges
Support	shop, laboratory, housekeeping
Location	convenient to the MSRD main plant
All-weather	sufficient to maintain schedules

Fig. 1 shows the relationship of minimum required range length, antenna size, and frequency. Various representative antenna developments are spotted, illustrating that most of the programs can be satisfied with a range length of 3000 to 4000 ft.

Interference is of two kinds, passive and active. Passive relates to those effects which prevent the antenna from being tested in a free-space environment: multi-path or unwanted scattering effects of ground reflections, buildings, and natural vegetation. Active interference includes all undesired radiation.

The ever-present ground is handled by either of two techniques:⁵ the test

antenna and source are elevated to minimize ground reflections, or the two end points are located close to the ground and the ground reflection controlled and used. The former is called an elevated range and the latter a ground-level range. In some instances advantage has been taken of two elevated points separated by a valley. South Jersey, unfortunately, does not boast such features. More generally one or both terminals are placed on towers and residual spectral ground reflections broken up or absorbed to some tolerable level. This is a type of range employed at MSRD for many programs.

The ground-level range requires carefully graded and controlled terrain between the test antenna and the source antenna to maintain a stable addition of the ground-reflection signal with the direct-link signal over the area of the test antenna aperture. This type of range is useful for certain sizes and frequencies.

Active interference is generated by many sources: some are licensed transmitters, others are incidental noise generators. The ever-increasing number of radar and communication stations puts almost any test site in an interference area. In addition, MSRD itself has a continuing number of radar and high-power transmitters under test. Source radiation of multiple ranges themselves may cause intra-range problems. Tolerable levels can be reached and maintained only by an across-the-board attack:

- 1) Elimination or reduction of the interference
- 2) Discrimination against the interference

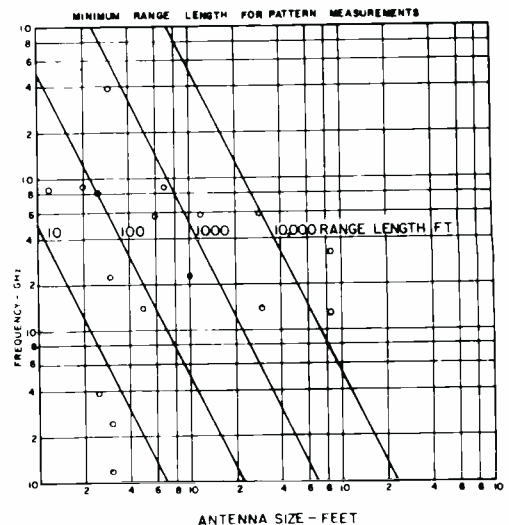


Fig. 1—Relationship of minimum range length, antenna size, and frequency.

The first works on the interference source, the second on the test antenna receiver.

Range plan

General

The general plan consists of four elements:

- 1) Location and layout
- 2) Building modifications
- 3) Interference control
- 4) Facilities and equipment

The major location of the range and its parts will be on the RCA Moorestown property, a triangular-shaped 400-acre piece of land (Fig. 2). The nucleus or hub of the range will be an existing building (Fig. 3); this can be used with only minor interior modifications. The interference control will extend to all phases, from prevention of interference generation to the op-

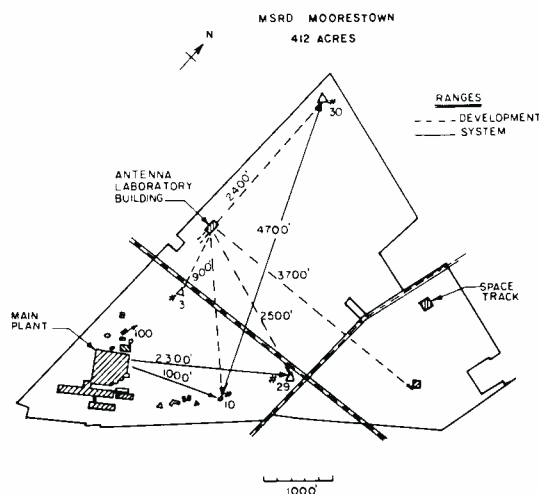


Fig. 2—Radar test ranges, MSRD.



Fig. 3—Antenna laboratory building.

eration in interference using sophisticated discrimination equipment. It includes technical management as well as techniques. The facilities and equipment consist of anechoic rooms, source towers, test equipment, surveyed and calibrated test ranges, and the accessory shop, laboratory, and computer support.

Location

The antenna laboratory building (Fig. 3) is located about 1/2 mile north of the main plant buildings and is surrounded by more-or-less open fields. It formerly housed the equipment used for outdoor backscatter and signature analysis measurements. After lying almost idle for some years, it was recently put into service for the AN/SPY-1 antenna measurements. This latter equipment and its arrangements, a major capital investment itself, will be incorporated into the overall range plans. Fig. 2 shows the relationship of the building to the property.

All but one of the ranges will have their terminus here. A short range is tentatively planned to be located on the existing RCA Gibbsboro site.³ This is about 14 miles, or 18 to 20 minutes, from Moorestown. The need and use for this range will depend on particular interference problems at Moorestown. Plans also include the use, if needed, of a small piece of land suitable for a source tower located at Arney's Mount, about 13 miles northeast of Moorestown. Activity at the leased Medford test site is to be phased out and terminated.

The plan includes renovation of the antenna laboratory building and some modifications. The basic building layout and major supporting walls fit into the range needs quite well. Fig. 4 shows the layout and planned use of the building interior.

Interference control

The interference control plan includes those areas of activity which will permit antenna measurements to be made throughout the Moorestown ranges with a minimum of interference. It is clear that there is no single solution, that there will be some periods of unavoidable conflict, and that the problems will require continual attention and periodic activity. On the

other hand, there is probably no location which is either completely free or could be sheltered from similar kinds of interference for any long period of time.

The interference control consists of two kinds of activity: technical investigation and control, and range management and control. The first has these steps:

- Interference measurement and analysis
- Development of techniques for discrimination
- Construction or modification of test equipment

Existing and potential interference sources have been defined by measurements and by tabulation of licensed transmitters. This data will be used to influence location and orientation of ranges as well as allocation of individual ranges to programs. It will pinpoint excessive levels and identify those which can be reduced.

Range management will include the establishment of a Range Control Board which will guide and control:

- all planned range use
- all range modifications
- all MSRD land use
- all range capital equipment

By these means, potentially serious conflicts can be averted, planned time sharing can be influenced, major interference sources can be prevented, and undesirable interacting activity can be minimized. This board will seek to optimize solutions for short-term problems while maintaining the long term integrity of the range capability and capital investment.

Radar-type Interference

One particularly troublesome type of interference is that from nearby radars, both operational and experimental or in test. These are located both off and on RCA property and naturally tend to be in the same general frequency bands as antennas to be developed. While frequency discrimination and modulation coding can do much, it cannot handle all situations. The pulse nature of the interference suggests that a blanking technique can have value. The low duty cycle of most antenna measurements will allow, in effect, time sharing of the same spectrum.

An experimental evaluation and

equipment development for this technique is underway and initial results are quite promising. Synchronization with the interference pulse is obtained from the leading edge for equipments off-property and beyond control. Those on-property can be synchronized likewise, or, for extreme high-level problems and pulse-rate-agile systems, hard-wired video or RF links can be used to completely blank the pulse. It is unlikely at a given frequency and situation, that more than one to three interfering equipments will be operational simultaneously. Thus the potential reduction in measurement data rate does not appear severe.

Description of ranges

The various existing and planned ranges are listed in Table I and their locations delineated in Figs. 2 and 5. Two important guidelines are being used in their design and construction:

- 1) Ranges will have permanent calibrated capabilities using dedicated equipment; and
- 2) Operating equipment and procedures will incorporate labor-saving and time-saving features.

A major portion of the required equipment is already owned and in general use. This will be rearranged and supplemented. Ranges 1 and 2 exist in part. Forms of ranges 5, 6, and 7 exist at other locations. Ranges 3 and 4 are in process of being built. The remaining three will be implemented as their need becomes more imminent.

All the ranges consist of the receiving end where the antenna under test is rotated through its various look angles, and the transmitting or source end from which a test signal is radiated. The receiving end will have a pad and pedestal with a drive system for rotating the antenna, a receiver, and recording equipment for sensing and documenting variations in the antenna performance. The transmitting source will generally be located on a tower and will be remotely controlled in orientation, polarization, and frequency. The use of phone lines and digital circuitry for control is planned. Some receiving sites will be enclosed for all-weather operation and to allow tests on antennas with particular environmental limitations, such as

those for space. A capability down to 200 MHz will be available in these chambers.

Range No. 1 is already in existence and in use. It was designed to test the AN/SPY-1 antenna—a high data-rate, wide-coverage, broad-band, electronic scanning antenna. This is a 900-ft-long elevated range, operating between a 150-ft-source tower and a 50-ft-high tower-mounted pedestal. The measurement and data requirements of this program dramatically illustrate the magnitude of modern antenna testing. This array has a $100 \times 90^\circ$ coverage with a less-than 2° beam. For each beam position, three monopulse patterns must be assessed: one sum and two difference patterns, and these at several frequencies. Gain, beam-width, lobe level, beam position, and error slope are only some of the data that must be gathered.

The pedestal and signal source as well as the antenna beam steering are controlled by a programmed computer (Digital Equipment Corp., Model PDP-11, with 18k core memory). Measured data is stored on magnetic tapes for evaluation and reprocessing for presentation. The computer also analyzes and presents spot data in real time to validate measurements being taken.

Ranges 3 and 4 are being built as a pair, using a common control room and source tower. Certain specialized recording and control equipment will also be shared. The two ranges have different but over-lapping frequency ranges. Likewise Ranges 1 and 2 will share a common control room and some equipment.

Conclusion

The complement of ranges as proposed will give RCA an antenna development and measurement facility fully suitable to the needs of the foreseeable future. These will support the product lines (other than broadcast) of the other four G&CS divisions as well as MSRD.

References

1. Beverage, H. H., "The Wave Antenna" *Trans. of AIEE*, Vol. 42 (1923).
2. See AEGIS papers in *RCA Engineer*, Vol. 17, No. 1 (June-July 1972).
3. Gehring, H. E., "The Broadcast Antenna Faculty" *RCA Engineer*, Vol. 8, No. 3 (1962).
4. Callaghan, J. and Peterson, D., "Television receiving antennas in blue and gold," *this issue*.

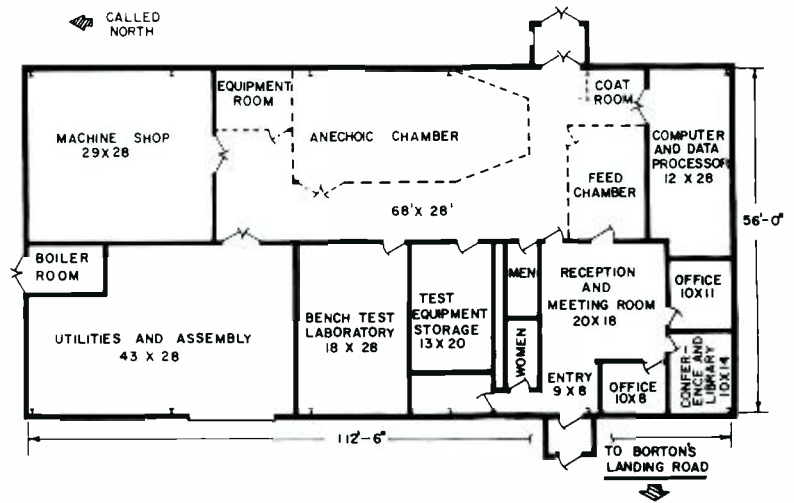


Fig. 4—Floor plan of antenna laboratory building.

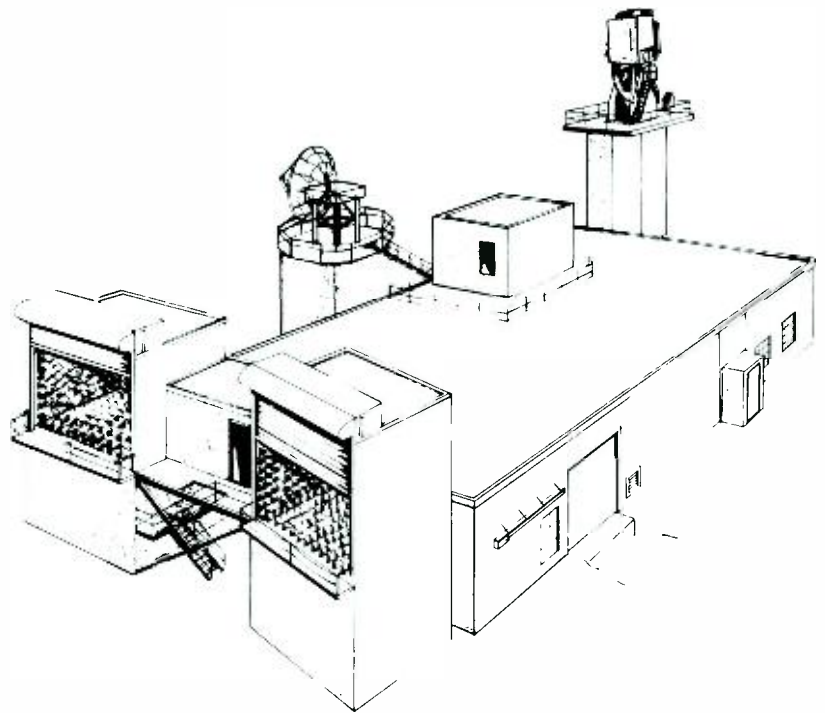


Fig. 5—Configuration of antenna laboratory facility.

Table I—Developmental ranges.

No.	Type	Height (ft)		Length (ft)	Min. freq. (MHz)	Remarks
		Transmit	Receive			
1	Elevated open	150	50	900		
		150	50	2500		
		200	50	3700		
2	Elevated open	150		2400		
		200		3700		
3	Ground level and elevated semi-anechoic	0 to 40	26	0 to 300	1000	
		200	26	2400	1000	
4	Ground level and elevated semi-anechoic	0 to 40	26	0 to 300	400*	
		200	26	2400	400*	
5	Anechoic room	—	—	10	1000	Feed and element tests
6	Shielded anechoic room	—	—	40	1000	Feed and element tests
7	Ground plane	0 to 150	0			HF scale model tests
8	Elevated range	Various	75	Variable		For high front-to-back and main-to-minor lobe ratios.
9	Elevated	25	25	0 to 100		Located at Gibbsboro for special interference problems.
10	Line of sight	300	50	70,000		Potentially useful.

* Useful to 200 MHz at some performance accuracy reduction.

New VHF filterplexer

D. G. Hymas | J. J. Matta | P. C. Noll | A. N. Schmitz

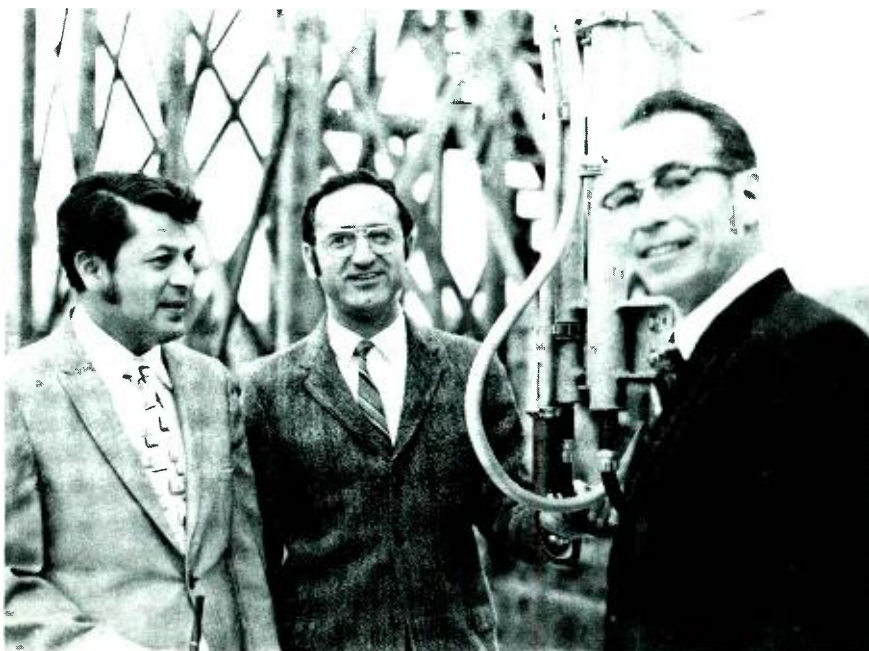
The recently introduced RCA TT50FH television transmitters for Channels 7 through 13 have a new filterplexer at the output shaping the lower sideband visual signal (50kW peak) and combining the aural signal (10kW) into a single coaxial transmission line. More stringent transmission standards have been introduced with increasingly more emphasis on idealized performance in all parts of the transmitter including the filterplexer.

Anthony N. Schmitz, Antenna Engineering Center, Broadcast Systems, Gibbsboro, New Jersey, received the BSME from California State Polytech in 1959. From 1959 to 1963, Mr. Schmitz was with the Missile and Surface Radar Division where he worked on the design of bandpass filters, temperature stabilized klystrons and high power RF loads. Since joining the Antenna Engineering Center, he has been engaged in the design of filterplexers, cavity temperature compensation systems, transmission-line components, 3-dB couplers, notch diplexers, sideband filters, antennas and RF load systems. He has a patent for a method to improve the average power capability of coaxial transmission lines and a patent pending on a heat resistant ferrite coating.

Joseph J. Matta, Antenna Engineering Center, Broadcast Systems, Gibbsboro, New Jersey, received the BS in Physics from St. Joseph's College in 1951. He subsequently completed post-graduate courses in Advanced Math from the Moore School of Engineering. His experience includes development of high power RF loads and transitions for the BMEWS project and includes a patent in conjunction with this project. In Commercial Broadcast TV Systems, he was project engineer for the first high power UHF waveguide filterplexer, also FM and VHF notch diplexers, triplexers, UHF hybrid filterplexer and the VHF coaxial filterplexer.

Donald G. Hymas, Ldr., Antenna Engineering Center, Broadcast Systems, Gibbsboro, New Jersey, received the BSEE from the University of Alberta, Canada in 1949 and the MSEE from Moore School, University of Pennsylvania in 1960. Following graduation, he worked for Canadian General Electric from 1949 to 1953 in radio receiver design and on various communication systems projects, the principal one of which was one linking Pinetree early warning radar sites. Since 1954 he has been with RCA working in the microwave communications field involving message, data, and television relaying, and since 1970 as Leader in Filter Products, Transmission Line and FM antennas at Gibbsboro, New Jersey. Mr. Hymas is a Registered Professional Engineer of the Province of Ontario and a member of the IEEE.

Authors (left to right) Schmitz, Matta, and Hymas.



MODERN television transmitting antennas for the VHF high-band channels (such as the RCA traveling-wave antennas) employ a single coaxial line as the feeder from the television transmitter to the tower-mounted antenna. The visual and aural transmitter outputs must be diplexed onto the single transmission-line feeder and in addition the double sideband visual signal from the transmitter must be filtered forming a vestigial sideband signal to confine the radiated modulation components within a 6-MHz channel assignment (see Fig. 1). A filterplexer combines the functions of vestigial sideband filter and diplexer.

The electrical operation of the filterplexer may be visualized by reference to the equivalent circuit (Fig. 2). Here, the resonant coaxial cavities actually used in the filterplexer are represented by lumped circuits. The 3-dB coaxial couplers used

Reprint RE-18-5-19
Final manuscript received October 12, 1972.

Phillip C. Noll, Antenna Engineering Center, Broadcast Systems, Gibbsboro, New Jersey received the BSEE from Purdue University in 1952 and MSEE from Drexel Institute of Technology in 1965. He continued with additional post-graduate study at the University of Pennsylvania. He joined RCA in 1952, working in the Vacuum Tube Division at Cincinnati, Ohio. In 1953, he transferred to the Antenna Engineering Center. Since that time, he has participated in design projects on sideband filters, filterplexers, and other high power circuit components. Mr. Noll's recent projects include Television and FM multiplexing equipment for the new World Trade Building in New York City. He is a member of Eta Kappa Nu, and IEEE.



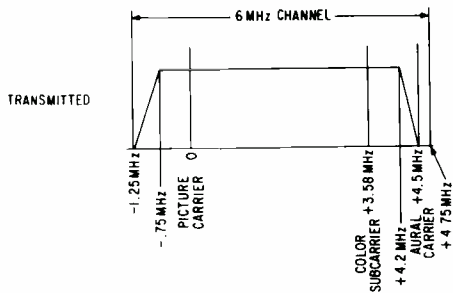


Fig. 1 — Idealized transmission characteristics.

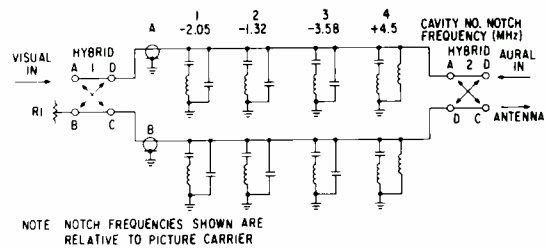


Fig. 2 — Filterplexer equivalent circuit.

at input and output are identified as hybrid 1 and hybrid 2. These 4-port devices may be visualized as tightly coupled directional couplers that have the following properties:

Power splitting

a) A signal applied at port A divides with half the power delivered to port C and half to port D and little or none at port B. The signals at ports C and D are in phase quadrature.

Combining

b) If equal-power quadrature-phase signals are applied at port A and B, the signals add at port C and little or none appears at port D.
 c) The bandwidth is 30 to 40 MHz. Despite the physical length of $\lambda/4$, the quadrature phase relationship holds for frequencies far off band center.

Diplexing

d) From b) above since port D is effectively isolated from port A, a second signal may be applied at port D and this signal from the symmetrical property of this device will be divided with half delivered to port A and half to port B with little or none to port C. The signals at port A and port B will be in phase quadrature.

Consider now the visual signal applied at port A of hybrid 1. The signal splits (quadrature phase, equal power) to feed the two coaxial lines (A and B), each with four cavities, series resonated at the following frequencies (referenced to picture carrier):

Cavity No.	Resonant freq. (MHz)
1	-2.05
2	-1.32
3	-3.58
4	+4.5

The four cavities are parallel resonated near picture carrier. Each cavity places a low impedance across the line at the series-resonant frequency so the energy at this frequency is almost totally reflected back to hybrid 1. The spacing of cavities on line A with respect to hybrid 1, port D, are the same as those on line B with respect to hybrid 1, port C. Therefore, the reflected signal from cavity 1A, for example, adds in phase with that from cavity 1B at hybrid 1, port B, where the unwanted signal is absorbed in load R1. Very little of this reflected signal is returned to hybrid 1, port A. The portion of the visual signal between -0.75 MHz and +4.18 MHz, relative to the picture-carrier frequency, passes through branches A and B with little attenuation and is delivered to the antenna at hybrid 2, port C.

then varied to establish required production tolerances for the required transmission performance specification.

The next phase of the program was the development of the resonant cavities with the required parameters. Particular attention at this phase was directed to designing safe voltage margins into the product. Each of the parallel lines of the filterplexer must handle 25 kW, peak visual power. Thus the peak voltage is given by

$$V_{\text{peak}} = \sqrt{2 \times 25,000 \times 80} = 1580 \text{ V}$$

The cavities were successfully tested with a transmitter at these peak powers. Tests were not extended to actual breakdown, as the transmitter power was not available at this time.

A most critical part of the design was the frequency stabilization of cavities against ambient temperature variation. The principle used is discussed in the next section.

Principle of cavity temperature compensation

The resonant frequency of a cavity can be represented by a series LC circuit where the resonant frequency is a function of the inductance and capacitance of the cavity. The inductance L is a function of the length the probe protrudes into the cavity and the capacitance C is a function of the gap between the probe tip and the cup. As the ambient temperature rises, the outer shell of the cavity and the probe increases in length causing the cavity to detune.

The problem then becomes one of controlling the probe length so the product LC remains constant. This was accomplished by making a compound rod with a portion of the length of invar and the remaining portion steel. Typical frequency shift curves are shown in Fig. 3.

The aural signal is applied to port D of hybrid 2 and is split (quadrature phase, equal power) to feed the two coaxial lines —A and B. Most of this signal is reflected by cavities 4A and 4B and returned to the antenna via hybrid 2, port C. Leakage of the aural signal past cavities 4A and 4B is absorbed in the terminating load R1 connected to hybrid 1.

Design program

The initial design was assisted by analysis of a mathematical model using a computer program developed in Fortran IV. A 2x2 matrix was formed for each of the parallel coaxial lines with cavities. These were combined into a 4x4 matrix which was then analyzed in tandem with a 4x4 matrix for each hybrid. Cavity slopes, resonant frequencies, and spacings were

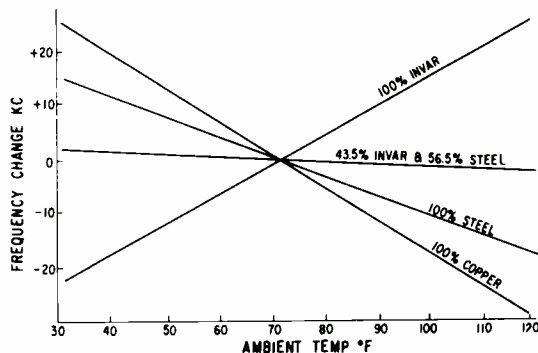


Fig. 3 — Frequency drift vs. ambient temperature.

Table I — Filterplexer specifications.

	<i>New Filterplexer</i>	<i>Previous product</i>
<i>Visual amplitude response (dB normalized)</i>		
-4.25 to -1.25 MHz	-20	-20
-3.58 MHz	-42	-42
-0.75 to 4.0 MHz	-0.6	—
-0.5 MHz	—	-0.75
0 to +4.0 MHz	—	+0.3 to -1.0
+4.18 MHz	-1	-1.5
<i>Input return loss (dB)</i>		
<i>Visual</i>		
-4.25 to -1.25 MHz	20.9	20.9
-1.25 to +4.0 MHz	31	26.5
+4.0 to -4.18 MHz	26.5	23.2
<i>Aural</i>		
	20.9	20.9
<i>Efficiency (%)</i>		
<i>Visual</i>		
	95.5	94
<i>aural</i>		
	90	92
Size LxWxH (in.)	96x47x34	90x87-1/2x29
Cooling	Forced air	Water

All cavities are cooled from a single forced-air blower and manifold distribution system properly portioning the flow to cavity pairs in relation to the heat dissipation requirements.

The probe is designed so that the power losses (due to heating of the probe assembly) influence the compensation. Air that is heated in proportion to power losses is circulated around the compound rod. Thus stabilization is optimized for varying power input level to the cavity as well as varying ambient temperatures.

This portion of the design program was accomplished in the following sequence:

- 1) Analysis of mathematical model of each cavity which included the temperature distribution along the cavity axis and radial distribution.
- 2) Synthesis of a model in breadboard form, using suitably placed heaters to achieve the temperature distribution postulated in the model.
- 3) Temperature compensation of the breadboard.
- 4) Power tests on the cavity model.
- 5) Selection of air-cooling system with proper manifolding for the complete filterplexer.
- 6) Power tests on the complete filterplexer.

Performance standards

What are the ideal standards for filterplexer performance and how closely are they approached with the new model? The standards are based on transmission characteristics for visual and aural

channels and effective isolation between these channels.

The Federal Communications Commission, the regulatory body governing domestic broadcast transmission, specifies that the shape of the transmitted visual channel shall be in accordance with Fig. 1. This illustrates the lower sideband shaping of the amplitude modulated visual signal required to confine the radiated modulation components in the assigned 6-MHz television channel band.

In addition to the amplitude shaping requirements, the filterplexer must provide a good impedance match throughout the modulation band to the transmitter and must have low attenuation (high transmission efficiency) at the visual channel carrier frequency.

The aural channel requires no amplitude shaping; however, a good impedance match and low attenuation must be provided across a band of ± 50 kHz centered at picture carrier frequency plus 4.5 MHz. The standards on isolation between visual and aural channels are set by the transmitter designer to:

- 1) Control level of intermodulation products that may be generated in the transmitter

Table II — Filterplexer measured data.

Frequency (MHz) <i>Rel. to pix carrier</i>	<i>New product, chan. 8</i>		<i>Previous product, chan. 8</i>	
	<i>Atten. (dB)</i>	<i>Normalized VSWR</i>	<i>Atten. (dB)</i>	<i>Normalized VSWR</i>
-4.5	21.7	1.03	25.6	1.03
-3.58	54.8	1.02	51.6	1.03
-3.2	31.1	1.01	21.6	1.025
-2.75	26.5	1.02	21.1	1.025
-2.05	57.2	1.035	20.6	1.02
-1.42	—	—	42.6	1.01
-1.6	21.7	1.050	42.6	—
-1.32	36.0	1.070	—	—
-1.25	21.0	1.065	21.6	1.01
-1.0	2.7	1.040	10.4	1.02
-0.75	0.3	1.040	3.6	1.03
-0.5	0	1.035	0.4	1.02
0	0	1.035	0	1.02
0.75	0	1.035	0	1.04
1.75	0.1	1.045	0.6	1.06
2.75	0.28	1.045	0.8	1.09
3.25	0.32	1.040	0.8	1.10
3.75	0.21	1.035	0.6	1.10
4.0	0.47	1.020	0.2	1.08
4.18	0.95	1.035	1.0	1.14
4.5	25.6	1.125	31.7	1.24
4.75	6.4	1.092	10.5	1.11

<i>Isolation (dB)</i>	36.4	31
Visual to Aural	36.41	31
Aural to Visual	50	47
<i>Efficiency (%)</i>		
Aural	90	91
Visual	95.5	95.5
<i>Aural VSWR</i>	1.02	1.17

output amplifiers if such isolation is not provided. These products may be radiated if not properly attenuated in the design.

- 2) Minimize effect on the output metering circuits of visual and aural transmitters particularly those monitoring output load VSWR.

A comparison of specifications for the new filterplexer and those for the predecessor are shown in Table I. Measured performance data on a production unit are shown in Table II together with corresponding data for the previous product.

Principal differences in this design from previous units are the following:

- 1) Addition of pair of cavities in the lower sideband to improve the response at -0.75 MHz.
- 2) Improved passband response.
- 3) Use of 3-dB coaxial coupler instead of bridge diplexer. This resulted in a more compact assembly despite the two additional cavities.
- 4) Forced-air cavity cooling instead of water.
- 5) Cavity temperature compensation.

Conclusions

Some of the design considerations of a television transmitter filterplexer have been described. Emphasis in the development program was placed on performing full power tests on cavity models as early in the program as possible to verify calculated voltage margins and temperature compensation requirements. Full power tests were also performed on a complete filterplexer prior to production for customer orders.

Future improvements in the design are under review. Significant product cost reduction might be achieved with the advent of high power circulators to isolate transmitter output amplifier from the filterplexer. With the consequent possible relaxation of input impedance requirements three visual cavities might be eliminated in the present eight cavity design. Improvements in material plating technology are being studied for possible lower cost substitutes for copper presently used in the cavities for high electrical and thermal conductivity as well as structural strength.

Acknowledgment

This development program was initiated under the direction of Roger E. Wolf now Manager Television Transmitter Engineering Meadow Lands, Pa.

Computer-aided design of vertical patterns for TV antenna arrays

Dr. Krishna Praba

A method for filling nulls in the vertical pattern of a broadcast TV antenna has been developed and applied. This computer-based technique, now being used by the Communication System Division, compares favorably with other methods. The computer program is versatile and the synthesis technique has been especially successful since the designer is in the decision loop. However, further work is needed to improve the optimization methods.

SEVERAL METHODS of synthesizing the vertical patterns of antenna arrays for television broadcasting have been developed.^{1,2,3,4} All of them refer to arrays having identical elements. In arrays consisting of panels that are themselves several wavelengths long, the vertical pattern of the panel itself may have, in effect, a null in the region of interest. To avoid such a null, the array can be made up of shorter panels, but the number of feed points is increased thus reducing reliability. Another method for overcoming the problem is to combine one short panel with several longer panels to make up the aperture. This combination of short and long panels established a need for a general method of solving a variety of null-filled patterns with simplified illumination currents. A computer-aided design technique was developed a few years ago to

assist in the synthesis of such arrays. The program, now available on a time-sharing terminal, allows the user to fill the nulls to the desired extent and also to reduce side lobes. When necessary, constraints may be imposed on the amplitude or phase of the currents in one or several panels.

The magnitude of the unfilled array pattern around the main beam is, of course, considerably greater than that at other angles. Further, the main beam may be tilted to any desired location by progressively phase-shifting the currents of the panels. A null-filled pattern can be considered to be made up of an unfilled primary pattern whose main beam is located at the desired angle and one or several more unfilled patterns whose main beams are located at the primary pattern nulls to be filled. The illumination currents for the final pattern are the sum of all these illuminations. Adjust-

Reprint RE-18-5-18
Final manuscript received October 12, 1972.

Dr. Krishna Praba
(formerly Dr. P. B. Krishnaswamy)
Antenna Engineering Center
Broadcast Systems
Gibbsboro, N. J.

received the BSc in Physics from Madras University (India) in 1951, the MSEE from Princeton University in 1962 and the PhD from the University of Pennsylvania in 1964. Prior to joining RCA, he was associated with Fischer & Porter Co., Warminster, Pa. where he developed flow instruments and process control systems, and with Drexel Institute of Technology as an Assistant Professor of Electrical Engineering. Since joining RCA in 1967, he has mainly been responsible for analytical work on antenna arrays. He has developed several computer programs for antenna design and has worked on the various multiple antenna installations that have been developed, or are under development, by the Antenna Engineering Center. He has published several papers on the above subjects and holds five U.S. Patents. Dr. Praba is a member of IEEE, a member of Sigma Xi, and a fellow of the British Computer Society.



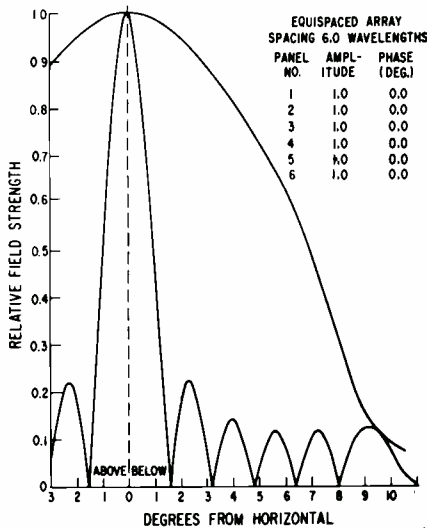


Fig. 1—Uniformly illuminated equiphase array.

ment of the phase of the secondary illuminations results in reducing or increasing the magnitude of the pattern at the desired angle, thus accomplishing null fill or side-lobe reduction. In general, the starting point is not restricted to unfilled array illumination. Thus, previous solutions can be improved upon, reducing the solution time considerably.

The technique compares favorably with all the other methods and has been extensively used in antenna array synthesis. When the current in a panel is constrained in magnitude or phase, that particular panel current is readjusted to the constrained value. The method is faster in that the null filling is restricted to the desired nulls only, instead of specifying the entire range. In addition, no gradient calculations are necessary, as is the case in steepest descent techniques.

General considerations

The vertical pattern $P(\theta)$ of an antenna consisting of N panels, at a depression angle θ is given by

$$P(\theta) = \sum_{i=1}^N p_i(\theta) A_i \exp(j\phi_i) \exp [j(2\pi/\lambda) d_i \sin \theta] \quad (1)$$

where $p_i(\theta)$ is the vertical pattern of the i^{th} panel; A_i is the amplitude of the current in the i^{th} panel; ϕ_i is the phase of the current in the i^{th} panel; and d_i is the location of the i^{th} panel. In TV applications, only the normal-

ized magnitude of the pattern is of interest.

For an array consisting of N identical panels spaced uniformly apart and carrying identical currents, the expression of the vertical radiation pattern is given by

$$|P(\theta)| = |p(\theta)| \left| \frac{\sin [(N\pi d/\lambda) \sin \theta]}{N \sin [(\pi d/\lambda) \sin \theta]} \right| \quad (2)$$

where $p(\theta)$ is the vertical radiation pattern of the panel and d is the spacing. When $p(\theta)$ is a constant (unity since it is a relative field pattern), the function $P(\theta)$ repeats itself for every λ/d in $\sin \theta$ and has nulls at $(Nd \sin \theta/\lambda) = \pm m$, for $m=1, 2, \dots$. A plot of Eq. 2 for $p(\theta)=1$ is available in many texts.³ The unfilled pattern for a six-layer Zee-panel array is shown in Fig. 1.

To provide adequate coverage for television broadcasting, the nulls in the radiation pattern in the coverage area cannot be tolerated. In most cases, the customer specifies the extent to which the nulls are to be filled. The desired amount varies with the type of coverage area, their distances from the antenna, the height of the antenna, its effective radiated power, etc. The desired pattern to achieve a 100-mV/m signal in the coverage area, is shown in Fig. 2, based on the FCC data.⁶

Any specified tilting of the beam below the horizontal is easily achieved by progressive phase shifting of the currents in each panel by an amount equal to $-2(\pi/\lambda) d_i \sin \theta_r$, where θ_r is the required amount of tilt. Minor corrections, necessary to account for the panel pattern, can be easily determined by iteration.

When the nulls of a pattern are filled, the directivity of the pattern is reduced. This reduction in gain is to be kept as low as possible. A typical gain loss of 1 to 2 dB is generally encountered.⁷ A good approximation of the gain reduction is the ratio of the beam maximum of Eq. 1 to that of an array in which the beam maximum is maximized for the same power input. In a uniformly spaced array with identical elements, the beam maximum is maximized when all the currents are equal in magnitude and the beam is tilted to

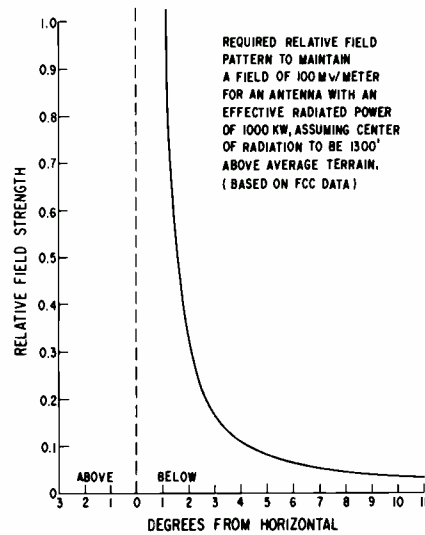


Fig. 2—Desirable relative field pattern.

coincide with the maximum of the element pattern.

In the case of an array with two different element patterns, the power into the panels is to be proportional to the gain of the panel pattern, assuming that the panel beam tilts are the same and mutual coupling between panels can be neglected.

In some cases, it is not only necessary to fill the nulls, but it is also desirable to reduce the levels of the sidelobes, so as to increase the gain of the pattern.

Null-filling methods

The variables available for pattern null filling are the spacings of the panels and the amplitudes and phases of the exciting currents. The spacings are generally chosen for the full utilization of aperture and the gaps between the panels are just sufficient to reduce mutual coupling between adjacent panels. Hence, the only variables available are the $2(N-1)$ amplitudes and phases.

In split-feed systems, one of the simple methods of null filling is by power division between the panels. For example, a 70:30 power division between each half of the array produces a 13% fill of the first null, but the even nulls are not filled. If this method is extended to fill all the nulls, the resultant power division is not acceptable in practice. But power division is usually employed where only the first null is to be filled. A typical pattern is shown in Fig. 3.

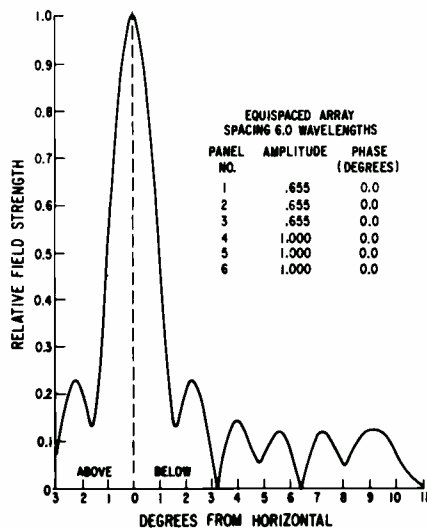


Fig. 3—Equiphase array with power division.

A similar approach to null filling by changing the phases of the currents is very useful, since the power fed to the antenna is maximized. In an array are equal for maximum power input; in some other arrays, the amplitudes are adjusted in proportion to the power ratings. For example, if the bottom and the top layers of an N -layer array differ in phase by ϕ from the rest, the first $[(N/2) - 1]$ nulls are filled. The amount of null fill is ap- of identical elements, the amplitudes proximately

$$(4/N) \sin(\phi/2) \cos[\pi N d \sin \theta / \lambda]$$

The side-lobe levels tend to be high.

One of the classical methods of null filling in which both phases and amplitudes are modified, is the "Woodward Quadrature Method."² The successive nulls are filled by the elementary uniform array which is shifted by progressive phase to the required null location and is in quadrature with the main illumination. The solution is the algebraic sum of all such elemental illuminations. The method has been used successfully in the design of antenna arrays.³ Generally, one has no control on the side lobes and constraints are not applicable. Equal amplitude constraint can also be imposed by correcting the amplitudes of the current back to unity.⁴

Computer-aided design

The following method is similar to "Woodward's" procedure except that the quadrature requirement for the

null filling part of the illumination is removed. A plot of the array pattern, as in Fig. 1, indicates that the magnitude around the main beam is considerably greater than that at other angles. The panel element pattern further enhances this effect by reducing the secondary main lobes as well. The main beam is shifted to any depression angle θ by progressively phasing the panel current by an amount equal to $(-2\pi d_i / \lambda) \sin \theta$. If the pattern is to be raised or lowered at any angle θ_M , a second illumination of the array with a progressive phase shift in the current and an additional constant phase is added to the primary illumination. In this case, the current I in the panel i is modified to

$$I_i = A_i \exp(j\phi_i) + \sum_{M=1}^L k \exp \{ j [(-2\pi/\lambda) d_i \sin \theta_M + \alpha] \}$$

If α is in phase with the pattern corresponding to all the A_i and ϕ_i , the resultant pattern due to the new currents is increased by an amount proportional to k at θ_M . If α is out of phase, the resultant pattern is reduced. If k is proportional to A_i , the normalization is accomplished. Minor variations in the pattern around the angle θ_M can be accounted for by successive iterations. If the currents are

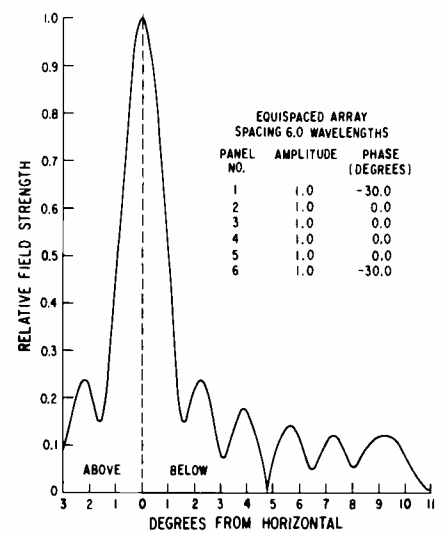


Fig. 5—Uniformly illuminated array with variable phasing.

to be fixed in any of the panels (for example, in the case of power constraint), the magnitude of the current is readjusted to the original value. In such a case, the resultant pattern improvement is reduced and more than one iteration is necessary. It has been found that the number of iterations to arrive at the final solution are reduced considerably if a partially filled pattern is chosen as a starting point. Hence, most of the derived solutions are generally stored for future use as a starting point.

Results

A computer program (Fig. 4) using the above method has been in use for several years. The following examples are illustrative of the results that have been obtained.

Example 1 (Fig. 5): With all the amplitudes equal, the first two nulls are filled by phase perturbation of the top and bottom panels of a six-layer antenna. This solution is often used as a starting point, as is the case for examples given below.

Example 2 (Fig. 6): The third null is filled by shifting the pattern to the depression angle where it occurs with an in-phase illumination. Two iteration steps were required to achieve 5% null, since all the amplitudes were constrained to be equal.

Example 3 (Fig. 7): From the above pattern, all the nulls were raised by removing the amplitude constraint. A second iteration was needed to raise the fourth null to 7.5% from 4.7%. The maximum power in any panel is

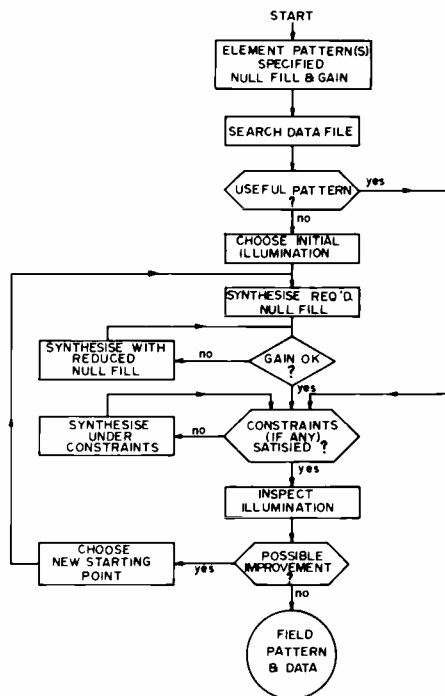


Fig. 4—Computer aided pattern synthesis, flow chart.

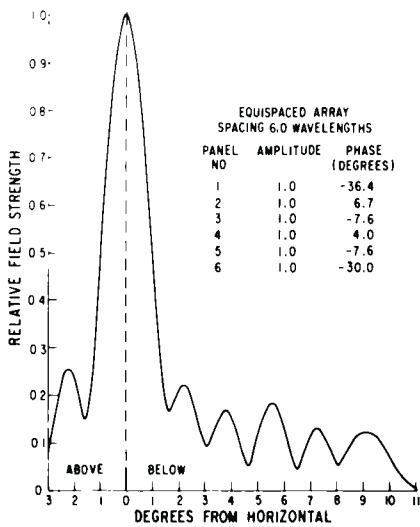


Fig. 6—Uniformly illuminated array with variable phasing, improved.

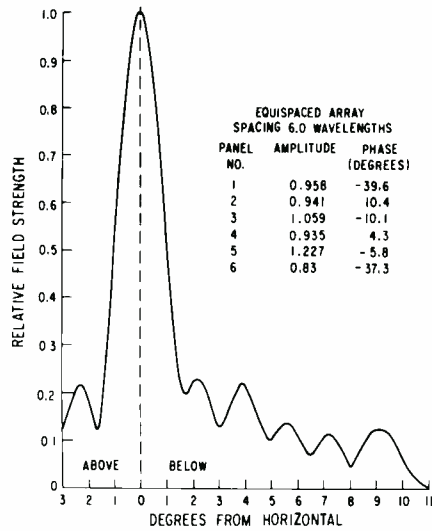


Fig. 7—Array with power division under phasing.

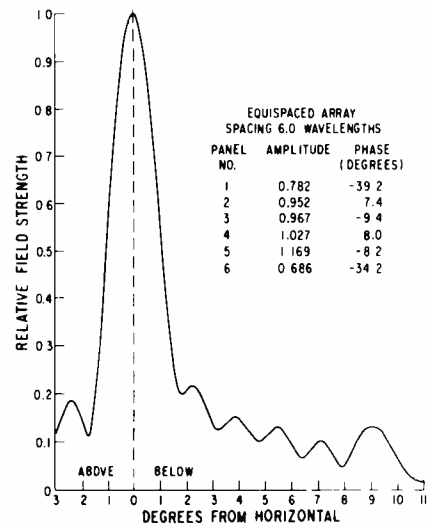


Fig. 8—Array with power division under phasing, improved.

24% instead of 16.7% in the equal-amplitude case.

Example 4 (Fig. 8): The second lobe at 3.7° below the horizontal in *example 3* is almost equal to the first lobe at 2.2°. This was reduced to produce a smoother pattern. Two iterations were required to keep the nulls filled to the same level.

Example 5 (Fig. 9): In this high gain antenna consisting of eleven panels, one of the middle panels is shorter than the other panels. The longer panels have a null at 9°. The array is tilted to 0.75° and the coverage is compared with 100-mv/mm curve derived from FCC data.

Only simple examples have been shown. The pattern shaping is not necessarily restricted to a null or side lobe. The computer program is quite versatile and the synthesis technique has been especially successful since the designer is in the decision making loop.

Further work

One of the major problems in antenna arrays is pattern stability across the channel bandwidth. The problem is more severe in the case of multiplexed antennas. Simplified feed-system compensation is not economical. In such cases, the compensation for phase changes in the feed system has to be accounted for. Work has been done on the optimization of antenna illumination taking into account the feed system of the array.¹⁰ Another problem is to determine whether any par-

ticular solution of the antenna array synthesis is the optimal one or whether a higher gain could still be obtained. An extension of the earlier work is underway.

References

1. "Woodward, P. M.," A method for calculating the field over a plane aperture required to produce a given polar diagram" *IEEE* Vol. 93 pt IIIA (1946) pp. 1554-1558.
2. Hill, P. C. J., "Methods for shaping vertical patterns of VHF and UHF transmitting aerials." *Proc. IEEE*, Vol. 116, No. 8, (Aug. 1969) pp. 1325-1337.
3. DeVito, G., "Considerations on antennas with no null radiation pattern and pre-established maximum-minimum shifts in the ver-

tical plane." *Alla Frequenza*, Vol. XXXVIII, No. 6 (1969).

4. Perini, J. and Ideslis, M. H., "Radiation pattern synthesis for broadcast antennas". *IEEE Trans. on Broadcasting* Vol. BC-18, No. 3 (Sept. 1972) p. 53.
5. Kraus, J. D., *Antennas* (McGraw-Hill Book Co.: 1950) pp. 521-534.
6. *FCC Rules and Regulations*, para. 3.699, Fig. 9.
7. Siukola, M. S. and Clark, R. N., "Various methods of determining the gain of a proposed TV Antenna", *RCA Engineer*, Vol. 16, No. 1.
8. Gihring, R. E. "Latest trends in TV broadcast antennas" *RCA Broadcast News* Vol. 105, (Sept. 1959) pp. 56-65.
9. Hill, P. C. J. "A method for synthesizing a cosecant radiation pattern by phase and variation of a constant amplitude equispaced array", in *Electromagnetic wave theory*" (Pergamon; 1967), pp. 815-850.
10. Crane, R. L., *et al*, RCA Laboratories, Princeton, N. J. *Private correspondence*.

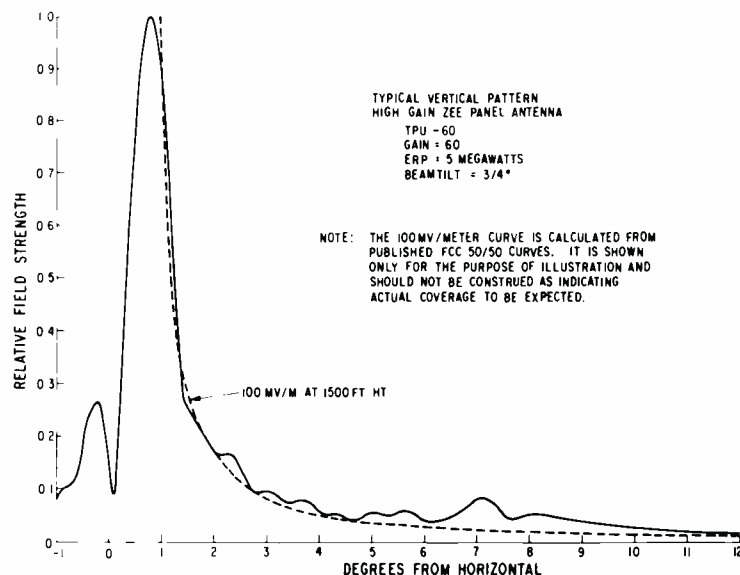


Fig. 9—Typical antenna patterns.

Lunar sounder experiment for Apollo 17

Dr. S. L. Goldman | E. J. Nossen

Early in 1971, North American Rockwell was authorized by NASA to request bids to design and develop a chirp radar for the Apollo 17 mission. The goal of the chirp radar (a coherent, synthetic-aperture type called the Lunar Sounder) was to record, on photographic film, radar signatures of the Lunar surface and sub-surface. RCA's part in this program was to design, develop and deliver a space-qualified chirp generator, transmitter, T/R switch, and receiver for installation in the Command Service Module.

Dr. Stephen L. Goldman

Communication Systems Engineering
Government Communication Systems
Communications Systems Division
Camden, N.J.

received the BSEE from Tufts University in 1962 and the MSE and PhD (EE) from the University of Pennsylvania in 1966 and 1971, respectively. Dr. Goldman's first assignment was altimeter circuit design for RCA-ACCD in Camden, N.J. From 1963 to 1965, at AED, he was concerned with satellite communication system analysis. From 1965 to 1967, at ASD, he was involved in the design, synthesis and analysis of FM and pulse radar altimeters and cavity design for Gunn Oscillators. In 1967 he was awarded a David Sarnoff Fellowship for PhD study. Since 1969 Dr. Goldman has been employed by GCS in Camden, N.J., where he has participated in the development of Time Division Multiple Access Communication Systems and the Apollo 17 Coherent Synthetic Aperture Radar. His tasks have also included the analysis of tracking loops, digital frequency synthesizer evaluation and analysis, HF/UHF subsystem design for the Integrated Radio Room and analysis of Nuclear EMP effects on various communication systems. He has participated as an associate instructor in RCA's after hours Education Program. Dr. Goldman is a member of Tau Beta Pi and IEEE.

Edward J. Nossen

Communication Systems Engineering
Government Communication Systems
Communications Systems Division
Camden, N.J.

received the BSEE from Newark College of Engineering in 1953; the MSEE from Drexel Institute of Technology in 1956; and has taken graduate courses at University of Pennsylvania. From 1953 to 1955 Mr. Nossen worked for Minneapolis-Honeywell in the instrumentation and process-control field. After joining RCA in 1955, he participated in the modernization of missile control auxiliaries of the MG3 airborne fire control system, design of the antenna and feedhorn nutation servos of the TALOS missile guidance radar, and special-purpose digital computers for airborne fire control and navigation. Mr. Nossen was responsible for system analysis and technique development in the field of electronic reconnaissance and electronic countermeasures. His study responsibilities have also included operation analysis and evaluation of military systems in an ECM environment. Recently he has been responsible for studies and technique development of pseudo-random noise and tone-ranging systems for communications and navigation applications. He is a member of Tau Beta Pi, Eta Kappa Nu, the IEEE and he was awarded RCA's 1969 David Sarnoff Outstanding Achievement Award in Engineering for his conception of and contributions to the Apollo VHF Ranging program. He holds three U.S. Patents.

THE LUNAR SOUNDER MISSION is illustrated in Fig. 1. The chirp radar is housed in the Command Service Module (CSM), which orbits the moon at an altitude of 110 ± 10 km with a nominal velocity of 1600 meters per second, thus completing a full revolution in about two hours. The Lunar Sounder uses three separate carrier frequencies—5 MHz, 15 MHz, and 150 MHz—to map the lunar surface and subsurfaces to a depth of as much as one kilometer directly beneath the orbital path of the CSM. By providing sufficient resolution and dynamic range in the reflected signal and by subsequent signal processing, the Lu-

Table I—Resolution goals.

Freq. (MHz)	Resolution (meters)*		
	Along-track (down-range)	Depth	Crosstrack
150	20	10	900
15	60	100	1500
5	360	600	3500

*To achieve a high resolution in depth, each frequency band uses a 10% bandwidth as follows: 5.0 to 5.55 MHz; 15.0 to 16.6 MHz; and 150 to 166 MHz.

nar Sounder should provide information about the location and characteristics of lunar subsurfaces and reflectors. The desired dynamic range is 60 dB, and the resolution goals are given in Table I.

Pulse-compression system

To avoid the use of high-peak-power narrow-pulse transmissions, a linear FM pulse-compression technique is used. This technique uses a periodic pulsed transmission whose instantaneous transmission frequency is linearly swept over a passband of width Δf . This type of pulsed transmission is known as a chirp. The received chirp echoes are compressed by a dispersive delay device so that most of the echo energy occurs within a much smaller time interval than the time interval

Table II—Coherent synthetic aperture radar (CSAR).

Parameter	HF: 5 MHz	HF: 15 MHz	VHF: 150 MHz
Initial frequency, f_0 (MHz)	5	15	150
Frequency sweep, Δf (MHz)	0.533 ···	1.6	16
Frequency rate, f_s (kHz/ μ s)	2.222 ···	20.0	2000
Pulse duration, T (μ s)	240	80	8
Pulse repetition period (μ s)	2520	2520	504
Time-Bandwidth Product, $T\Delta f$	128	128	128
Pulse energy (Joules)	0.02 to 0.026	0.007 to 0.009	0.0007 to 0.0009
Risetime (%)	3.6 ± 0.4	3.6 ± 0.4	10 ± 0.5
Receiver output freq. range (MHz)	0.233 to 0.766	0.9 to 2.5	3.0 to 19.0

Authors Nossen (left) and Goldman with a model of the lunar sounder.



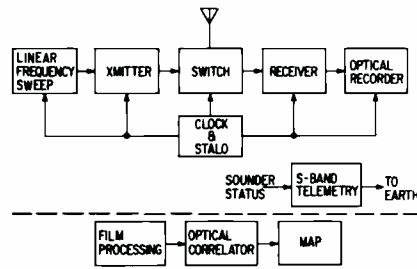
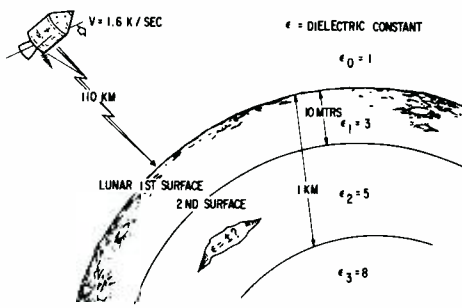


Fig. 1 (left)—Lunar sounder mission.
Fig. 2 (above)—Lunar sounder block diagram.

that the transmitted chirp occupied. The ratio of the time duration of the transmitted chirp to the time duration of the compressed chirp is the *pulse-compression ratio*. The pulse-compression ratio is also equal to the product of the time duration and the spectral bandwidth (time-bandwidth product) of the transmitted signal.

With a pulse-compression system, the increased detection capability of a long-pulse radar system is achieved while retaining the range-resolution capability of a narrow-pulse system. Several advantages are obtained. Transmission of long pulses allows more efficient use of the average-power capability of the radar. Generation of high-peak-power signals is avoided. The average power of the radar can be increased without increasing the PRF (pulse repetition frequency) and hence decreasing the radar's unambiguous range. An increased system resolving capability in doppler is also obtained as a result of the use of the long pulse. In addition, the radar is less vulnerable to interfering signals that differ from the transmitted chirp signal. Some of the radar parameters are shown in Table II.

Optical processing

Rather than compressing the chirp echoes during Lunar Orbit, the uncompressed chirp echoes are recorded on photographic film by an optical recorder. On earth, the film is developed and fed into an optical correlator to produce a map. This correlator processes the information on the developed film to extract the lunar surface and subsurface features. One of the correlator functions is to perform the pulse compression; its other function is doppler processing to achieve improved resolution along the spacecraft's track as projected on the Lunar surface. The block diagram of the

Lunar Sounder is shown in Fig. 2 and the signal flow is shown in Fig. 3.

Time sidelobes

If the Lunar target were an isolated corner reflector, the received echo would be an attenuated, time-delayed, doppler-shifted replica of the transmitted chirp. Thus, the received echo of the transmitted envelope would essentially be maintained intact. Compression of the received chirp echo, whether done by a compression line or by an optical correlator, would yield approximately a $(\sin t/t)$ envelope in the time domain. A preferred time domain envelope would be

$$y(t) = \frac{\sin t}{t} \quad (\text{for } |t| \leq \pi) \\ = 0 \quad (\text{elsewhere})$$

which represents a $(\sin t/t)$ envelope without sidelobes. *Sidelobes* are all the local maxima of the $(\sin t/t)$ envelope other than the maximum at $t=0$ (the main lobe). These sidelobes are undesirable because they can mask echoes from smaller targets at ranges different from the range of the largest aperture target. When masking occurs, resolution is degraded since the ability to identify adjacent echoes is degraded. By rounding the corners of the envelope of the transmitted chirp, the sidelobe levels of the compressed chirp can be reduced, thus improving the radar's depth-penetrating capabilities by reducing the masking effect caused by the sidelobes. The process of shaping the envelope of the transmitted chirp is called *weighting*.

Fig. 4 illustrates one-half the time waveform of an unweighted and a weighted, compressed-chirp-time waveform. The weighted chirp envelope is described by a cosine-squared function. That is, for a chirp transmitted in the time interval $(|t| \leq T/2)$, the envelope of the transmitted chirp is $\cos^2 \pi t/T$.

Note that the weighted chirp sidelobes

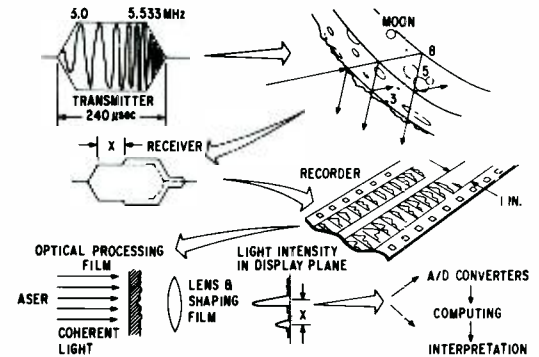


Fig. 3—Lunar sounder signal flow.

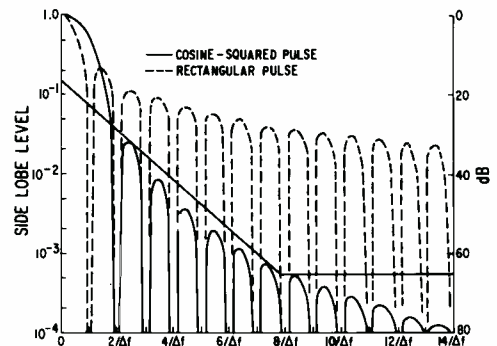


Fig. 4—Comparison of sidelobe levels.

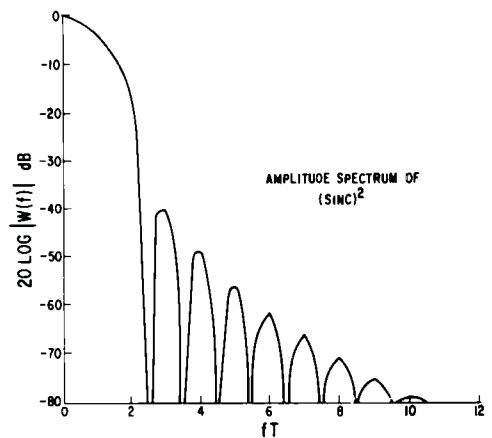


Fig. 5—Sidelobes with a sinc^2 -weighted pulse.

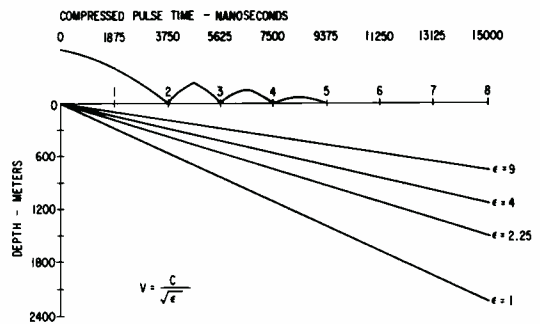


Fig. 6—HF1 (5 MHz) resolution.

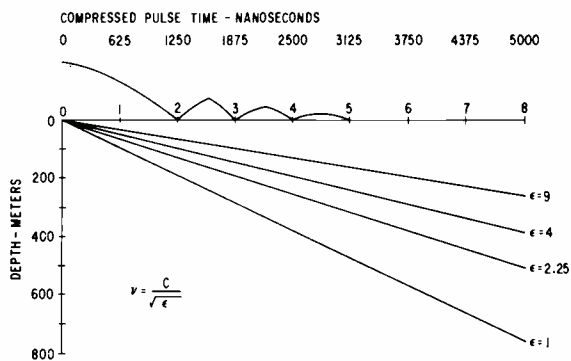


Fig. 7—HF2 (15 MHz) resolution.

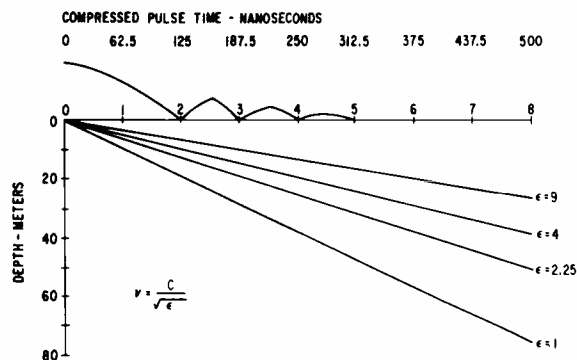


Fig. 8—VHF resolution.

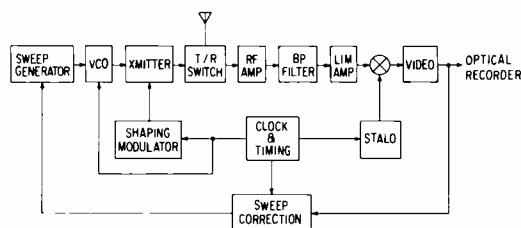


Fig. 9—Typical CSAR channel

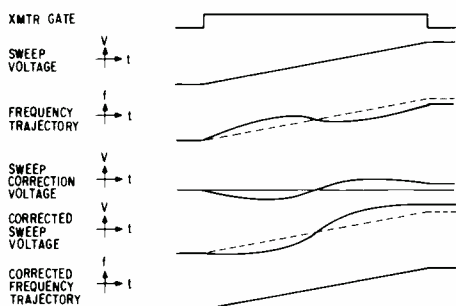


Fig. 10—Frequency sweep linearization sequence.

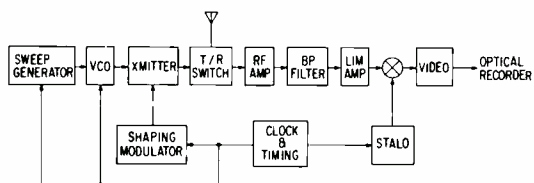


Fig. 11—Open-loop chirp transmitter and receiver.

are much lower than the unweighted chirp sidelobes, thus reducing the masking effect of sidelobes. An undesired side-effect of weighting is broadening of the main lobe (see Fig. 4). Cosine squared weighting doubles the time duration of the main lobe between nulls, thus halving its range resolution. It was for the convenience of specifying and testing the radar by itself that a cosine-squared weighting function was postulated. However, for the Apollo 17 mission, the optical processor will use sinc² weighting which exhibits sidelobes as illustrated in Fig. 5.

In most applications of range measurement, the velocity of wavefront propagation can be assumed to equal the velocity of light in a vacuum. However, in mapping the sub-lunar profile, the geometric distance between reflecting interfaces can not be determined without knowledge of the dielectric constant of the sub-lunar soil. Since a relative dielectric constant greater than 1.0 slows down the velocity of a wavefront, the effective resolution of the chirp radar is improved for higher values of relative dielectric constant, ϵ . This effect is illustrated by Figs. 6, 7, and 8 which relate the lunar depth vs. sidelobe location as a function of ϵ for the three Lunar Sounder transmission bands.

Effects of amplitude and phase non-linearities

If the chirp frequency-time trajectory is non-linear, or if the chirp transmitter, antenna, or receiver exhibits either non-flat amplitude response or non-linear phase over the chirp passband, the time sidelobes illustrated by Fig. 4 are distorted. The most serious types of distortion are either significant broadening of the main lobe or elevation of one or several of the sidelobes.

The former effect reduces resolution close to the main target while the latter misleads the radar by simulating the presence of a false target. Amplitude or phase ripple that is virtually immeasurable by standard techniques can cause significant distortion to the time sidelobes illustrated by Fig. 4.

The solid line on Fig. 4 illustrates the original goal for Lunar Sounder sidelobes. At $t=0$, the line intersects the ordinate at -16.1 dB below the main

lobe, rolling off to -65 dB at $t = \pm 8/\Delta f$. The amplitude and phase linearity goals were such that all distortion sidelobes should fall beneath this line. For example, if 8 cycles of amplitude ripple existed over the chirp passband, the peak magnitude of amplitude ripple that would generate an interference echo (simulated false target) 65 dB below the main lobe would be 0.1% peak (0.008 dB peak). Similarly, 8 cycles of phase ripple of peak magnitude 0.07 degrees would also generate an interference echo -65 dB below the main lobe.

System block diagram

The original concept for the Coherent Synthetic Aperture Radar (CSAR) used a closed-loop chirp generator that promised to equalize the effects of transmitter/receiver phase non-linearities. Fig. 9 illustrates the closed-loop chirp generator block diagram. The video output is sampled and error-correction voltages synthesized over a sequence of many chirps. The error-correction voltages are applied to the sweep generator where they pre-distort the chirp frequency-time trajectory so that, at the video amplifier output, the chirp frequency-time trajectory will be linear. Fig. 10 shows the frequency sweep linearization sequence. The first chirp sweep voltage increases linearly with time. However, the VCO frequency trajectory is non-linear. Thus, at the sample times, voltage zero-crossings do not occur. The zero-crossing time displacements result in sampled error voltages that pre-distort the linear sweep voltage to minimize the video waveform voltage zero-crossing time deviations from the closed-loop sampling times. Ultimately, the corrected sweep voltage increases non-linearly with time to generate a chirp frequency-time trajectory that is linear at the CSAR video amplifier output.

The combination of schedule constraints and excellent performance of the CSAR chirp generator with an open loop resulted in the program decision to provide an open-loop chirp generator for the Lunar Sounder experiment. Fig. 11 illustrates the open-loop chirp generator. Since the effects of transmitter/receiver phase non-linearities are not equalized by an adaptive closed loop, the transmitter/receiver filter phase functions must be

carefully controlled over the chirp passband. The open and closed loop systems are described in detail in Ref. 1. Figs. 9 and 11 indicate that the transmitted chirp envelope is "shaped" by a shaping modulator. The effects of varying the envelope rise and fall times is examined in detail in Ref. 2.

Techniques for evaluating chirp quality

Three techniques were identified for evaluating the quality of the chirp and the effects of transmitter, antenna, and receiver non-linearities upon it. They are illustrated in Fig. 12.

- 1) Use of a dispersive delay line as a pulse compression line;
- 2) Crosscorrelation of the chirp with a reference chirp; and
- 3) Autocorrelation of the chirp.

Pulse-compression line

Since classical chirp radars use compression lines, the obvious technique for evaluating the chirp quality was by means of a compression line. However, the performance goal illustrated by Fig. 4 represented more of a technical challenge than any vendor was willing to assume in the time interval available. If the first few attempts at building a compression line to achieve this goal failed, an unacceptably high floor would be imposed on the demonstratable quality of the chirp and its associated transmit-receive chain.

Crosscorrelation

A second technique is the multiplication (correlation) of the Lunar Sounder chirp with a reference chirp to yield a constant frequency (dechirped) pulse. However, with this technique, the non-linearities of the reference might dominate and mask any distortion echoes due to the chirp being measured. Furthermore, since the non-linearities of both chirps are virtually immeasurable without an

ideal compression line, the better of the two chirps could not be identified.

Autocorrelation

Autocorrelation is similar to cross-correlation except that the Lunar Sounder chirp is split into two paths, one of which contains a non-dispersive delay line. The two paths then join at separate input ports of a correlator (balanced modulator). The correlator output is the dechirped pulse whose spectrum envelope is analogous, with a few minor but defineable exceptions, to the time envelope of a chirp waveform at the output of a compression line. The only disadvantages of the autocorrelation technique are the discrepancies between the time envelope at a compression line output and the spectrum envelope of the autocorrelated chirp.^{3,4}

Using the autocorrelation technique, the reference display of Fig. 13 was generated. As explained in Ref. 3, the display of Fig. 13 was photographed from the CRT of a spectrum analyzer; the straight-line sidelobe goal levels of Fig. 4 are reproduced. If a chirp is perfectly linear, its display would appear as illustrated by Fig. 13.

Fig. 14 is the spectrum of a chirp before compression. Fig. 15a illustrates the quality of a chirp generated by one of the early vco breadboards. Fig. 15b illustrates the quality of a chirp generated by an engineering model of the vco (final mechanical and electrical configuration). Note the improved definition of sidelobe structure. Also note that the main lobe of the engineering model vco is significantly narrower than the main lobe of the breadboard vco. As the main lobe narrows, system resolution improves.

The sensitivity function of the chirp autocorrelator magnifies or suppresses interference sidelobes generated by

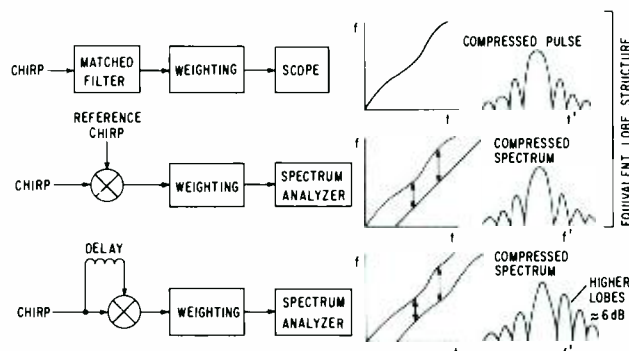


Fig. 12—Sidelobe test methods.

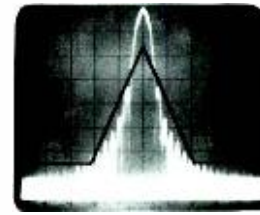


Fig. 13—Sidelobe levels of a linear chirp.

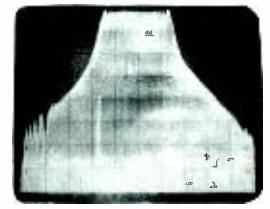
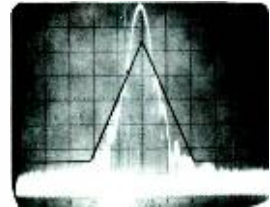
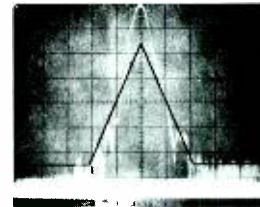
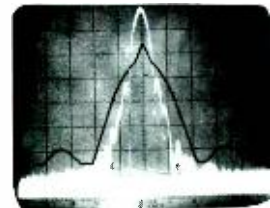
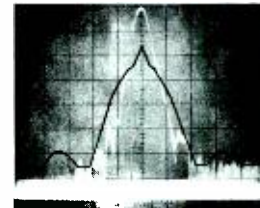


Fig. 14—Spectrum of an uncompressed chirp.



a) Early VCO breadboard b) Engineering model VCO
Fig. 15—Sidelobe-measurement-equipment display of autocorrelated chirps.



a) Early VCO breadboard b) Engineering model VCO
Fig. 16—Sidelobe-measurement-equipment display of autocorrelated chirps with modified-sidelobe-goal levels.

amplitude and phase non-linearities.³ This effect results in a modification of the straight-line sidelobe goals illustrated in Figs. 4, 13, and 15. The sidelobe-goal line, modified to illustrate the autocorrelator's sensitivity function, is illustrated by Fig. 16.

Figs. 15 and 16 indicate the improvement achieved between breadboard and engineering model vco implementation. They also demonstrate the successful achievement by the CSAR of the program goals: low-interference sidelobe levels.

Acknowledgment

The authors acknowledge the efforts of S. Klein, J. Daniel and D. Wern in the development of the sidelobe measurement equipment which was used to generate the displays illustrated in Fig. 13, 15, and 16.

References

1. Goldman, S. L. and Nossen, E. J., *private communication*.
2. Volertas, V. F., *private communication*.
3. Goldman, S. L. and Nossen, E. J., *private communication*.
4. Goldman, S. L., *private communication*.

Displays for modern radar systems

G. A. Senior

Introduction of the digital computer into radar systems has made possible great flexibility of operation, adaptability of the system to the environment, sophistication of signal processing, and nearly fully automatic operation. However, a system with these features can produce an overwhelming volume of data with far too great resolution for effective visual display. Means of editing this wealth of data to a level useful to the operator are described in terms of the Video Formatter designed and built for the AN/SPY-1 radar.

RADAR SYSTEMS have evolved into vastly complex electronic systems that are no longer well served by the relatively simple traditional displays. Features that contribute to this complexity are the use of one or more electronically steerable phased-array antennas, digital computer control, frequency agility over wide bandwidth, a variety of coded waveforms that permit sophisticated signal processing, and the means for automatic detection and classification of targets. With these operational features, the function of the display has been significantly modified and reduced in importance.

Display problem

The character of the display problem is greatly altered from that of more simple days. The agility of the antenna beam allows interleaving of both search and track functions in near real time. Computer control of operation mode permits the utilization of different waveforms, different pulse repetition frequency, different frequency of operation, and different signal processing techniques as the situation requires. In fact, more than one antenna face may radiate simultaneously. The result of these widely varying operating conditions is that the data accumulated are far too great in volume and resolution for meaningful display. The displays also are called on to show the nature of the electronic environment so the operator can select radar features to counter the environment.

Operator training requires that the data be displayed in conventional

form: plan position indicator (PPI), range height indicator (RHI), range versus amplitude (A-scope), etc. The problem, then, becomes one of editing, compressing, storing, and formatting the wealth of radar returns to a meaningful data set to be displayed for human supervision of the automatic operation of the system.

The Missile and Surface Radar Division

George A. Senior, Ldr.
Displays and Monitoring
Signal and Data Processing Engineering
Missile and Surface Radar Division
Moorestown, New Jersey
attended the U.S. Naval Academy from 1934 to 1937 and received the BSEE and MSEE from MIT in 1940. He served in the U.S. Navy until 1946, where his duties were related to instruction and preparation of manuals on maintenance and tactical use of radar. He joined RCA in 1946, where his assignments have included RF heating applications, a radar coordinate-translation display system, closed-circuit TV design and application, supervision of development and design of the high-power RF equipment for the C-Stellarator nuclear fusion research center, and 12 years of supervision of a wide variety of digital data handling, radar display and performance monitoring systems. Mr. Senior is a registered professional engineer in the State of New Jersey. He is one of the authors of the widely known Army-Navy texts *Radar Electronic Fundamentals* and *Radar System Fundamentals*.

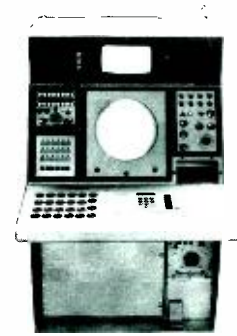


Fig. 1—AN/UYA-4 Data Display Group.

sion is currently participating in design and testing of the AN/SPY-1 radar system for the AEGIS Program. This system features phased array antennas, extensive digital data processing, computer control of signal processing and mode of operation, and coverage of a large volume of space with high-resolution search and tracking beams. Thus, the display problems encountered in this system may be taken as typical of current large radars. The solutions are discussed in this paper, although security restrictions prevent detailed explanations that would involve sensitive operating parameters. No new display devices are used in this radar; the novelty lies in the manner of handling and formatting data in a way useful to the operator. The radar is intended to be fully automatic. Thus, the displays are not operationally critical. Instead the displays are provided for the following reasons:

- 1) To permit monitoring of radar performance by the observer, but not operation of the radar in the older sense,
- 2) To permit operator analysis of the electromagnetic environment, and
- 3) To allow operator intervention and assistance in detecting and tracking under adverse conditions.

The existing AN/UYA-4 Data Display Group (Fig. 1) is used with the AN/SPY-1 radar. This system, which has been designated as standard display equipment for shipboard use, provides a number of functions. It will accept radar data from several sources, generate symbology and alphanumeric to identify targets on the screen, and provide widely different display range scales, sector coverage, formats, and character of video shown, under the independent selection of each of the observers at the display consoles. Data



are displayed on a screen consisting of long-persistence P19 phosphor. Additionally, several special-purpose A-scope formats are provided in the radar control console of the AN/SPY-1.

AN/SPY-1 radar features

A summary of the salient operating features of the AN/SPY-1 radar will indicate the versatility of the system, and hence the difficulty of displaying its data. Four array faces are disposed about the ship to provide essentially hemispheric coverage. The scan is performed in discrete beam positions, with each dwell normally limited to one interpulse period which is variable with the range suitable to the beam. The computer normally produces an orderly scan program, with the beam scanned upward from the horizon in a fan, and counterclockwise in azimuth. The scan pattern is stabilized in space against the ship's motion. However, the orderly scan may be interrupted periodically for special scans, for tracking of targets, for moving target processing, or for other similar requirements. It is apparent then, that the radar may be considered a surface search unit, a conventional fan-beam air search radar, a height-finding radar, or a tracking radar. These multiple functions are carried out under computer control, and the amount of time allowed for each is adapted to the operational environment.

Radar returns digitized to 6 bits of amplitude are fed from the signal processor to the Video Formatter. This unit converts the radar data to a form suitable for use by the display systems. The radar returns may be processed to furnish at least four kinds of digitized video outputs:

- 1) Ungated (sometimes called non-cross gated)—high-resolution data processed through the pulse compression network.
- 2) Gated—video returns from all targets not being tracked by the computer.
- 3) Log video—signals of relatively low resolution but capable of showing all targets in view, including clutter.
- 4) Moving target indication (MTI)—produced automatically by computer command when appropriate, or manually under the operator's control.

Resolution of the video available is of sufficiently high order that approximately 10^7 target cells exist in the coverage area, which could be overwhelming to the display, but necessary to the automatic operation of the system.

Video formatter

Fig. 2 shows a simplified block diagram of the Video Formatter. Information on the mode, range, etc. of the next dwell is fed for control purposes to the Formatter from the computer. Digitized video of several types is made available from the signal processor, and reduced in precision from 6 bits to 2 bits of amplitude as the first step in limiting the volume of data to be handled. Next, signals in four adjacent range cells are tested to determine the greatest amplitude among the four. The four cells are collapsed to one, in which this maximum value is reported. The result of these two operations is a significant saving in memory requirements. These involve the processing, the reduction of resolution of data to a level compatible with the display surface capability, and the development of enough processing time to allow sequential transfer of data to the display from fore and aft faces, even though the data are received simultaneously. The

range-collapsed digital video is stored in buffer memories as received, but is read out under display and timing control for feed through the D/A converter to the radar data distribution switch-board of the AN/U YA-4 display system.

A-scope digital video is processed in full 6-bit amplitude precision. Appropriately selected data are stored as received during a track beam, read out at reduced bandwidth, reconverted to analog form, and fed to radar control computers along with associated timing signals.

Precision reduction

The 6 bits of amplitude data for each range cell represent a greater dynamic range than can be observed in the brightness modulation of a long-persistence phosphor. Accordingly, the precision of each sample is reduced so that there are only 2 bits in each sample for PPI and RHI video data fed to the AN/U YA-4 displays. The two bits, which represent black and three brightness levels, are defined in terms of threshold values that range from zero to 63, corresponding to the 6 bit input video data. The threshold values are a function of the radar mode, but are fixed for each mode. Thresholds are identical for fore and aft Channel A and Channel B video. Each radar mode, except MTI modes, is assigned three threshold values.

A simplified block diagram of the precision reduction function is shown in Fig. 3. Threshold values are stored in programmable logic matrix boards, from which the required threshold values are transferred to the buffer. During the interval between radar dwells, the mode information for the next dwell is made available from the

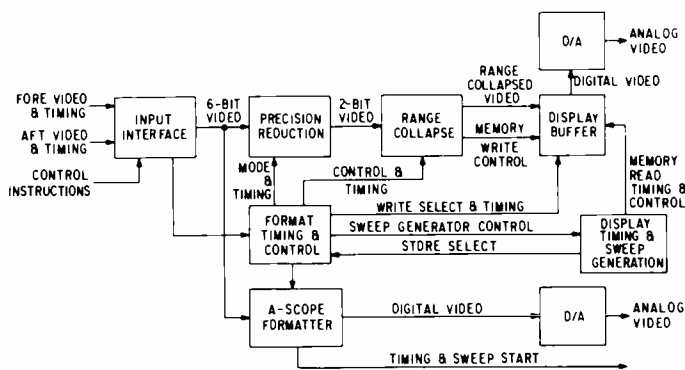


Fig. 2—Simplified block diagram of Video Formatter.

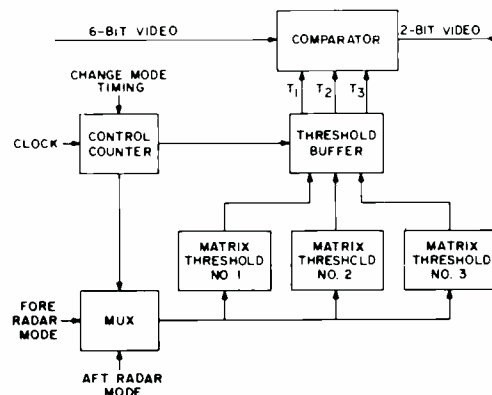


Fig. 3—Simplified block diagram of precision reduction function.

radar computer. The "change mode timing" signal causes the control counter to generate the buffer transfer pulses and multiplexer (MUX) control pulses to transfer the required threshold numbers. The comparison logic consists of comparators, parallel decoders, serial-to-parallel converters, and control logic. The 6-bit word is applied to three comparators which compare the three thresholds (T_1 , T_2 , and T_3) stored in the threshold buffers. Five outputs from the three comparators are processed in the parallel decoder to determine the reduced precision output 2-bit word. The decoder produces a "one" for the most significant bit if the comparators indicate that the video is not less than T_2 . As shown in the tabulation below, the least significant bit is a "one" if the video is greater than T_3 , or greater than T_1 and less than T_2 , or equal to T_1 or T_3 . The two output bits are loaded into

Threshold	Video
6-bit precision	2-bit precision
$< T_1$	00
$\geq T_1$ but $< T_2$	01
$> T_2$ but $< T_3$	10
$\geq T_3$	11

a shift register for parallel to serial conversion. The input video word in the system consists of five 6-bit words, or 30 bits, which are collapsed to 10 bits, and shifted out serially to the range-collapse function.

A specific threshold is established for log video when it is present, and this threshold is not changed as radar mode changes. When Channel A and Channel B video are selected, both are compared against the same thresholds.

Range collapse

Range-collapse circuits are provided for each of the four video channels. Timing for the collapse is controlled by the associated variable sequence generator, which is provided to effect the change of time base from AN/SPY-1 to the NTDS scale. For simplicity, it has been indicated that the collapse is in the ratio of 4:1; because of the time-base difference between radar and display, the ratio is actually 61:16 or nearly 4:1. Comparison is made among three cells instead of four at three places in the sequence to accommodate this difference. Fig. 4 shows the block diagram of the range

collapse function, in which the 2-bit video is fed into the input buffer. The contents of this buffer are compared with the state of the feedback storage registers, and the larger of the two numbers is inserted into the feedback storage register on the next clock pulse. After four (approximately) comparisons, the last "greatest of" decision is transferred to the output data storage and the feedback storage is cleared.

Display memory

The AN/UYA-4 display uses a single-gun cathode ray tube. This requires storing data from the fore and aft faces when they are received so that the data may be read out sequentially to accommodate the single gun. Memory is provided in the form of MOS module cards. Conceptually, the rather straightforward approach is taken of providing two memories for both fore and aft video words—one in which to write and one from which to read. The memory organization provided in the Video Formatter is rather complicated. Hence, it will be dismissed with only the concept, except to note that identical memories must be provided not only for fore and aft faces, but also for the Channel A and Channel B video.

Timing and sweep generator

A display timing and sweep generator is provided to send range zero pulses and trains of pulses of variable frequency for the X and Y deflection of the display. In the PPI mode of display, a train of ΔX pulses proportional in frequency to the sine of the azimuth angle is generated to produce left-right deflection. A sign bit is used to resolve the left-right ambiguity. Vertical deflection is produced in like manner proportional to the cosine of azimuth angle. In RHI mode, ΔX and ΔY pulse trains are produced proportional to the cosine and sine of the elevation angle. The data so produced, in synchronism with the shift out of the video amplitude data, are self-consistent so that each console operator may select range scale, offset, and format to suit his mission. Symbols necessary to identify targets on the display are generated within the AN/UYA-4 system, and may be independently called up by each operator.

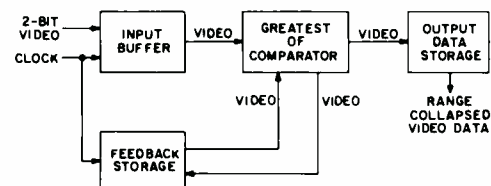


Fig. 4—Block diagram of range collapse function.

A-scope formatter

A-scope signals are generated in a separate part of the Video Formatter. When the radar mode portion of the dwell data word indicates that the next dwell is to be a target track, for which an A-scan display is indicated, this information is fed to the programmer (Fig. 5), which then sets up the appropriate controls for the timing generator. Full-precision Channel A video data are gated into the A-scope memory for a preset period of time that brackets the tracking gate. On readout from memory, the digital signal is reconverted to analog for use by the display at the control console. The memory is read out repeatedly for each loading, and several successive returns from the tracked target loaded in the sequence that the computer commands. Thus, the effective refresh rate on the A-scope is approximately 30 times/s. Although the data as received are of high resolution, and hence wide bandwidth, the signal path to the A-scope is of modest bandwidth only because of the relatively slow rate of readout. Timing and start of sweep signals are sent to the A-scope in synchronism with the synthetic video.

Acknowledgments

Concept of the Video Formatter was developed by E. G. Lurcott, C. A. Hobbs, and the author. Detailed design was carried out by I. N. Zoltan and D. Caplan of Support and Special Communications Engineering Group, Government Communications Systems.

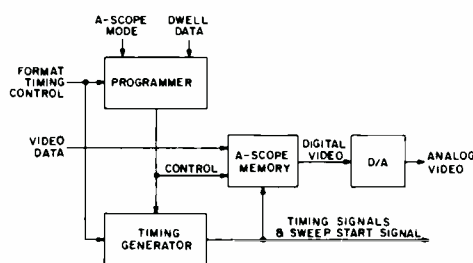


Fig. 5—Block diagram of A-scope formatter.

Phase shifter and driver design for the AN/SPY-1 phased array

N. R. Landry | H. C. Goodrich

Norman R. Landry

Radiation Equipment Engineering
Missile and Surface Radar Division
Moorestown, New Jersey

received the BSEE with High Distinction from Worcester Polytechnic Institute in 1957 and the MSEE from Drexel Institute of Technology in 1965. Prior to joining RCA, Mr. Landry served two years in the U.S. Army as an electronics instructor. His first assignment with RCA was in the design, fabrication and checkout of a very high power, high-frequency transmitter. He was then associated with a full-scale radar range where he designed system improvements and wrote several technical articles on radar cross-section measurement techniques and results. His major designs were the microwave system of an L-band cross-section measurement range and, at a later date, a coherent transmitter using microwave pulse shaping and traveling-wave-tube amplification to 50 kW of peak power. With this equipment, the phase and amplitude of the backscattered radar energy could be simultaneously measured. Mr. Landry has done applied research into an L-band super-cooled Tunnel Diode Amplifier which operated at cryogenic temperatures, and he has designed and built a low-loss, high-isolation PIN diode limiter for C-band. For the past seven years, he has been involved in the design of ferrite phase shifters for use in microwave phased array radar systems. Two designs were used in model arrays while three designs were produced for the AN/SPY-1 radar for the AEGIS system. He has written several technical articles and made ten patent disclosures relative to phase shifters. During this later period he has also contributed to various system and component designs and proposals. In a recent effort, he was a member of the task team that worked on the successful CAMEL proposal. Mr. Landry is a member of the Eta Kappa Nu, Sigma Xi, and the IEEE.

Hunter C. Goodrich

Advanced Systems and Technology
Missile and Surface Radar Division
Moorestown, New Jersey

received the BA in physics from Wayne State University in 1942 and the MSEE from Drexel University in 1967. After three years as a civilian engineer with the Signal Corps Engineering Laboratories, he joined RCA's Advanced Development Group of the Consumer Product Division in 1945. For the next fifteen years, he produced numerous consumer product advance developments in the area of transistorized radio and TV circuits, remote control, signal seeking and electronic tuners, and color TV demodulation and convergence systems. In 1960, he transferred to the Advanced Signal Processing Group of MSRD. There he has developed a variety of signal processors and correlation devices and also received the Chief Engineer's Technical Excellence Award for his work on the flux feedback driver, used in the AEGIS system. He has published several technical papers and has over thirty-five issued U.S. patents.

Three microwave garnet phase-shifter designs are used in the AEGIS weapon system. The microwave design is straightforward except that the toroid assembly is potted with silicone rubber to increase its power handling capability and the magnetizing wires are shielded with a spiral-wrapped wire to prevent the propagation of higher order modes. The driver circuit uses a new "flux feedback" concept for improved accuracy and employs monolithic circuits, hybrid circuits, and discrete components. Design of the interfaces with mating components is an important cost consideration and the chosen designs are described in detail. A table of typical performance data for each of the phase shifters is followed with a discussion of three techniques for improving factory yield.

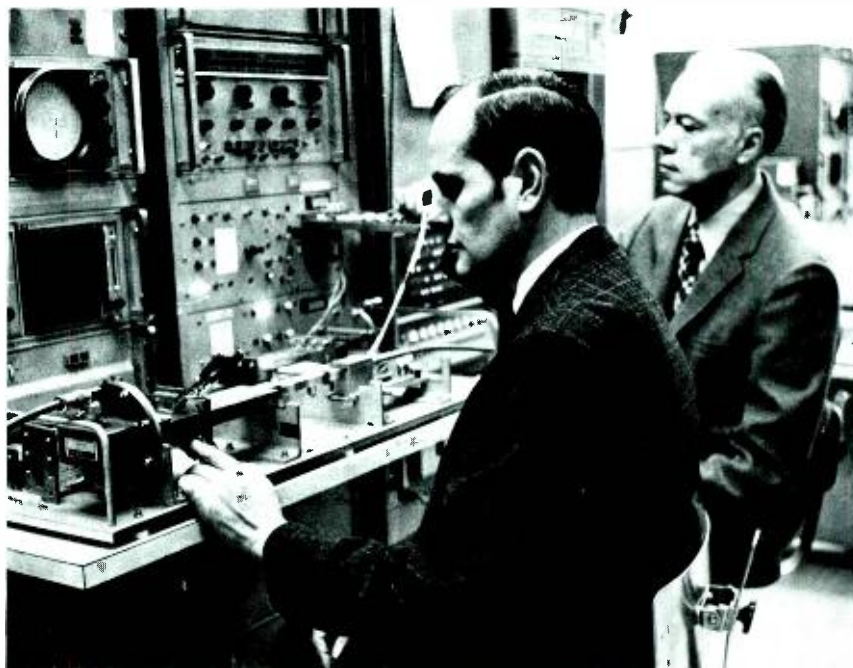
THE AN/SPY-1 phased-array radar uses subarray steering to minimize the number of phase commands that must be generated. This requires three phase shifter designs (Fig. 1). Transmit phasers are used at the inputs to the final crossfield amplifier tubes, receive phasers are used at the inputs to the receive beamformer, and antenna phasers are associated with each radiating element.

All three designs can be described as being of the waveguide, non-reciprocal, flux-drive, latching-garnet variety.¹ The garnet used is manufactured by Trans-Tech, Inc. and is their G-1004 with manganese substitution.² Each phaser has a rectangular toroid of garnet mounted in the longitudinal center of a rectangular waveguide. The toroid

Reprint RE-18-5-11

Final manuscript received December 4, 1972.

Authors Landry (left) and Goodrich.



slot contains two magnetizing wires and is otherwise filled with a ceramic that has a relative dielectric constant of 50, except for the transmit phaser for which the dielectric constant is 16. An impedance-matching transformer is used at each end of the toroid to provide a low VSWR over the frequency band. The transmit and receive phase shifters require greater phase accuracy than the antenna phaser. To accomplish this, the precision units have sturdy housings with waveguide interfaces and have a mated driver which is adjusted during production for optimum performance.

Microwave design

Phase-shifter design usually starts with the selection of the toroid and waveguide cross sections. Using an analytical model, a number of characteristics are considered:

- Differential phase versus frequency,
- Power handling capability,
- Propagation of higher order modes,
- Matching transformer design, and
- Toroid switching requirements.

The model used to predict the performance of various phase shifter designs has been described in the literature.^{3,4}

A sketch of this model with a list of variants is given in Fig. 2. The characteristic equation is obtained by incorporating the garnet tensor permea-

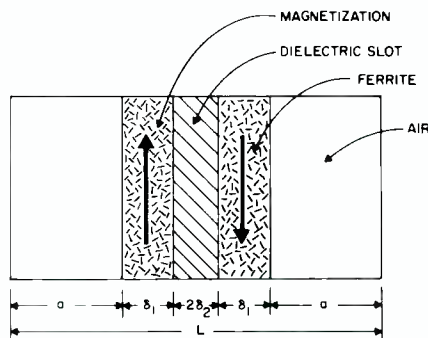


Fig. 2—Cross section of analytical model of phase shifter.

bility into Maxwell's equations and solving the appropriate boundary value problem; this technique gives a good approximation to device performance. This is true even though the top and bottom bridges between the twin garnet slabs are ignored and internal magnetization is generated with external fields; whereas in the actual device, internal magnetization is generated through hysteresis effects and the applied field is zero.

Interaction between the DC magnetization and the propagating RF field causes the propagation constant to either increase or decrease from the value that would exist if only the dielectric properties of the material were considered. The amount of interaction is a function of the level and direction of magnetization and the direction of propagation. For a given

design, differential phase shift is obtained by changing remanent magnetization to whatever is required for the desired change in propagation constant. This characteristic is nearly linear for the phasers being described.

Toroid and waveguide widths for the three designs were chosen to provide a nearly constant differential-phase-shift vs. frequency characteristic. High-dielectric-constant inserts^{2,5} were used to reduce phase-shifter size, weight, cost, and switching time and energy requirements. Matching transformers for the waveguide phase shifters can be designed using the model of Fig. 2 and setting the width of the garnet slabs to zero. In general, a ceramic matching transformer with two quarter-wave matching sections (maximally flat) was used at each end of each toroid assembly.

The analytical model can also be used to calculate electric and magnetic field strengths across the waveguide cross section. Such a calculation for the antenna phaser shows that an electric field strength of 3020 V/in. can be expected for a power level of 6 kW. At small air gaps, this field strength is multiplied by the dielectric constant of the inserts and becomes 151 kV/in. From Cobine,⁶ the arc-over strength of air increases with reduced air gap and is 45 kV/cm for a distance of 0.1 cm and 95 kV/cm for a distance of 0.01 cm. A 40-mil air gap, then, should have a breakdown strength of 114 kV/in. while that of a 4-mil air gap is 240 kV/in. To insure that all air gaps are small, the toroid assembly is potted with a silicone rubber that is injected under pressure. This encapsulant tends to fill all air gaps and reduces the voltage stress by its dielectric constant which is 2.6. The resulting stress in the silicone is about 60 V/mil while its rating is 550 V/mil. Without potting, the design would be marginal; with potting, it is conservative and much more reliable. The transmit and receive phasers are also potted to improve their power-handling capability and reliability.

The plot of insertion phase vs. toroid magnetization shown in Fig. 3 illustrates a shortcoming of the analytical model. The problem results from assuming that magnetization is uniform across the toroid leg while the squareness of the **B-H** loop requires switch-

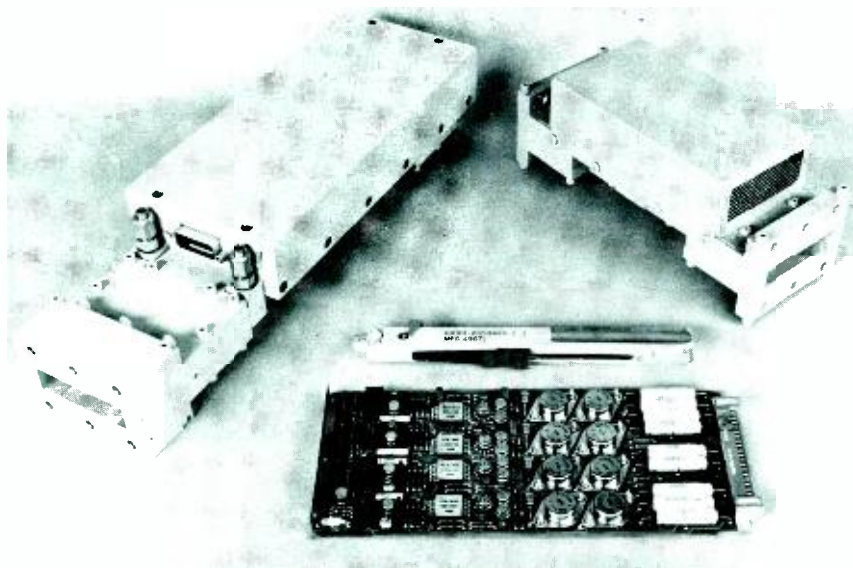


Fig. 1—Three phase shifter designs. At upper left is a transmit phase shifter assembly, at the right a receive phase shifter assembly, in the middle is an antenna phase shifter, and at the bottom, drivers for four antenna phase shifters.

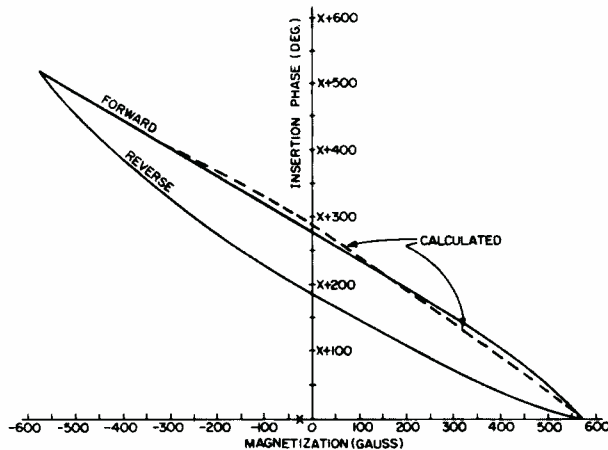


Fig. 3—Insertion phase vs magnetization, antenna phaser (calculated and expected).

ing to start from the internal edge of the toroid and progress outward. The two experimental curves are useful in describing the phase characteristics of a phaser. The curve labeled “forward” has a nearly linear characteristic and is the one used in generating differential phase shift. As temperature is increased, the maximum remanent magnetization is decreased and the extremities of the curves are reduced. To a first-order approximation, the curve labeled “forward” decreases its slope slightly and the curve labeled “reverse” moves upward to close the two curves at their extremities. This tends to stabilize insertion phase over temperature and is the result of several compensating effects. The two-way electrical length, sometimes called reciprocal phase, at any bit setting is the sum of the insertion phases represented by the two curves. This characteristic may be important in some applications and for the antenna phaser amounts to a variation of $\pm 30^\circ$ over the bit settings.

One of the problems associated with garnet phase shifter design is the potential existence of narrow-VSWR and insertion-loss spikes within the operating band of frequencies. These resonances are due to the propagation of undesired modes within the garnet-loaded portion of the phaser. At appropriate resonant frequencies, the garnet section acts as a cavity and energy is absorbed. The amount of energy absorbed is a function of the Q of the resonant cavity and the coupling coefficient of the mode exciter.

Propagation of undesired modes is controlled by lowering the Q of the cavity by selective absorption and by reducing the coupling coefficient by careful assembly. To lower the Q , the magnetizing wires are shielded with a fine wire wrapped in a spiral around them. This spiral-wrapped wire presents a larger resistance and inductance to longitudinal RF currents and effectively suppresses the undesired modes. To reduce the coupling coefficient, a good fit between the inserts and the toroids and between the toroids and the housing must be obtained.

Driver design

Fig. 4 illustrates the magnetic cycle through which the garnet toroid is driven during a transmit/receive

sequence. The “past history” of the core is first wiped out by applying a negative RESET pulse whose magnetizing force is several times the coercive force. At the conclusion of the RESET pulse, the core is left at its major loop remanent state B_{r1} . This represents a reference point from which the SET flux is measured. The transmit SET pulse is a positive pulse of amplitude e_s . During the pulse, the core flux changes according to the relationship $d\phi/dt = -e_s$. When the flux has changed by the desired amount— $\Delta\phi$, plus a small fall-back increment $\Delta\phi_f$ —the SET pulse is terminated. The phaser will now produce the desired phase shift for the transmitted pulse. The core is RESET and SET for receive in a similar manner, except that the polarity of the pulses is reversed.

To control the phase shift to the order of a few degrees, the flux placed in the garnet core must be controlled to an accuracy of 1 to 2%. The flux feedback concept shown in Fig. 4 was developed to achieve accurate control in a reliable and economical manner. The dual windings, A and B , are used for bidirectional magnetization of the garnet core. For RESET, the appropriate amplifier A or B (depending on the desired magnetizing polarity) is gated on. The magnetizing current flows through a sampling resistor R_s . The voltage across R_s is applied to an integrated-circuit RESET comparator, which is also supplied with a reference voltage. When the desired RESET current level is reached, the voltage from R_s exceeds the reference, causing the comparator to change state and turn off the gated amplifier.

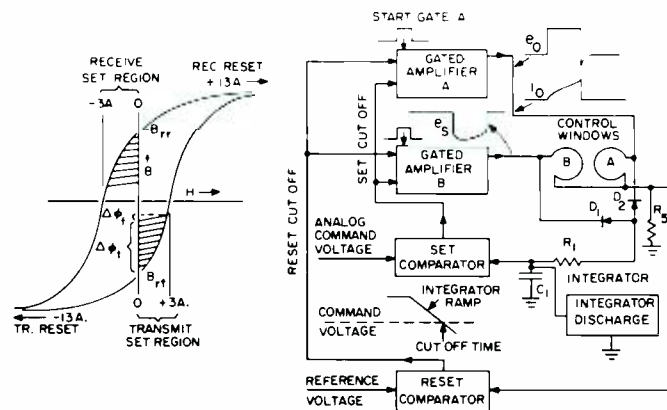


Fig. 4—Flux feedback driver.

When the phaser is to be SET for a given phase shift, an analog command voltage, proportional to the desired phase shift, is applied to an integrated-circuit SET comparator. The appropriate amplifier is next gated *on*, and the undriven winding *A* or *B* is used as a sense winding to measure the level of flux change. This winding develops a voltage, $e_s = -d\phi/dt$, that is exactly equal to the instantaneous rate of flux change. This voltage is integrated via R_1C_1 to produce a voltage ramp. The level of the voltage ramp at any instant is proportional to the induced flux at that instant. When the flux has built up to the desired level, the integrated voltage will exceed the command voltage, causing the SET comparator to change state and quickly shut *off* the gated amplifier.

In the flux-feedback approach, the driver accuracy is primarily determined by the comparator thresholds and the integrator time constant R_1C_1 . Long-term stability can be readily achieved for these parameters. Substantially eliminated as causes of flux variation are normal garnet permeability changes, amplifier temperature and aging effects, drive lead voltage drop, and supply voltage fluctuations as thousands of high current drivers turn *on* simultaneously. Its tolerance to amplifier characteristic variations makes flux feedback readily adaptable to integrated-circuit construction. Present drivers use hybrid integration (incorporating a standard monolithic comparator) for the control circuit, a specially developed monolithic dual-gated amplifier, and discrete amplifier output transistors. An LSI monolithic control circuit is under development.

Mechanical interfaces

Mechanical packaging of the phase shifters into the array antenna often requires special input and output matching structures. The transmit and receive phase shifters mate with waveguide components and pose no special problems. The antenna phaser, however, must provide an end-launched coaxial connector⁸ at one end to mate the loaded waveguide to a coaxial power divider and a blind connection with a radiating horn at the other end where no mechanical fasteners are allowed.

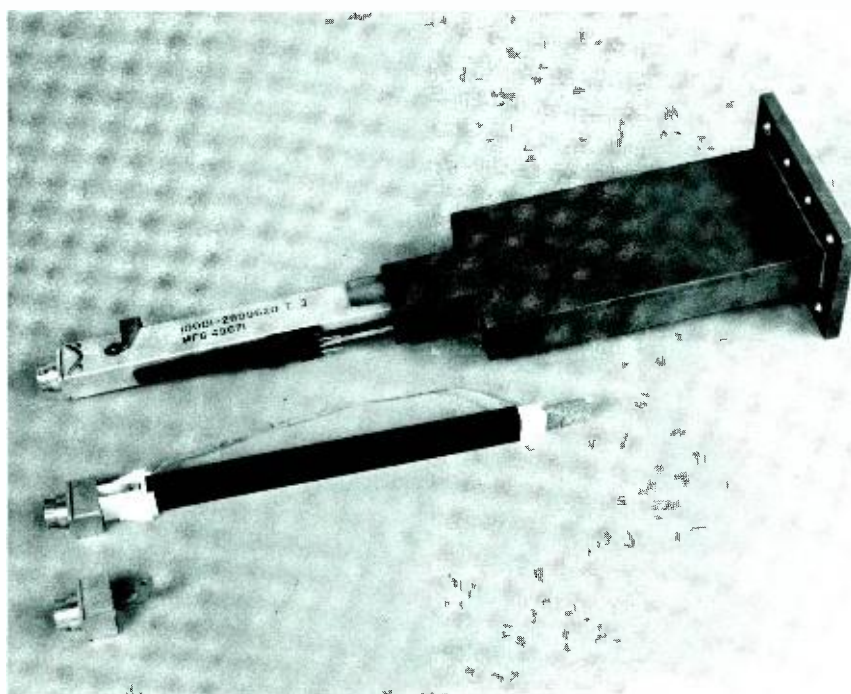


Fig. 5—Antenna phaser interfaces.

The coaxial connector, exciter, and transformer, together with a phase shifter inserted in a radiating horn, are shown in Fig. 5. The coaxial connector, exciter, and transformer were designed empirically. The resultant connector has a 60-ohm section, the exciter has a trapezoidal cross section, and the transformer has a dielectric constant of 16. The transformer is bonded to the garnet stack while the connector butts against the transformer, with the exciter fitting into the transformer slot and attached to one of the waveguide broadwalls with a small screw. The exciter shape provides the capacitance required between the exciter and the side walls of the transformer and automatically provides centering of the exciter in the transformer slot. The exciter is formed through powder metallurgy, has no sharp edges, and preserves the high-power-handling capability of the garnet toroid assembly. Nickel plating is used on the coaxial center conductor to make it compatible with the gold plating in the power divider; the exciter is tin plated to make it compatible with the aluminum phaser housing. Nickel and tin also form a compatible couple.

The phase shifter is mounted to the power divider with a spring clamp that allows misalignment from perpendicularity by $\pm 0.5^\circ$. The other end of the

phaser uses a standard two-step waveguide transformer. The first step is of ceramic and the second step is of Duroid. This end of the phaser slips into the radiating horn and uses nickel-plated stainless-steel spring contacts to make the connection between the phaser and horn. Electrical performance of this design provides a VSWR and insertion loss which are essentially independent of the position of the phaser in the horn; insertion phase changes by $\pm 4.5^\circ$ for a change in insertion depth of ± 0.062 in. The spring mounts at each end of the antenna phaser satisfy the design concept of providing self-alignment between the power divider and the horn cluster.

Performance data

Data measured on production units of the three phaser and driver designs show that differential phase shift is linear with command within an RMS error of less than 2.5° . Over a $\pm 40^\circ\text{F}$ temperature range, insertion phase changes $\pm 5.0^\circ$ and differential phase at the maximum bit command changes $\pm 6.0^\circ$. Differential phase errors as functions of operating frequency are small and are included in the above figures.

Insertion loss for the antenna phaser is typically 0.95 dB when averaged over

frequency and command settings, while that of the transmit and receive phasers is typically 0.90 dB. VSWR is low in all designs and power handling capability is tailored to the various requirements. Table I lists the specification requirements and typical performance of the three designs. Differential and insertion phase errors include the effects of ambient temperature, RF power, DC power supply drift, and an estimate for aging. Phase errors for the antenna phaser are considerably below the specification values. This is attributable to the limited production (5000 units) where each constituent part is purchased from one vendor. As the number of suppliers for each part is increased, variability will also increase. Switching energy includes that which is delivered to the toroid and switching wires as well as driver efficiency. MTBF for the antenna phaser and driver is allocated as 200,000 hours for the phaser and 160,000 hours for the driver. Since they are not a mated pair, malfunctioned drivers can be replaced during normal maintenance while defective phasers will wait for depot repair. Testing during vibration has indicated several small mechanical vibrations, but these had no measurable effect on the performance characteristics.

Production considerations

Several techniques for improving production yield are being used in phaser

production. These are, in addition to the normal purchased material inspection, care in assembly, in-process tests and inspections, and quality-control procedures. One technique is to measure the maximum remanent magnetization of the garnet toroids, their most sensitive parameter, and select a set of three toroids for each phase shifter. In this manner, a toroid with low remanence can be paired with one of high remanence to partially balance their effects. Toroids are being purchased with a remanence tolerance of $\pm 5\%$ and the selection is reducing this to $\pm 2.5\%$ for the toroid sets.

Another technique used for the antenna phasers is to categorize them as *A*, *B*, or *C* depending on their differential-phase vs. switched-flux characteristics. Type *A* provides too much differential phase for a level of switched flux; type *B* is average; and type *C* provides too little. By having three types of drivers, it is possible to compensate the *A*- and *C*-type phasers and, for a given population, either reduce overall error or increase yield. In practice, sets of 32 *A*-, *B*-, or *C*-type phasers are assembled into array modules so that an array module has all of one type and is so marked.

A third technique is to trim insertion phase. This is done electronically in the mated drivers of the transmit and receive phase shifters. For the antenna phaser, it is done with inductive iris

triplets that can be inserted in the side of the phaser housing. Three triplets provide a trim of $\pm 24^\circ$ in steps of 8° , change insertion loss by about ± 0.04 dB and have a negligible effect on VSWR.

Acceptance testing

Phaser acceptance testing is done with Hewlett-Packard Automatic Network Analyzers.⁹ Special computer programs and interface equipment allow the analyzer to automatically measure the VSWR, insertion loss, and insertion phase of the units at selected frequencies and bit settings. Nine frequencies and 32 bits are measured for the transmit and receive phasers, while five frequencies and eight bits are used for the antenna phasers. Typical temperature characteristics are stored in the computer and the computer translates the room-temperature data to expected performance at an average operating temperature. Analysis has shown that this temperature extrapolation is not critical over the specified temperature range, and extrapolation errors as large as $\pm 40\%$ can be tolerated. Actual error is probably less than $\pm 10\%$ and is small compared to the savings enjoyed by testing phasers at room temperature rather than average operating temperature.

References

1. Ince, W. J. and Temme, D. H., "Phasers and Time Delay Elements", Project Report RDT-14, Contract AF19(628)-5167, MIT Lincoln Laboratory, (July 11, 1967).
2. Ince, W. J., Temme, D. H., Willwerth, F. G., and Huntt, R. L., "The Use of Manganese-Doped Iron Garnets and High Dielectric Constant Loading for Microwave Latching Ferrite Phasers", *GMTT 1970 International Microwave Symposium Digest*, pp. 327-331.
3. Ince, W. J. and Stern, E., "Nonreciprocal Remanence Phase Shifters in Rectangular Waveguide," *IEEE Transactions on Microwave Theory and Techniques*, Vol. MTT-15, No. 2 (Feb. 1967) pp. 87-95.
4. Whicker, L. R. and Jones, R. R., "Design Guide to Latching Phase Shifters", *Microwaves* (Nov. 1966) pp. 31-39 and (Dec. 1966) pp. 43-47.
5. Landry, N. R., "Microwave Phase Shifters", RCA Reprint RE-15-3-5; *RCA Engineer*, Vol. 15, No. 3 (Oct./Nov. 1969) pp. 20-25.
6. Cobine, J. D., *Gaseous Conductors, Theory and Engineering Applications*, (Dover Publications, Inc.; New York, N.Y.; 1958) p. 166.
7. Goodrich, H. C. and Tomsic, R. J., "Flux Feedback Boosts Accuracy of Phased Array Radar Systems", *Electronics*, Vol. 43, No. 24 (Nov. 23, 1970) pp. 77-80.
8. Wheeler, G. J., "Broadband Waveguide to Coax Transitions", *IRE National Convention Record, Part 1* (1957) pp. 182-185.
9. Hackborn, R. A., "An Automatic Network Analyzer System", *Microwave Journal* (May 1968) pp. 45-52.

Table I—Phased-shifter characteristics.

	Antenna phaser		Receiver phaser		Transmit phaser	
	Spec	Typical	Spec	Typical	Spec	Typical
Freq (GHz)	—	—	—	—	—	—
VSWR, (max)	1.35	1.25	1.25	1.20	1.25	1.15
Insertion loss (dB, ave)	1.1	0.95	0.9	0.90	1.2	0.90
Insertion loss (dB, peak)	1.5	1.15	1.2	1.10	1.5	1.15
No. of bits	5	5	5	5	5	5
$\Delta\phi$ error (deg., RMS)	9.5	5.0	4.5	4.0	4.5	4.0
IP error (deg., RMS)	14.2	6.0	4.0	3.0	4.0	3.0
Power (ave, W)	12	12	—	—	120	120
Power (peak, kW)	1.5	1.5	—	—	15	15
Power (peak survive, kW)	6.0	16.0	10.0	16.0	40	80
Temp (operating, °F)	80 to 160	80 to 160	80 to 105	80 to 105	80 to 105	80 to 105
Temp (survive, °F)	-80 to 167	-80 to 167	-80 to 167	-80 to 167	-80 to 167	-80 to 167
Sw speed (RESET, μ s)	10 for both	4	7	5	13	6
Sw. speed (SET, μ s)	—	2	6	3	10	4
Sw. rate (ave, Hz)	800	800	800	800	800	800
Sw. energy, per PRF (μ J)	—	600	—	600	—	800
Sw. current (peak, A)	13 \pm 1	13	—	13	—	18
MTBF (hrs.)	88,700	—	83,333	—	85,300	—
Shock	MIL-STD-202D		MIL-STD-202D		MIL-STD-202D	
Vibration	MIL-STD-167		MIL-STD-167		MIL-STD-167	
Humidity (dewpoint, °F)	50		50		50	

Note: Typical values include an estimate for measurement error, power supply drift, and aging.

High-efficiency avalanche diodes (TRAPATT)* for phased-array radar systems

Dr. K. K. N. Chang | Dr. H. Kawamoto | H. J. Prager
 Dr. J. Reynolds | A. Rosen | Dr. V. A. Mikenas

The high-efficiency avalanche (TRAPATT)* diode is capable of generating high pulsed microwave powers. The progress made at RCA Laboratories both in theory and in technology under a continuous and intensive development program has firmly established this device as one of the front contenders for solid-state phased-array radar systems. Current effort has resulted in significant advances in diode performance capabilities, as, for example, 50 W peak output power was obtained over a 10% bandwidth at S-band with 10 dB gain, 16% efficiency, 5.6% duty cycle and 10 μ s pulse width. Under different test conditions, substantially better individual performance results have been demonstrated.

*TRAPATT (Trapped Plasma Avalanche Triggered Transit)

THE RAPID DEVELOPMENT of microwave solid-state sources has resulted in considerable interest in a solid-state approach to phased-array radar design. Several solid-state phased-array radar systems have already been designed using the transistor as the basic building block for the microwave power source. Indeed, it has been shown that such an approach offers many advantages over the conventional design approach (which uses a high-power-tube transmitter) in the areas of reliability, size, weight, cost, flexibility, etc. Unfortunately, the transistor is basically a CW device and is peak-power limited. In many cases, this characteristic imposes severe limitations on radar system design making it a much less attractive candidate. On the other hand, TRAPATT (Trapped-Plasma Avalanche-Triggered-Transit) devices offer very high peak-power capabilities, making them excellent candidates for radar system applications. In addition, recent development work by RCA has advanced the TRAPATT diode performance capabilities to a point that is very attractive to radar system designers. This paper discusses some of this recent progress in S-band TRAPATT amplifiers.

Basic TRAPATT diode-circuit interactions

When the high-efficiency (TRAPATT) mode was discovered at RCA,

it was considered to be "anomalous": the oscillation efficiencies were markedly higher than had been observed with existing IMPATT avalanche diodes, and the oscillation frequencies were lower than those predicted by the transit-time theory for an avalanche diode. The subsequent computer simulations and detailed analytic theory have established the basic physics of the operating mechanism—the existence of a high-density, slow-moving electron-hole plasma during part of the oscillation cycle.

In very simple terms, an electron-hole plasma is "turned" on and trapped in the presence of an RF signal. The operation thus drastically deviates from that of the IMPATT mode where no plasma is formed. Furthermore, one of the prerequisites for the formation of such a plasma is a substantially higher current density than that required for the IMPATT mode.

The TRAPATT-mode operation involves a complex interaction between

the device and the RF circuit. In essence, the device can be viewed as a nonlinear switch that possesses a specific I - V characteristic [$I = \text{func.}(V)$] for a given doping profile. The RF circuit is a linear network with an impedance matrix (Z). Impedance values at the various Fourier components of the signal frequency are of specific interest. The circuit can be realized either by a lumped-element circuit, or by distributed transmission lines, such as coaxial lines, microstrip, waveguides, etc. A simple schematic representation of the TRAPATT amplifier is shown in Fig. 1.

The avalanche diode has DC terminals for the bias supply. The linear network has four-terminals: two for the diode, and two for the oscillator output load or the circulator amplifier output. The model shown in Fig. 1 is a simplified representation of the actual physical mechanisms. The reader should, for example, be reminded that the switching-time function of the diode is not independent of the frequency characteristic of the network and that switching time and impedance characteristics are interrelated because the plasma is turned on by the RF signal at the circuit terminals.

In principle, the frequency of the signal delivered to the load can be at any desired Fourier component of the interaction; therefore a low-pass filter is necessary for the fundamental power output, while a band-pass filter is needed for a harmonic power extraction. Microstrip line has been an attractive medium for circuits in the frequency range of 1 to 8 GHz. Compared with other distributed circuits, like coaxial lines and waveguides, the microstrip circuit is more compact and more accessible to testing. Also, the microstrip ground plate lends itself to device heat sinking.

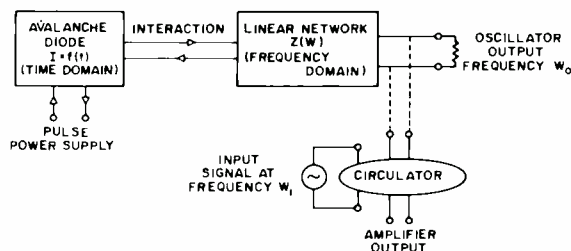


Fig. 1—Diode-circuit interaction.

Device fabrication problems increase as the desired frequency of operation is increased. Diodes operating in the fundamental mode above 3 GHz require very thin depletion layers. To ease processing problems on diodes that operate at frequencies above S-band, harmonic instead of fundamental power extraction has been considered to be more practical. The advantage lies in the fact that the high-frequency results can be achieved with relatively inexpensive low-frequency diodes and simple circuits.

Device technology

Diode design and fabrication

The approach to diode fabrication was based on theoretical guidelines¹

Reprint RE-18-5-13

Final manuscript received October 24, 1972.

The research reported in this paper was concurrently sponsored by the Army, Navy, and RCA Laboratories, Princeton, N.J.



Dr. Vitas A. Mikenas

Advanced Microwave Techniques
Missile and Surface Radar Division
Moorestown, N. J.

received the B.A.Sc. from the University of Toronto in 1962 and the M.Sc. and Ph.D. from the University of Illinois in 1964 and 1967 respectively. In 1967, he joined RCA where he has been engaged in research and development related to numerous aspects of microwave phased-array technology. In 1967 he was involved in a cooperative program with RCA Laboratories in the development and evaluation of ferrite materials for high power phase shifters. Subsequent to this program, he performed analyses of HF log-periodic dipole arrays and investigated the effect of practical ground and ground screen systems on HF antenna performance. In 1968, he undertook an IR&D program to investigate new techniques of designing low cost HF phased array antenna systems. From 1970 to the present time, he has been concerned with the development and evaluation of the microwave portion of various solid state radar systems including LITS, CAMEL, AN/TPS-59 and the S-Band Module. At the present time, he is engaged in a cooperative program with RCA Laboratories in the development of a solid state S-band module using Trapatt diode technology.

Dr. Kern K. N. Chang, Communications Research Laboratory, RCA Laboratories, Princeton, N.J. received the BS from National Central University, Chungking, China in 1940; the MSEE from the University of Michigan in 1948; and the PhD from the Polytechnic Institute of Brooklyn in 1954. From 1940 to 1945, he was associated with the Central Radio Manufacturing Works, Kuming, China, working on broadcasting and communication receivers, and from 1945 to 1947, he was a radio instructor in the Office of Strategic Services, U.S. Army, China Theatre. Since 1948, Dr. Chang has been a member of the technical staff at RCA Laboratories. In 1953 he did original work on periodic field focusing for traveling-wave tubes which has culminated in an RCA commercial line of traveling-wave tubes. In 1957 he was one of the pioneers who explored the principle of parametric amplification and conversion. In 1959 he invented a low-noise tunnel diode amplifier and converter. In 1967 he and his co-workers discovered a new high efficiency mode of operation in silicon avalanche diodes. Dr. Chang is the author of 50 original technical papers and holds 40 U.S. patents in the field of microwave tubes and solid-state devices. He is the author of *Parametric and Tunnel Diodes*. He was the recipient of 1956 and 1950 RCA Achievement Awards. He was also the 1964 achievement award winner of the Chinese Institute of Engineers, New York, Inc. In 1967 he received the David Sarnoff Outstanding Achievement Award in Science. Also, in 1967 he was appointed a Fellow of the RCA Laboratories. He is a member of Sigma Xi. He has also been selected for listing in the *American Men of Science*.

Hirohisa Kawamoto, Communications Research Laboratory, RCA Laboratories, Princeton, N.J., received the BS in Electronics from Kyoto University in 1961. He received the MS in 1966 and the PhD in 1970, both in Electrical Engineering and Computer Sciences from the University of California at Berkeley, where he held a University Scholarship and a Research Assistantship. From 1961 to 1964 and from 1966 to 1968 he worked at Matsushita Electronics Corporation, Osaka, Japan. He studied the second breakdown of p-n junctions and contributed to the development of high-frequency transistors that were resistive to a high pulsed-power dissipation. He developed several transistor circuits for television sets. In 1967, he was responsible for the entire operation of quality assurance in the Integrated Circuit Division. From 1964 to 1966 and from 1968 to 1969, he worked for the Electronics Research Laboratory at the University of California. In 1970, he was an Acting Assistant Professor at the Department of Electrical Engineering and Computer Sciences at the University of California. He joined RCA Laboratories in 1970 and has been working on high-efficiency microwave avalanche diodes. Dr. Kawamoto is a member of IEEE, Eta Kappa Nu, and Sigma Xi.

H. John Prager, Communications Research Laboratory, RCA Laboratories, Princeton, N.J., received the BSEE from the University of Vienna in 1938 and the MSEE from the University of Michigan in 1940. From 1940 to 1942, he was associated with the Research Laboratory of the Detroit Edison Company. In 1943 he joined the Electron Tube Division of RCA as a production engineer of small power and receiving tubes. In 1944 he transferred to the Receiving Tube Development Group where he worked as Design Engineer, Technical Coordinator and Unit Leader until 1959. In 1959 he became a Member of the Technical Staff at RCA Laboratories. He has since been engaged in various studies on microwave semiconductor devices, such as varactors, tunnel diodes, Hall-effect devices, solid-state optical devices and avalanche diodes. In 1960 he was co-recipient of an RCA Achievement Award for team work on research leading to the first tunnel diode amplifier and down-converter. In 1967 he was again presented with an RCA Laboratories Achievement Award for outstanding team performance "in the development of greatly improved avalanche-diode oscillators". Mr. Prager is a member of the IEEE.

Dr. James F. Reynolds, Microwave Technology Center, RCA Laboratories, Princeton, N.J. received the BEE, MEE, and PhD from Rensselaer Polytechnic Institute in 1964, 1965, and 1967, respectively. Since joining the RCA Microwave Technology Center in 1967, Dr. Reynolds has been engaged in work on silicon and GaAs active microwave devices. In 1968, he received an RCA Laboratories Achievement Award for his research on transferred electron oscillators. His recent work has been concerned with the development of TRAPATT diode sources for military and commercial systems. Dr. Reynolds is the author of 20 technical papers and holds 1 patent with 2 patents pending. He is a member of Tau Beta Pi, Eta Kappa Nu, and an associate member of Sigma Xi.

Arye Rosen, Microwave Technology Center, RCA Laboratories, Princeton, N.J., received the BSEE from Howard University in 1963, and the MScE from Johns Hopkins University in 1965. He was an instructor at Johns Hopkins during the year 1963-64, and presently is enrolled in the PhD program at Jefferson University. From 1964 to 1967, Mr. Rosen was concerned with systems design at General Telephone and Electronics International, and with antenna and circuit design at Channel Master, Inc., and American Electronic Laboratories, Inc. In 1967, Mr. Rosen joined the RCA Microwave Technology Center where he is presently engaged in the study and development of microwave circuits for solid state microwave oscillators and amplifiers. Mr. Rosen is a member of Tau Beta Pi, Sigma Xi, and the Association of Professional Engineers of British Columbia. He is the author of 15 technical papers and presentations and holds 3 patents with 2 patents pending in the microwave field.

Authors (left to right) Prager, Reynolds, Kawamoto, Chang, and Rosen.



and practical experience, which in the past has resulted in successful TRAPATT diodes. The design theory was developed for p⁺-n-n⁺ structures, but is also useful for complementary n⁺-p-p⁺ diodes; both types are being explored in current programs. Diodes for fundamental- and harmonic-power extraction are under development. Thus for the S-band radar, the fundamental-extraction diode is a 3.2-GHz diode, while for the second-harmonic extraction the diode is designed as a 1.6-GHz diode.

The first step in the design of a TRAPATT diode relates the depletion width, W , of the n-region (in the conventional p⁺-n-n⁺ structure) to the center frequency, f_c , of the operating band,

$$W = 7/f_c \quad (1)$$

For $f_c = 1.6$ GHz (a second harmonic diode), the depletion width should be approximately $5 \mu\text{m}$. The next step concerns the doping density of the n-region. For operation with high peak-power output and high duty factor the doping-density \times depletion-width product (nW) should be

$$nW = 4 \times 10^{11} \text{cm}^{-2}$$

This corresponds to a doping density of $8 \times 10^{14} \text{cm}^{-3}$ for a second harmonic diode. The design theory shows that TRAPATT diodes of the area \times impedance product (AZ_o) have an optimum value equal to 0.15 ohm-cm^{-2} ; thus for a 25-ohm characteristic impedance, the area, A is $6 \times 10^{-3} \text{cm}^2$ (875- μm diameter). Similarly for fundamental frequency operation, the depletion width, $W = 2.2 \mu\text{m}$; the doping density, $n = 1.8 \times 10^{16} \text{cm}^{-3}$; and for an optimized $AZ_o = 1.2 \times 10^{-2} \text{ ohm-cm}^2$, the area, A is $5 \times 10^{-4} \text{cm}^2$ (250 μm diameter).

Diodes were fabricated following the above-outlined design and fabrication guidelines. The wafers were prepared with a borosilicate glass deposition, followed by a diffusion. Both the in-diffusion depth from the surface and the out-diffusion from the substrate must be considered in determining the required overall thickness of the depletion layer. It has been demonstrated in the past that in order to consistently fabricate reliable large-area TRAPATT diodes, it is important to have a certain amount of out-diffusion from the substrate, thus

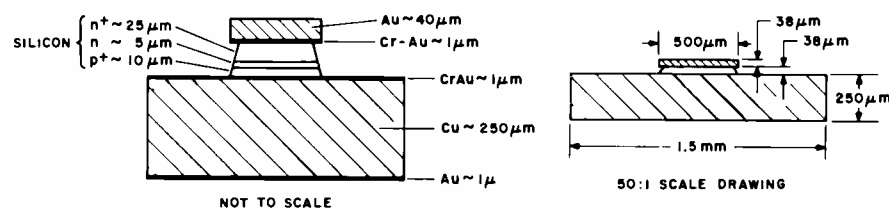


Fig. 2—Diode configuration.

eliminating a possible failure mechanism associated with an abrupt epitaxial-substrate interface. In the p⁺-n-n⁺ diodes, the required amount of out-diffusion from the n⁺ to the n-region necessitates an accompanying deep diffusion from the p⁺ into the n-region. This is required because the available substrate (n⁺) material is either antimony- or arsenic-doped, and therefore has a diffusion coefficient about two orders of magnitude lower than that of boron, the dopant of the p⁺ layer. For these reasons, epitaxial layers were chosen to be of substantial thickness, *i.e.*, 20 to 30 μm , thus allowing 15 to 20 μm for the required in-diffusion depth of the junction. Diodes made according to this procedure have given reliable operation and high peak-power output at moderate duty factors and pulse widths. At high duty factors or long pulse widths, the thickness of the in-diffused region and its contribution to the thermal resistance becomes increasingly critical.

Complementary diodes

Although most of the silicon avalanche diodes (both TRAPATTs and IMPATTs) have been made of p⁺-n-n⁺ structures, there has recently been a great deal of interest in the complementary n⁺-p-p⁺ structures. The complementary structure attracted this interest because several studies had indicated that better efficiencies for IMPATT diodes could be expected from this structure. The reasons for turning toward the complementary structure were dictated not only by the expectation of better efficiencies and lower threshold current, but also by the promise of better thermal dissipation, which is one of the goals of our research.

The improved thermal dissipation is feasible with the complementary diodes since it is possible to use thinner in-diffused junctions, and therefore the heat sink can be placed

closer to the junction. To accomplish this with the complementary n⁺-p-p⁺ structures, boron was chosen as the dopant for the substrate (p⁺), while the junction is formed by diffusion of phosphor (n⁺) into the epitaxial p-layer. Because the boron and the phosphor have nearly identical diffusion coefficients, the device has a nearly symmetrical diffusion profile; that is, the out-diffusion depth (from p⁺ into p) is the same as the in-diffusion depth (from n⁺ into p). This feature allows one to fabricate reproducible high-power large-size TRAPATT diodes with a much thinner diffused junction depth.

The proper choice of doping density and thickness of the active region in the complementary TRAPATT diodes can be designed following the same guideline described for the conventional TRAPATT diodes. Starting with an epitaxial layer of only 9 μm , and diffusing to a junction depth of only 3 μm , an almost symmetrical doping structure results. The out-diffusion is sufficient to give reliable and reproducible operation, free from microplasmas and premature failures, while the in-diffusion is of a very shallow type consistent with the design goal of improved thermal resistance.

Integrated heat sink

In addition to developing these basic diode fabrication techniques, we are developing a technology of heat sinking that will help us toward the design goals of long-pulse and high-duty-cycle operation. The heat sinking of TRAPATT diodes is especially important since the generation of high-power microwave output depends on the adequate dissipation of the heat generated at the p⁺-n junction. A generally applied technique for heat dissipation consists of "flip-chip" bonding, in which the p⁺ surface is brought in contact with the heat sink through thermal compres-

sion. While this technique is effective for very small diode diameters, it becomes quite poor for the large diodes with which we are dealing. The reason is found in the inadequacy of surface finishes over a large area, and the incomplete thermal contact resulting from it. Therefore, we have chosen to use an integral copper heat spreader that is achieved by either electroplating a heavy copper layer or diffusion-welding a heavy copper disk² to the p⁺ side of the metallized wafer.

The procedure for electroforming is as follows:

- 1) After the wafer has been diffused, a chromium-gold film is evaporated on the p⁺ surface. Chromium is used primarily for adherence between the silicon and gold. The chromium layer has a thickness of a few hundred Angstroms thick.
- 2) A layer of copper is then electroplated on the gold surface. The structure and appearance of the copper layer are carefully watched to obtain a dense and clean deposit. Usually 150- μ m-thick copper can be plated. A thin layer of gold is applied for further protection.
- 3) The silicon wafer, which was about 200 to 250 μ m thick at the start, is now thinned (from the n⁺ side) by lapping and chemical etching to approximately 25 to 40 μ m thickness.
- 4) A chromium-gold film is then evaporated on the n⁺ surface, with the same thicknesses as before on the p⁺ side.
- 5) Photoresist is applied to this back contact, and 500- μ m diameter holes are opened in it.
- 6) A heavy gold layer is electroplated through these holes into the gold contact of the n⁺ surface.
- 7) The photoresist is removed and mesas are etched (using the heavy gold layer

as masks for the silicon etch). The resultant mesas are shown in Fig. 2.

- 8) Photoresist is applied to the copper-plated surface, and a grid-raster 1.5 \times 1.5 mm (with 125 μ m line thickness) is obtained in concentric alignment with the 500- μ m mesas (of the silicon side).

- 9) The copper is etched along the grid lines, and hence the individual chips are separated from each other. The completed diode chip is shown in Fig. 2.

In addition to producing good thermal contact, this procedure offers proper shaping of the electric field profile at the surface of the mesa. Secondly, the heavy copper layer supports the silicon mesa and allows handling of the chips, even after they have been thinned down to about 25 μ m. This becomes especially important in the case of certain geometrical structures such as multiple stripes, rings, and dots (described later).

Specially shaped structures

One method to increase the diode's input-power capability is to reduce the thermal resistance by using special structures other than the disk shape. Investigation of special multiple-stripe and ring structures has been done in a past program. In extending the idea of the stripe structure, we now plan to use a long single-stripe, 0.13 \times 2.3 mm (5 \times 90 mils) in shape. The advantages in using the long-stripe structure are as follows:

- 1) The thermal resistance is reduced;
- 2) The long-stripe diode geometrically matches the microstrip line better than other shaped diodes, (Fig. 3); and
- 3) parasitic inductances due to connecting wires are reduced.

The thermal resistance of the stripe is given by:

$$\theta_{in} = (\gamma KWL)^{-1} [W \sinh^{-1}(L/W) + L \sinh^{-1}(W/L)]$$

where γ is a constant determined by the shape of the heat sink, K the thermal conductivity, W the width of the stripe, and L the length of the stripe. For a stripe of 127 \times 2285 μ m, for instance, the thermal resistance, $\theta_{in} = 2.2^\circ\text{C}/\text{W}$. The maximum input power is 102 W for a junction temperature of 250°C and 25°C ambient temperature, which is just equal to the power required from our specification, and therefore one striped structure should be sufficient to handle the required average power.

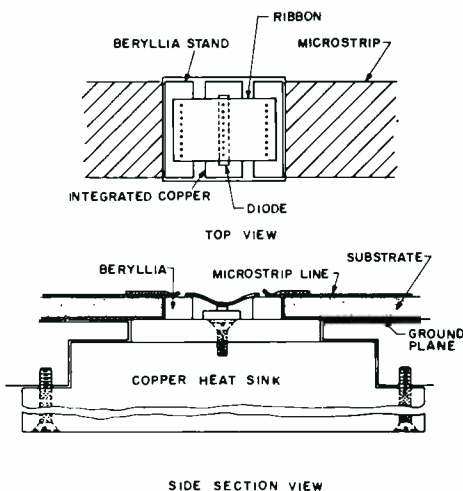


Fig. 3—Top and side views of a long striped diode mounted with a copper heat sink in a microstrip line circuit.

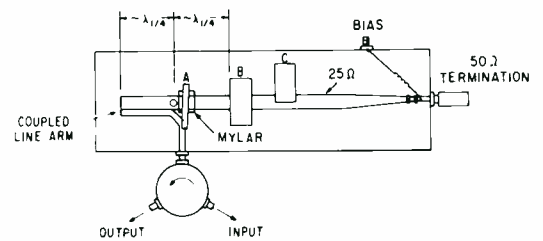


Fig. 4a—Duroid-substrate microstrip-circuit amplifier.

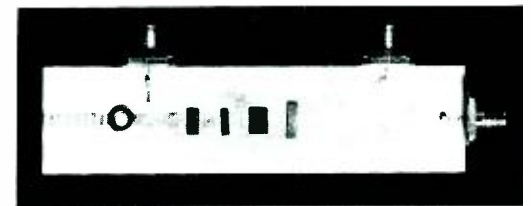


Fig. 4b—Alumina-substrate microstrip-circuit amplifier.

Circuit development

Two types of microstrip circuits for fundamental and second-harmonic power extraction, namely the singly-coupled and the multiple-coupled circuits, have been used experimentally in this program. The coupled circuit has proven itself an excellent wide-band amplifier circuit. Both circuits are usually operated in a class-A mode, *i.e.*, the diode is biased at a nominal operating current level. Recently, class-C mode, which biases the diode at very low currents, has also been successfully demonstrated.

Singly-coupled microstrip circuit

1) Duroid Substrate

Fig. 4a shows a new circuit developed for 3-GHz operation. The diode is placed in the middle of the transmission line. One end of the transmission line is open-circuited and the other end is terminated by a 50-ohm load. The distance between the diode and the open end is 2.7 cm. The input-output line makes a 90° angle with the main line, and the end of the input-output line forms a coupled transmission line with the open end of the main line. A narrow bar, A, bridges the output line and the main line. The tuning plates, B and C, comprise a reflection plane for all frequencies.

The circuit was tested with a variety of diodes. Representative results are:

- $I_{in} = 4 \text{ A}$
- $V_{in} = 80 \text{ V}$
- $P_{out} = 50 \text{ W}$
- Efficiency = 16%
- Frequency = 3.3 GHz (fundamental mode)
- Bandwidth = 330 MHz (10% at 3dB)
- Gain = 10 dB
- Pulse width = 5 μ s
- Duty cycle = 1%

Fig. 5 shows the frequency spectrum of the power output. Waveforms of a

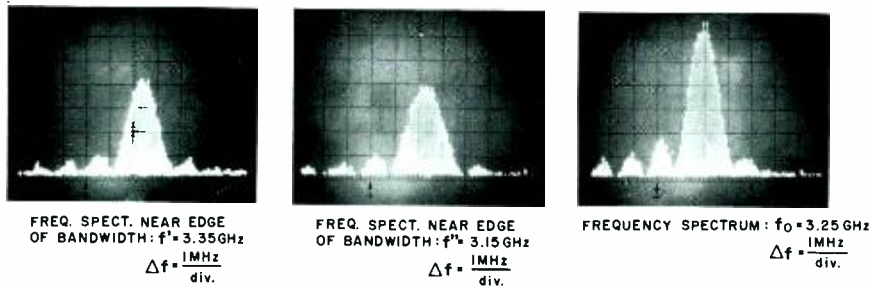


Fig. 5—Frequency spectrum of the RF output from the second-harmonic amplifier.

similar amplifier operating with a second-harmonic extraction were measured with a 12-GHz sampling oscilloscope. The bottom picture of Fig. 6 shows the waveform measured at the output terminal. This output waveform is sinusoidal and has a repetition period of 320 ps corresponding to the output frequency of 3.15 GHz. The top picture of Fig. 6 shows the waveform at the diode as measured through a 1000-ohm microwave resistor connected to the diode. The diode waveform is similar to those generally observed in actual and computer-simulated performances of high-efficiency avalanche diodes: an over-voltage followed by a voltage drop representing the sequence leading to the trapped-plasma state. Note, however, that the repetition period of the trapped-plasma occurrence is twice as long as the repetition period of the output signal. This indicates that both the input and output signal are second harmonics of the trapped-plasma occurrence.

2) Alumina substrate

Compared with the organic duroid, alumina is an inorganic material and has a higher dielectric constant ($\epsilon = 10$). Therefore, microstrip circuits

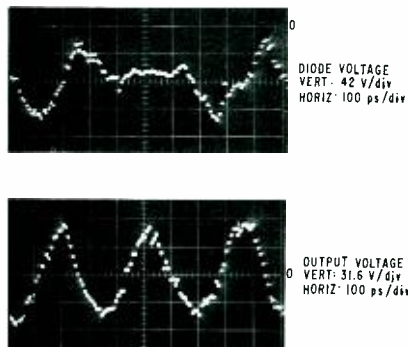


Fig. 6—RF voltage waveform at the diode (top) and the output terminal (bottom) of the second-harmonic amplifier circuit.

made of alumina substrate are small in size. A standard S-band reflection-type circuit shown in Fig. 4b, for example, has an overall dimension $1 \times 5 \times \frac{1}{4}$ in. This circuit has been used to evaluate most diode samples in the fundamental mode as both oscillators and amplifiers. To the left of the diode is an open-circuited section of transmission line which determines the frequency of operation. The tuning elements to the right of and around the diode are used to impedance match the diode at the fundamental frequency and to reflect the harmonics in the correct phase. An external three-port circulator is used to provide the duplexing function for the input and output ports. Typical results achieved with this circuit include oscillator performance in which 84 W were generated at 2.91 GHz with an efficiency of 35%. Some typical amplifier results obtained with this circuit are shown below:

$$\begin{aligned}
 P_{out} &= 133 \text{ W} \\
 \text{Freq.} &= 3.2 \text{ GHz} \\
 V &= 65 \text{ V} \\
 I &= 10 \text{ A} \\
 \text{Efficiency} &= 20.5\% \\
 \text{Gain} &= 8.7 \text{ dB} \\
 \text{Bandwidth} &= 1.2\%
 \end{aligned}$$

The relatively narrow bandwidth results shown above prompted an investigation of diode-circuit requirements at the fundamental as well as at the second, third, and fourth harmonic frequencies. This investigation resulted in an improved circuit design in the form of a coupled bar circuit which increased the operating bandwidth to almost 4%. Further computer-aided design techniques resulted in a circuit consisting of a two-section low-pass filter on a 10-mil alumina substrate. This circuit resulted in a 9.5% operating bandwidth but at a slightly reduced power output level of 50 W.

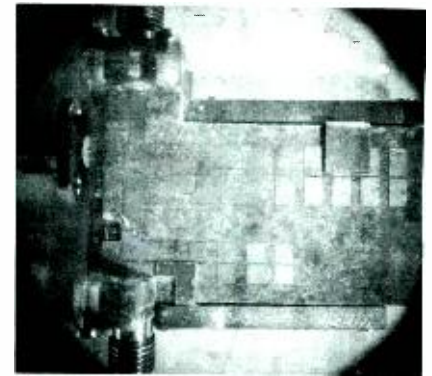


Fig. 7—Photograph of coupled-line circuit.

Microstrip-coupled-line circuit

Another circuit configuration that has been used to achieve broadband amplification is the second-harmonic coupled-line circuit shown in Fig. 7. It consists basically of two coupled lines whose length and spacing can be varied to achieve a given impedance transformation and operating frequency. The larger pair of lines introduces a high reactive impedance at the trapped-plasma (fundamental) frequency, thus trapping the fundamental component. The smaller pair provides tuning and matches the device to the output load at the second-harmonic frequency.

By use of this circuit, S-band amplifiers have been developed that provide a 3-dB bandwidth of 15% with maximum gain of 4.2 dB, and 3-dB bandwidth of 10% with maximum

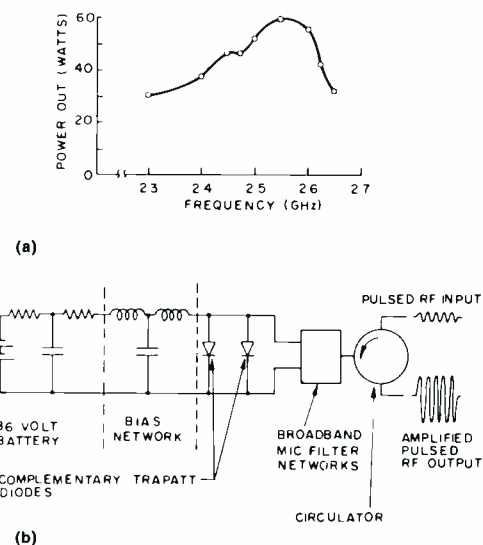


Fig. 8—(a) Power output vs. frequency characteristic of a wideband class-C amplifier and (b) a diagram of the setup for the class-C amplifier.

gain of 6 dB with output power in the order of 50 W.

Class-C operation

The modulator for TRAPATT amplifiers is usually provided by switching the DC bias *on* and *off* with the desired pulse width and duty cycle. In a practical system, this would mean using a transistor-driven pulse modulator. Such an approach has a number of disadvantages: it is complex, expensive, and bulky; the modulator can be almost as large and expensive as the basic amplifier. For this reason, class-C operation of TRAPATT amplifiers is highly desirable. In class-C operation, the TRAPATT diodes are DC biased below breakdown, so that only negligible DC current, mainly leakage current in the order of $10 \mu\text{A}$ is drawn by the diode when there is no RF input to the amplifier. When RF is applied to the amplifier, the diodes are driven into the trapped-plasma state, large DC currents are drawn from the power supply, and the RF input signal is amplified. As soon as the RF drive is removed, the amplifier is automatically shut off again.

The feasibility of wide-band TRAPATT amplifiers operating under class-C conditions has been demonstrated.

A diagram of the setup for a class-C amplifier is shown in Fig. 8b. Typical amplifier results are shown in Fig. 8a. A 3-dB bandwidth of 14.2%, maximum gain of 6.5 dB, and 60 W maximum output have been obtained in a microstrip-coupled-line circuit.

Phase measurements on TRAPATT amplifiers

Phase characteristics, and phase and gain tracking characteristics, are important in phased-array radar applications. To perform the phase measurements, it was necessary to set up a special test station suitable for pulsed measurements of the TRAPATT device. The method used to make the measurements is a straight forward phase bridge that makes use of the precision line stretcher in the standard Hewlett-Packard reflectometer head.

Fig. 9 is a plot of the gain and relative phase characteristics as a function

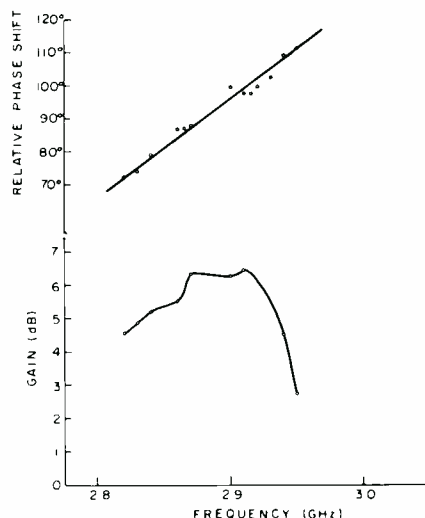


Fig. 9—Relative phase and gain characteristics of TRAPATT amplifier as a function of frequency. Power output is 62 watts.

tion of frequency for a microstrip-coupled-line amplifier. The amplifier circuit used in the measurement is the microstrip-coupled-line circuit. The amplifier was delivering 62 W with a 4% bandwidth. As can be seen, the phase shift deviates from linear by $+3.5^\circ$ and -2.5° .

Fig. 10 shows phase and gain tracking measurements on two separate amplifiers. These amplifiers incorporated three coupling bars in each resonator instead of the usual two in order to obtain increased bandwidth.

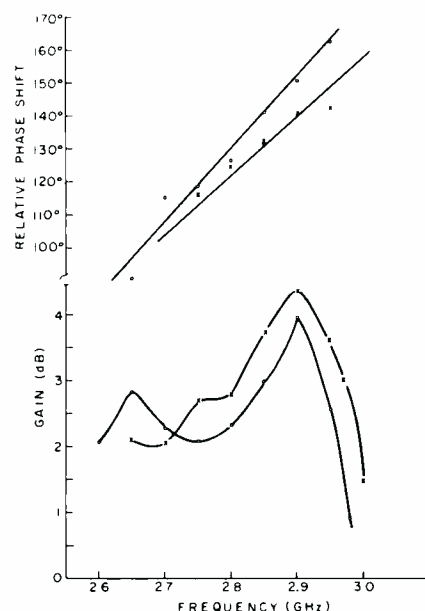


Fig. 10—Relative phase and gain characteristics of two TRAPATT amplifiers.

Table I—Maximum individual characteristics for S-band amplifier.

Characteristics	Individually
Frequency	3.3 GHz
Bandwidth	14.6% (-3 dB)
Output peak power	150 W
Duty Cycle	15.6%
Pulse width	$40 \mu\text{s}$
Gain	18 dB
Efficiency	19.3%
Phase linearity	$+3.5^\circ, -2.5^\circ$
Unit-to-unit gain variation	1 dB
Unit-to-unit phase variation	18°

Table II—Overall performance of an S-band Amplifier—characteristics achieved simultaneously in an amplifier.

Characteristics	Overall
Frequency	3.3 GHz
Bandwidth	10% (-3 dB)
Output peak power	50 W
Duty Cycle	5.6%
Pulse width	$10 \mu\text{s}$
Gain	10 dB
Efficiency	16%

The gain between the two amplifiers varies less than 1 dB and the phase, less than 20° over a 12% bandwidth.

Summary of achievements

The present status of the S-band TRAPATT program is summarized in Tables I and II. Table I summarizes the maximum performance for each characteristic individually, without regard to other characteristics. Table II is an overall performance summary and shows characteristics that have been achieved simultaneously.

Future work on the program will be aimed at achieving higher power, gain, pulse width, and efficiency.

Reference

1. Clorfeine, A. S.; Ikola, R. J.; and Napoli, L. S.; "A Theory for the High-Efficiency Mode of Oscillation in Avalanche Diodes," *RCA Review*, Vol. 30 (Sept 1969) 397-421.
2. Assour, J. M.; Murr, J., Jr.; and Tarangoli; "On the Fabrication of High-Efficiency Silicon Avalanche Diodes," *RCA Review*, Vol. 31 (1970) p. 499.
3. Rosen, A.; Reynolds, J. F.; Liu, S. G.; and Theriault, G. E.; "Wideband class-C TRAPATT Amplifiers," *RCA Review*, Vol. 33 (1972) p. 729.

Acknowledgment

The authors acknowledge the technical assistance of E. L. Allen, V. Lawson, L. Semenistow, and S. Weisbrod.

High power latching ferrite phase shifters for AEGIS

L. J. Lavedan, Jr.

As part of the AEGIS AN/SPY-1 radar, a high power, ultra-precision phase shifter was designed and later produced in quantity. The design, as produced, is a complete entity and includes microwave and electronic hardware as an integrated package. To attain the required performance, it was necessary to combine microwave, electronics, thermal, and materials disciplines in a manner that would optimize production yield. Adequacy of the design is evidenced by a study of production data which indicates that the phase shifters produced equal or better all initial design criteria, with a yield approaching 100%.

THE THEORY of latching-phase-shifter operation has been discussed in detail in the literature.^{1,2,3,4} For high power operation, this basic design information must be expanded to include the effects of arc-over, limiting, and internally-generated (due to RF losses) thermal variations and gradients.

This paper describes these high power effects and the necessary design concepts for obtaining a practical high power phase shifter. In addition, a design example of a high power phase shifter used on the AN/SPY-1 phased array radar is included along with a summary of production data evaluation.

Design consideration

Typically, a waveguide latching "ferrite" phase shifter for use at low to moderate powers consists of a microwave magnetic material with toroidal geometry (to assure remanent properties) centrally located within a waveguide structure (see Fig. 1). A dielectric material may be used internally to the toroid to enhance RF field concen-

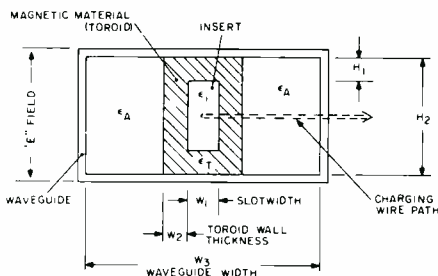


Fig. 1—Typical cross-section of a latching ferrite phase shifter.

tration within the magnetic material and a wire, oriented for minimum RF coupling is threaded through the toroid such that the magnetization of the toroid can be modified by external means.

From suitable theoretical design equations and with the aid of computer

Louis J. Lavedan, Jr.

Radiation Equipment Engineering
Missile and Surface Radar Division
Moorestown, New Jersey
received the BS in Physics from Loyola University of the South in 1954 and the MS in Physics from Louisiana State University in 1956. From 1956 to 1962, Mr. Lavedan was a member of the microwave component development activity at RCA Moorestown, specializing in high power effects and duplexer design for BMEWS and TRADEX radars. In 1962, he joined the Sperry Rand Corporation, Clearwater, Florida, where he began specialization in the field of microwave ferrite phase shifters. In 1970, he returned to RCA and continued work in the specialized field of microwave phase shifter design and production assistance on the AEGIS AN/SPY-1 development program. He is currently engaged in continuing AEGIS Program work as well as related efforts on other microwave component design programs.

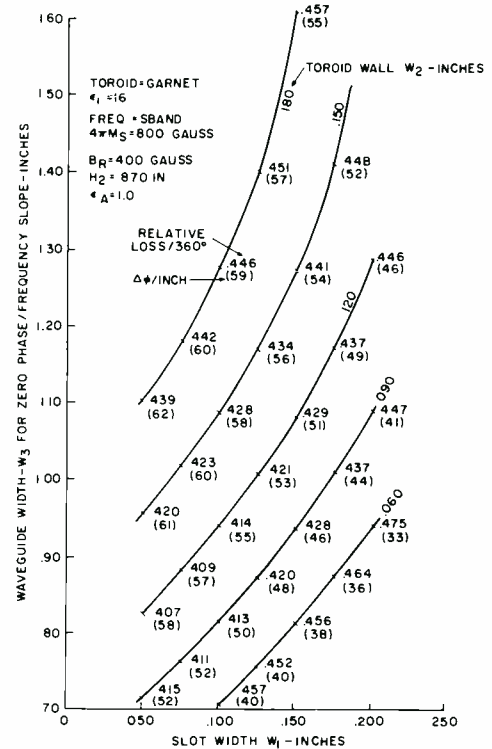
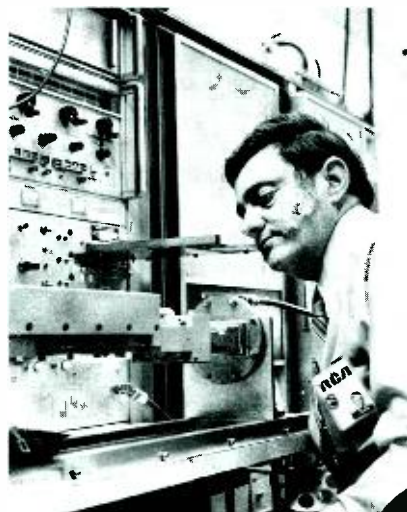


Fig. 2—Phase shifter design curves.

programs, the typically specified device parameters of differential phase per linear inch of material, insertion phase length for the demagnetized toroid state, relative insertion loss, frequency response, and RF fields within the microwave material can be generated as a function of mechanical dimensions and magnetic and dielectric properties.

Such a resulting computer-produced design curve is given in Fig. 2. Using these curves for a fixed set of magnetic and dielectric properties, performance characteristics are modified as a function of dimensional parameters.

All such theories necessarily assume that all properties, especially microwave material properties as entered into the equations are realizable; in practice, this is not possible. Within the bounds of practical design, typical limitations include:

- 1) The loss properties of magnetic and dielectric microwave materials cannot be made vanishingly small.
- 2) Physical fit between dielectric insert, toroid, and waveguide cannot be made perfect.
- 3) Magnetic properties of the material employed are temperature sensitive.
- 4) The charging wire has physical dimensions and will influence RF response.
- 5) End use usually places restrictions on overall device physical characteristics of weight, length, height and width.

High peak-power effects

At high peak powers, it is necessary to consider two potential failure mechanisms: arc-over (which is usually catastrophic) resulting from excessive E field stress and limiting (which is a magnetic material phenomenon) resulting in increased losses over those encountered at low power and in itself is reversible.

Arc-over

The first of these effects is primarily a physical assembly problem, the magnetic and dielectric materials themselves (all ceramic) possessing sufficient breakdown characteristics to withstand the fields encountered. Referring to Fig. 1, ionization of air within the microwave structure is the primary source of arc-over with a permanent deterioration resulting from the generation of carbon paths. Air in a region of high electrical stress can occur at the boundaries between toroid and waveguide wall, and toroid and dielectric insert. Voltage gradients across the air gaps can become excessive due to the high dielectric constant materials (toroid and insert) normally employed. Thus, to minimize breakdown, air gaps are filled with a suitable potting material. This technique has been successfully employed and has resulted in increases in arc-over power levels of 2 to 5 times the value without potting.

Limiting

Limiting is a magnetic material phenomenon related to frequency, RF field strength, saturation magnetization of the material, and spin wave line width of the material by the following equation:

$$P_{LIM} = (H_{CRIT}/h)^2 \quad (1)$$

where h is the field strength per watt of RF power within the magnetic material, and P_{LIM} is the peak limiting power. H_{CRIT} is the minimum field strength for limiting, expressed by

$$H_{CRIT} = A(\Delta H_K/m_s) \quad (2)$$

where ΔH_K is the spin-wave line width; A is a variable inversely proportional to m_s (for $m_s > 0.5$, $A \approx 1$ and for

$$m_s = \gamma(4\pi M_s)/f \quad (3)$$

with γ as the gyromagnetic ratio (2.8); $4\pi M_s$ representing the magnetic saturation magnetization; and f representing the frequency (in GHz).

Fig. 3 is a plot of H_{CRIT} as a function of m_s for various realizable values of ΔH_K based upon experimental results. For typical cross sections, $h \approx 0.03f$ Oersteds. Therefore, for any given physical geometry and frequency of operation, all values of ΔH_K and m_s which produce P_{LIM} greater than that required by operating specifications are acceptable. This is definitely constrained by:

- 1) Overall device loss increases with ΔH_K ,
- 2) Overall device length increases with $1/m_s$, and
- 3) The number of proven material choices available is severely limited.

High average-power effects

Fig. 4 includes typical response curves for microwave ferrite and garnet materials as functions of temperature. [The word *ferrite* as used here applies to the family of materials which includes compositions of magnesium-manganese, nickel, and lithium; whereas *ferrite*, as used in the title of this article, applies to industry terminology wherein devices employing any microwave magnetic materials are misnamed ferrite devices.] Since these material parameters indicate varying degrees of temperature sensitivity, the device em-

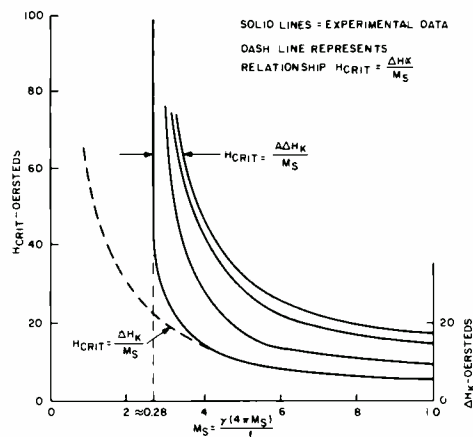


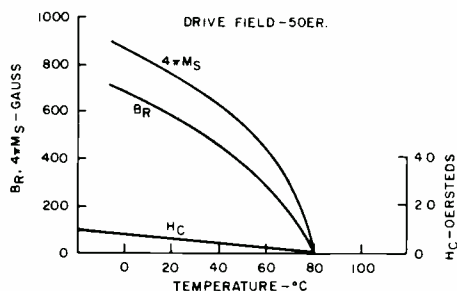
Fig. 3— H_{crit} vs. M_s for various ΔH_K .

ploying these materials will also show a similar sensitivity.

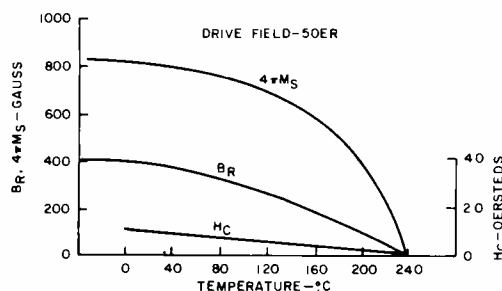
The RF losses appear as heat generated within the toroid and the insert used in the phase shifter. Because of the typical configuration employed and the poor thermal conductivity of these materials (ceramics), these RF losses can result in large temperature rises and gradients within the toroid structure.

In addition to the variations shown in Fig. 4, one must include magnetostrictive effects wherein a stress within the magnetic material from any cause will appear as a change in magnetic properties. Gradients in temperature create such stresses which therefore influence operational device properties. The RF magnetic materials in the garnet family possess such magnetostrictive properties unless specially doped with impurities, whereas the ferrite family is typically lacking in such variations.

It is theoretically possible to attain adequate high average power performance by proper doping of the material. For practical designs, however,



a) Magnesium-manganese ferrite.



b) Gadolinium-aluminum-doped yttrium iron garnet.

Fig. 4—Typical response curves for ferrite and garnet vs. temperature.

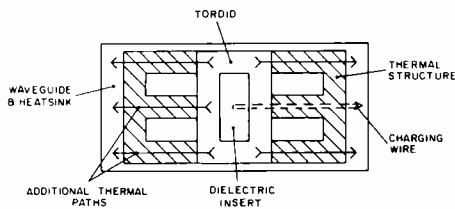


Fig. 5—Modified cross-section of latching ferrite phase shifter for high average power.

electrical and physical constraints along with material availability are imposed, and it is necessary to devise other methods to directly control temperature rise, and therefore gradients, rather than relying on material performance over temperature. Specifically, auxiliary thermal paths from the toroid structure must be designed. Fig. 5 shows a cross section with such a path added.

It is of importance to consider the properties of this added thermal path:

- 1) It is located within the waveguide in the RF field;
- 2) It must not only reduce overall temperature rise but must reduce gradients;
- 3) While accomplishing its prime task of temperature stabilization, it must create a minimum perturbation to the RF properties.
- 4) It must be a non-conductor with minimum dielectric constant.

Two such materials are available: boron nitride and beryllium oxide. Although boron nitride possesses a lower thermal conductivity, it is easily machinable, non-toxic, and has a lower dielectric constant; therefore, it is used extensively throughout the industry to

improve thermal efficiency of RF devices.

Fig. 6 shows a plot of anticipated temperature superimposed upon the cross-section of Fig. 5 for the condition of approximately 3 W RF dissipation per inch within the toroid material. If the boron nitride structure was removed, there would be a notable increase in temperature near the center of the toroid. Since both thermal transfer materials referenced above possess dielectric constants other than 1, curves similar to Fig. 2, with suitable loading factors, can be generated. The introduction of such loading results in a change in waveguide width and a reduction in differential phase of less than 10% when properly designed for minimum RF interaction.

Design verification

Based upon design criteria outlined above, a high power phase shifter was developed for operation in the transmit signal path of the AN/SPY-1 phased array radar. This array, using subarray steering, requires the use of phase shift elements in transmit and receive signal paths to permit adjustment between subarrays.

Instantaneously a phase shifter can have only one value of electrical length for each direction of RF propagation. (For non-reciprocal devices, the values are not equal for the two propagation directions.) In any array employing multiple phase-shift elements, it is the instantaneous difference in path lengths between elements that is of prime importance. To obtain this information directly at test would not

be feasible; therefore, a set of practical test definitions has been devised.

Insertion phase

Each phase shifter is switched into a predetermined magnetic state at test and the resultant phase length is compared to an arbitrary reference, usually the mean of all phase shifters. Deviations of all units about the mean are converted into a standard deviation for the array. In addition to the array standard deviation, any one unit is usually specified as to maximum error allowable from the reference, assuring minimum drift in the mean over production.

Differential phase

Each phase shifter is switched through a series of predetermined magnetic or phase states, and the insertion phase length of each phase state is compared to the reference state: thus, a difference or differential phase. Again these differential phase values are compared to the ideal response and errors in terms of RMS deviation can be noted.

Because of the random nature of these errors, the array RMS error is the sum of insertion and differential phase errors. Note that only the error from the mean is important for insertion phase whereas the absolute error from the ideal is important for differential phase.

Phase shifter tolerances

Each transmit phase shifter must produce the desired phase shift with a maximum differential phase error of 4.5° RMS and a maximum insertion phase error of 4.0° RMS over all operating conditions of temperature and power.

To meet the close phase tolerances specified, the unit was designed for water cooling with a water temperature variation of 80°F to 105°F and a maximum instantaneous water temperature gradient of 5°F and with the electronic driver as an integral part of the device.

It was determined that instantaneous power levels could vary from half to full power, which corresponds to RF average input powers of 60 to 120 W.

A study of internal losses and thermal transfer characteristics yielded a possible toroid temperature of 80°F to 120°F with a maximum unit to unit

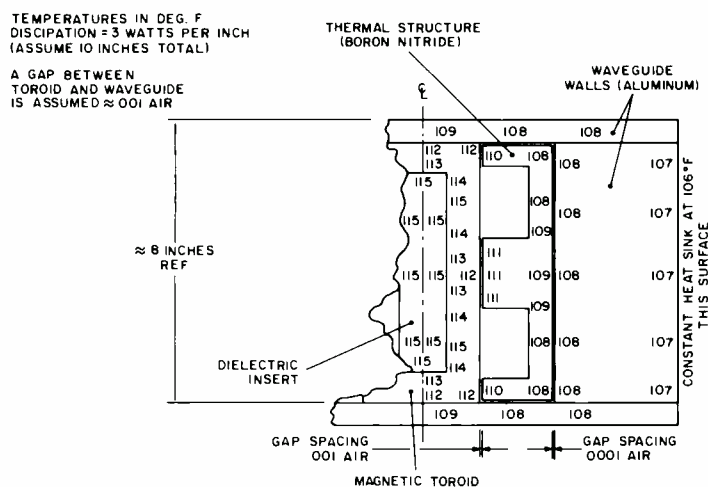


Fig. 6—Cross-section of high power phase shifter with temperature profile.

temperature gradient of 12.5°F (5° due to water, 7.5° due to power). Worst-case peak power was 15 kW.

From Eq. 1, assuming the conditions $m_s \geq 0.5$ and $h \approx 0.1$ Oe.

$$P_{LIM} = 15 \times 10^3 = (H_{CRIT}/0.1)^2 \quad (4)$$

Thus,

$$H_{CRIT} = 12.25 \text{ Oe.}$$

and, from Eqs. 2 and 3,

$$\Delta H_K / (4\pi M_s) = 1.11 \times 10^{-2} \quad (5)$$

Referring to Fig. 3, any value $H_{CRIT} \geq 12.25$ Oe will yield the desired limiting threshold. It is, however, necessary to choose values of ΔH_K and $4\pi M_s$ which yield a unit of reasonable physical length.

Because of physical length limitations, the maximum allowable toroid length was 10 in. A minimum value of $B_H = 550$ gauss was required to attain the desired phase shift in this 10-in. length throughout the range of temperatures and practical drive conditions, while limiting the insert dielectric constant to a maximum of 16 (h increases as dielectric constant, requiring higher values of H_{CRIT}).

To attain this minimum value of B_H , it was necessary to select a value of $4\pi M_s$ of 800 gauss or greater, and from Eq. 5, $\Delta H_K \geq 8.9$ oersteds is required.

The requirements of high spin-wave line width (ΔH_K) and temperature stability point directly to the use of garnet rather than ferrite as the magnetic medium for the device.

The material finally chosen had the properties:

$$\begin{aligned} 4\pi H_s &= 800 \text{ gauss} \\ B_H &= 560 \text{ gauss for drive} = 4H_s \\ H_c &\approx 0.8 \text{ Oe} \end{aligned}$$

and is a garnet of the YIG (yttrium iron garnet) family doped with gadolinium—for temperature stability; aluminum—for $4\pi M_s$ adjustment; homium—for adjustment of ΔH_K ; and manganese—for reduction in magnetostrictive effects.

The cross section chosen was based on the data presented in Fig. 2 where:

Slot width was held to a maximum, consistent with good design practices for minimum overall waveguide width to minimize thermal paths;

Wall thickness was also minimized to reduce thermal paths; and

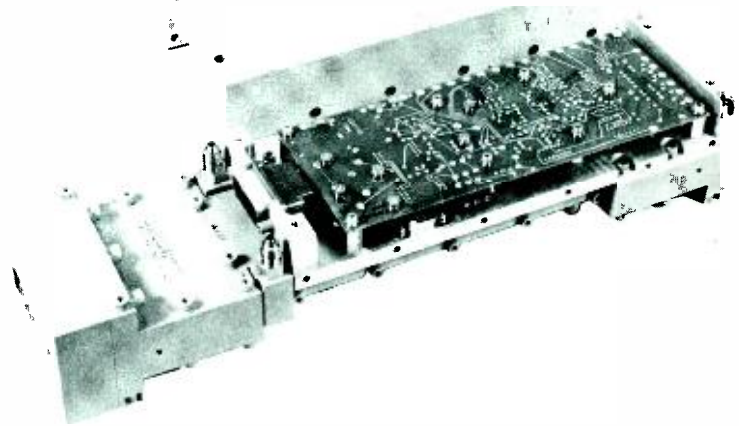


Fig. 7—Transmit high power phase shifter for AN/SPY-1 radar.

Waveguide height (0.800 in.) was chosen as a compromise between limiting threshold (which is directly proportional to height) and proper suppression of unwanted modes within the structure.

The production result was the phase shifter shown in Fig. 7. Thirty-three such units were produced for the array (32 for system plus one qualification unit) with the following results:

Parameter	Specification	Response
Peak vsWR	1.25	1.103
Avg. insertion loss (dB)	1.20	0.79
Peak insertion loss (dB)	1.50	1.009
Differential phase error* (RMS—degrees)	3.0	2.033
Standard deviation of insertion phase* (degrees)	2.0	0.7
Total differential phase error (RMS—degrees)	4.5	3.20
Total standard deviation of insertion phase (degrees)	4.0	2.26

*These values were measured on each unit at nine frequencies and 32 bits (phase states) at room temperature translated to a base-line temperature of 100°F.

The total values of phase error are based upon experimental results over power (peak and average) and temperature assuming a maximum instantaneous unit-to-unit temperature gradient of 12.5°F anywhere in the operating temperature range.

The unit was evaluated for limiting (design specification of 15 kW) and was found to exceed 20 kW. This margin of safety is considered necessary because of the normal tolerances of $4\pi M_s$ associated with material manufacture.

Each unit was internally (between toroid and dielectric insert) filled with a silicone gel to minimize voids. With such filling of voids, the unit was subjected to formal testing of 40 kW peak power in the presence of a radioactive source for two hours (equivalent to several hundred hours of life test) with no arc-over or damage. The unit was also informally subjected to powers in excess of 80 kW peak. The anticipated arc-over level is in excess of 150 kW peak.

Summary

A high power phase shifter was designed with constraints imposed on maximum length and cross section. This design was placed in production and subjected to extensive evaluation. The results of test indicate that all parameters were sufficiently below specification levels that the unit can be produced with an expected yield approaching 100%.

References

- Ince, W. J. and Stern, E., "Nonreciprocal Remanence Phase Shifters in Rectangular Waveguide", *IEEE Transactions on Microwave Theory and Techniques*, Vol. MTT-15, No. 2 (Feb. 1967) pp. 95-97.
- Landry, N. R., "Microwave Phase Shifters", RCA reprint booklet, *Microwave Technology*, PE-452; *RCA Engineer*, Reprint RE-15-3-5, (Oct./Nov. 1969) pp. 20-25.
- Goodrich, H. C. and Tonisie, R. J., "Flux Feedback Boosts Accuracy of Phased Array Radar Systems", *Electronics*, Vol. 43, No. 24, (Nov. 23, 1970) pp. 77-80.
- Hodges, L. R. and Harrison, G. R., "Temperature Stability in Yttrium-Gadolinium-Aluminum-Iron Garnets", *J. of the Amer. Ceramic Soc.*, Vol. 48, No. 10 (Oct. 1965).

High-frequency high-power multi-octave distributed-amplifier-transmitter

D. L. Pruitt

A multimewatt distributed-amplifier transmitting system for use in a VHF radar system was designed and constructed by the Missile and Surface Radar Division in the late 1960's. This transmitting system occupies 18,000 square feet of floor space and employs 72 power tetrode tubes. The system—believed to be the world's highest-power distributed-amplifier transmitter—is now operational. This paper describes the basic transmitter configuration, including the high-power amplifier chains, the protection of power tubes from arcing, the high-voltage power supply system, the intermediate-power driver amplifiers, and the transmitter cooling system.

DISTRIBUTED-AMPLIFIER techniques have been used for years. At first, in 1936,¹ they were used in "low-power video" amplifiers.^{2,3} Distributed amplifiers were developed in later years for high-power applications, such as ionospheric sounding and ECM in the VHF and low-UHF ranges.⁴

Since the mid-50's, the prospect of VHF radar systems has been an intriguing one, but one that required new approaches to power amplification. Broadband transmitter systems were most desirable, with goals of 2½-to-3-octave instantaneous bandwidths, set for operation in the low-VHF range. In the late-60's, the Missile and Surface Radar Division undertook the development of a very-high-power broadband VHF transmitter system: distributed-amplifier techniques

were successfully applied to solve the technical problems involved.

The transmitter system described in this paper was developed for broadband operation, and achieved a bandwidth of almost three octaves with multimewatt peak-power output and duty cycles up to 11%. The development and subsequent analysis of this transmitter system included extensive analytical computer studies of high-power distributed-amplifier operation.^{5 6 7 8 9 10}

Configuration and performance

Fig. 1 is a block diagram of the transmitter system. Six high-power amplifier (HPA) chains are used to generate the total output power. Each HPA has a separate distilled-water cooling system; one "raw water" cooling system is used for the entire transmitter. A single high-voltage DC power supply and capacitor storage bank system supplies DC power to all six amplifier chains. Four levels of

high-voltage DC are fed to each amplifier: 4, 11, 13, and 15 kVDC. As indicated in Fig. 1, each HPA feeds a separate antenna, with the total output power combined in space.

The transmitter system, exclusive of the high-voltage power supply (HVPS) and cooling equipment, occupies 90x100 ft (9,000 square feet) of high-overhead floor space. The HVPS capacitor bank occupies an additional 20x120 ft of floor space. The HVPS units are located outdoors. The distilled-water cooling system occupies 60x120 ft of floor space. Total floor space required by the transmitter system is then 18,600 square feet.

High-power amplifiers

Fig. 2 is a simplified schematic of a single high-power amplifier (HPA). Each of the six HPAs uses 12 RCA 4641 power tetrodes in a distributed-amplifier circuit.

Grid-line impedance is 5½ ohms. Broadband ferrite core transformers are used to match the grid line to a 50-ohm source at the input end and to a 50-ohm termination at the output end. Operation is essentially Class A, with all 12 HPA tubes operated at the same grid-bias voltage.

The screen grid of each power tetrode is individually pulsed, and the peak-pulse voltages are adjusted to obtain the desired "video" plate currents. These video plate currents are set with zero RF input drive. When RF drive is applied, the peak-pulse plate currents increase due to non-linearity in the 4641 tube characteristics.

As shown in Fig. 2, the low-pass grid line is made up of inductors L40, L41, . . . , L52 in conjunction with the tube-input capacitances plus the circuit capacitance. As mentioned previously, impedance is 5½ ohms. Networks (C53, L55, R14) introduce high frequency loading to help suppress parasitic oscillation. The input drive power is transformed from 50 to 5½ ohms by RF transformer T1. The drive power is terminated in R26 (50 ohms).

The plate line consists of inductors L1, . . . , L13 in conjunction with tube-output capacitances plus circuit capacitances. The plate-line cutoff frequency is the same as that of the grid line, so that plate-line phase shifts match the grid-line phase shifts. Plate-line impedance is tapered from a high impedance (at reverse termination R1) to



D. L. Pruitt
Radiation Equipment Engineering
Missile and Surface Radar Division
Moorestown, New Jersey
received the BSEE from Iowa State College in 1949. He joined RCA in April of that year, and after a year on the specialized training program, moved to the Radar section in Camden, N.J. in 1950. Since then, he has been involved in the design of microwave components, modulators, and transmitters for various radar systems. His experience has ranged from transistorized pulse and RF circuitry to a two-megawatt-average-power ignitron pulse modulator and multimewatt peak-power tetrode transmitters. He had primary technical responsibility for the RF circuitry of the transmitter described in this paper.

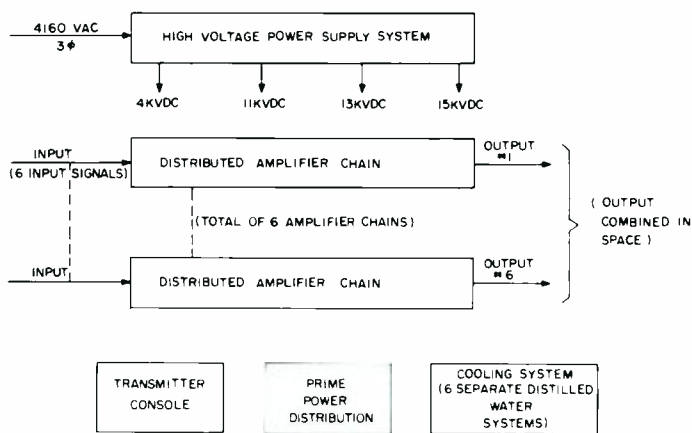
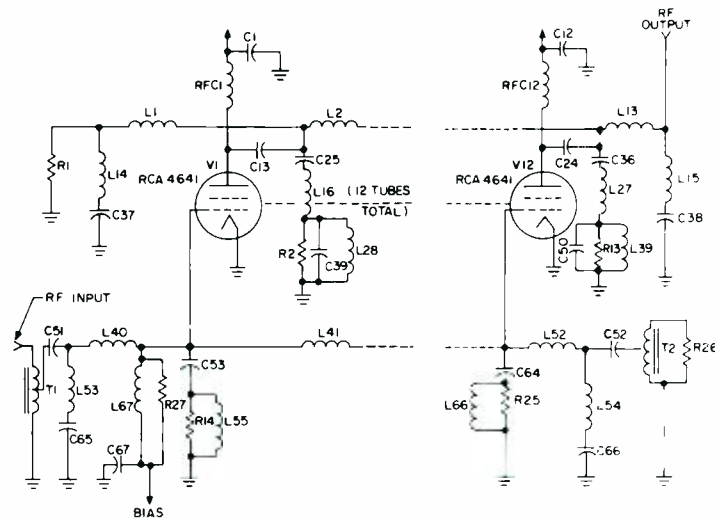


Fig. 1 — Transmitter System block diagram.

Fig. 2 — Simplified schematic of a single high-power amplifier; six HPA's are used in the transmitter system.



a lower impedance at the RF output. The output line is a 6 1/8-in.-diameter 50-ohm coax.

Harmonic content in the plate-current waveform is high because of characteristic tube nonlinearity—as high as -12dB for the second harmonic and -15dB for the third harmonic. These harmonics are removed in a high-power harmonic filter, located between the transmitter and the antenna.

Since the plate and grid line mid shunt impedances theoretically go to infinity at the cutoff frequency, the amplifier will tend to oscillate at or near cutoff. This tendency is prevented by plate-line networks (C25 L16 L28 C39 R2) and eleven other identical networks. These "oscillation suppressors" are double-tuned circuits, tuned slightly below the cutoff frequency, which couple 50-ohm loads tightly to each plate at the tuned frequency.

The DC plate voltage is fed to the HPA tube plates via RF choke coils RFC1, RFC2, ..., RFC12. The RF voltage present on the plate line builds up gradually from input end to output end, *i.e.*, the maximum RF voltage appears at the plate of tube V12, and minimum RF voltage appears at tube V1, as a general rule. Reflected power from the load (VSWR) and plate-line imperfections may partially upset this simple picture, without changing the general pattern. Since the RF voltage varies from tube to tube, efficiency can be maximized by "grading" or "tapering" the DC plate voltage. In the HPA's of this equipment, the DC plate voltage is graded as follows: tubes V1 to V4, 11 kVDC; tubes V5 to V8, 13 kVDC; and tubes V9 to V12, 15 kVDC.

The 15-kVDC level used on V9 through V12 provides a generous minimum plate voltage for ideal conditions. High VSWR loads, coupled with the rise in circuit mid-shunt impedance at the top of the band, cause a reduction in the minimum plate voltage for some tubes. For example, a VSWR of 2:1 coupled with maximum frequency operation could cause inadequate minimum plate voltage at tube #12. Excessive screen current is prevented by use of a "soft" screen supply (using a series resistor). This also causes a small drop in total power output, which is tolerated for these extreme conditions.

The HPA tubes are screen pulsed, from individual screen pulse "regulators." Peak screen voltages are adjusted at the HPA local control panel, which also displays the resulting peak plate currents.

Fig. 3 shows a finished HPA unit. Several of the RCA 4641 tetrode tubes may be seen in this photograph. Fig. 4 is a photograph of the HPA control panel (local control console) outside the HPA room. HPA tube filament and screen voltages are individually controlled, and peak plate currents, peak screen currents, and peak screen voltages are monitored on peak reading meters at this console.

Each HPA assembly is 5 ft wide, 20 ft long, and about 8 ft high; it is housed in a shielded HPA Room measuring 30 ft square and 12 ft high. The 12 HPA screen voltage pulsers and 3 crowbar units are also housed in the HPA Room.

HPA tube arc protection

It is well known that high-power tubes are subject to internal flash arcs during operation—the "Rocky Point effect."¹¹ If

not interrupted, the arc will damage, or destroy, the tube.

In the design, a conventional ignitron crowbar¹¹ is used to interrupt the power-tube arc. Plate arcs are sensed by thresholding the signal from a plate-pulse current transformer, feeding logic circuitry which fires the appropriate crowbar for the tube concerned. A memory circuit lights a lamp to show which tube arced. There is one crowbar for each voltage level on each HPA — *i.e.*, three crowbars per HPA and 18 crowbars per transmitter system.

Each HPA crowbar chassis receives plate voltage from the high-voltage power supply system via a high-voltage silver/sand fuse. When the crowbar fires, the associated fuse opens up, thus isolating the faulted unit from the HVPS. The remaining five HPA's continue to operate as if nothing had happened. A remotely operated fuse changer is used to switch to a new fuse, thus returning the HPA involved to operational status. Each fuse

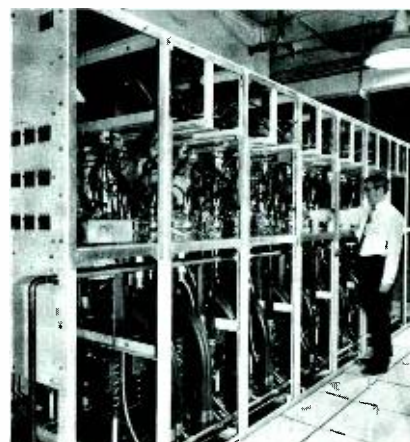


Fig. 3 — High-power amplifier.

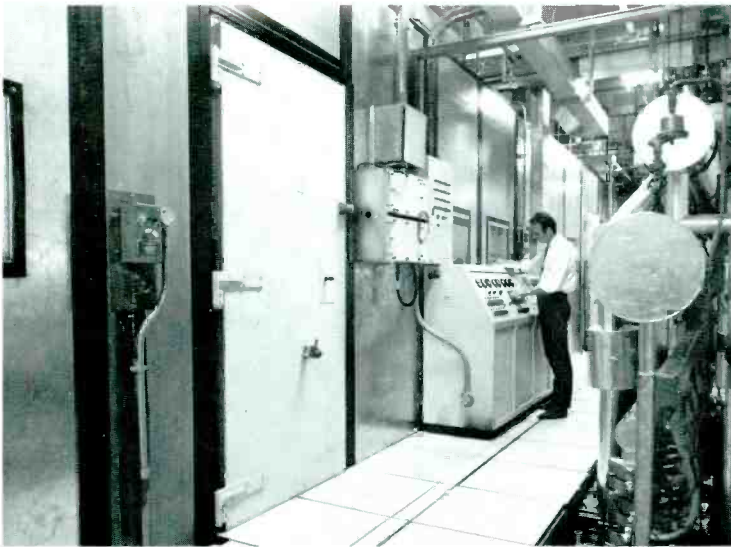


Fig. 4 — HPA control panel



Fig. 8 — Capacitor-bank room.



Fig. 5 — HPA room.

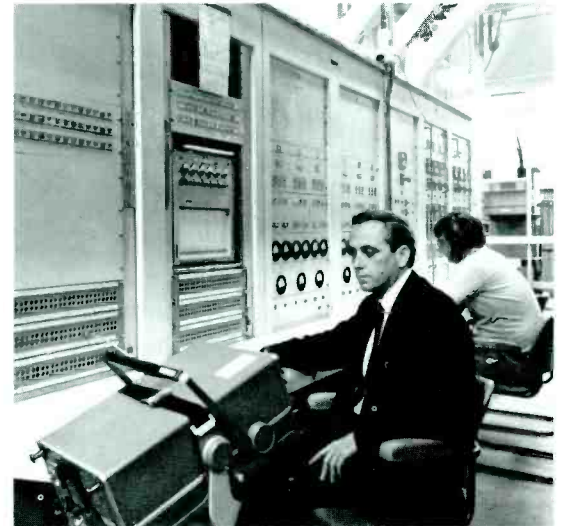


Fig. 9 — Transmitter control console.



Fig. 7 — High-voltage DC power supplies.

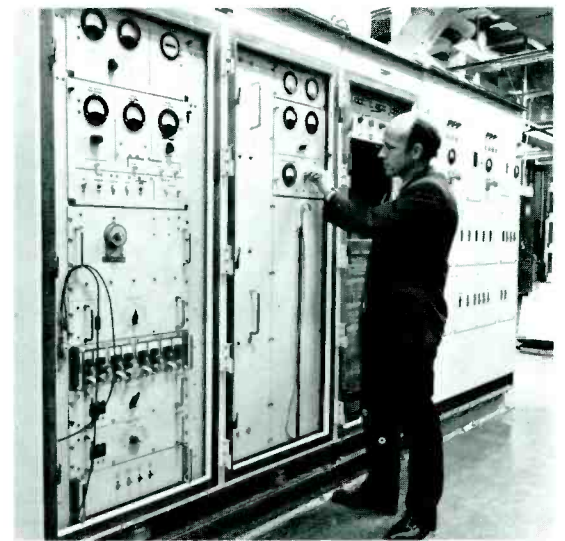


Fig. 10 — IPA-driver, fault logic, and load center.

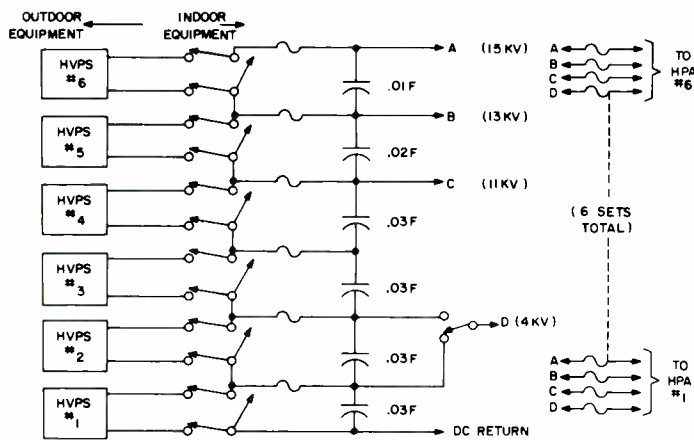


Fig. 6 — High-voltage power supply (HVPS) system.

changer contains five fuses. After five operations of a given crowbar chassis, the HPA room is opened up to replace the blown fuses. The fuse is designed to allow for easy field replacement of the fuse wire.

Fig. 5 shows a view inside the HPA room, with the fuse changer in the foreground. The row of 12 screen-pulse regulators is in the middle of the room, with the high-power amplifier in the background.

High-voltage power supply system

Fig. 6 is a block diagram/simplified schematic of the HVPS and capacitor bank system.

Six identical high-voltage DC power supplies are used, with the outputs connected in series. Each supply is fed from a 4160V AC, three-phase source, and each supply contains its own 4160V AC three-phase circuit breaker. Each supply is 12½x14x9 ft high. The output rating per supply is 2 to 5 kVDC (variable by remotely-controlled load-tap changer). Thus, the HVPS system is capable of a maximum output voltage of 30 kVDC, although the typical operating value is 15 kVDC maximum.

An indoor switch matrix permits isolation of any of the six supplies for repair or maintenance as required. The system can supply full required voltage with any one supply down, though the tapered-plate-voltage feature is partially lost if either supply #5 or #6 is down.

The pulse currents are drawn from the series-connected capacitor banks. As shown in Fig. 6, the six capacitor banks vary in size from 0.01 to 0.03 F. Max-

imum rated energy storage capacity is 1.875 mJ; normal storage is 0.55 mJ.

Twenty-four large coaxial cables (similar to RG-17) feed the four high-voltage levels (4, 11, 13, and 15 kVDC) to the six HPA's. Each line has a protective input fuse, or backup fuse for the crowbar fuse.

The six high-voltage power supplies are individually controlled from a remote, centrally located console. ON/OFF and RAISE/LOWER controls are provided, with complete voltage and current metering.

Fig. 7 shows the six outdoor-mounted HVPS units. Fig. 8 is a view of the capacitor room, with the switching matrix on the wall to the left and the capacitor banks to the right in the photograph. Fig. 9 is a view of the central transmitter control console (TCC). The HVPS controls and various monitoring functions are located at the TCC.

Driver amplifiers

The intermediate-power amplifier/driver must supply a minimum of 800W peak RF drive power to each HPA input. Six driver units are used, one for each HPA.

The input from the system exciter is 60 MW peak to each of the six IPA/driver cabinets. The intermediate-power amplifier (IPA) is a small distributed amplifier containing six type-8233 tetrodes. IPA grid-line impedance is 50 ohms, thus matching the 50-ohm exciter cable with no requirement for impedance transformation. IPA plate-line impedance is 300 ohms, and typical power output is 3 W peak. A 2:1-voltage-ratio RF transformer matches the 300-ohm IPA plate line to a

75-ohm coaxial line which carries the 3 W IPA output to the driver input.

The driver grid-line impedance is 75 ohms, and the driver plate-line output impedance is 200 ohms. The driver is another small distributed amplifier, using 12 type-8121 tetrodes. The driver output power (800 to 1000 W peak) is transformed to the 50-ohm level by a 2:1 (voltage ratio) ferrite transformer, and fed to the HPA via 7/8-inch 50-ohm coaxial line.

Fig. 10 shows the IPA-Driver, fault-sensing logic, and "local-load-center" cabinets. The IPA-driver circuitry occupies a 2½ cabinet at the left, while the fault-sensing logic occupies a single cabinet in the center.

Cooling system

The six outdoor units of the HVPS are self-cooled, with oil-to-air radiators to transfer the waste heat to the atmosphere. All indoor units are in an air conditioned environment, with forced, cooled air circulated continuously.

Waste heat from the HPA tubes, HPA filament power supplies, and HPA screen pulsers, is removed by a distilled-water system. Each HPA tube plate is cooled by a 60 gal/min flow of high purity water (720 gal/min for all 12 tubes in an HPA). Typical flow for the remaining water courses is 1 to 2 gal/min/water course.

The water system (for each HPA) consists of a 2000-gal stainless-steel storage tank, demineralizing equipment, a 1000-gal/min, 100 psig pump, and copper distribution piping with flow interlock switches. Secondary (raw water) cooling is provided by outdoor cooling towers.

References

1. Percival, W. S., British Patent Specification No. 460,562, applied for 24 July 1936.
2. Ginzton, Hewlett, Jasberg, and Noe, "Distributed Amplification," *Proceedings of the IRE*, (Aug. 1948).
3. Horton, Jasberg, and Noe, "Distributed Amplifiers: Practical Considerations and Experimental Results," *Proceedings of the IRE*, (July, 1950).
4. Rodgers, P. H., "Large Signal Analysis of Distributed Amplifiers," Engineering Research Institute, University of Michigan, Technical Report No. 52, Contract No. DA-36-039 s c 63203, July, 1955.
5. Douma, L., *Private Communication*.
6. Douma, L., *Private Communication*.
7. Douma, L., *Private Communication*.
8. Douma, L., *Private Communication*.
9. Douma, L., *Private Communication*.
10. Hoover, W. and Prutt, D., *Private Communication*.
11. Parker, W. N. and Hoover, M. V., "Gas Tubes Protect High Power Transmitters," *Electronics*, (Jan., 1956).

Low backlobe antenna for airborne missile-warning system

H. Honda

Antennas used in certain airborne applications, must have very low backlobes to reduce ground clutter, yet they must be as compact and simple as possible for aircraft installation. This paper describes techniques for reducing the backlobes of a dielectric-rod antenna over a broad angular region (namely, over the entire rear hemisphere of the radiator) while providing wide angular coverage by the use of devices that are simple to implement. A method of enhancing the directivity for such a radiator by step-indexing of the material is also discussed. The theory of these techniques is briefly described, and experimental results showing verification of the theory are presented. The theoretical effects of metal structures close to the radiator and of the presence of radomes are discussed, and experimental data are presented.

DEFENDING AN AIRCRAFT against missiles and other aircraft requires a tail warning system with low false alarm and a capability of providing an automatic alert for appropriate maneuvers. For a sensor system that consists of a pulse doppler radar (PDR), the false alarm may arise from ground clutter. Clutter rejection in a simple and cost-effective PDR system may be accomplished by use of a low sidelobe antenna, if that radiator is simple and cost-effective. Such a radiator is the dielectric rod antenna.



Because of its low profile, the dielectric rod radiator is attractive from the standpoint of use in a rear-looking antenna system on high speed aircrafts. However, this type of radiator is not generally noted for its low backlobes. A technique has been developed to reduce these lobes. This technique, as well as a method of enhancing the gain, and the measured performances of the radiators implementing these

H Honda
Radiation Systems Engineering
Aerospace Systems Division
Burlington, Mass.

received the BSEE from the University of Pennsylvania, the MSEE from Drexel Institute of Technology, and MS (physics) from Northeastern University. Mr. Honda worked for four years on the design and development of microwave components for airborne radars and communications relay systems. He has worked for six years on the design and development of microwave and UHF antennas for radar, communication sonobuoy systems, and in the analysis of communication antennas from the standpoint of anti-jam capabilities. Mr. Honda has spent two years supervising the development of low cost microwave relay systems and printed microwave circuitry. He has also applied microwave techniques to computer systems and, in particular, has investigated variable capacitance phase-locked oscillators. He investigated optical radar processing techniques for ICBM detection and advanced microwave antenna techniques, including integrated circuit active element phase array. He has analyzed monopulse systems, particularly as related to antenna systems from the standpoint of boresight shift and spurious responses. He has investigated electrically small UHF and VHF antennas. His most recent activities include the development of broad-beam low-backlobe antennas for applications to PDR systems on tactical and strategic aircrafts, and analysis of the minor lobe requirement for these radiators from the standpoint of ground clutter reception. Mr. Honda is a member of IEEE, of Eta Kappa Nu, and of RESA (the industrial branch of Sigma Xi).

techniques are discussed in this paper.

The salient electrical requirements to which this type of antenna was developed are:

- Operating Frequency in the upper D-band and in the E-band;
- Gain in the 11 to 15 dBi range;
- Minor lobes in the entire rear hemisphere of the antenna (backlobes) of the order of 35 dB down from the peak of the main beam.
- Compact size.

Backlobe suppression

The technique used for backlobe suppression over a wide angular region is a simple concept, and its principle may be described as follows: It is a well established concept that the total radiation pattern of the dielectric rod antenna may be considered to be the vector sum of the feed point and terminal radiations. For the radiators of interest, the patterns of the feed point radiation and of the terminal radiation in the rear hemisphere are at most within the first few sidelobes of the pattern. If the energy in these lobes is anti-phase, the lobes tend to cancel. By spacing the "phase centers" of the feed point and terminal radiations, so that the end-fire condition is met, the radiation in the rear hemisphere tends to cancel and is enhanced in the forward hemisphere. For good cancellation over wide angular region, the rearlobes for the two components must match in amplitude. Thus, the techniques become a function of the two

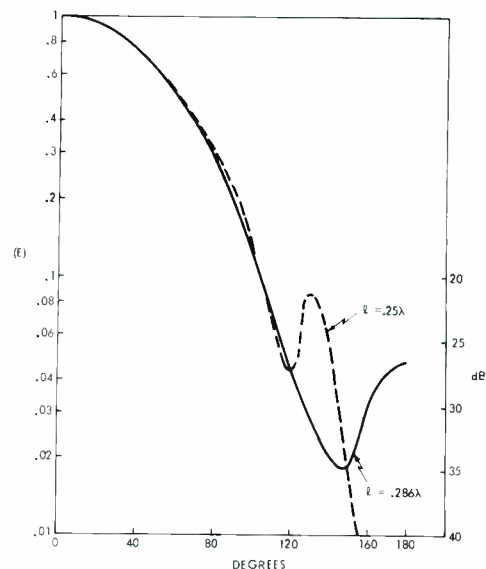


Fig. 1—Effect of phase center distance.

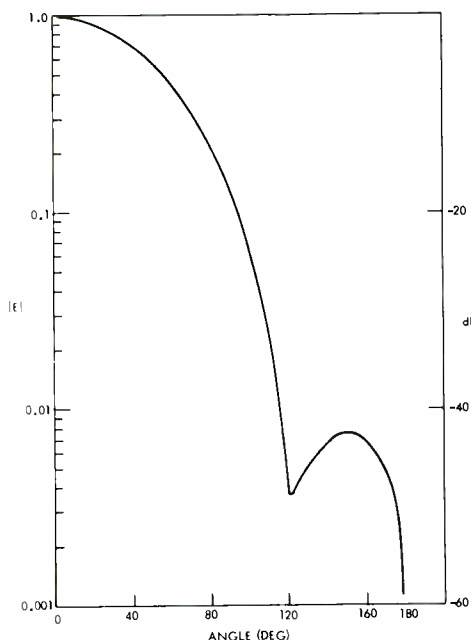


Fig. 2—Resultant pattern with tapered distribution.

radiation patterns and the launching efficiency.

In practice, these factors are not easily controlled. However, if we introduce auxiliary radiators of proper amplitude and phase, the radiation in the backlobe region can be further suppressed. For dielectric rods, the auxiliary radiators may take the form of a simple band on the cylindrical portion of the rod, which introduces a discontinuity in a normally non-radiative line. The width of the band controls the amplitude of radiation; its position controls the phase.

Calculations were made to check the backlobe suppression principle assuming the backlobes of the feed point and terminal radiations to be equal, using theoretical patterns for the feed point and terminal radiations. Fig. 1 and 2 show the resultant pattern assuming uniform and tapered aperture distribution, respectively, for the terminal radiation. Fig. 2 shows that backlobe suppression of over 40 dB (relative to the peak of the main beam) over a 70° region about the rear axis of the radiator is possible under these conditions. These calculations were made for shorter rods than those of primary interest in this paper.

Enhancement of directivity

If relatively high gains are desired in the radiator, the rod radiator loses some of its attractiveness because of

its increased length. If high gain is achievable with short lengths, while maintaining a small cross-sectional area, the usefulness of the radiator is enhanced.

In a surface-wave transmission line, most of the energy propagates outside the dielectric. For such a line, the smaller the diameter the lesser is the field confined near the rod; or more precisely, the lesser the difference in phase velocity between that in the rod and that in free space, the greater is the extent of the field outside the rod. If a discontinuity is introduced so that radiation occurs (as in the case of the dielectric rod radiator) the directivity of this radiation depends on the extent of the field at the plane where the discontinuity occurs. This then implies that the smaller the radiator diameter, the greater is its directivity. Further, since the field is more confined by higher dielectric constant, the lower the constant, the higher the directivity for a given diameter rod.

In a practical radiator, there is a limit to the minimum diameter utilizable, since the dipole mode field is usually launched from a circular waveguide, which would prevent propagation if the diameter becomes too small. Also, with decrease in aperture size, the launching efficiency is decreased and energy is directed into the direct radiation (feed point) which tends to spread the energy and thus reduce the gain.

To circumvent this restriction, a material of lower dielectric constant may be introduced between the basic rod and air (free space). This reduces the difference between the phase velocities and the field decays less rapidly away from the rod (while propagating parallel to the rod). The effective aperture is thus increased. [The layers of dielectric is referred to as a "liner." The liner was first used for mechanical consideration by P. Tremblay.]

This is perhaps an oversimplified description of the theory, since it is based upon the surface-wave propagation concept. A tapered rod also radiates by leaky wave, so that the mechanism for increased gain is not so simple as stated above. On this basis, it may be expected that the rod with more gradual taper may be influenced more by a liner.

Experimental results of radiators in free space

Both the techniques of backlobe suppression and gain enhancement discussed above were implemented and measurements made on radiators of various lengths, *i.e.*, for radiators of various gain. Radiators with gains ranging from 11 dBi to 13 dBi were tested. In previous studies, rods with about 5 dBi and 14 dBi gains were measured.

In much of the present study, the two techniques were implemented at the same time and the best performance characteristics were obtained by this simultaneous application, *i.e.*, the sharp "cut-off" in beam characteristics obtained by the liner aids in reducing the rearlobes over a broader angular region, as well as enhancing the gain. An example of such a radiator used in the experimental studies is shown in Fig. 3, where a fiberglass liner is fitted over a rod of high- K styrene-based material ($\epsilon=9\epsilon_0$) incorporating a band.

A typical example of the backlobe reduction achieved by use of the band (no liner) is shown in Fig. 4. The pattern shown is that in the E-plane, for a 0.244λ -diameter rod with an 0.81λ -diameter ground plane. Reduction in rearlobe level from -22 dB (relative to peak of main beam) to -31 dB, over $\pm 90^\circ$ about the rear axis of the antenna is seen.

As mentioned, the backlobe level depends on the feed-point-to-terminal spacing. The E-plane pattern characteristic as a function of this spacing is shown in Fig. 5 for a particular rod. The characteristic is also dependent upon the ground plane size, as may be expected—not only because it changes the feed-point radiation pattern but also because it tends to diffract the terminal radiation. For small

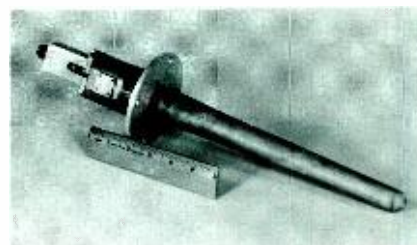


Fig. 3—Experimental dielectric-rod radiator.

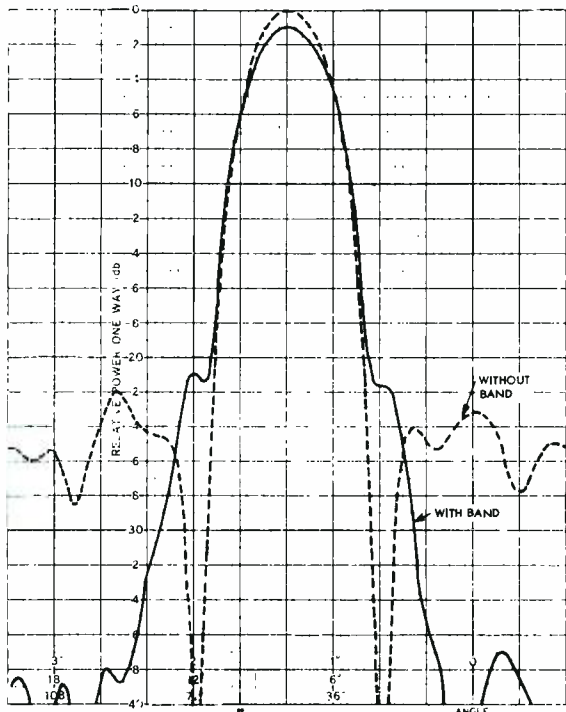


Fig. 4—Backlobe reduction by use of bands.

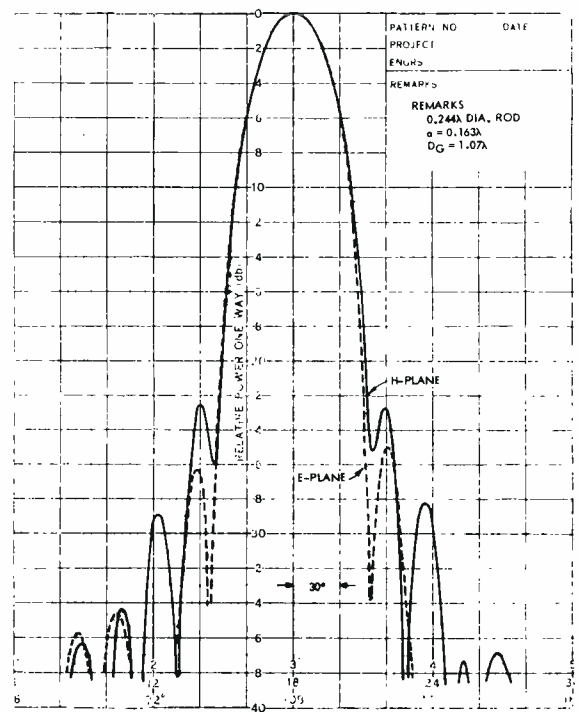


Fig. 8—Principal plane patterns with teflon liner.

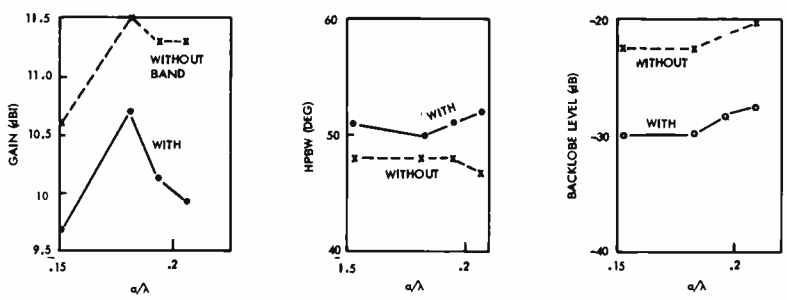


Fig. 5—E-plane characteristics with bands as function of feed-point-to-taper spacing.

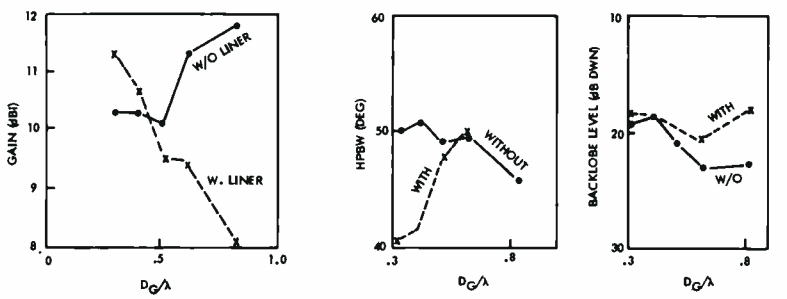


Fig. 6—Characteristics of 0.244 rod with teflon liner.

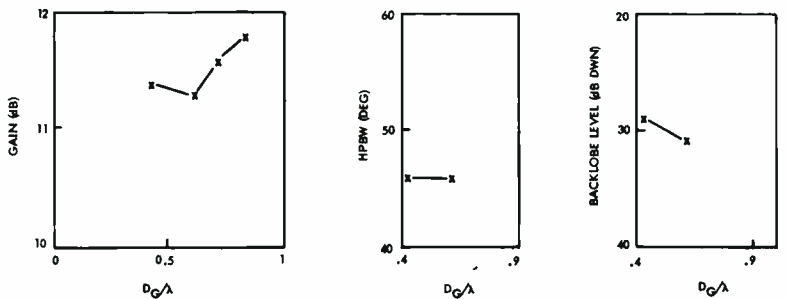


Fig. 7—E-plane pattern characteristics with backlobe suppression.

ground planes, there is a cyclic change in rearlobe characteristics as the plane is increased in size.

The investigation of the increase in directivity engendered by the use of liners was rather limited, primarily because of the cost of the material and of the fabrication. The materials used in the study were teflon, fiberglass, and foams of various density. Liners of these materials were tested with rods of various diameter and lengths. Fig. 6 and 7 summarize some of the results of this investigation.

The use of liners is most effective for small ground planes with the higher-dielectric-constant materials, as seen from the gain characteristics of Fig. 6, where the performance of a rod with teflon liner but without backlobe suppression are summarized. The results in Fig. 7 are for teflon liners with backlobe suppression. The liner dimension was held constant and the ground plane diameter varied.

Representative of the patterns resulting from a rod with liner and backlobe suppression are those shown in Fig. 8, where the principal plane patterns of a rod with teflon liner (base diameter: 0.305λ) and with 1.07λ -diameter ground plane are plotted. Fig. 9 shows the pattern for a rod with a high-density foam liner.

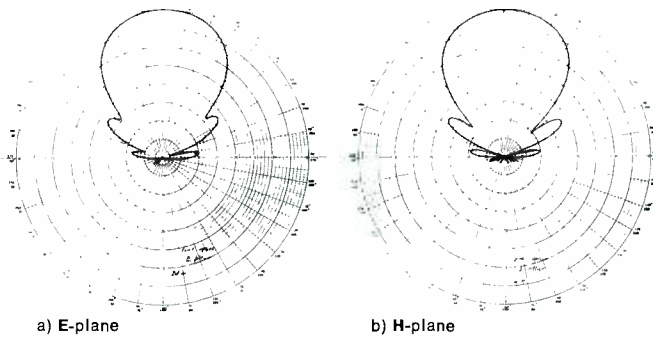


Fig. 9—Polar pattern of dielectric rod with foam liner.

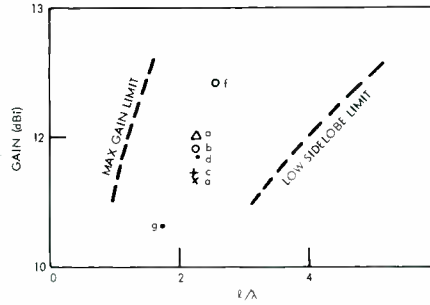


Fig. 10—Effectiveness of liners.

CONDITIONS

	D_0/λ	D_G/λ	D_L/λ	LINER
a	.244	.61	.305	TEFLON
b	.244	.81	.305	TEFLON
c	.244	.81	.27	FIBERGLASS
d	.244	.81	.81	FOAM
e	.223	.81	.305	TEFLON
f	.223	.81	-	-
g	.223	.71	-	-

D_L - LINER BASE DIA.
 D_0 - RCD DIAMETER
 D_G - GROUND PLANE DIA.

The effectiveness of the backlobe-suppression technique has been demonstrated, but that of gain enhancement by the mechanism discussed above is less evident. Increase in gain by use of stepped-index dielectric is obtained, but other mechanisms, such as "back-fire" and focusing effects may be the more dominant factors. Regardless of the mechanism, the results can be assessed by comparing them with those obtained by other investigators using more conventional techniques.

Zucker gives a plot of gain and beamwidth versus electrical length for surface-wave antennas. For a given gain, there is a range of values for the length, dependent upon the design: the lower limit determined by maximum gain design and the upper limit by minimum sidelobe design. The latter is of interest here.

The results of the liner investigation are summarized in Fig. 10, where the measured gains are plotted as functions of the overall length of the liner, for the best backlobe characteristics obtained. In some of the cases, the plotted points are without liners, since the liners used resulted in large degradation in backlobe characteristics without appreciable improvement in gain. The results indicate that the length of the radiator is reduced to almost one-half that of the "conventional" low-sidelobe rod.

Applications

This type of radiator may be installed on either tactical or strategic aircraft; studies were made to determine the effect of installation upon the antenna performance, where mockups of parts of aircraft structures were prepared

and the radiator performance was measured in the proximity of such structures. For a high performance tactical aircraft, a representative location of the radiator is atop the vertical stabilizer; in the study of this type of installation, a mechanically positioned antenna was considered to be located in a radome as shown in Fig. 11. The effect of the radome and of the support structure were examined. The resulting principal plane patterns are shown in Figs. 12 and 13. In the E-plane, the radome aids in the suppression of the backlobes. The radome mounting structure does not degrade the performance a large amount.

For the strategic aircraft application, installation on the side of the fuselage was considered. (Installation on the tip of the horizontal stabilizer will be

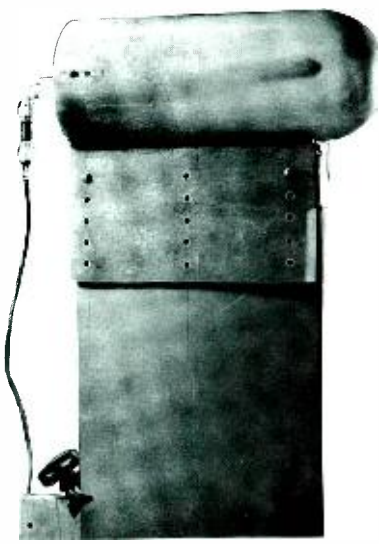
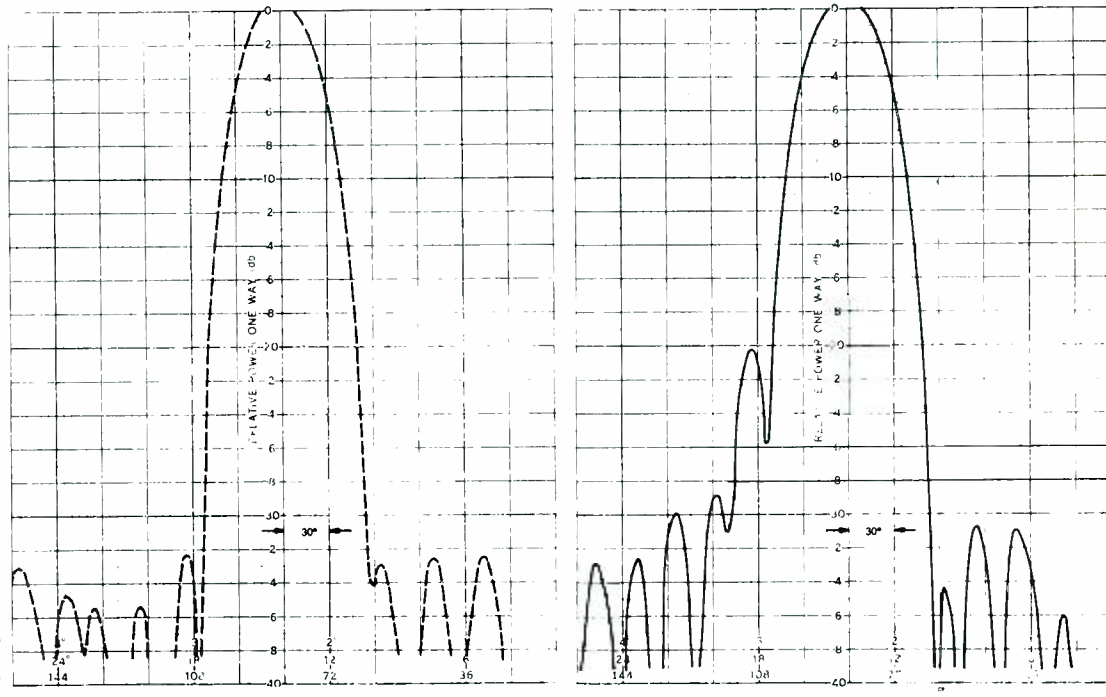


Fig. 11 (above)—Single-radiator configuration. Fig. 12 (right)—E-plane pattern of mechanically switched rod. Fig. 13 (far right)—H-plane pattern of mechanically switched rod.



investigated. Here, the radiation characteristics are essentially those of free space.) The backlobe suppression technique previously discussed makes the radiator relatively insensitive to backlobe degradation by proximity to structures near the radiator. Theory and measurements indicate the backlobes are formed quite close to the radiator, so that the structures in back of the radiator do not appreciably affect the performance. Structures to the side of the radiator may have appreciable effect. They may be considered as those in the near zone, metal surfaces may be as close as a wavelength from the radiator without appreciably degrading the backlobe characteristics. Thus the radiator which is canted at an angle to the fuselage may be recessed some distance within the fuselage, without appreciably altering the characteristics. Structures in the Fresnel zone is less obvious to assess. However, the field in this region tends to be "collimated" for short distances from the effective aperture. In fact, the 3-dB width of the pattern is equal to the aperture width at a distance of D^2/λ (for uniform illumination). In the far field, the multipath condition exists and the reflections from the metal structures perturb the pattern. The amount, of course, depends on the cant angle.

Measurements were made with radiators mounted on a flat metal surface simulating the aircraft fuselage. The pattern is dependent upon the location of the radiator with respect to the edge of the fuselage and upon its separation from the fuselage. Fig. 14 shows the E-plane pattern for a radiator canted 30° from the surface.

A radar system utilizing this type of radiator installed in a strategic aircraft (Fig. 15) was successfully flight tested. The radiator was mounted in the tail section of the aircraft.

Acknowledgment

Most of the work in the development of this radiator was done under IR&D funds. The author thanks the many individuals in the Aerospace Systems Division for their assistance. In particular, the support of L. Andrade, Dr. W. C. Curtis, and P. A. Michitson is gratefully acknowledged.

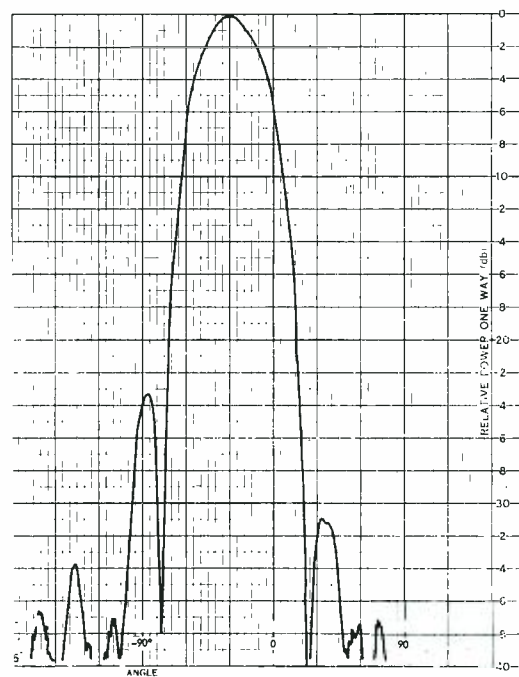


Fig. 14—E-plane pattern for radiator canted 30° from ground.

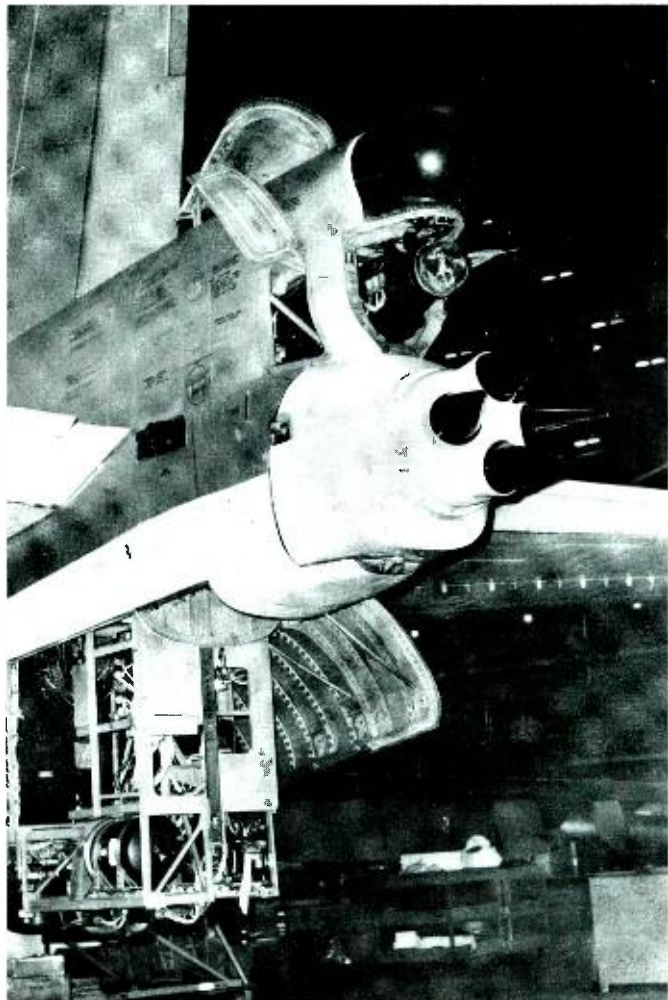


Fig. 15—Photograph of clusters of four dielectric rod radiators on aircraft.

Ultra-lightweight deployable antennas

W. S. Sepich

Two deployable antennas were used on the Apollo program for direct communications between the lunar surface and earth. Other publications have described the LM erectable antenna used on earlier Apollo missions. This paper makes a technical comparison between the two antennas, concentrating on the S-band high-gain antenna used on the Lunar Rover Vehicle with the Lunar Communications Relay Unit.

FOR BETTER communication with earth during the astronauts' extravehicular activity (EVA) on the lunar surface, early Apollo missions required a high-gain antenna that could be easily and quickly erected on the surface of the moon. The astronauts communicated directly with earth through this S-band antenna which was first used on Apollo 11. The Missile and Surface Radar Division (MSRD) successfully designed and built the 10-ft-diameter erectable antenna.¹ The antenna was fabricated with 21 ribs that were spring

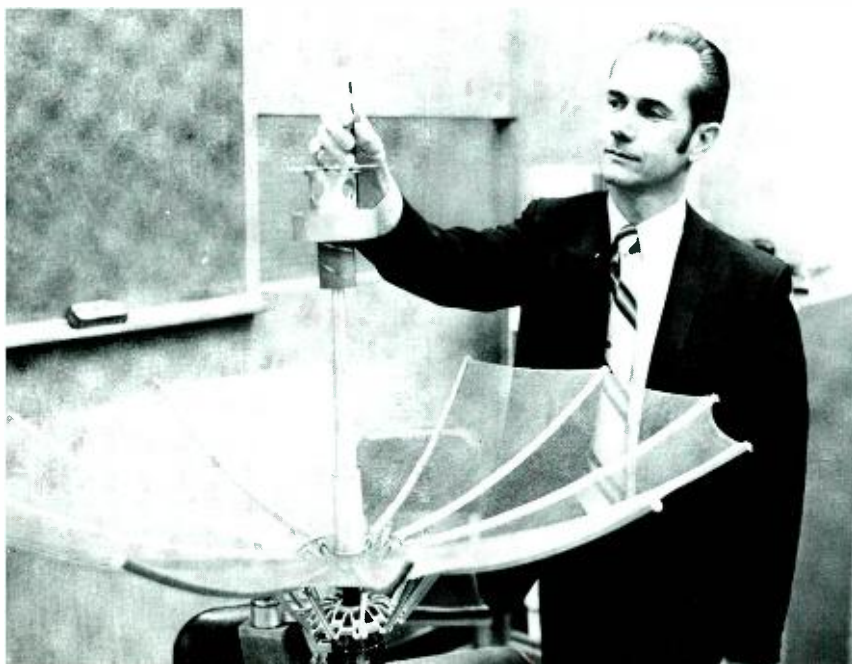
hinged near the parabola vertex and also at the halfway point to reduce package size for the trip to the moon. The reflecting surface was formed across the ribs from a tricot-knit wire mesh of 0.0005-in.-diameter nickel chromium wire, gold plated to improve reflectivity. The antenna feed was a single-element, end-fire helix with a cup-shaped reflector mounted on a telescoping boom. The entire antenna was tripod mounted and the reflector was deployed through the use of stored energy in leaf-type springs at the joints of the reflector rib sections. This

William S. Sepich, Mgr.

Mechanical and Structural Engineering
Missile and Surface Radar Division
Moorestown, New Jersey

received the BSME from the University of Pennsylvania in 1954 and the MSME from Drexel University in 1960. He joined RCA in 1954 as a design engineer on antenna pedestals. In 1960 he was promoted to group leader. He

has been responsible for design studies of the SAM-D missile launcher and for the design of the AN/MPS-36 antenna, pedestal, and trailer. He has been Manager of Mechanical and Structural Engineering since 1969, where his responsibilities have included the design of the LCRU antenna, mechanical design of the AEGIS AN-/SPY-1 phased array, and the antennas to be landed on Mars for the Viking program.



Reprint RE-18-5-6
Final manuscript received December 6, 1972.



Fig. 1 — LM erectable antenna on the Moon during Apollo 12 mission.

antenna is shown in Fig. 1 during the Apollo 12 mission on the lunar surface.

The early Apollo missions required one astronaut to remain within sight of the Lunar Module (LM) to maintain contact with the earth. This restricted EVA to within one or two miles of the LM and prevented both astronauts from exploring deep craters together. To give the astronauts greater mobility, the Lunar Rover Vehicle was developed for use on Apollo 15 for the first time. The use of the Rover required a new communications system that could be mounted on the vehicle to maintain direct communications with earth. The Communications Systems Division developed the Lunar Communications Relay Unit (LCRU) for this purpose, and MSRD provided the S-band high-gain deployable antenna for the LCRU. (The UHF and S-band low-gain antennas on the LCRU are not discussed in this paper.)

The LCRU has successfully transmitted voice, telemetry, and color TV from the



Fig. 2 — LCRU antenna mounted on lunar roving vehicle on the Moon during Apollo 15 mission.

Table I — Comparison of the LM erectable and LCRU S-band high-gain antennas.

Parameter	LM erectable antenna	LCRU S-band high-gain antenna
Weight (lbs)	14.0	2.6*
Diameter (in.)	120	38.8 (max.)
Dimensions		
stowed (in.)	10 dia. x 39	5.5 dia. x 24.88
F/D ratio	0.54	0.38
Surface tolerance (in., RMS)	0.15	0.15
Number of ribs	21	12
Pointing accuracy (°, max.)	±0.25	±0.8
Transmit freq. (MHz)	2282.5 ± 10	2265.5 ± 10
Receive freq. (MHz)	2101.8 ± 10	2101.8 ± 10
Polarization	RH circular	RH circular
Axial ratio	2dB ± 1.3° BW	3dB ± 2.5° BW transmit
Transmit gain	32dB ± 1.3° BW	23dB ± 2.5° BW
Receive gain	31.2dB ± 1.3° BW	22.0dB ± 2.5° BW
Side-lobe level (dB)	20	15
Transmit VSWR	1.2	1.2
Receive VSWR	1.8	1.5
Impedance (ohms)	50	50
Power handling (W,CW)	10	15

*Without optical sight

astronauts and has received transmissions from earth without using the Lunar Module as a relay point. The LCRU has also transmitted, through the deployable antenna, the first "live" color TV coverage of the LM's lunar blast-off. Fig. 2 shows the LCRU S-band high-gain antenna on the LRV on the lunar surface during the Apollo 15 mission.

LCRU antenna configuration

The LCRU deployable antenna is used at S-band. From earth launch to lunar landing, the antenna is folded as part of a hinged mast assembly within a stowage container. After lunar landing, it is carried from the LM and connected to the Lunar Rover, where it is manually deployed into a 38-in.-diameter parabolic reflector. It is aimed at the earth through its optical sight, and is then ready to transmit and receive signals at specified frequencies.

Table II — LCRU S-band high-gain antenna surface contour error.

Error source	RMS contour deviation (in.)	
	10 ribs	12 ribs
Geometry (function of no. of ribs)	0.159	0.102
Wrinkles in fabric	0.03	0.03
Tolerances of components	0.005	0.005
Assembly variances	0.08	0.08
Deployment force variation	0.01	0.01
Thermal distortions	0.06	0.06
Summary RMS value of deviations	0.188	0.146

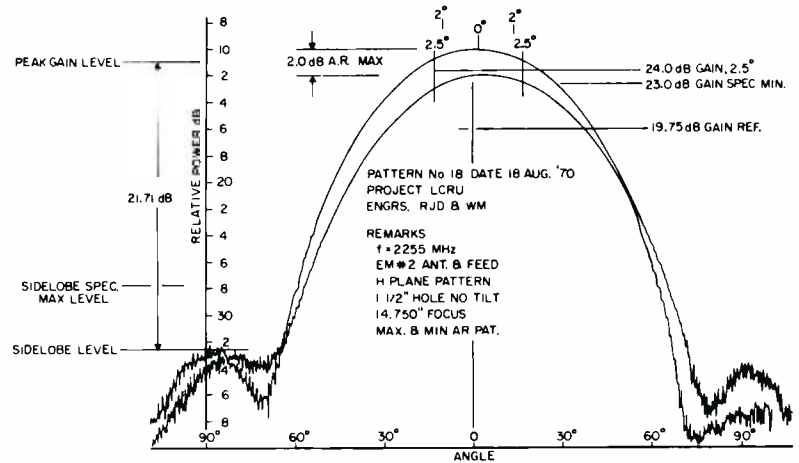


Fig. 3 — Typical LCRU antenna pattern taken on engineering Model No. 2.

The design of the 38-in.-diameter LCRU parabolic antenna took full advantage of the experience gained in the design of the 10-ft.-diameter LM erectable antenna. There are a number of similarities between the two antennas, such as the basic rib design, use of a tricote-knit wire mesh for the reflecting surface, and the use of a single end-fire helix antenna feed with a cup reflector. There were also, however, a number of significant differences between the antennas besides the obvious size relationship. Since the LCRU antenna was to be mounted on a mast on the LRV, it had to be designed to withstand the vibrations encountered when traversing the lunar surface. The antenna had to be mounted to the mast in either the folded or deployed configuration during a mission; unlike the LM erectable antenna which was deployed only once during a mission, the LCRU antenna was designed to be opened or folded as many as 100 times

during the mission. This requirement precluded the use of stored energy in the form of springs being used for deployment. Instead, a manual push-pull actuator guiding a rib-lifter linkage mechanism was utilized similar to an umbrella mechanism, except that it must operate from the convex side of the parabola to minimize aperture blockage. The large number of actuations also dictated the use of a heavier wire mesh for the reflecting surface than that used for the LM erectable antenna. Table I shows data comparing the LCRU antenna to the LM erectable antenna.

To meet the gain specification for the LCRU antenna, the surface contour accuracy must be held to 0.15 in., RMS. The surface contour is a function of the number of ribs used to form the surface, since the mesh is stretched tight between ribs. Obviously, the larger number of ribs used, the greater the contour accuracy.

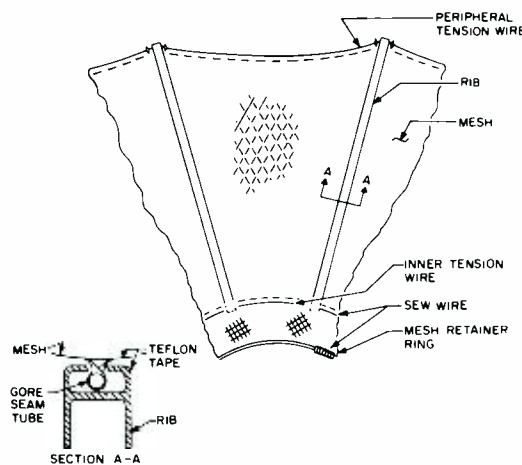


Fig. 4 — LCRU reflector construction.

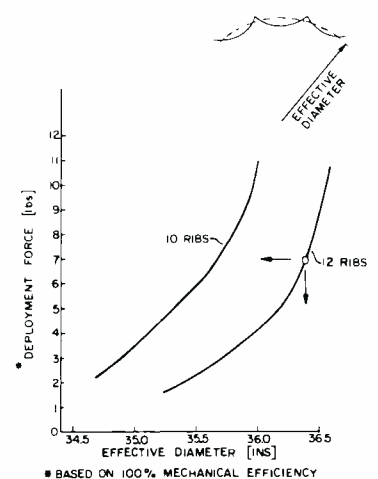


Fig. 5 — LCRU deployment force vs. effective diameter.

However, the weight of the antenna is also a function of the number of ribs used. Table II summarizes the surface-contour error analysis which led to the decision to use a 12-rib antenna. Fig. 3 shows a typical antenna pattern taken during testing of the engineering model.

The wire mesh is attached to the ribs by folding over, inserting through a slot in the rib, then sliding a piece of flexible tubing into the fold as shown in Fig. 4. The tubing diameter is larger than the slot in the rib, thus trapping the mesh in the rib. The mesh is protected with Teflon tape where it enters the rib slot. The same figure shows a view of a gore of material between two ribs. Note that since the mesh is tensioned in the radial direction by inner and peripheral tension wires, a scalloped effect takes place at the periphery of the antenna. Thus, although the ribs form a diameter of 38 in., the effective diameter for electrical purposes is somewhat less. This effective diameter becomes a function of the amount of tension in the peripheral tension wire, which in turn affects the amount of force required in the deployment mechanism to fully open the antenna to its locked position. Fig. 5 shows the results of the analysis which related effective diameter to deployment force. While a larger effective diameter was desirable to enhance electrical performance, human factors limited the allowable deployment force. The specification allowed a deployment force of 10 lb maximum. For the 12-rib configuration, a deployment force of 7 lbs was selected, which results in an effective diameter of 36.4 inches.

The deployment mechanism shown in Fig. 6 is actuated by rotating the actuation grip out of its locking detent, then pulling or pushing the actuation grip axially. This force acts on the rib-lifter which forces the 12 ribs open or closed through the 12 links shown. This mechanism may also be seen in Figs. 7 and 8 which show the antenna in the closed and open positions respectively. The rib lifter motion on the shaft is guided by stainless steel balls rolling in grooves machined in the mating aluminum parts.

A dust shield made from Kapton film material protects the balls and ball paths from contamination by lunar dust. To lock the antenna in either the open or closed position, the actuation grip is

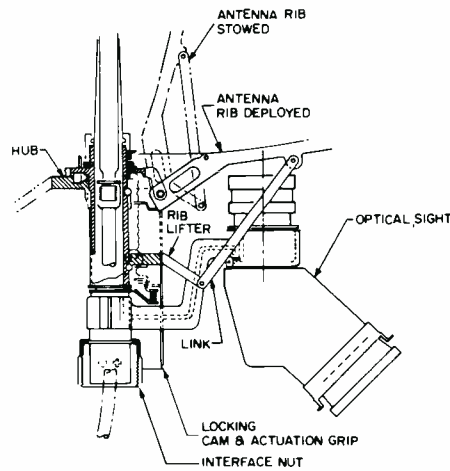


Fig. 6 — LCRU deployment mechanism and locking device.

rotated 30°; this activates a ball/cam action in either of the extreme positions.

The antenna feed can be seen at the top of Fig. 8. The end-fire helix shown has been electroplated on a hollow fiberglass cylinder which is then filled with polyurethane foam for rigidity. This helix is dual wound as compared to the single-wound helix used in the LM erectable antenna, with consequent improvement in axial ratio and beam squint. The cup-shaped reflector reduces side-lobes and back radiation. The feed support boom also serves as the RF transmission line. A printed-circuit transformer mounted to the back of the cup matches the feed to the transmission line

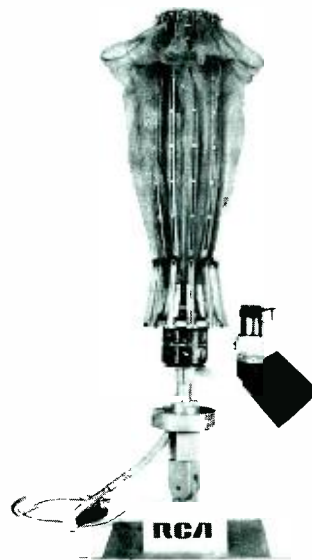


Fig. 7 — LCRU Antenna in folded position.

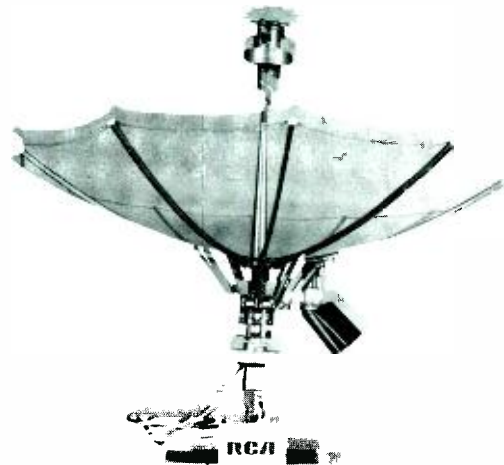


Fig. 8 — LCRU antenna deployed.

Also shown in the lower right portions of Figs. 7 and 8 is the optical sight which is used by the astronauts to aim the antenna at the earth. This sight was developed by Advanced Technology Laboratories specifically for the LCRU application.

Conclusion

The hostile environments encountered during space travel and lunar exploration require an extension of the engineer's ingenuity and analytical capabilities far beyond that normally required for the design of a communications antenna. Only a few of the tradeoffs, studies, and analyses that went into the development of these two ultra-lightweight space antennas have been illustrated in this article. The successful missions performed by these antennas without a failure are proof of the diligence and thoroughness of all those individuals who have contributed to their development.

Acknowledgments

Thanks to R. J. Mason, E. Schwartz, and W. C. Wilkinson for their assistance in the preparation of this article.

Reference

1. Mason, R. J. and Wezner, F. J., "An Erectable Antenna for Space Communication," *The LEM Program at RCA*, RCA reprint PE-453; *RCA Engineer*, Vol. 11, No 5 (Feb-Mar 1960).

Communication antennas for Viking Mars lander

W. C. Wilkinson | W. A. Harmening | O. M. Woodward

In 1976, the United States will soft land a scientific satellite on the surface of Mars. Its communication system, furnished by RCA, will use three antennas for contact with earth. These antennas are described. The mission and Martian environment are the principal design constraints. One narrow-beam antenna is steered in two axes and the other two antennas are fixed, with broad patterns. All have circular polarization and stringent pattern requirements. Test data from initial models are indicative of successful designs.

VIKING* is the United States effort to soft land twin spacecraft on Mars. The unmanned landers will sense the Martian air, the local environment, take pictures, seek life forms, and transmit their findings to earth during a three-month active period. The first of these vehicles will reach Mars on July 4, 1976, in a life-sterile condition. Fig. 1 summarizes the mission.

Each launch configuration will be a spacecraft consisting of an orbiter and a lander** with launch times one month apart in the August-September period of 1975. After an eleven-month earth-Mars transit, each spacecraft will be injected into a Mars orbit and seek a favorable spot for its lander. Each lander will be separated to thrust its way into an entry trajectory, will be slowed by a deployed parachute, and then gently dropped to the hostile Martian surface using its own engines. The orbiters will continue to orbit at altitudes of approximately 1000 miles, collecting their own data and acting as communication relay stations between the landers and earth.

Reprint RE-18-5-19

Final manuscript received February 1, 1973.

* The Viking Program is managed by the Langley Research Center, NASA.

** Martin Marietta Aerospace (MMA) is the prime contractor on the lander.

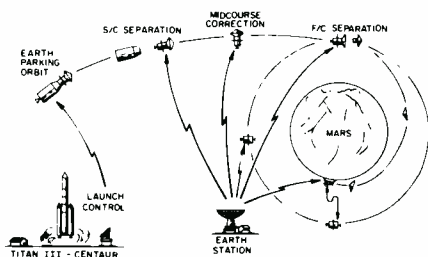


Fig. 1 — Viking mission sequence.

Communication system

Two communication routes are available to handle transmission between the lander and earth. One is via the orbiter, which receives at 381 MHz from the lander and transmits to earth at 2300 MHz. [All frequencies quoted in this paper are nominal.] This route is the only link during the period from separation to landing, and the prime link after landing. The second route is a direct earth-lander link: up at 2100 MHz and down at 2300 MHz. This is the backup link for data after landing and throughout the three-month-long Martian operation. Commands to the lander are carried only over the direct S-band link.

The direct Earth-Mars link poses severe problems. The nominal distance is 125-million miles with a round trip signal travel time of about 25 minutes. Mars has a daily rotation rate nearly the same as that of earth. Thus, either a broad-pattern, low-gain, fixed-beam antenna or a narrow-pattern, high-gain, steered-beam antenna can be used. The Viking direct link uses the former for initial receive and the latter for transmit and receive. The relay link also uses a low-gain, broad-pattern, fixed-beam antenna to cover the lander attitude variations during entry and the changing position of the orbiter both during lander entry and after landing. Fig. 2 illustrates the lander on Mars and the location of the three communication antennas.

Antenna system

The three communication antennas are designated by type:

- S-band high-gain antenna (HGA)
- S-band low-gain antenna (LGA)
- UHF low-gain antenna (LGAA)



Fig. 2 — Lander deployed for operation.

Design and development of these antennas is the responsibility of MSRD as part of the communications subsystems which AED is handling for the Viking Program [under subcontract from Martin Marietta Aerospace]. The HGA configuration is based upon previous RCA space program antennas: the Lunar Orbiter, the Lunar Excursion Module erectable antenna for Apollo, and the Apollo Lunar Communication Relay Unit antenna. The configuration common to the LGA and LGAA is a new concept. The designs of all three antennas trade heavily upon techniques and knowhow derived from RCA's space antenna experience.

The Viking mission includes a new environment, however, and has particular difficulties differing in important aspects from previous space communication systems.

These in brief are

- 1) Sterilization by high temperature soak prior to launch;
- 2) Transmission during Martian entry; and
- 3) Two-axis steerable antenna operation under high wind and dust conditions.

The first difficulty — heat sterilization — dictates careful material choice. Transmission during Martian entry by the LGAA antenna presented a difficult power-breakdown problem. The need for full hemisphere steering of the HGA on the Martian surface during dust-storm conditions and during the extreme temperature range of the Martian day has added several new constraints to those of past space antennas.

High-gain antenna

Configuration

The basic configuration selected for the HGA is based on a series of mission, communication, and antenna studies carried out during a period of more than eight years. The frequency, gimbal arrangement, type and size of antenna, and orientation logic were major choices. The minor choices were reflector, feed and transmission line type, drive and

Table I — Performance specifications high-gain antenna.

	Transmit	Receive
Frequency (MHz)	2790 to 2800	2110 to 2120
Gain (dB, min.)	22	21
VSWR (max.)	1.2	1.4
Polarization		Right hand circular
Axial ratio (dB, max.)		
0°	1.5	4.0
5°	3.0	4.0
Beamwidth (°, min.)		
-3 dB	11.5	—
-1 dB	6.4	—
Sidelobes (dB, min.)	22	22
Power (W, max.)	40	—
Step increment (° command)		0.3
Step rate (° S)		3.6
Angle readout accuracy (bits)		10
Weight (lb, max.)		16.7
Reflector size (in., dia.)		30
Temperature, sterilization (°F)		+280
Temperature, Mars (°, max.)		+145
Temperature, Mars (°F, min.)		-195
Wind, Mars (mi. hr. max.)		160

mechanism type, and orientation readout type.

Fig. 3 is a photograph of the HGA; Table I lists the performance characteristics. The radiation aperture is a front-fed parabolic reflector. It is oriented by an elevation-over-azimuth type of gimbal arrangement. Gimbal axis and reflector offsets are kept small to minimize wind and static mass unbalance torque. The two drive and resolver-readout mechanisms are contained in the common housing immediately to the rear of the reflector. A short mast supports the drive-reflector assembly. The pattern is steered by on-board computer-generated commands to initially acquire and then maintain pointing at the earth.

Antenna mechanisms

The antenna, when deployed on Mars, is directed to point at the earth during its visible periods, to establish a communications link. This link can then be maintained with low angular velocities about either of the antenna axes. However, torques from the high winds in conjunction with low peak and average available electrical power narrows the choice of suitable drives. The long-duration high-vacuum flight to Mars and the wear during the 90-day surface operation made the choice of a lubricant-drive system difficult. After numerous tradeoff studies, a modified stepper motor was selected in conjunction with a high-ratio spur-gear train.

The stepper-motor modification consists of increasing the normally undesirable residual magnetic torque present when de-energized. The residual or detenting

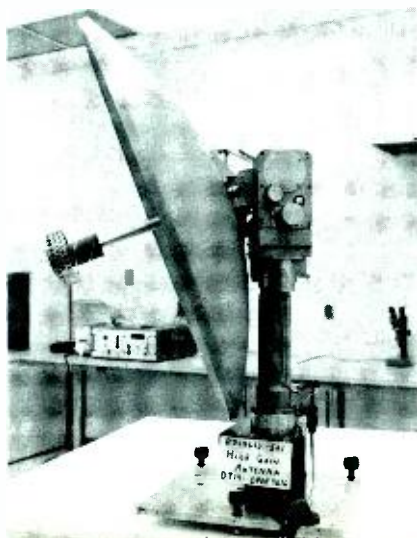
torque is increased to a level such that the wind torques will not cause antenna motion when drive power is off. This feature minimizes power drain. Other schemes such as worm gearing could accomplish the same result, but at the expense of considerable frictional and rubbing abuse of the lubricant not obtained with spur gears.

The motor turns 90° each time a current pulse is applied; in this case, a train of four pulses is generated by a command. With the 1195:1 gear ratio used, one command moves the antenna approximately 0.3°, and the motor is capable of executing at least two commands per second. The antenna uses identical drives in each of the two axes. In addition to the stepper motors, each axis includes a standard resolver to obtain angle data. A four-mesh straight spur gear train connects a motor to its load.

Mechanically, the design is similar to other space hardware. However, the mission time duration and temperature range impose unusual problems with regard to thermal expansion and lubricant life. The differential expansion problem posed by the extreme temperature range (-195°F to +280°F) was solved by selection of aluminum alloy 4032 for the gear box and A286 stainless steel for all gears. The bearings are of 440C stainless steel. In addition, the bearing and gear mesh clearances were made as large as possible, within the allowable antenna pointing error, to avoid jammed gear meshes or overloaded bearings.

The gear lubricant consists of a molybdenum disulfide and binder coating (Ball Bros., Type II) applied to gear teeth with abnormally large face widths to obtain low stress and thereby a long-lived lubricant. The bearings are

Fig. 3 — High-gain antenna (HGA).



lubricated with pure MoS₂, applied by a sputtering process to maintain thin highly adherent films on the bearing races.

Two flexible RF cables cross the limited travel (112") of the elevation axis. For the larger azimuth-axis travel (676"), a cable wrap scheme is used for one (sampler) RF cable as well as the signal leads serving the motors and resolvers. The prime signal-path line uses a non-contacting RF rotary joint.

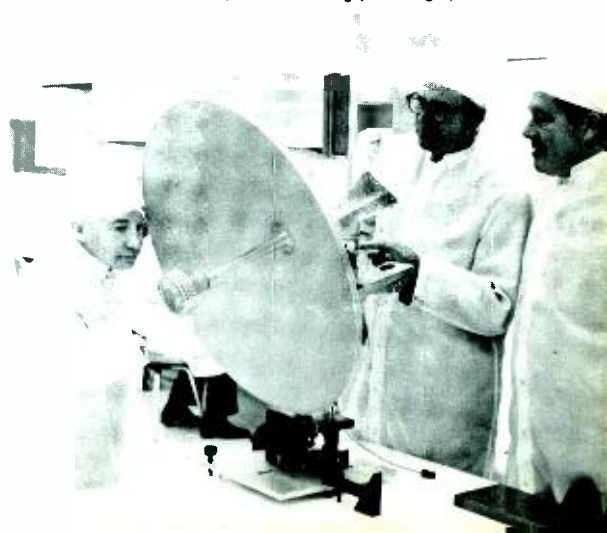
Although weight limited, the antenna

Mr. Wilkinson's biography appears with his other article in this issue.

Oakley M. Woodward, Jr., Radiation Equipment Engineering, Missile and Surface Radar Division, Moorestown, New Jersey received the BSEE from the University of Oklahoma in 1938. From 1938 to 1941 he was employed by the Seismographic Service Corporation of Tulsa, Oklahoma involved in US and foreign geographical exploration. He joined RCA in 1941 as a research engineer at the RCA Manufacturing Company in Camden. In January 1942 he became a member of the technical staff at the RCA Laboratories in Princeton, engaged in research in antenna technology. This assignment continued until 1940, when he transferred to the Missile and Surface Radar Division as a staff member in the antenna skill center. Since that time he has been active in research, design, and development of antennas and microwave components and has served as a consultant to other divisions on special antenna problems. Mr. Woodward has published more than 50 technical papers and reports on antenna and microwave topics, and has had 22 patents issued in his name. He received four special awards at the RCA Laboratories for outstanding work in research, and is the recipient of the 1971 MSRD Annual Technical Excellence Award for his work in development of the Viking antennas and other specialized antenna developments.

Wayne A. Harming, Radiation Equipment Engineering, Missile and Surface Radar Division, Moorestown, New Jersey received the BS in Aeronautical Engineering from the State University of Iowa in 1951. He received the MS in Applied Mathematics from Adelphi University in 1959. For two years he was employed by the McDonnell Aircraft Corporation in design of helicopter control systems. From 1953 to 1959 he worked for the Republic Aviation Corporation in the aircraft dynamic analysis section. Mr. Harming joined RCA in 1959 and was assigned to the instrumentation radar section as a pedestal and mechanisms engineer. He was responsible for the development of hydraulic drives for these radars and he received a patent on a mechanical drive system arrangement. He has been heavily involved in the design of airborne and space antennas including three antennas used on the Apollo program.

Authors Wilkinson, Woodward, and Harming (left to right).



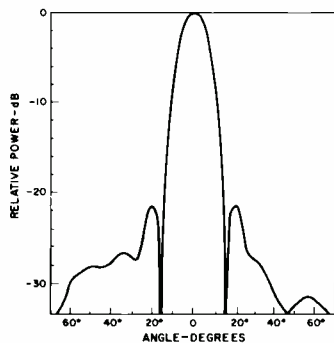


Fig. 4 — HGA radiation pattern.

must achieve a minimum 25-Hz resonance when deployed to avoid interference with a seismometer experiment.

RF system

The technique and types of component being used in the RF system are well proven by previous use in space programs. An air coaxial line is combined into the mast with a non-contacting-choke azimuth rotary joint located within the azimuth drive mechanism. The teflon core flexible line which carries the signal across the elevation axis has a one-turn loop to relieve strain at low temperatures. A 30-dB coupler, used for checkout testing, is contained in the feed assembly coaxial line and consists of a simple resistive-terminated loop. The sampled signal is carried around the azimuth axis in the control cable wrap and down the mast in a small diameter coaxial line.

The feed is a helix type with a tapered dual winding. This winding, with a cylindrical-cup ground plane, generates a circularly polarized excitation with good axial ratio and an excellent symmetry. The cup has been perforated to reduce weight and to prevent Martian dust build-up. A printed-circuit board contains matching elements and a power-splitting balun for driving the two windings from the coaxial feed line.

Although this type of feed is simple and reliable for generating circular polarization, it interacts with the re-radiation from the main reflector, affecting axial ratio. This effect becomes more serious for relatively low-gain reflectors

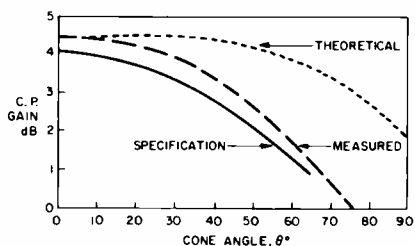


Fig. 5 — Coverage of low-gain antennas.

Table II — Specification highlights, low-gain antennas.

	S-Band LGA	UHF LGAA
Frequency (MHz)	2110-2120	381 ± 2
Gain (dB)		
0° cone angle	4.0	4.0
±65° cone angle	0.8	0.8
±90° cone angle	—	-4.0
Polarization (dB)	RH circular	RH circular
Axial ratio (dB)		
0°	1.5	1.5
±65°	4.5	4.5
±90°	—	8.0
VSWR (max.)	1.3	1.2
Power handling (W)	—	60
Signal sampler		
Coupling (dB)	20 ± 3	—
Directivity (dB)	27	—
Weight (lb. max.)	0.8	4.0

such as this. The feed location can be set optimally for narrow band operation, but a compromise position must be picked for the frequency range here required. This has been done, with the transmit band favored. A typical radiation pattern of the HGA is shown in Fig. 4.

Storage and erection

The HGA is stowed along the side of the lander within a restricted envelope. A pyrotechnic pin puller device is mounted on a hinged link to prevent angular motion about the antenna elevation axis and the deployment hinge axis. A pair of tabs on the link mate with the antenna to prevent angular motion about the azimuth axis. The spring-driven erecting mechanism at the deployment axis, the pyrotechnic device, and the link are separately supplied devices. The stowage arrangement provides direct load paths for the more severe loading conditions such as launch/boost vibration or Mars landing shock, while preventing exposure of the antenna drive trains to these loads.

After release of the antenna by firing of the pyrotechnic pin puller, the antenna is slowly moved to the erect position for operation (Fig. 2). The deployment force is supplied by negator springs at the deployment axis; an escapement mechanism controls the rate of deployment.

Low-gain antennas

Concept

Both the LGAA antenna at UHF and the LGA at S-band must radiate over approximately a hemisphere to satisfy mission needs. Although the patterns will be affected somewhat by location of the antennas on the lander and its nearby objects, the patterns are specified in free

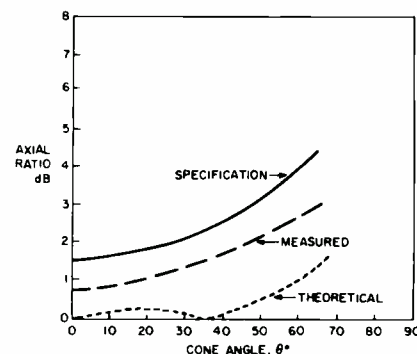


Fig. 6 — Axial ratio of low-gain antennas.

space. Modeling measurements on the lander have shown the order of these effects.

The right-hand, circularly polarized pattern shape and gain, as specified through any planar cut containing the axis of the antenna, are plotted in Fig. 5. The axial ratios are shown in Fig. 6.

Table II lists other specified values for the two antennas. If one integrates this pattern shape over the full sphere, a margin of about 1.25 dB is indicated. This margin must account for variations of the realized pattern shape, losses, axial ratio variations, and measurement errors.

This type of radiation pattern cannot be obtained with the usual Turnstile¹ antenna of crossed dipoles over a ground screen or crossed slots cut in a conducting plane. Both of these antenna types basically generate only radial currents emanating from the antenna center. Theoretical studies² have shown that an additional mode of radiation is required to achieve the desired broadbeam radiation characteristics. This so-called axial mode is an "error" pattern type, consisting of a doughnut shape with its null aligned along the axis of symmetry of the antenna. The relative amplitudes and phases of these two radiation modes may be selected to achieve the specified pattern shapes with a small margin of safety. The dotted curves of Figs. 5 and 6 illustrate the gain and axial ratio

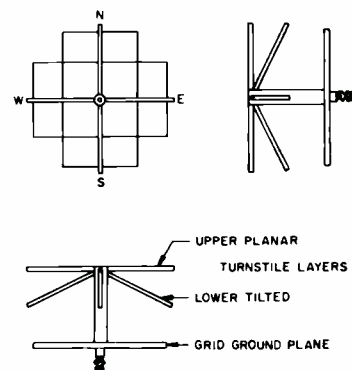


Fig. 7 — Configuration of low gain antennas.

characteristics that can be obtained theoretically under ideal conditions and with a perfect ground plane.

A common geometric design was chosen for both of the low-gain antennas. This is shown in Fig. 7 and consists in effect of two superimposed turnstile antennas spaced above a ground-screen reflector. One of the turnstile layers consists of crossed dipoles aligned parallel to the reflector plane; the other turnstile elements are inclined downward to introduce the axial-mode component parallel to the axis of the antenna. The desired radiation characteristics in the upper hemisphere are achieved by proper choice of the lengths and inclination angles of the radiating elements and their heights above the reflector.

The reflector itself is a tuned wire-grid type developed some years ago at RCA. The geometry and dimensions of the grid-wire configuration, having a maximum size of less than one-half wavelength, are chosen such that suppression of the backward radiation is greater than would be obtained with a much larger continuous sheet of metal. Added advantages are greatly reduced weight and wind resistance.

S-band low-gain antenna

Fig. 8 is a photograph of the first model of the LGA. Quadrature excitation of the orthogonal radiating elements is achieved by methods developed during the present program. For the LGA, a "split-drum" balun is used to feed only the north-south dipoles directly. These same feed terminals are connected to the east-west dipole elements through series condensers. The antenna impedances and condenser reactances are such that the orthogonal currents are equal in amplitude and in phase quadrature. Vernier capacity elements, printed on the protective plastic radome of the antenna, supplement the final adjustments. The circularly polarized gain and axial ratio

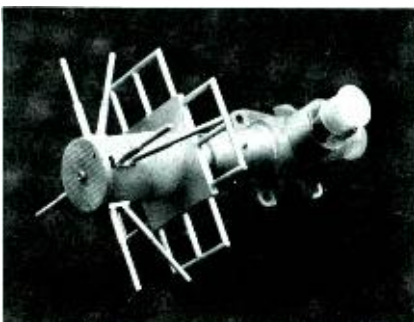


Fig. 8 — S-band low-gain antenna.

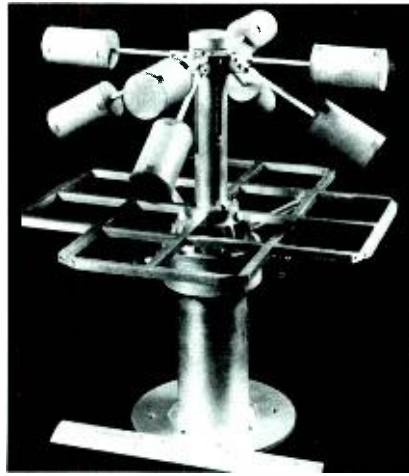


Fig. 9 — UHF low-gain antenna.

characteristics obtained from typical measurements of the S-band low-gain antenna are plotted as the dashed curves shown in Figs. 5 and 6. Measured data for the UHF low-gain antenna is similar to that of the S-band antenna.

UHF low-gain antenna

Fig. 9 is a photograph of the first model of the LGAA. Because the UHF low-gain antenna (LGAA) is physically much larger, the external capacitances are not desirable, because of the added wind resistance and the increased voltage-breakdown problems. For this application, a different approach was developed, consisting of a cylindrical sleeve surrounding the feed balun. Four longitudinal slots are cut in this sleeve with diagonal pairs of slots having different lengths. These slots are filled with dielectric rods to provide greater power-handling capability as well as to prevent entry of Martian dust particles. Vernier adjustments of the slot reactances are provided by small metal tabs attached near the lower ends of the four dielectric rods. The electrical configuration is equivalent to a bridge circuit in which the east-west dipoles are joined across one pair of the bridge output terminals; the north-south dipoles and the power input terminals are joined across the other pair of output terminals, and the bridge legs are made up of alternating inductances and capacitances. This method has an advantage in that circular polarization may be obtained for any value of the dipole-radiation impedance merely by properly adjusting the slot lengths.

Power breakdown

Achieving a reliable power breakdown design for the LGAA proved to be very difficult. Because the antenna operates

during descent to the Martian surface, it passes through the worst-case pressure condition for breakdown. Initial tests showed that the central-feed region and the radiator-tip region were both vulnerable. Measurement difficulties were aggravated by the need to simulate Martian atmosphere, by apparent lowering of breakdown levels due to surface contamination, and by interaction with low-pressure test chambers. Constraints of size and weight also limited the range of solutions.

The high voltage regions of the central feed lines and tuned elements were loaded with teflon and fiberglass-epoxy dielectrics to reduce the atmospheric gradients to tolerable levels. The radiator elements were brought under control by increased rod diameter and by use of metal corona balls on the tips encased within cylinders of polyurethane foam.

Cleanliness

The program goal of biological assay on Mars is reflected in the antenna configuration and program. The choice of materials and the manufacturing and testing of the three antennas must meet stringent requirements on cleanliness. Particular attention has been taken to minimize the presence of organic materials. Pre-assembly cleaning, strict white-room assembly, and protection during test are part of the procedures. All three antennas are enclosed by protective plastic bubbles during RF tests on the pattern range and during transport.

Current status

All three designs have been developed through breadboard stages with performance to specification. The first space hardware versions — Development Test Models — are now in test and are demonstrating successful performance.

Acknowledgment

As in all such programs, many at MSRD have made important contributions. Of special note is the contribution of W.H. Mulguez who is the engineer responsible for all three antennas.

References:

1. Brown, G. H., "The Turnstile Antenna" *Electronics*, (April, 1936).
2. Woodward, O. M., "A Mode Analysis of Quasi-Isotropic Antennas", *RCA Review* (March 1965)

Decoder for delay-modulation coded data

J. Lewin

Delay modulation, originally developed in conjunction with high density digital (saturation) tape recording, combines the advantages of the narrow bandwidth of pulse-code modulation (PCM) nonreturn to zero (NRZ) and the advantages of self-timing information inherent in phase modulation. This paper describes a decoding technique for the conversion of delay-modulation digital data to NRZ (c) data. A potential time-phase ambiguity in reception and decoding of delay-modulated data is resolved in real time, through monitoring the data stream for a unique waveform inherent in delay-modulated data. Statistical backup is provided. Included are logic implementation and timing diagrams.

DELAY MODULATION¹, originally developed in conjunction with high density digital (saturation) tape recording, combines the advantages of both nonreturn-to-zero (NRZ) and phase modulation. In Fig. 1, waves *A* and *B* demonstrate phase modulation in the form of biphasic space or biphasic level. Unlike phase modulation, which has two transitions per bit when viewed at the maximum character rate (consecutive spaces as shown in Fig. 1, waveform *A*), delay modulation requires at most one transition

Reprint RE-18-5-17

The work described in this paper was performed by the Astro-Electronics Division of RCA for the Goddard Space Flight Center of NASA under Contract NAS5-10396.

An earlier version of this paper appeared in **IEEE Transactions on Communication Technology** Vol. COM-19, No. 5 (Oct 1971).

J Lewin

Spacecraft Systems Engineering
RCA Astro-Electronics Division
Princeton, N.J.

received the BSEE from Northeastern University in 1957, the Master of Management Science from Stevens Institute of Technology in 1967, and completed graduate courses in Computer Science at Polytechnic Institute of Brooklyn in 1968. Mr. Lewin has 15 years experience in system design, analysis and testing in digital communications, data processing, command and control, and computer programming and applications. He joined the RCA Communications System Division in 1959, and was assigned to the Advanced Communications Techniques Laboratory where he analyzed Fleet communications for automation of shipboard message processing; developed concepts for secure communications for the Minuteman Command and Control System; directed system studies on synchronization and timing, failure modes, self-verification techniques, communications jamming susceptibility, and tamper resistance. He transferred to the Astro-Electronics Division in 1967 where he has been engaged in the design and development of spacecraft data processing, data collection, command and controls and telemetry subsystems on the ERTS program as well as on classified programs. He also performed system study and definition of a wide-band digital video data buffer for use with RCA's Laser Beam Image Reproducer (LBIR). From 1957 to 1959, Mr. Lewin was employed by the U.S. Army Signal Research and Development Laboratory, where he developed mobile digital computers and computer programs for Army field use.



per bit (see Fig. 1, waveform *C*) and thus permits a higher packing density. Therefore, delay modulation, while requiring approximately the same bandwidth as NRZ modulation² (which is half the bandwidth of phase modulation), affords the advantage of inherent self-timing information of phase modulation not present in NRZ modulation.

A potential time-phase ambiguity exists in the reception and decoding of delay-modulated data when the timing information is extracted from the transitions in the incoming data bits. A clock phase shift of 180° can occur when the receiver synchronizes to the wrong transitions. Proper phasing of receiver clock and data must be ensured at all times for reliable decoding operation.

The following describes the procedure for decoding delay-modulated data.

Delay-modulation-data rules

The rules for encoding digital data, such as NRZ data, into delay-modulated data include the following:

Rule 1: A mark (*M*) is represented by transition (from either level to the other) in the center of the bit cell.

Rule 2: A space (*S*) is represented by no transition except in the case of the two or more consecutive spaces, in which case transitions are placed at the bit-cell edges.

Rule 3: There is no transition at the bit-cell edges when a space is followed by a mark, or vice versa.

A representative waveform, as a consequence of these rules, is shown in Fig. 1, waveform *C*.

Mark detection

Marks are uniquely defined as transitions at the center of a bit (Rule 1). This characteristic of delay-modulated data is used in the following decoding scheme.

Detection of marks or transitions at the center of a bit can be accomplished by comparing the two levels of the half-bits within the bit cell. If the two half-bit levels within the bit cell are different, then the bit is a

mark. If the two half-bit levels are the same, then the bit is a space.

In the decoder, this comparison is accomplished by

- 1) Delaying the delay-modulated data (Fig. 2, line B); and
- 2) Modulo-two addition of the incoming data (Fig. 2, line C) with the delayed data.

Line A represents the incoming phase-delay data. The delay in line B is one-quarter of a bit period and is achieved through timing T_E .

It should be noted that for every transition in the incoming data (Fig. 2, line A), a pulse one-quarter bit wide is generated in line C. Inspection of line C shows that the pulses generated correspond to the marks and consecutive spaces. Predictably, the pulses corresponding to the marks occur toward the middle of the mark bit cell (third quarter), whereas the pulses corresponding to the consecutive spaces lies at the edge of the space bit cell (first quarter).

To separate the mark transitions from the space transitions, line C is inspected with a clock pulse lying in the third quarter of the bit cell, and is one-quarter bit wide. Thus, the logical product of line C and line D will yield one-quarter-bit RZ pulses representing marks (line E), which correspond to those marks in the original data.

Space detection

The ambiguous definition of spaces requires detection (or regeneration) by inference. Inspection of line C (transition pulses) and line D (clock) shows that while a coincidence of inspection pulses exists corresponding to marks in the data, no coincidence of pulse exists between line D and line C corresponding to spaces in the data. The logical product of the inverse of line C (line C') and line D, therefore, will result in properly sequenced pulses corresponding to spaces. This result is shown in line F.

NRZ (c) generation

The next step is the generation of NRZ (c) data, which requires a flip-flop (FF). Using line E (marks) to set the FF and line F (spaces) to reset the FF will generate the required NRZ (c).

Logic implementation

Fig. 3a is a logical implementation of the described delay modulation to NRZ converter. Emphasis was given to the minimization of crossover spikes (hazards). This implementation requires two flip-flops, three 2-input gates, and one or two inverters, depending on the availability of the inverse of the data input.

In addition to the basic decoder, Fig. 3 contains timing generation and control circuitry as well as phasing-error detection circuitry. These are discussed in subsequent paragraphs.

Timing generation

The circuitry in Fig. 3b generates the necessary timing. It is assumed that an in-phase bit-rate clock and a 90° out-

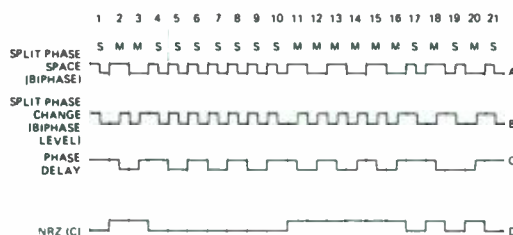


Fig. 1—Pulse-code-modulation waveform comparison.

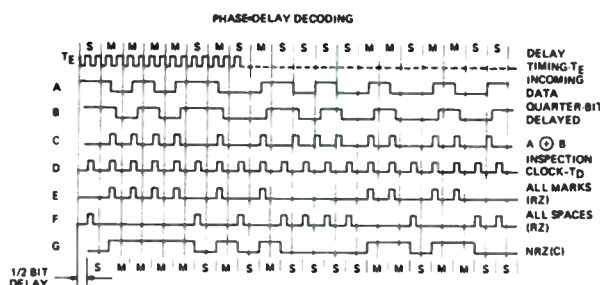


Fig. 2—Delay-modulation to NRZ conversion—timing diagram.

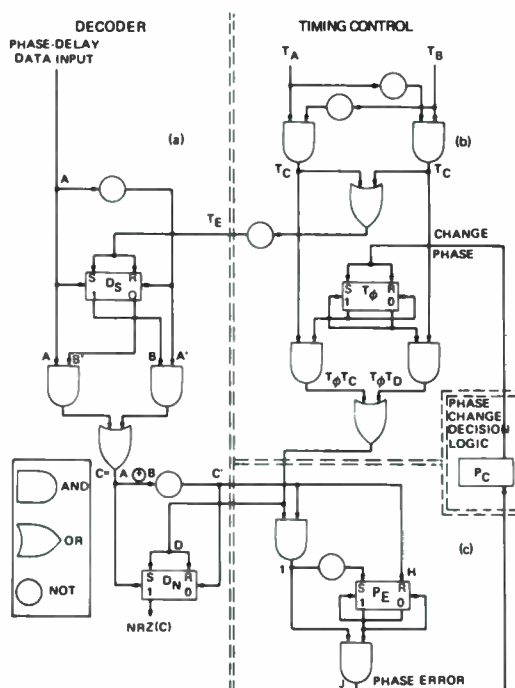


Fig. 3—Delay-modulation to NRZ converter—logic diagram.

of-phase bit-rate clock are the available inputs. These input clocks are illustrated in Fig. 4 as T_A and T_B . The phase modulation to NRZ converter requires three clocks for its operation. A clock (50% duty cycle) at twice the bit rate and 180° out of phase with the input data (T_E , Fig. 4) is used to delay the input data by one-quarter bit (see Fig. 2, line A and T_E) by re-clocking the input data at $FF D_s$ (Fig. 3).

Two additional clocks (25% duty cycle, first and third quadrant T_C and T_D , Fig. 4) are required for transition sampling (line D, Figs. 2 and 5), one each, for the two possible input phasing conditions.

All the timing is generated from inputs T_A and T_B with three 2-input AND gates and three inverters. (Two of the three inverters are needed only if inverses of T_A and T_B are not available as inputs.)

Phasing

The timing information inherent in delay-modulated data contained in the transitions is ambiguous. Recall that transitions occur at both the center of each bit, which is a mark, and at the ends for consecutive space bits. Should the local receiver phase up to the wrong transitions, that is, one-half bit out of phase, the resultant NRZ (c) output would be in error.

Inspection of the waveform shown in Fig. 1, line C indicates that consecutive marks and consecutive spaces are identical in waveform and are only distinguished from one another by reference to receiver timing; that is, by defined bit-cell edges. Similarly,

the space-mark and mark-space waveforms offer no uniqueness when displaced by one-half bit.

The only unambiguous waveform in delay-modulated data is a mark-space-mark (101) bit combination. Under phase shift, this combination results in an "illegal" waveform. When examined by the converter, this waveform will decode as two consecutive spaces (00) in place of mark-space-mark (101); this fact is used for phasing-error detection.

Phase-error detection

Delay-modulated data, when subjected to a phase shift of one-half bit from the correction reference will, upon conversion to NRZ data, result in the incorrect decoding of the input data to $(n-1)$ marks for (n) consecutive spaces, and spaces for all other bit combinations. This result is illustrated in Fig. 5a, line G. Examination of the space line (line F) and the data line (line A) on Fig. 5a and comparison with the corresponding lines in Fig. 2, shows the following.

Under correct phasing (Fig. 2), the number of spaces occurring on the space line (line F) and bracketed by the interval defined by the waveform MSM (101) on the data line (line A) is, as expected, one space.

Under condition of phase error (Fig. 5a), the number of spaces occurring on the space line (line F) and bracketed by the internal MSM (101) on the data line (line A) is, as observed earlier, two spaces.

No other occurrence of two spaces bracketed by any other interval can be found, regardless of phasing. This

unique condition facilitates phase-error detection.

Fig. 5b shows the pertinent timing corresponding to the implementation shown in Fig. 3c. In Fig. 5b, line H defines the waveform intervals of the incoming data (transition pulses). Line I represents the erroneously decoded spaces. Line K give the resultant phase-error pulse for each condition where two decoded spaces are bracketed by a given input waveform as defined by line H; that is, for every mark-space-mark (101) input.

Detector implementation

The phasing-error detector consists of one FF, two 2-input AND gates, and one inverter. The error detector FF P_E is reset ($P_E=0$) by each leading edge of the waveform shown in line H. The inverse of line I (I') is used to set FF P_E ; that is, P_E is set ($P_E=1$) by the trailing edge of each pulse in line I. An output (shown as line K), denoting a phasing error, will occur when $P_E=1$ (line J is high) and the presence of a pulse in line I.

Thus, a phasing error having occurred, the phasing-error detector will generate an output pulse (line K, Fig. 5) every time a mark-space-mark (101) bit combination occurs in the data.

Phase-error correction

Having determined that a phase error has occurred, it becomes a matter of sampling the modulo-two product [Fig. 5a, line C] with a clock that is displaced by one-half bit from the original sampling clock (replace T_D with T_C , see Fig. 4) to correctly decode the incoming data.

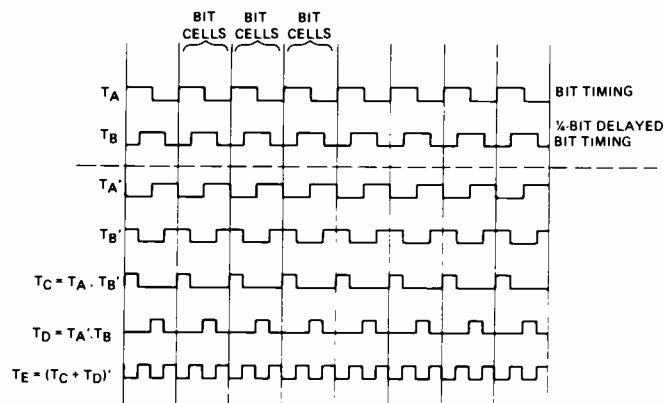


Fig. 4—Decoder timing diagram.

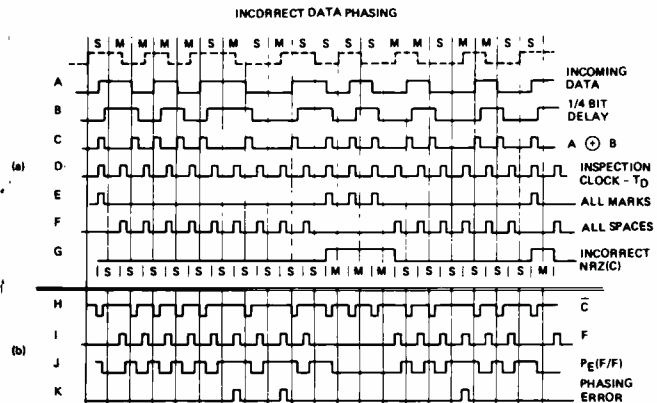


Fig. 5—Phase-error detection—timing diagram.

Fig. 3b, labeled "timing control," selects the correct sampling clock as a function of the indications received from the error detector; that is, a phase-error pulse will toggle flip-flop T_0 and change the sampling timing by gating to the decoder either T_r or T_v clock (applied to FF D_n for the modulo-two output sampling). Correct decoding will ensue. The decoder will thus track the correct input phase of the data. Phasing recovery within less than 1-bit time is possible.

The implementation of the "phase-change decision logic" (Fig. 3) is a function of the noise susceptibility of the phase delay to NRZ converter and the corresponding bit error rate; that is, the probability of generating mark-space-mark due to noise as well as the probability of occurrence of the required mark-space-mark (101) bit combination (P_m) in the input data bit stream.

At low bit-error rates, it may be desirable to integrate over a given interval of two or more detected phasing errors, to preclude unnecessary decoder rephasing due to bit errors. The phase-change decision logic could be implemented to change phase within the desired number of detected errors.

Assuming incorrect phasing due to initial mis-synchronization (acquisition) or single-bit errors, recovery is determined by the frequency of occurrence of 101-bit combinations in a given input bit stream and the phasing-error indications required to activate the phase-change decision logic (see Fig. 3). The periodic occurrence of 101 in a given bit stream can be guaranteed by the deliberate introduction of the 101 configuration: for example, word sync, containing the 101-bit combination(s). Thus, for a word length of m bits and containing a single 101, a worst case recovery is guaranteed with $(m+3)$ bits, assuming that a single phase-error indication per unit time is needed to generate a change-phase command. If an arbitrary number, n , of phase-error indications per unit time are required to generate the change-phase command, guaranteed recovery will take place within $n(m+3)$ bits.

The preceding discussion ignores the occurrence of 101-bit combination in the data.

Assuming randomness of the data bit stream, the probability of occurrence of one or more 101-bit configurations is relatively high and increases rapidly as m , the number of bits in the data word, increases. Fig. 6 shows the probability of k or more ($K=1, 2, 3, 4$) 101-bits in a random bit stream of m bits. As can be seen on Fig. 6, for $k=1$ and $m=10$, the probability of one or more (101's) is 65.7% (within 10 bits). For 30 bits ($m=30$), the probability of occurrence of one or more 101-bit configurations is 97.5%. Therefore, the implication is that for most applications, reliance of the random occurrence of 101's to maintain proper phasing is feasible; that is, no deliberate periodic insertion of 101's is needed. Transmission efficiency is thus increased.

The equations used to generate the curves on Fig. 6 were derived by observation of the truth table. The validity of the equations has been verified manually for $m=3, 4, 5, \dots, 11$ bits. The equations are as follows.

For $k=1$,

$$P_m[101 \geq 1] = \frac{1}{2^m} \sum_{i=3}^m (a_m)_i,$$

$$a_m = 2^{m-3} + a_{m-1} + \sum_{i=3}^{m-3} (a_m)_i,$$

where P_m is the probability of occurrence of k or more 101-bits in a random bit stream of length m and a is the number of m -bit words where k or more 101-bits occurred.

For $k=2$,

$$P_m[101 \geq 2] = \frac{1}{2^m} \sum_{i=5}^m (b_m)_i,$$

$$b_m = b_{m-1} + a_{m-2} + \sum_{i=5}^{m-3} (b_m)_i.$$

Table I—Probability calculations

m	2^{m-3}	a_{m-1}	$\sum_{i=3}^{m-3} (a_m)_i$	a_m	$\sum_{i=3}^m (a_m)_i$	2^m	p_m
3	1	0	0	1	1	8	0.1250
4	2	1	0	5	4	16	0.2500
5	4	3	0	7	11	32	0.3439
6	8	7	1	16	27	64	0.4220
7	16	16	4	36	63	128	0.4920
8	32	36	11	79	142	256	0.5550
9	64	79	27	170	312	512	0.6094
10	128	170	63	361	675	1024	0.6572
11	256	361	142	759	1452	2048	0.6992
12	512	759	312	1583	3015	4096	0.7361
15	1024	1583	675	3280	6295	8192	0.7684
14	2048	3280	1452	6760	13055	16384	0.7968
15	4096	6760	3015	13871	26926	32768	0.8217

$$p_m[101 \geq 1] = \frac{1}{2^m} \sum_{i=3}^m (a_m)_i, \quad m \geq 3, \quad \text{where} \quad a_m = 2^{m-3} + a_{m-1} + \sum_{i=3}^{m-3} (a_m)_i \quad (m-3) \geq 3.$$

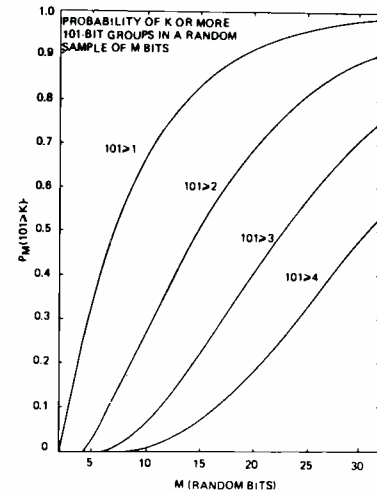


Fig. 6—Phase error detection—probability curves.

For $k=3$,

$$P_m[101 \geq 3] = \frac{1}{2^m} \sum_{i=7}^m (C_m)_i,$$

$$C_m = C_{m-1} + b_{m-2} + \sum_{i=7}^{m-3} (C_m)_i,$$

Table I shows some sample calculations.

Phase-change decision logic

The logic configuration and the necessary algorithm for the operation of the phase-change decision logic would have to be obtained empirically and be based on results of error-rate testing of the phase delay to NRZ converter. The propensity, if any, of phase-delay modulation to the generation of 101-bit configurations when subjected to noise will determine the reliability of operation of the phase-delay to NRZ converter.

References

1. G. Jacoby, U.S. Patent 3 414 894, Dec. 5, 1968.
2. M. Hecht and A. Guida, "Delay modulation," *Proc. IEEE (Lett.)*, vol. 57, July 1969, pp. 1314-1316.

Simple analytical model for the envelope distribution of a sinusoidal carrier in atmospheric radio noise

C. V. Greenman

Charles V. Greenman

Electronic Warfare Systems
Communication Systems Division
Government and Commercial Systems
Camden, New Jersey

received the BSEE with High Honors from Michigan State University in 1959 and the MSEE from the University of Pennsylvania in 1962. Since joining the Communication Systems Division in July of 1959, he has worked in the field of the propagation of ELF and VLF radio waves. On a number of classified Government contracts, he also contributed analyses dealing with communication techniques for multipath channels, spread-spectrum anti-jam systems, FM system optimization, and the performance of matched-filter signal processing systems in a randomly refractive and absorptive plasma channel. In 1965 Mr. Greenman joined the technical staff of the Communication Research Laboratory, RCA Laboratories, Princeton where he worked on the U.S. Navy's Project SANGUINE, a major government contract dealing with Polaris communications. He contributed a cost-effectiveness study comparing a number of long-range communication modes for the weapon force and assisted in preparing a state-of-the-art summary report for advanced naval communications concerning HF data transmission techniques. Since joining the Electronic Warfare Systems activity of Camden in late 1970 he has contributed an analysis of end-to-end performance for the *La Faire Vite* proposal effort and performed studies in support of a VLF signal processing system. Mr. Greenman is a charter member of the Honors College of Michigan State University (1957) and is a member of Eta Kappa Nu and Tau Beta Pi.

A recent article by Omura and Shaft¹ proposed modeling atmospheric radio noise as a narrowband process having a log-normal envelope distribution. Based on such a model, an approximate expression is derived for the envelope probability distribution of a sinusoidal carrier in atmospheric radio noise. The results are compared with measured distribution of the instantaneous amplitude out of a wideband envelope detector (Watt and Plush), and show good agreement over the range of input carrier-to-noise ratios for which measurements were made.

MOST INFORMATION AVAILABLE ON atmospheric radio noise is in the form of measured data on the envelope (RMS value and amplitude probability distribution, APD, as specified by the RMS-to-average noise voltage ratio, V_a). Models for the noise process have been based in the past on graphical displays of the APD. Little measured data exists on the combination of signals and atmospheric radio noise.²

Several analytical models for the instantaneous noise process have appeared in recent years that give good

agreement with the measured first- and second-order statistics of atmospheric noise. In this paper, one of these analytical models is described, and the statistics of the carrier-signal envelope in atmospheric radio noise are derived. The expression derived for the amplitude distribution applies for high exceedence probabilities—those that are of main interest in a practical sense (*i.e.*, detection probabilities greater than 50%).

Following Omura and Shaft¹, the noise-voltage model ("Log-Normal Noise Model") is given by

$$a(t) = A \exp[n(t)] \cos[\omega t + \theta(t)] \quad (1)$$

where $n(t)$ is the Gaussian noise process, zero mean, and variance σ^2 (σ^2 is related to the parameter V_a by the rela-

Reprint RE-18-5-3

Final manuscript received September 27, 1972

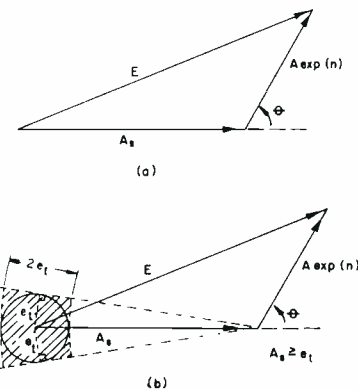


Fig. 1—Phasor diagrams showing the relationship of the envelope to the instantaneous carrier (A_s) and noise (A) amplitudes, and the random relative phase angle (θ).

tion $V_d = 10\sigma^2 \log_{10}(e)$ where e is the natural logarithmic base; and $\theta(t)$ is the random phase process, independent of the Gaussian noise $n(t)$, uniformly distributed $(0, 2\pi)$.

The instantaneous RMS level of the noise is simply $A \exp(\sigma^2) / 2^{1/2}$, while the envelope RMS level is $A \exp(\sigma^2) - 3$ dB above the instantaneous RMS level.

If $E(t)$ is the envelope of a sinusoidal signal $(A, \cos \omega t)$ plus atmospheric noise $a(t)$, one can easily show that

$$E^2(t) = A_s^2 + 2AA_s \exp[n(t)] \cos \theta(t) + A^2 \exp[2n(t)]$$

or abbreviating,

$$E^2 = A_s^2 + 2AA_s \exp(n) \cos \theta + A^2 \exp(2n) \quad (2)$$

where n and θ are independent random variables.

The last equation can be shown in phasor form noting its similarity to the Law of Cosines formula [Fig. 1a].

For the moment, let us concern ourselves only with the case where A_s is greater than some envelope value e_i and we wish to determine $\text{Prob}(E > e_i)$. This can be diagrammed as in Fig. 1b. First we approximate the probability that the random variable E falls within the circle of radius e_i , i.e., $\text{Prob}(E \leq e_i)$, by the probability that E falls within the shaded rectilinear area shown, and then $\text{Prob}(E > e_i) = 1 - \text{Prob}(E \leq e_i)$. The probability that E lies in the shaded area requires θ to be in an angular sector of $2 \sin^{-1}(e_i/A_s)$ radians simultaneously as $A \exp(n)$ lies in the range $(A_s - e_i) \leq A \exp(n) \leq (A_s + e_i)$. The second relation can be expressed as

$$\ln[(A_s - e_i)/A] \leq n \leq \ln[(A_s + e_i)/A] \quad (3)$$

Consequently,

$$\text{Prob}(E > e_i) \approx 1 - \frac{1}{\pi} \sin^{-1}(e_i/A_s) \left\{ \Phi\left(\frac{\ln[(A_s + e_i)/A]}{\sigma}\right) - \Phi\left(\frac{\ln[(A_s - e_i)/A]}{\sigma}\right) \right\} \quad (4)$$

subject to the constraint $A_s \geq e_i$, where

$$\Phi(x) = (2\pi)^{-1/2} \int_{-\infty}^x \exp(-u^2/2) du$$

(Standardized Normal Distribution Function).

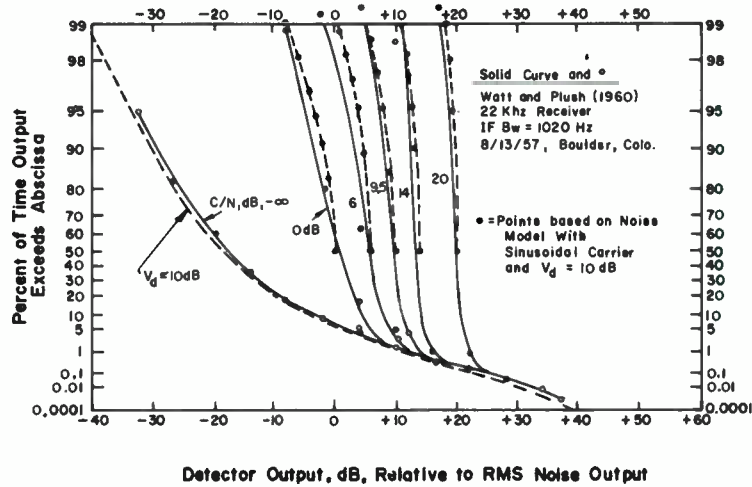


Fig. 2—Cumulative distributions of detector output for various ratios of carrier to atmospheric noise.

Using the foregoing relationships, the exceedence probability for the envelope of a carrier plus atmospheric noise can be written

$$\text{Prob}(\rho > \rho_0) \approx 1 - \frac{1}{\pi} \sin^{-1}(\rho_0/\rho_i) \left\{ \Phi\left(\frac{\ln(\rho_i + \rho_0) + \sigma^2}{\sigma}\right) - \Phi\left(\frac{\ln(\rho_i - \rho_0) + \sigma^2}{\sigma}\right) \right\} \quad (5)$$

where

$$\rho_i = A_s / [A \exp(\sigma^2)] \quad (\text{the instantaneous RMS carrier-to-noise ratio}) \quad (5a)$$

$$\rho_0 = e_i / [A \exp(\sigma^2)] \quad (\text{the envelope of the carrier plus atmosphere noise, normalized by the RMS level of the noise envelope}) \quad (5b)$$

subject to the constraint $\rho_0 \leq \rho_i$.

One may consider Eq. 5 as approximating the exceedence probability distribution for the output signal-plus-noise-to-RMS-noise ratio ρ of a wideband envelope detector having an input RMS carrier-to-noise ρ_i , where the atmospheric radio noise is characterized by an envelope RMS-to-average ratio of V_d dB. Direct comparisons can be made, therefore, with the measurements of Watt and Plush.³

Fig. 2 compares the empirical data of Watt and Plush with values computed using the foregoing equation. The

curve shown for $C/N \rightarrow -\infty$ dB represents the detector output for atmospheric noise alone (no carrier signal). Comparing such curve with CCIR Report 322,⁴ a value for V_d of approximately 10 dB has a probability distribution (shown by the dashed line), which agrees reasonably well with the measured data. The computed points for a sinusoidal carrier in atmospheric noise based on the analysis given here show good agreement with the measured detector output distributions over the range of input carrier-to-noise ratios considered. As mentioned previously, the derived equation for the detector output amplitude probability distribution is valid for exceedence probabilities greater than 50%.

References

1. Omura, J. K., and Shaft, P. D. "Modem Performance in VLF Atmospheric Noise," IEEE Trans. Commun. Technol., vol. COM-19, No. 5, October 1971, pp. 659-668.
2. The data of Watt and Plush for the wideband detected envelope of a carrier in atmospheric noise ($V_d \approx 10$ dB) are, to the author's knowledge, the only information available; see Watt, A. D., and Plush, R. W. "Measured Distribution of the Instantaneous Envelope Amplitude and Instantaneous Frequency of Carriers Plus Thermal and Atmospheric Noise," in *Statistical Methods in Radio Wave Propagation*, W. C. Hoffman, Ed. (New York: McGraw-Hill, 1967) pp. 544-551.
3. See the previously cited reference 2, or Watt, A. D., *VLF Radio Engineering* (London: Pergamon Press; 1967) pp. 544-551.
4. Documents of the Xth Plenary Assembly, "World Distribution and Characteristics of Atmospheric Radio Noise" (CCIR Report 322; Published by the International Telecommunication Union; Geneva; 1964). Pergamon Press; 1960) pp. 233-247.

RCA — MIT Research Review Conference

W. O. Hadlock, Editor

The information summarized in this article has been compiled from notes, information provided by the speakers, and recordings made during the MIT-RCA Seminar. In some cases, more information is available.

AT A RECENT RCA-MIT conference, selected faculty of Massachusetts Institute of Technology, Cambridge, Mass., conducted a special two-day seminar for the benefit of about 60 RCA research, engineering, and technical planning personnel. Discussed during the sessions was current progress being made in areas of contemporary research, preselected topically by RCA for consideration. The seminar is only one of the various services being provided by MIT under the RCA-MIT Industrial Liaison Program agreement.

RCA is one of about 100 companies presently participating in the Industrial Liaison Program. In return for an annual fee, RCA obtains the potential of quick access to and an active communications channel with research programs that align with RCA's current and possible future business interests.

The two-day briefing highlighted oral presentations by MIT faculty members and question-answer discussions concerning several areas of major research being conducted by MIT.

Topics at the conference included the areas of 1) materials and devices, 2) applications of computer systems and 3) marketing and management.

Summaries of presentations

The summaries reported in the following pages are intended to provide a general overview of the technical presentations; additional information and details may be available from Frank W. Widmann, Manager, RCA Engineering Professional Development, Corporate Engineering Services Programs or by direct contacts with MIT personnel through J. Peter Bartl, MIT's Industrial Liaison Officer.

Supplements RCA program

RCA's own research program is aimed primarily at supporting the most critical needs of the Company in currently identified business areas. However, many important areas of research and advanced technology that also merit continued study must be bypassed because of economic priorities and limitations.

Thus, the MIT research program supplements the RCA program and complements it where RCA has the need for awareness but has not invested directly.

ILO office

MIT administers the program through an Industrial Liaison Office (ILO), staffed by Industrial Liaison Officers. One of the six officers, J. Peter Bartl, is assigned to interface with RCA in rendering the services available under the program. Mr. Bartl maintains direct contact with key people in each of RCA's divisions, and with Frank W. Widmann, who administers the Program at RCA.

Benefits entire technical staff

RCA engineers and scientists in all areas are eligible to benefit from the services provided under the MIT-RCA Industrial Liaison Program (see summary of concluding remarks by J. Peter Bartl).

Acknowledgements

Credit is given to Hans K. Jenny, Mgr., Microwave Solid-State Devices Operations, Electronic Components, Harrison, N.J.; who provided the Editors with copious notes. The photographs for this article were provided by Frank W. Widmann, Mgr., RCA Engineering Professional Development, Corporate Engineering Services. Special thanks also to be Conference speakers and J. Peter Bartl, MIT-RCA Industrial Liaison Officer.

Photos show some of participants at the special two-day research and business review seminar. Top left is Professor Charles P. Kindleberger, Department of Economics, who delivered a talk on "The Economics and Politics of International Business." Flanking the dinner speaker are: right, Dr. J. Hillier, Executive Vice President, RCA Research and Engineering; and left, E. J. Dailey, Staff Vice President, International Planning, RCA Corporate Planning. Top right is a scene during a laboratory presentation by Prof. Don Steinbrecher (left) and by Mrs. Anne Hirsch, Industrial Liaison Officer. Other photos show sections of RCA participation during evening dinner session.



Trends in engineering

Dean Keil reviewed the outlook and the role for the scientist and engineer in helping to solve social problems. Engineering has a critical responsibility to contribute to the progress of society. MIT President, Dr. J.B. Wiesner emphasized the need for public support of technology and the engineers role in achieving this objective.

Public support of technology

Dr. Jerome B. Wiesner
President, MIT



By public support I mean more than just money: when general public support is lacking, the money will be as will students who should concern us more. Public support includes an understanding of the benefits of research and development; an enthusiasm for its accomplishments; and, an eagerness to see it prosper and grow. It is only within the past decade that this has become a serious question, brought on by real problems which concern us all.

At the start of the last decade, the public regard for technology and for universities as intellectual and research centers was at an unparalleled high. There was a feeling within our society that it was only a matter of time until technology would conquer any ill we might care to direct our attention to and we would live in an even more utopian society. Almost everyone accepted the premise that the pursuit of basic and applied research in the physical sciences in universities was of vital importance to the military security of the United States and to the nation's economic well-being. This confidence in the value of research carried over to the health-related areas and stimulated funding for ever-growing programs in the biological sciences.

About 1968 to 1969, questions began to be asked about the importance of research and the image of the university faded a bit. Thus, a little over two years ago, I found myself delivering a dinner address entitled, "Can the University Continue to be an Important Source of Scientific Research", a question which a few years earlier would have appeared frivolous. Today, the American public, as well as decision makers at all levels in our government - national, state and urban - have begun to realize that science and technology can bring undesirable and unexpected side effects, as well as great benefits. Along with this change in attitude on the part of the public towards science and technology, the public's outlook on life has also changed. In the early 1960's there was a feeling that we had to meet the scientific challenge posed to us by the Russian's dramatic launching of Sputnik. Now we are planning many joint space programs. Defense does not loom so great. But, as a world society, there was also a feeling that life was good and would get better. Today, we hear from some that we live in a finite world, and the spectre of Malthus is again with us on a larger scale, only delayed a bit by the industrial revolution and perhaps more recently, by the green revolution.

Here at M.I.T., Dr. Forrester's study on World Dynamics has received considerable attention, if that isn't too modest a description for the reaction he has drawn. His study points out that unless man begins corrective actions, we can expect a world catastrophe, quite possibly, within our lifetimes. Actually, I believe that those corrective actions have already been taken. A key difference now is that in the past, social deficiencies were blamed on forces beyond man's control - natural catastrophes such as droughts, floods or epidemics, or social catastrophes such as depressions (which were regarded almost akin to natural phenomena), or the acts of evil men such as a Hitler or a Stalin. Today, it is generally believed that we have the means to provide the opportunity for a decent life for everyone. It is the bittersweet character of the modern world - the contrast between the world that is and the world that could be - that leads to the disenchantment we see on all sides. Thus, we see a demand from the public and its decision makers to develop technology without bad side effects, and a need to develop policies and actions that will keep mankind away from the catastrophic course many now feel it is on. It is a truism that these have not been typical concerns of scientists and engineers in the past and even discussions about these questions have frequently been excluded from the agenda of their professional societies. Fortunately, this is now changing.

Most agree that science and technology has provided the basis upon which we have formed our contemporary society, as good or bad as it is, even though we have not been required to design a public policy for science and, I dare say, we don't know how to design such a policy today to ensure the continuing favorable development of science and technology. It is only in the past couple of years that the government has begun to provide support for the fields of behavioral and social sciences. Advanced mathematical and engineering concepts, including modeling, can be used to analyze or predict the behavior of sectors of the society itself. I suspect that we could have avoided some of our worst mistakes in planning domestic legislation if such capabilities had existed in the past (Examples - Housing, Medical Plan). We would have recognized some of our present crisis such as pollution, earlier, I believe. An impending major crisis for this country which could alter the entire course of our economy is a potential shortage of energy. Here, at MIT and in industry, we have an opportunity to see whether our analysis and planning abilities can be developed and employed effectively. We have emerged from a period where every proposed development was blindly supported in the belief that it was needed for defense or the economic well-being of the nation, to a time where it is being demanded that the side effects, both bad and beneficial, of technological programs be judged before they are implemented. This, then, requires a widened scope for our engineering considerations. A scope which, in addition to the traditional basic science and mathematical training and the special skills and knowledge of a specific engineering discipline will also include a deep understanding of the social sciences and the humanities.

Future of engineering

Dean A. H. Keil
Dean, School of Engineering



The service role of the engineering profession began with the development of technological devices to satisfy narrowly-defined human needs. It gradually expanded and, during the past few decades, has come to encompass broadly-defined technical analyses and the design of complex physical systems. It must now expand again in response to the rising problems of a society which has become increasingly dependent on technology and suffers increasingly from its abuse.

The engineering profession must now accept the additional responsibility of playing a leading role in providing Needs Analyses and Impact Analyses as the bases for decisions on how to resolve society's major problems, all of which are technology-related but which likewise involve major social, political and economic factors.

Engineering education must respond to this broadening scope of engineering and accept the fact that several types of engineering activities are emerging which can be characterized in a simplified manner as the technologist; the practicing engineer and designer; the engineering scientist; and the broad systems engineer who related technology and society in identifying workable solutions.

All four types of engineering activities are crucial in developing effective uses of technology for the benefit of society. Schools of engineering must decide which type or types they wish to develop in order to maximize their contribution to society through education and research.

Materials and devices

Papers by Aggarwal, Gatos and Dresselhaus provided an idea of the scope of research at MIT in the fields of quantum electronics and materials research.

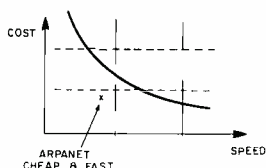
Quantum electronics

R. L. Aggarwal
Francis Bitter National Magnet Laboratory*
Massachusetts Institute of Technology



A brief review of the work (work supported in part by the Office of Naval Research) on tunable infrared lasers was given. In particular we

ARPA Network. I note that an arm of RCA is also engaged in work on the ARPANET.



Essentially, the ARPANET is the interconnection of about 50 (mainly large and medium-scale) computers (called "hosts") through a nationwide packet-switching telecommunication system consisting of 50-kilobaud lines, and about 35 (small) computers (called "interface message processes" or "IMPs"). Four MIT computers are connected to the IMP in Technology Square: the MULTICS Honeywell 645 and three Digital Equipment PDP-10s. Through the network, we and our programs can interact with colleagues at Harvard, Carnegie Mellon, Utah, Stanford and other institutions engaged in computer research and gain access to such specialized facilities as the flexibly (micro-programmable) Standard IC-9000 computer at the Institute for Informative Sciences at the University of Southern California. The communication network itself (lines and IMPs) introduces very little delay (usually about 0.1 second) into on-line transactions. The network-control programs in the host computers in some instances make interaction a bit sluggish, but on the whole, one can work in a remote computer via the ARPANET almost as well as in a local computer.

We are engaged in several network activities, which I shall mention here:

Developing a network service source

The MULTICS System has several features that qualify it to be an excellent network service system: very large address spaces (64,000 x 64,000 words), unusually advanced arrangements for information security, hierarchical file structures, and others. The Computer Systems Research Division of Project MAC is using MULTICS and the ARPANET to develop the concept of "information utility".

File transfer

Although much of the early use of the ARPANET is simply use of remote computers through local terminals, more sophisticated applications are coming into the picture. We have been active with other ARPANET groups in developing and implementing a standard protocol for the transfer of information files among host computers. Abhay Bhushan is chairman of the File Transfer Task Force. Marc Seriff is developing a virtual network file system that will bring into one coherent functional array files that actually reside in diverse, distributed file systems.

Convenience of use

When one has 50 different computer systems effectively within reach, he begins to realize that their diversity is a serious obstacle to his exploitation of them. We have been exploring the problem of how to make functional simplicity out of physical and logical complexity. The main approach, of course, is through standardization of protocols to govern what is transmitted over the lines. That approach is supplemented by "local sugaring". For example, we can see who is working in any one of the network computers we use most frequently simply by adding its name, e.g., "NIG", to our own "WHO" command. If we spot the initials of a friend in the resulting list, we can communicate with him directly almost as readily as if he were logged into our local computer. Or we can send him "mail" by typing, for example:

MAIL RMM UTAHT
Will you be at the SF mtg. on the 23rd? Lick.

Using remote programs and subprograms

One of the most important applications for us will be the use of remote programs and subprograms. We are developing that capability with the hope of making several remote programs and subprograms appear as augmentations of our local on-line software library.

The datacomputer

The Computer Corporation of America, a neighbor in Technology Square, is developing a very large computer-based file system for the ARPANET. We are cooperating in that effort as an early user. The prospect of access to a trillion-bit file is quite exciting.

Cost

Working at a console within seconds of any part of such far-flung resources makes it easy to visualize a great revolution in man's use of information: Mail delivered in a minute, computer-based teleconferences, reading from electronic books, and all the rest. Such visions are usually quickly cooled by thoughts of cost. The cost of transmitting bits via ARPANET technology, however, is not a severe damper. After one has an IMP, the present cost is about 30 cents per thousand packets, each packet carrying up to 1,000 bits. If the packets are half full, on the average, that is 60 cents per million bits or about 2cents per equivalent typewritten page. When ARPA-like networks are operated commercially, the costs will no doubt be increased by such factors as marketing, but there may be counterbalancing economies of scale and improvements in technology. There is reason to hope, therefore, that dreams may indeed be realized in the world of computer-communication networks.

The new automation

Professor Edward Fredkin
Director, Dep't., Electrical Engineering
Project MAC



Advances in computer technology are taking place in which the costs are being decreased by a factor of two every two years. This pace will continue in the foreseeable future. The costs of computation and the processing of information will decrease by a factor of 1000 every 20 years. Today, calculators can be obtained for about \$400 with stored programs that can perform substantial mathematical operations.

The existing technology appears able to sustain or improve this rate of advance with the advent of integrated circuit technologies. The time will arrive when computers will be available for a few dollars. As these advances occur, there will be more and more uses for the computer.

Project MAC at MIT is concerned with a new technology evolving in which computer programs are created so that computers "know something". Prior to this, computers were full of data and were thought of as rapid, mechanical idiots. However, the new domain invades the scope of what people can do. In addition to bookkeeping and routine business tasks, the new computer's brain will lead to automation of all kinds of processes that may combine modern machinery with old time craftsmanship. Automatic assemblies by computer program are now more common but this new approach involves a step beyond in which (for example) integrated circuits can be selected and produced as a result of decisions concerning the location of pins and leads, packaging configurations and the refinement of other tasks at hand.

At project MAC, the development of "common sense" computer systems is progressing within very narrow domains and still requires much effort. However, the approach allows direct communication with the computer via typewriter in which problems are presented for solution. The computer can meet a situation not anticipated by its designer/programmer. In this way, a business manager can "be his own programmer" and solve problems directly by the computer.

The computer that "knows something" will figure out solutions and solve mathematical problems involving symbolic integration, factoring, and taking limits better than anyone, except possibly a very gifted person.

The true definition of "understanding" is difficult to establish; however, we learn to represent knowledge via the computer as a combination of data and algorithms. The capability (for example) of solving problems involving a world of blocks where the computer uses sequences other

than those anticipated by the builder was cited. Techniques that enable computers to gather information from, and interact with their environment, can be visualized, for instance - as a robot with eyes and hands coordinated to carry on tasks unaided by human control.

Management and marketing

Papers by Little, Kindleberger, Farris, Roberts, and Hollomon dealt with the areas of predicting marketing results through models motivating performance, studying consumer durables in the world market, and generating new business through entrepreneurship. In concluding the seminar, Mr. Bartl described the liaison services available to RCA.

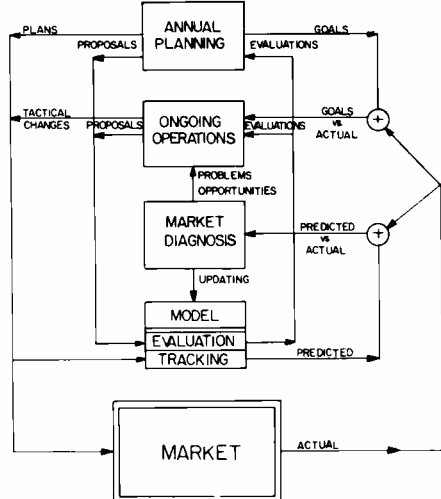
Decision support systems in marketing

Professor John D. C. Little

Alfred P. Sloan School of Management
Director, Operations Research Center



Marketing managers make decisions about price, advertising, promotion, and other marketing variables on the basis of factual data, judgments, and assumptions about how the market works. A decision support system (DSS) is a set of data, techniques, and associated computer software for assisting a manager in this work. Four major components of a DDS are: (1) A data bank that receives a continuous flow of new information from the environment. (2) A set of models or theories about how the market works. (These may be implicit in the manager's mind or explicit in mathematical form.) (3) A set of statistical tools and techniques with which to relate models and data. (4) An optimization capability to aid in the comparison of alternative actions. (The techniques may be as simple as ranking and sorting or as complicated as nonlinear mathematical programming.)



The concept and the use of a DSS is illustrated by a three-year case study of marketing consumer product.

The model plays a key role because it gives structure to the decision problem, identifies data to be collected, and guides data analysis and interpretation. In the marketing management process the model not only provides a basis for evaluating strategies in annual planning and day to day firefighting but, if properly used, becomes part of a monitoring system which compares predictions with actual sales to uncover marketing problems and opportunities and focus managerial attention on them.

Further reading:

J. D. C. Little, "BRANDAID: An On-Line Marketing Mix Model." Sloan School of Management Working Paper 586-72, February 1972.

The economics and politics of the multinational corporation

Professor C. P. Kindleberger

Department of Economics



The theory of direct investment is found to belong not to that of international capital movements but to the theory of oligopolistic competition. Companies go abroad essentially when they have advantages over their local competitors. These advantages are largely technological, but include, on occasion, the coordination of complex operations at successive stages of production, in which the corporation is more efficient than the disaggregated market.

When the corporation is exploiting its advantages through direct investment, it increases world efficiency. On occasion, however, such investment can work against efficient resource allocation, when for example, direct investment extends monopoly, or in the case of defensive investment which is undertaken not to make positive profits but to insure against possible losses.

The resistance to direct investment in home and host countries alike is largely unrelated to questions of efficiency. Forces in the home country are largely interested in income distribution, which is the basis of the Burke-Hartke opposition. In the host country, the bases are more cultural and political, and rest on nationalistic, populist, mercantilist etc. grounds. It seems likely that this opposition will decline as the economic benefits are spread more widely, just as the local opposition to the national corporation was finally overcome.

Motivating performance in a stable organization

Professor George F. Farris

Alfred P. Sloan School of Management



Several models to explain the motivation of technical performance were advanced, leading to the conclusion that technical performance is a multiplicative function of the individual's abilities, motives, technical information, expectancies that technical performance satisfies personal goals, and the incentive value of these goals.

Motivational models	Image	Management Strategy
Creative genius	Superstar	Benign neglect
Socioeconomic incentive	Businessman	Financial + promotion incentives
Info. available	Info. processor	Provide tech. info.
Creative tension	Envir. products	Create security + challenge
Creative climate	Indep. creator	Autonomy for creativity
Negotiation cycle	Negotiator	Construct + negotiate goals, career ops.

A new stable organization was seen to be very similar to an expanding organization in most of these factors, except that the work force is apt to be older and less current technically, job security may become an issue, and promotional opportunities will probably be limited. Several



managerial strategies based on the author's research were suggested to "unstable" the stable organization. Each strategy involved renewal through renegotiation of the technical person's career opportunities, roles in the informal organization, and work goals.

Specific suggestions to motivate an organization included clarification of job security, a professional growth program, encouraging more technical collaboration in the informal organization, increasing external contacts, re-grouping of technical teams, assigning people to multiple tasks, increasing time pressure, and rewarding good performance with greater challenge.

How large corporations generate new business

Professor Edward B. Roberts

Alfred P. Sloan School of Management



The wearing thin of traditional routes to corporate growth highlights the attractiveness of new venture-oriented strategies. Traditional approaches to growth include increased penetration and broadening of existing markets and movement into foreign markets. But market saturation combined with heavy competition from Europe and the Far East are eroding these traditional alternatives; one after another major North American firms have recognized that new venture approaches can provide viable opportunities for growth and diversification. Several entrepreneurial venture methods being adopted are:

1. Venture capital investments in new or small firms;
2. Joint ventures between the large corporation and small high-technology companies;
3. Venture packaging and sponsored spin-off of technical groups within a firm to semi-independent status outside the company;
4. Internal entrepreneurial activities based on new organization concepts.

The venture approaches outlined above rely upon investing in or combining with entrepreneurs outside of the larger firm, or of moving internal entrepreneurs into an external relationship with the originating firm. From our research, we have seen all of these approaches tried in large firms, sometimes with promising success, sometimes with clear failure. The resources available to the corporation, its competition, its traditions all affect whether any of the externally oriented venture methods can be successfully adopted.

Internal entrepreneurship

Internal entrepreneurship relies upon recruiting within the corporation champions for new products and services, stimulating them toward entrepreneurial behavior, and aiding them in developing business growth. The activities often are separated from the rest of the company's product lines to provide greater independence, freedom from short-term pressure, different rewards, improved visibility and access to the top.

Entrepreneurship in new independent firms usually starts with an idea for a new product or a dramatic improvement in an existing product, not merely a modest improvement in a standard line. Behind the idea is one or more entrepreneurs often frustrated in attempts to gain support. Even though the initial idea may be for one product only, with limited market potential, the entrepreneur assembles around him two or three others, similarly spirited but with different skills for building a company. Initial capital needs to get underway are usually small and risked by the entrepreneurial team itself. But a wide variety of investment banking and venture capital sources are accessible for the raising of more substantial funds when needed. If they fail, the entrepreneurs may lose some of their own capital and will have to go back to looking for a job. But if they succeed in growing their venture, the entrepreneurs stand to gain substantial financial rewards.

Many of the elements associated with successful new company entrepreneurship can also be found in the situation at the 3M Company, a multi-billion dollar firm noted for its successes in internal entrepreneurship, its continuing innovation, and its compelling growth record. One key element of the 3M entrepreneurial strategy is the lack of minimum size constraints for approval for a new product team

endeavor. To be sure, 3M would prefer the promise of a \$100 million market rather than merely a \$5 million forecast for a new product. But it does not reject opportunities that appear small at the beginning. This is comparable to the founding of a new company based on one product. Who can tell where it will lead?

Creating an entrepreneurial climate

Most professional organizations have people who, if given the opportunity, would behave like entrepreneurs. The major deterrents are the organizational policies, procedures and modes of operation that do not stimulate and may, in fact, inhibit entrepreneurial activity.

Internal entrepreneurship in corporations can be effectively stimulated and nurtured by direct and rapid channels through which new product ideas can pass and be reviewed. One company accomplishes the objective of providing quick and direct access to "seed money" for potential entrepreneurs by allocating limited funds earmarked for the preliminary investigation of new product ideas. The entrepreneur must go before a review board for approval. If approved, objectives, time-table and budget are set and the entrepreneur at that point has full authority within the scope of his budget to reach the objectives.

A company, serious about promoting internal entrepreneurship, should see that new product ideas do not suffer in competition with present products by setting aside a fixed percentage of the budget for them. Some companies put as much as 30% of their R&D resources into the research for and development of new venture opportunities.

Planning an entrepreneurial strategy

A first step in promoting internal entrepreneurship can be top management communicating that it is searching for new ventures to be piloted by internal entrepreneurs. Top management may have restrictions for new venture investment and these should be communicated as well. Other steps that are likely to be necessary include:

1. Set up a department (New Ventures, or New Business Development).
2. Establish a review panel to examine and select new ideas.
3. Re-examine the company's compensation scheme to see if it is sufficiently flexible to recognize risks and provide rewards.

In review, we have pointed out the increased need for and trend toward venture growth strategies that emphasize linking entrepreneurial behavior with corporate resources. In particular, the strategy of internal entrepreneurship is an attractive approach.

References

The following references are of special interest to those considering an internal entrepreneurship strategy for their firms.

1. Martin, Richard "Venturing Out", *Wall Street Journal* February 1, 1972
2. Morgenthaler, George "Utilizing R&D By-Products" *Innovation*, Number 20, 1971
3. Park, Ford "The Technical Strategy of 3M", *Innovation*, Number 5, 1969
4. Roberts, Edward B. and Frohman, Alan L., "Entrepreneurship: Strategy and Growth", *The Business Quarterly*, Spring, 1972
5. Roberts, Edward B. "Entrepreneurship and Technolog.", *Research Management*, July, 1968
6. Roberts, Edward B. "Recognizing and Keeping Entrepreneurs", *Innovation*, Number 7, 1969
7. Schon, Donald A. "Champions for Radical New Inventions", *Harvard Business Review*, March-April, 1963
8. U.S. Department of Commerce *Technological Innovation: Its Environment and Management* U.S. Government Printing Office, 1967

Policy alternatives

Dr. J. Herbert Hollomon

Director, Center for Policy Alternatives



The new Center for Policy Alternatives has the objective of examining major policies and programs, both private and public, and to suggest alternatives. The Center intends to study policy alternatives, prepare draft legislation, suggest regulation, and propose policies. In doing this, many alternatives must be considered and the impact of each alternative evaluated.

One of the major studies of the center relates to the effective use of technology in the U.S. economy. Since technology is socially determined and differs in every nation (picture differences between Nigeria and United States), the individual economy, the society, the myths, and the cultures combine to produce the unique needs of a country and ultimately its economy. Therefore, the manner in which the country is changing and the rate of its change alter the technological needs of a society.

Technology in the U.S.

The U.S. is changing. The U.S. is considered the richest country in the world based upon the way we measure richness in terms of output of goods and services. The spread of the income distribution in the U.S. is relatively great, and the distribution has remained essentially unchanged for the past 20 years. Productivity of agriculture has increased much more than in industry. One of the great changes has been from an agriculture-industry based economy to one based primarily on the supply of services. However, there has been a migration of 23 million workers who comprise the least skilled, the poorest, and the ghetto workers to our cities. The problems of the cities result in part from this great migration.

Our country has the highest productivity in the world and one of the lowest rates of improvement. Today, we are increasing our productivity at only 2.5 percent per year compared with Japan's increase of 15 percent per year.

In the last 5 years, the rate of increase in the U.S. was less than that of any other industrialized nation except England; it was only about 1.5 percent. At the same time, we have a growing, negative balance of trade. We must stimulate exports or restrict imports or change the value of the dollar in the world market. It is clear that our decrease in productivity has contributed to inflationary trends.

Ours is one of the very few industrialized countries that has a substantial unemployment problem. At present, there is an economic crisis and a political crisis in Australia, where unemployment is 1.8%. However, in other countries workers must be imported to satisfy employment needs with no unemployment problems existing except for the United Kingdom and to some degree in the Netherlands.

With the growing affluence and industrialization, the availability of high grade mineral and fuel resources has declined. Their prices will rise, and we will need to operate with more conservative methods. In total our relative influence in the world economy has declined as the European Common Market and Japan have expanded. There is now an over supply of technical people.

The support for science and engineering compared to other countries has substantially declined. The ratio of major technical efforts devoted to commercial activities is greater in other countries than in the U.S. In recent years the amount of R&D supported by the federal government has declined in the U.S. The relative price for technical personnel is now falling, but there will be a shortage of engineers in 1974-75; thus in some areas hiring should begin in anticipation of this.

There are numerous studies being conducted by the Center which provide comparisons between our country and others. These comparative studies involve what other countries do to stimulate industrial development and the effectiveness of these measures. We now know that we can learn much from the experience gained by other countries of the world. Below are some of the comparative studies being conducted by the center.

1) Supply and demand: the supply and demand of professional manpower has a cyclic behavior in which there appears to be a six-year time lag between the supply and demand commonly called the "corn-hog cycle." We have either too many engineers or too few.

2) Manufacturing: studies of the various processes, materials fabrication, and the production of individual parts versus newer approaches possible such as the computer control of manufacturing. What other technology is available; how can that technology be applied; what are the software problems; and what is the total effect on manpower? These are all questions requiring study. In computer-controlled manufacturing one does not have to be restricted to routinized or standardized machines for production of components. Instead a variety of parts can be accepted and processed, eliminating expensive inventories.

3) Consumer durables: how does the production service work? What are the systems costs of producing, servicing, and disposing of consumer durables?

The RCA/MIT liaison program

J. Peter Bartl

Liaison Officer

MIT Industrial Liaison Office



In concluding the meeting, the services available to the managerial and technical teams of RCA through the Industrial Liaison Program were reviewed. The Program was formed in the late 1940s to provide a vehicle through which a large corporation could learn about the Institute's research and advanced development activities. The Program is, as far as we know, the first of its kind and RCA was one of the early participants. In its twenty-some years of existence, the Program has grown to a point where twenty staff members, headed up by six Liaison Officers and a Director are associated with it.

All Liaison Officers are graduates of MIT and form a highly flexible and personal interface between MIT and the participating companies. In addition to introducing companies such as RCA to MIT's research, the Liaison Program also hopes to introduce the MIT faculty and staff to industrial research and needs.

Several formal vehicles have been developed to stimulate interaction between the Institute and participating companies. The first of these is a directory of current research. Published annually, the current edition lists over 1700 research projects representing an annual research activity of over \$200 million. Typically, the work ranges from the soft sciences such as management, economics, political science, medicine, etc., to the more traditional hard sciences. A reference sheet is maintained on each project and, as is true of all Liaison Program services, can be obtained free of charge. Secondly, the Liaison Program sponsors spring and fall series of private, informal symposia. This spring, meetings will be held on "Opto-Electronics" (March 1), "Fracture Mechanics" (March 23), "Ceramics and Glass" (April 5), "Marketing Models and Systems" (May 2), "Combustion" (May 10), "Industrial Noise Control" (May 17), and "Technology Assessment" (May 24).

Nothing can substitute for face-to-face interaction, and as you develop new interests, the Liaison Program is prepared to identify faculty with similar interests and to arrange meetings to discuss these common interests at MIT. These visits are not meant to serve the role of a consulting relationship. However, when your needs require such a relationship, the Liaison Office will suggest consultants appropriate to your needs and arrange an introductory meeting. Consulting relationships with MIT faculty members are private relationships between the faculty member and RCA and do not involve the Institute in any way.

Each month, the Liaison Program abstracts a selected group of journal preprints, internal working papers and progress reports and makes these available. This *Monthly List of Publications* is distributed throughout RCA. Publications are available, free of charge, up to two years after appearing on this list and afterwards for the cost of reproducing the documents. The Liaison Program will also issue library cards and thus make the facilities of the MIT Libraries available to RCA personnel. In order to limit the paperwork of this system, it is requested that library cards be issued only to key personnel and that others borrow the cards from these individuals.

As mentioned previously, we aim to provide RCA with a flexible personal service. We are therefore interested in learning more about individual interests and needs and using our knowledge of the MIT community to create appropriate matches.

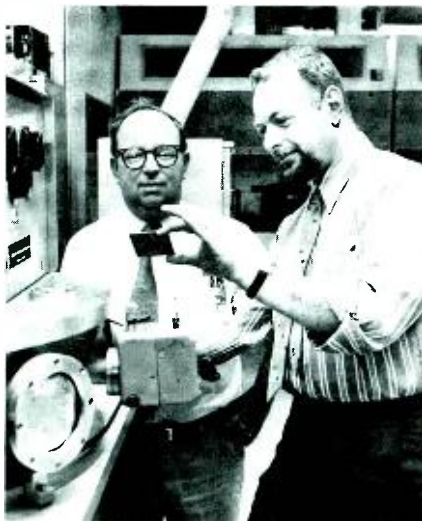
References

- 1) 1973 "Directory of Current Research"
- 2) "Monthly List of Publications"
- 3) "Announcement of 1973 Spring Series of Symposia"

Advanced packaging with thin-film microcircuits

W. J. Greig | R. Brown

A facility capable of high-volume manufacture of thin-film hybrid microcircuits is in operation in the Solid State Technology Center (SSTC) Somerville, N.J. Present and future larger scale integration needs indicate the relevance of applying thin-film and beam-lead technologies to advanced microelectronic packaging. Especially so, because this approach offers low-cost and high reliability.



Authors Greig (left) and Brown.

William J. Greig, Ldr.

Hybrid and Packaging Technology
Solid State Technology Center
Research and Engineering
Somerville, New Jersey

received the BS in Physics from Fordham University in 1953. He subsequently joined Electronic Components as a trainee and was assigned to the Semiconductor Department upon completion of the program. He served in the USAF from 1954 to 1956. Mr. Greig has been active in materials and process development covering all phases of semiconductor technology. He has been engaged in development of advanced assembly techniques fabrication of flip-chips and development of beam-lead technology. He is presently responsible for development of thin-film technology as it applies to advanced multi-chip packaging. Mr. Greig has had five patents issued and has several pending. He has authored or coauthored several technical papers. He is a member of the American Vacuum Society.

Richard Brown

Hybrid and Packaging Technology
Solid State Technology Center
Research and Engineering
Somerville, New Jersey

received the BS in Chemistry from Wagner College in 1951. He served in the USAF from 1952 to 1956. He attended Seton Hall University for graduate work and in 1959 joined Bell Telephone Laboratories where he was active in their thin-film program. He joined RCA in 1971 and has been working on the development of thin-film technology as it applies to advanced multi-chip packaging. He has several patents pending and has authored in a number of publications. He is a member of the American Ceramic and the Electro-chemical Society.

AN EXPANDING THIN-FILM TECHNOLOGY, based primarily upon manufacturing experience gained on the Safeguard Program, is used in SSTC for fabrication of packages for multi-chip arrays. These packages which have the capacity for multiple-level wiring when combined with beam leads provide an approach ideally suited to meet the increasing demands for more complex, higher density circuits.

Beam leads and thin film

The microcircuits shown in Fig 1 are typical of the types produced on the Safeguard Program. They consist of beam-lead chips and a thin film on ceramic interconnect composed of layers of titanium, palladium, and gold.

By using beam leads and thin films, an approach to multi-chip packaging has evolved offering high reliability and low cost. While reliability is always desired, the need increases significantly as the number of chips per pack-

age increases. However, if reliability can only be obtained by an attendant increase in cost, the multi-chip packaging approach to large-scale integration could quickly become economically impractical. The beam-lead, thin-film approach has several features which make it ideally suited for advanced packaging, yet maintaining low cost. Beam leads, for example, simultaneously provide both a degree of reliability not attainable with standard wirebonding techniques and a low-cost, high-yield assembly operation.

The thin-film metallization, which is equally reliable and compatible with beam-lead bonding, allows for high-density wiring with interconnects that are obtainable using well-defined standard-processing techniques—techniques that are readily controlled and monitored. The beam-lead, thin-film combination also features reparability which permits removal and replacement of defective chips. Additionally, because of the intrinsic hermeticity of the beam-lead device by virtue of its structure i.e., passivating dielectric and precious metal metallization and corrosion-free interconnects, a non-hermetic package enclosure may be utilized. This has a significant cost impact in terms of yield.

Reprint RE-18-5-21

Final manuscript received April 27, 1972.

The work reported herein has been supported in part by the Air Force Materials Laboratory, Air Force Systems Command, Wright-Patterson Air Force Base, Ohio, Contract F33615-71-C1085 (MMP516-0).

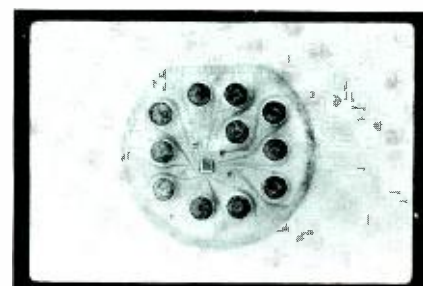
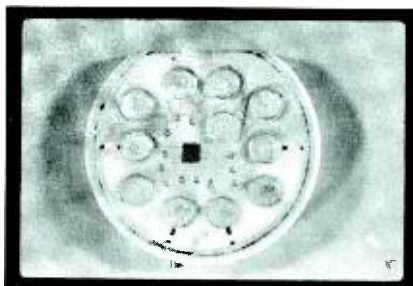


Fig. 1—Safeguard circuits.

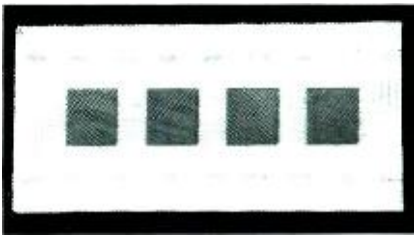


Fig. 2—1-k word x 1-bit memory array (0.400 x 0.900 in.)



Fig. 3—Cross section of bonded beam-lead chip.

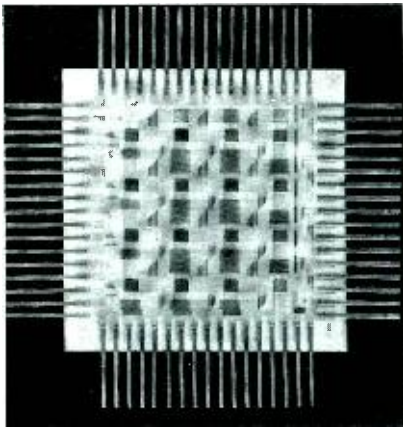


Fig. 4—16-chip ROM.

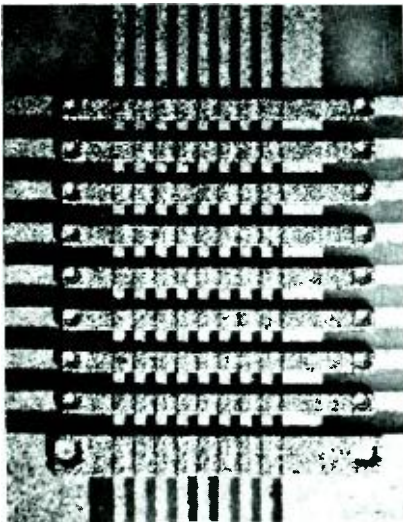


Fig. 5—Closeup of beam crossovers.

Fig. 2 shows a package containing four chips. In this case another feature of the beam lead is exploited, i.e., the “bugging” action of the chip which enables conductor lines to run under the chip. Fig. 3 shows a metallographic cross section of a bonded beam-lead chip and illustrates the chip “bugging”. The four chips are therefore interconnected using a single level of wiring. Should more than one level of wiring be required, a technique using air-insulated crossovers (micro-bridges or beam crossovers) is employed. Fig. 4 shows a 16-chip package requiring multi-level wiring using beam crossovers. A closeup of the crossovers is shown in Fig. 5.

Fabrication of multi-level microcircuits

The thin-film conductors are titanium, palladium, and gold. The choice of material is dictated by the desire to use a system having reliability equivalent to that of the chip and compatible with thermal-compression bonding, gold beam leads, the air-insulated crossover technique, and a non-hermetic package.

The processing consists of the following steps:

- 1) Vacuum deposition of the base metals—titanium, palladium, and gold.
- 2) Application of photoresist and defini-

tion of the base metal pattern (see Figs. 6a and 6b).

- 3) Vacuum deposition of copper and subsequent electroplating of copper to a thickness of approximately 1 mil over the entire substrate.
- 4) Application of photoresist and etching of holes through copper-to-base metal (see Fig. 6c).
- 5) Application of photoresist and opening area for subsequent gold plating for beam crossover.
- 6) Electroplating gold to a thickness of approximately 1 mil in crossover area only (see Fig. 6d).
- 7) Etching away all copper, leaving air-insulated crossovers.

The processing basically involves well-established procedures and techniques, all capable of high yields and high volume.

Ceramic substrate

A 3¾ x 4½-in. substrate size has been adopted as standard with multiple circuits per substrate being generated to reduce processing costs. Individual circuits are separated upon completion of the processing using laser scribing. The CO₂ laser used is shown in Fig. 7.

The substrate material is normally ceramic of high alumina content, usually 96 or 99.5%, with a surface finish ranging from 20 μm (center line average) to less than 1 μm. The actual material or finish will depend upon the particu-

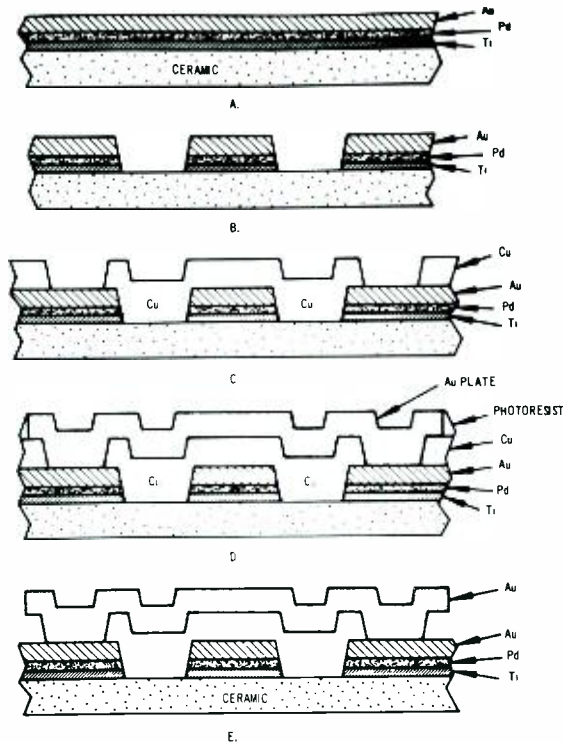


Fig. 6—Schematic of crossover process.

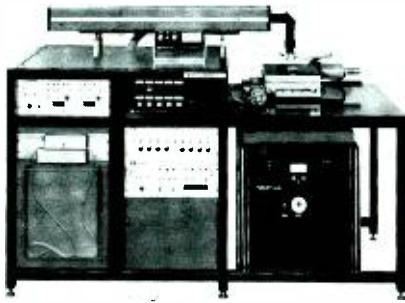


Fig. 7—CO₂ laser scriber.

lar circuit to be fabricated with the finer conductor lines (both line width and spacing) requiring the finer finish and the higher alumina content.

Thin-film metallization

The titanium, palladium, and gold layers are easily deposited by electron-gun evaporation. Two guns are used in a conventionally trapped diffusion pump system. The titanium and palladium are evaporated from a 4-pocket source and the gold from a single-pocket unit.

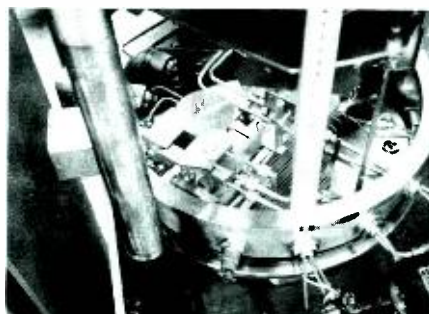
The actual system shown in Fig. 8 is capable of coating eight 3¾×4½ in. substrates. Each substrate yields over 12 in.² of useful area for a total in excess of 180 in.² per run. Uniformity of deposition is enhanced by using a planetary system capable of providing ±8% uniformity across an 8-in. diameter substrate holder. Increased capacity can be obtained by an appropriate change in fixturing.

Sputtering is another process available for conductor fabrication. Fig. 9 shows a three-target (12-in. target diameter) sputtering system. The system is equipped with a load lock to facilitate loading and unloading without opening the main chamber.

Fig. 8—Evaporation systems.



a) Crucible E-gun assembly with driver.



b) Single crucible E-gun.



c) Vacuum system rear view.

Photolithography

The fabrication of multi-chip arrays utilizing beam crossovers involves a minimum of three photolithographic steps per substrate. For high volume and low cost, multiple patterns per substrate are generated.

Photoresist application—The photolithographic processes use a positive photoresist exclusively. The resist is applied by spraying, since this method offers the high-volume capability desired as well as versatility with respect to accepting a wide variety of substrate sizes. The spray booth is shown in Fig. 10.

Alignment—all pattern alignments are accomplished mechanically rather than optically. The mask aligner used is shown in Fig. 11. It is capable of handling photomasks up to 5×7 in. and substrates as large as 5×5 in.

Electroplating

Approximately 1.0 mil of copper is electroplated onto a previously evaporated copper layer to form the spacer layer which determines the bridge-conductor separation.

Although the copper is ultimately dissolved, it exerts a considerable influence on the crossover processing. The plating should be homogeneous to insure uniform etching of the pillars over the entire substrate. Also, the copper surface affects the photoresist adhesion and the growth habit of the electroplated gold beams.

The gold bridges are electroplated by standard DC techniques. Control of the usual variables such as bath temperature, pH concentration, and current density results in controlled grain growth and plating thickness.

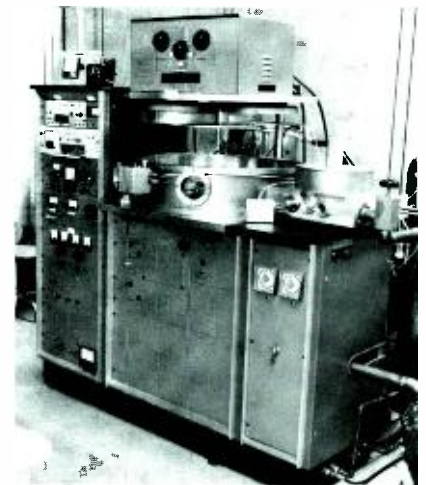


Fig. 9—Sputtering system.

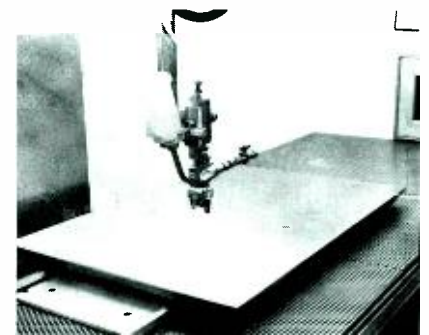


Fig. 10—Photoresist spray booth.

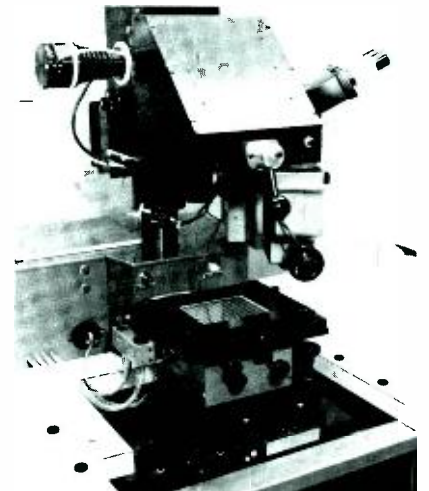


Fig. 11—Alignment and exposure unit.



Fig. 12a—Wobble head bonder.



Fig. 12b—Compliant bonder.



Fig. 13—Lead frame bonder.

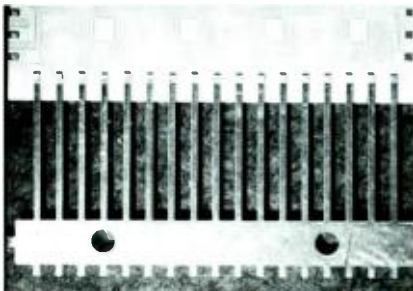


Fig. 14—Thermocompression bonded lead frame.

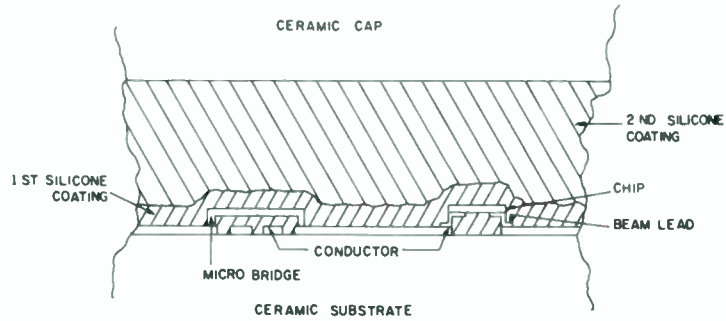


Fig. 15—Cross section of finished package.

Package assembly

Chip attachment—The beam-lead chips are thermocompression bonded to the thin-film conductors using either a “wobble head” bonder or a compliant bonder, shown in Fig. 12. In either case, all beams are attached simultaneously.

Lead frame—Fig. 13 shows a lead frame bonder used to thermocompression bond a nickel- and gold-plated copper lead to the thin-film termination pads. The mechanism is identical to that used with the chip. Again multiple leads are bonded simultaneously. Fig. 14 shows a bonded lead frame.

Encapsulation and capping—The encapsulation consist of an overcoat of a silicone varnish (Dow Corning R-6-2047) directly over the chips and the metallization, followed by a coating of RTV-3145 to provide added mechanical protection and to act as an adhesive for the ceramic cap. Fig. 15 is a schematic representation of a cross section of a finished package.

Microcircuit applications—Typical of the types of microcircuits being fabricated are those used in the 72,000-bit COS/MOS memory module being built for the Air Force Materials Laboratory. The module, shown in Fig. 16, consists of 10 ceramic circuits comprising 8 memory planes (arranged as a 1-k word by 9-bit memory), 1 address register, and 1 data register. The circuits are interconnected on the printed wiring board to function as an 8-k word by 9-bit memory.

Fig. 17 shows the three circuits with chips mounted but prior to encapsulation and capping. The type of circuits shown in Fig. 17 amply demonstrates the complexity and density obtainable

with this type of advanced packaging approach.

Acknowledgment

The authors wish to thank A. S. Rose for his suggestions and encouragement.

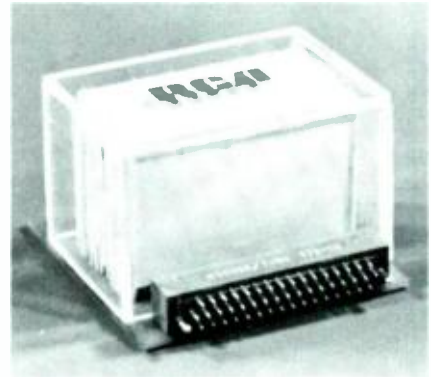


Fig. 16—Memory module.

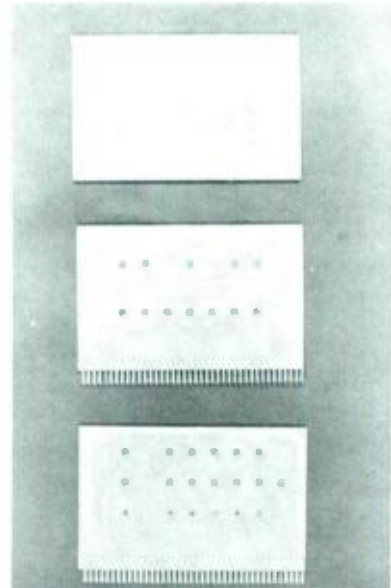


Fig. 17—Memory plane (top); address register (center); data register (bottom).

Charge-coupled devices and applications

Dr. J. E. Carnes | Dr. W. F. Kosonocky

Charge-coupled devices (CCD's) represent a new concept for silicon integrated circuits. This article reviews the basic operation of CCD's, including their basic operating limitations, methods of fabrication, and state-of-the-art experimental results; the various potential applications are then described in more detail.

THE CHARGE COUPLED DEVICE^{1,2} (CCD) is a new device concept which was introduced three years ago. It is an analog shift register, and as such has potential application in a variety of areas such as self-scanned image sensors, electronically-variable analog delay lines, matched filters, and autocorrelators. In addition, the simplicity and compactness of CCD's should result in their use as low cost, high capacity digital serial memories. Progress in CCD research has been rapid. Initial announcements told of devices having just eight stages with an efficiency per stage of approximately 99%.² In the succeeding years, the length of devices and their transfer efficiencies have increased at the rate of approximately one order of magnitude per year, so that present devices have as many as 500 stages³ and efficiencies of 99.99%.^{4,5} Devices with this type of performance are satisfactory for most of the applications mentioned and it is anticipated that

Reprint RE-18-5-22-
Final manuscript received August 25, 1972.

Authors Kosonocky (left) and Carnes.



CCD's will soon find their way into marketable products.

MOS capacitor

Since a CCD is physically just a linear array of closely-spaced MOS (metal-oxide-semiconductor) capacitors, it is important to understand the MOS capacitor and how the surface potential, V_s (the potential at the Si-SiO₂ interface relative to the potential in the bulk of the silicon), depends upon the various parameters involved.

Fig. 1 shows a cross-sectional view of an MOS capacitor with a p-type silicon substrate. When a positive step voltage is applied to the gate of such a structure, the majority carrier, holes, are repelled and respond within the dielectric relaxation time. This results in a depletion region of negatively-charged acceptor states near the surface of the

Dr. Walter F. Kosonocky
Process and Materials Applied
Research Laboratory
RCA Laboratories
Princeton, New Jersey

received the BSEE and MSEE from Newark College of Engineering in 1955 and 1957, respectively, and the ScD in Engineering from Columbia University in 1965. From June 1955, he has been employed at RCA Laboratories, where after one year as a Research Trainee, he became a Member of the Technical Staff and since that time he has been doing research on new solid-state devices and circuits. Since the spring of 1970, Dr. Kosonocky has been working on the study of performance limitations of CCD's and the development of charge-coupled devices for digital memories and self-scanned image sensors. Dr. Kosonocky received two RCA Laboratories Achievement awards in 1959 and 1963, and was awarded a David Sarnoff Fellowship for the academic year 1958-1959. During 1958-1959 and 1965-1966, Dr. Kosonocky was a lecturer and then Adjunct Professor of Electrical Engineering at Newark College of Engineering, and since 1969 he has been a lecturer at LaSalle College. He has published 24 technical papers, and has been issued 23 U. S. patents. Dr. Kosonocky is a member of Tau Beta Pi, Eta Kappa Nu, Sigma Xi, the American Ordnance Association, and a Senior Member of IEEE. Dr. Kosonocky is also a member of the IEEE Solid State Circuit Committee.

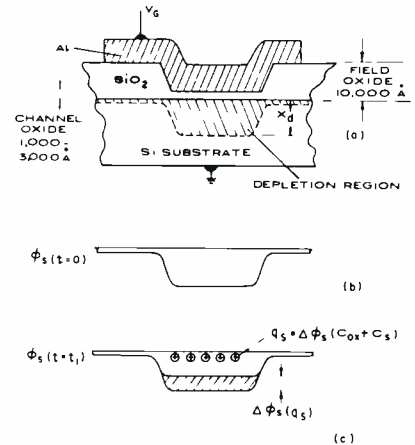


Fig. 1—(a) Cross-sectional view of an MOS capacitor representing element for charge-coupled circuit; (b) Surface potential profile just after application of step voltage V_G ; (c) Surface potential profile with charge signal q_s in the potential well.

silicon. The applied gate voltage is dropped across the series combination of the oxide and the depletion region in the silicon. Solution of the one-dimensional Poisson's equation subject to the appropriate boundary conditions, and including two-dimensional sheets of charge at the Si-SiO₂ interface due to fixed oxide charge (Q_{ss}) and signal charge represented by minority carriers (Q_{sig}), shows that the surface potential V_s is given by:

$$V_s = V_G' - B \left[\left(1 + \frac{2V_G'}{B} \right)^{1/2} - 1 \right] \quad (1)$$

where

$$V_G' = V_G + (X_{ox}/\epsilon_{ox}) (Q_{ss} + Q_{sig}); V_G \text{ is}$$

Dr. James E. Carnes
Process and Materials Applied
Research Laboratory
RCA Laboratories
Princeton, New Jersey

received the BS in Engineering Science from Pennsylvania State University with distinction in 1961. After four years in the U.S. Navy, he entered Princeton University and received the MA and PhD in Electrical Engineering (Solid State Device Physics) in 1967 and 1970, respectively. His PhD dissertation was an investigation of photo-induced currents and charge transport in polyvinyl-carbazole, an organic polymer. During the summers of 1966 and 1967, Dr. Carnes was employed at the David Sarnoff Research Center doing experimental work with evaporated metallic contacts and DC electroluminescence in strontium titanate. Since September 1969, when he joined the RCA Laboratories staff, Dr. Carnes has studied electrical breakdown, conduction and interface properties of various thin insulating films on silicon, including silicon dioxide, silicon nitride, and aluminum oxide. He is currently involved in the investigation of charge-coupled devices. Dr. Carnes is a member of the American Physical Society, Tau Beta Pi, Phi Kappa Phi, and IEEE.

the applied gate voltage; Q_{ss} is the fixed oxide charge; Q_{sig} is the signal charge of minority carriers (inversion layer charge); $B = qN_A \epsilon_s X_{ox}^2 / \epsilon_{ox}^2 = 0.15 (N_A/10^{16}) (X_{ox}/1000\text{\AA})^2$; q is the electronic charge in coulombs; N_A is the doping density in acceptors/cm³; ϵ_s is the dielectric constant of silicon; ϵ_{ox} is the dielectric constant of the oxide layer; and X_{ox} is the thickness of the oxide layer. Eq. 1 is a most important one in CCD design.

Just after the step voltage is applied to the gate and in the absence of signal charge Q_{sig} (the introduction of signal charge will be discussed in the next section), the silicon conduction band at the surface is well below the equilibrium Fermi level and electrons, the minority carriers, will tend to gather there. However, it takes a rather long period of time for thermally-generated minority carriers to accumulate in sufficient numbers to return to the system to thermal equilibrium. We have measured thermal relaxation times for MOS capacitors ranging from 1 to 100 seconds in good agreement with the predicted⁶ values assuming bulk thermal generation of minority carriers:

$$T = \tau N_A / 2n_i \quad (2)$$

where τ is the minority carrier life-time; N_A is the doping density; and n_i is the intrinsic carrier concentration (1.45×10^{10} cm⁻³ for silicon).

When minority carriers do accumulate at the surface, they start to create an inversion layer which resides within 100\AA of the interface. This negative charge tends to reduce V_s according to Eq. 1. When V_s goes to zero, no more charge can be accumulated or stored in the potential well. The capacitance of the potential well, C_{well} , consists of two capacitances in parallel: the fixed oxide capacitance, $C_{ox} = \epsilon_{ox} / X_{ox}$, and the capacitance associated with the depletion layer of the silicon, $C_d = (2qN_A \epsilon_s / V_s)^{1/2}$. Since C_d depends upon V_s , C_{well} is not constant for all values of V_s and, therefore, the concept of a potential well capacitance has limited usefulness. However, for large enough values of V_s , $C_d \ll C_{ox}$ and $C_{well} \approx C_{ox}$. For V_s values greater than $200B$, C_d will be less than 10% of C_{ox} , and C_{well} is essentially constant at C_{ox} .

Thus, the following fluid model of the MOS capacitor emerges: a potential

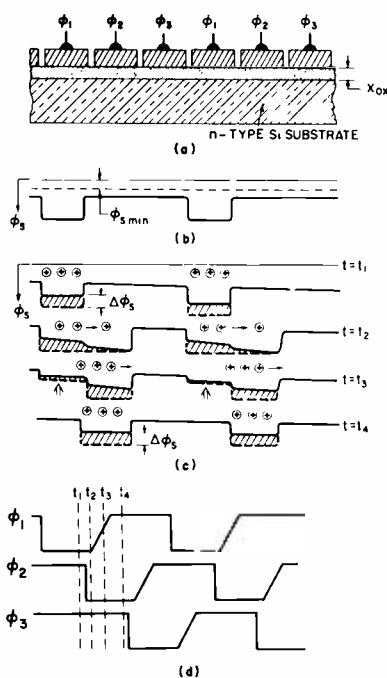


Fig. 2—Operation of a 3-phase charge coupled shift register: (a) Cross section of the structure along the channel oxide; (b) Surface potential profile for $\phi_1 = -V$, $\phi_2 = 0$, $\phi_3 = 0$ forming a potential well under the phase-1 electrode; (c) Transfer of charge from the potential wells under the phase-1 electrode to the potential wells under the phase-2 electrode illustrated by the profiles of surface potential at times shown in (d); (d) Waveforms of the phase voltages.

well for minority carriers can be created by applying a step voltage to the gate and this well will take a relatively long period of time to accumulate charge thermally. For times much shorter than this thermal relaxation time, a potential well exists at the surface, and the depth of this well can be altered by changing the gate voltage. When minority carriers are introduced as signal charge in the potential well, they tend to reduce the depth of the well according to Q_{sig}/C_{ox} , so they tend to fill up the well much like fluid in a container.

Basic charge-transfer action

A three-phase CCD is just a line of these MOS capacitors spaced very close together with every third one connected to the same gate, or clock voltage as shown in Fig. 2a. If a higher positive voltage is applied to the ϕ_1 clock line than ϕ_2 and ϕ_3 , the surface potential variation along the interface will be similar to Fig. 2b. If the device is illuminated by light, charge will accumulate in these wells. Charge can also be introduced electrically at one end of the line of capacitors from a source

diffusion controlled by an input gate. To transfer this charge to the right to the position under the ϕ_2 electrodes, a positive voltage is applied to the ϕ_2 line. The potential well there initially goes deeper than that under a ϕ_1 electrode, which is storing charge, and the charge tends to move over under the ϕ_2 electrodes. Clearly, the capacitors have to be close enough so that the depletion layers overlap strongly, and the surface potential in the gap region is a smooth transition from the one region to the other. Next, the positive voltage on the ϕ_1 line is removed to a small positive DC level, enough to maintain a small depletion region, increasing the surface potential under the ϕ_1 gates in the process. Now the ϕ_2 wells are deeper, and any charge remaining under ϕ_1 gates spills into the ϕ_2 wells. The charge, at least most of it, now resides one-third of a stage to the right under ϕ_2 gates. The charge is prevented from moving to the left by the barrier under the ϕ_3 gates. A similar process moves it from ϕ_2 to ϕ_3 and then from ϕ_3 to ϕ_1 . After one complete cycle of a given clock voltage, the charge pattern moves one stage (three gates) to the right. No significant amount of thermal charge accumulates in a particular well because it is continually being swept out by the charge transfer action.

The charge being transferred is eventually transferred into a reversed-biased drain diffusion and from there it is returned to the substrate. The charging current required once each cycle to maintain the drain diffusion as a fixed potential can be measured to determine the signal magnitude (current-sensing) or a re-settable floating diffusion which controls the potential of a MOSFET gate can be employed (voltage-sensing).⁷

The operation of the input and the output circuits for CCD's are described in more depth later in this paper (see *Experimental Results*). One can visualize a CCD shift register as a multi-gate MOSFET in which the charge signal is moved as charge packets from the source diffusion to the drain diffusion under the control of phase clock voltages applied to the gates.

Limitations on speed and efficiency

Clearly, 100% of the charge cannot move instantaneously from one poten-

tial to another. Also, some of the charge gets trapped in fast interface states at each site and cannot move at all. Therefore, in a given clock period not quite all of the charge is transferred from one well to the next. The fraction of the total that is transferred (per gate) is called the transfer efficiency, η . The fraction left behind is the loss per transfer, denoted ϵ , so that $\eta + \epsilon = 1$. Because η determines how many transfers can be made before the signal is seriously distorted and delayed, it is a very important figure of merit for a CCD. If a single charge pulse with initial amplitude P_0 is transferred down a CCD register, after n transfers the amplitude P_n will be:

$$P_n = P_0 \eta^n \approx P_0 (1 - n\epsilon) \quad (\text{for small } \epsilon) \quad (3)$$

When $n\epsilon = 1$, the original pulse is completely lost and distributed among several trailing pulses. Clearly, ϵ must be very small if a large number of transfers are required. If we allow an $n\epsilon$ product of 0.1, an overall loss of 10%, then a 3ϕ , 330 stage shift register requires $\epsilon \leq 10^{-4}$, or a transfer efficiency of 99.99%.

The maximum achievable value for η is limited by how fast the free charge can transfer between adjacent gates⁸ and how much of the charge gets trapped at every gate location by fast interface states.⁹

Three separate mechanisms cause the free charge to move from one well to another: self-induced drift, thermal diffusion, and fringing field drift. Self-induced drift¹⁰ is a charge-repulsion effect which is only important at large signal charge densities ($\geq 10^{10}$ charges/cm²) and is not particularly significant for achieving very high transfer efficiencies. Thermal diffusion results in an exponential decay of charge under the transferring electrode¹¹ with time constant

$$\tau_{th} = L^2 / 2.5D \quad (4)$$

where L is the center-to-center electrode spacing; and D is the diffusion constant.

By means of thermal diffusion alone, 99.99% of the charge is transferred each cycle at frequencies f_s (in Hz) given approximately by:

$$f_s(\text{thermal diffusion}) = 5.6 \times 10^7 / L^2 \quad (5)$$

assuming $D = 6.75$; L is center-to-

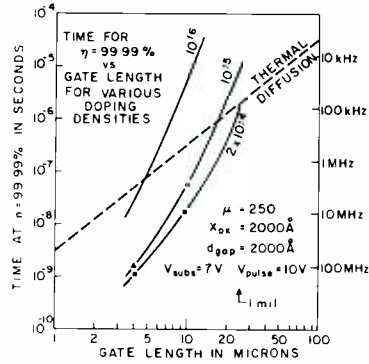


Fig. 3—Time required to achieve $\eta = 99.99\%$ vs. gate length for various doping levels. The thermal diffusion line is the maximum time required in any case.

center spacing measured in μm . Fringing field drift can help to speed up the charge transfer process considerably. The fringing field is the electric field along the direction of charge propagation at the Si-SiO_2 interface. This field will vary with distance along the gate with the minimum occurring at the center of the transferring gate. The magnitude of the fringing field increases with increasing oxide thickness and gate voltage and decreases with increasing gate length and doping density.¹² The effect of the fringing field upon charge transfer is difficult to assess analytically. A computer simulation of the transfer process under influence of strong fringing fields has indicated that the charge remaining under the transferring electrode still decays exponentially with decay time.

$$\tau_f = \frac{L^3}{20\mu X_{ox} V} \left[\frac{5Xd/L + 1}{5Xd/L} \right]^4 \quad (6)$$

where V is the clock-pulse voltage; and X_{ox} is the depletion layer thickness at the center of the transferring electrode.

Fig. 3 shows the time required to reach $\eta = 99.99\%$ as a function of gate length for various substrate doping densities. According to these calculations for a p-channel CCD, $\eta = 99.99\%$ is possible at clock frequency of 10 MHz with gate length $L = 7 \mu\text{m}$ and substrate doping of 10^{15}cm^{-3} . This assumes that trapping effects are negligible.

Charges can be lost from the signal into fast interface states because, while the filling rate of these states is proportional to the number of free carriers, the empty rate depends only upon the energy level of the interface state. Thus, even though a roughly

equal amount of time is available for filling as for emptying, many of the interface states can fill much faster than they can empty, and thus retain some of the signal charge and release it into trailing signal packets.⁹ This type of loss can be minimized by continually propagating a small zero-level charge or fat zero through the device. This tends to keep the slower states filled so they do not have to be filled by the signal charge. An analytical expression for fractional loss into fast interface states ϵ_s is given by:

$$\epsilon_s = \left(\frac{1}{\frac{n_{s,0}}{n_s} + 1} \right) kTN_{ss} \ln \left(1 + \frac{2f}{k_1 n_{s,0}} \right) \quad (7)$$

where $n_{s,0}$ is the fat zero carrier density in charges/cm²; n_s is the signal density in chgs/cm²; kT is in units of eV (0.026 at room temperature); N_{ss} is the fast state density in states/(eV-cm²); f is the clock frequency; and k_1 is a constant depending upon the trapping cross-section ($\sim 10^{-2} \text{cm}^2/\text{sec}$).

Eq. 7 implies that, without fat zero, $\epsilon_s \approx 10^{-2}$ for $N_{ss} = 10^{11} (\text{cm}^2\text{-eV})^{-1}$, and $\epsilon_s \approx 10^{-3}$ for $N_{ss} = 10^{10} (\text{cm}^2\text{-eV})^{-1}$ at 1-MHz clock frequency. By introducing $n_{s,0}$ equal to approximately 10 to 25% of a full well, ($\sim 2 \times 10^{11} \text{cm}^{-2}$), interface state losses can be essentially eliminated. For example, suppose $n_{s,0} = 2 \times 10^{11}$, $n_s = 10^{12}$, and $f = 10^6$. Then:

$$\epsilon_s = 2.2 \times 10^{-7} \text{ for } N_{ss} = 10^{10} \\ 2.2 \times 10^{-8} \text{ for } N_{ss} = 10^{11}$$

Methods of fabricating CCD's

Three-phase single-level metal CCD's

The three-phase CCD whose operation was described earlier can be made by standard p-MOS or n-MOS techniques. Only one level of metal is required in addition to source and drain diffusions. The gap between adjacent electrodes presents the major problems.

The gap should be as small as possible to insure good coupling between gates without any bumps or barriers in the surface potential. Thus 0.1-mil etching between metal electrodes is desirable but is a non-standard process. Furthermore, if the oxide in these gaps is exposed to the ambient air, the surface potential in the gaps is largely uncontrolled, and CCD operation can be adversely affected. Single-level metal

devices will, therefore, require some type of overcoat or resistive sea layer over the gap regions to control and stabilize the surface potential there. Another disadvantage of any three-phase system is a topological one. To contact the three-phase electrodes at least one cross-over or dig-down structure is needed at each stage.

The main advantage of the three-phase single-metal CCD is that it can be made with the minimum number of processing steps. The price for this is the definition of 2 to 3- μm gaps between the gates. Also, the best and more reproducible transfer efficiency has been obtained up to now with closely spaced CCD's in the form of polysilicon gates overlapped by aluminum gates, which are described in the next section.

Two-phase CCD's

In three-phase CCD's the potential wells are symmetrical, and the directionality of charge flow is maintained by the asymmetry of the clocking voltages as seen in Fig. 2. However, if each potential well had a built-in asymmetry to determine the direction of charge flow, then a symmetrical two-phase clocking scheme could be used to drive the device. The potential well asymmetry required is that the well must be deeper in the direction of charge transfer. This can be achieved by having two thicknesses of oxide under one electrode or by having a variation in substrate doping [See Eq. 1]. A two-phase device has clear topological advantages over a three-phase device since no dig-downs are required for access to the electrodes.

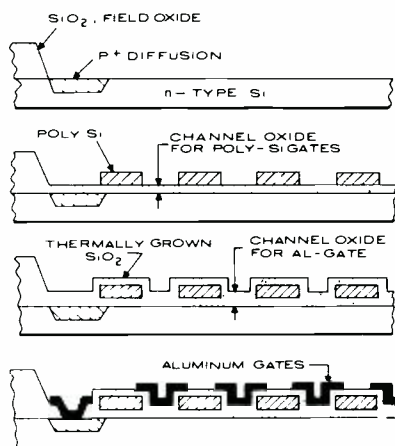


Fig. 4—Construction of the experimental charge-coupled devices.

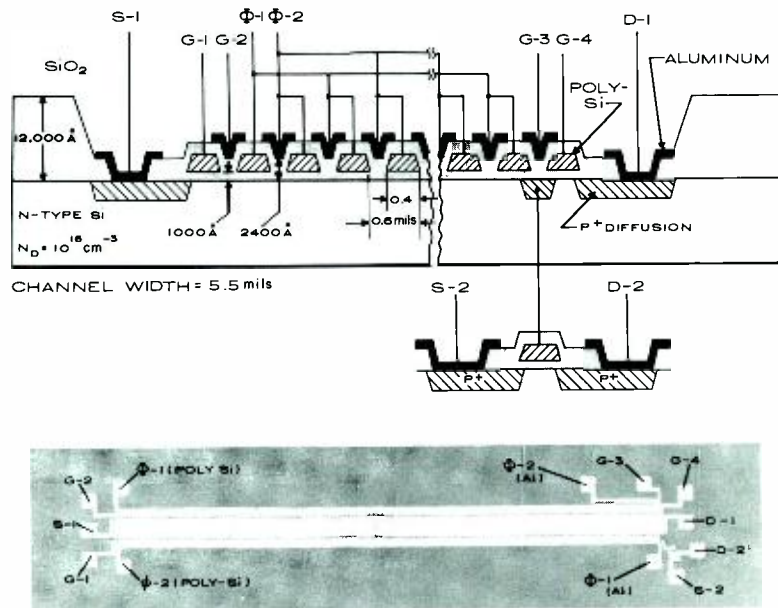


Fig. 5—Cross-sectional view and labeled photograph of CCD-T 128-stage shift register.

A particularly advantageous method of constructing two-phase CCD's which results in two thicknesses of oxide to provide signal directionality consists of polysilicon gates overlapped by aluminum gates. The method of making these devices is shown in Fig. 4. After definition, the polysilicon gates are partially oxidized to form an insulating layer and to increase the oxide thickness in the region between the gates. The aluminum is deposited and defined so that it overlaps the polysilicon gates as shown. The spacing between electrodes is determined by the polysilicon oxide thickness—typically 2000 \AA . No gaps are exposed to ambient and standard alignment (0.1 mil) and etching (0.2 mil) techniques result in 1.2 mil per stage (two polysil-

con gates and two aluminum gates) spacing. Such devices have been built and experimental results have been obtained.

Experimental results

A variety of CCD device structures have been fabricated at RCA Laboratories in the past two years, including three-phase single-level metal p- and n-channel devices and two-phase polysilicon overlapped by aluminum devices. The two-phase devices have generally been more well behaved and predictable than the single-level metal devices, probably because of the absence of gaps in the two-phase structures.

The cross-sectional view of a 128-stage two-phase CCD is shown in Fig. 5. In

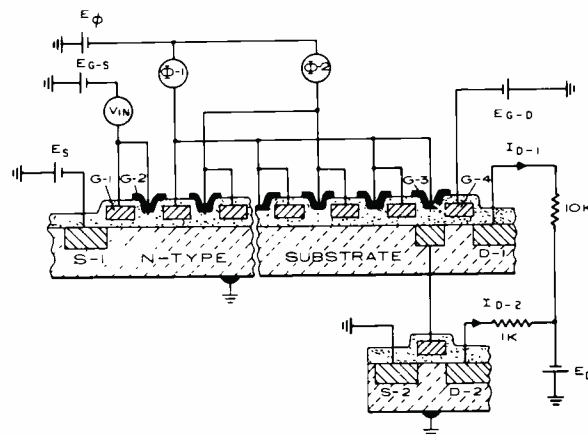


Fig. 6—Circuit diagram for the tests of two-phase charge-coupled shift registers.

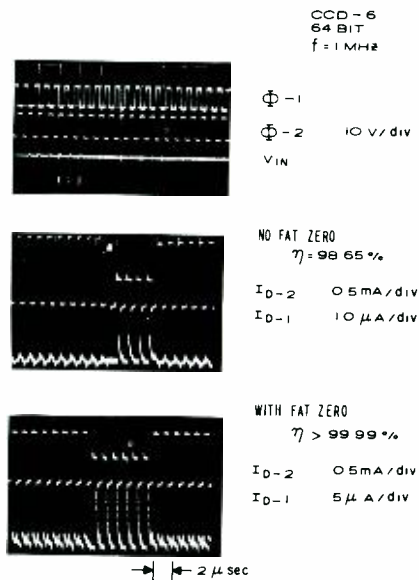


Fig. 7—Typical waveforms for CCD-6 64-stage shift register at 1 MHz.

the operation of this shift register (Fig. 6) the input charge signal is introduced by input pulses V_{in} and the bias voltages E_s and E_{g-s} . The output is detected either directly by “current sensing” as I_{D-1} current or as I_{D-2} by “voltage” or rather “charge-sensing” in which case the potential of a floating diffusion controls the gate of a MOSFET amplifier.

Fig. 7 shows typical oscilloscope waveforms for a 64-stage, two-phase device on a (111) substrate. The improved operation is clearly evident when fat zero is introduced. The experimental measurements of transfer efficiency vs. frequency on the two-phase devices have confirmed many of the analytical predictions discussed earlier, especially concerning the transfer of free charge by thermal diffusion and losses due to fast interface states. Fig. 8 shows the

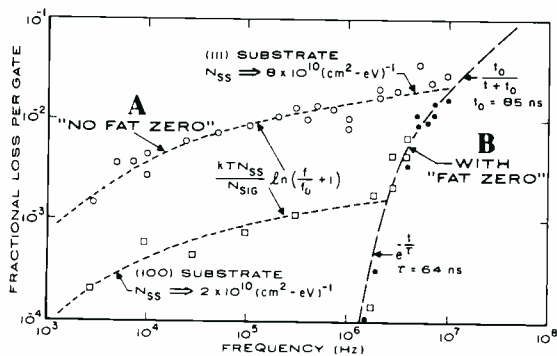


Fig. 8—Fractional loss per transfer vs. frequency for 128-stage shift register with and without fat zero.

fractional loss per transfer vs. frequency for a 128 stage, two-phase p-channel device with a 10- μ m-long polysilicon gate. First, the two left branches of the curve show the loss vs. frequency when no fat zero is introduced and fast state losses are expected to dominate. The top curve is for a device built on (111) silicon substrates with expected N_{SS} values of approximately 10^{11} ($\text{cm}^2\text{-eV}^{-1}$), and the bottom one is for (100) material with fast state densities expected to be $\sim 10^{10}$ ($\text{cm}^2\text{-eV}^{-1}$). A fit of the data to Eq. 7 yields a value of 8×10^{10} for the (111) device and 2×10^{10} for the (100) device, close to the values expected. The n_{ss} values deduced from the plots were consistent with those expected for thermal generation.

The right branch of the data in Fig. 8 shows the measured loss when a fat zero (10 to 20% of a full well) was intentionally introduced. The fast state losses have been reduced to an immeasurably low level and CCD operation is limited at the higher frequencies by free charge transfer. The doping of the substrate here is 10^{16}cm^{-3} —too high for fringing fields to be appreciable. Thus, the free-charge transfer is dominated by thermal diffusion. The dotted line shows the loss expected for a 10- μ m-gate device—indicating excellent agreement with the actual results. A hole mobility of $250\text{cm}^2\text{-(V-sec)}^{-1}$ was assumed.

Analog signal processing

Charge-coupled devices represent a new LSI technique for the processing of analog information. With charge-transfer loss (inefficiency) $\epsilon = 10^{-4}$ per stage, a figure which has been demonstrated experimentally (as discussed earlier), the analog signal can be transferred through up to 1000 stages of CCD with only minor amplitude and phase degradation which should be acceptable for most applications. One can see, therefore, delay lines for video and audio signals which can be operated with fixed or electronically-variable time delay as one of the direct and obvious applications of CCD's. The time delay, τ_d , for a CCD delay line is

$$\tau_d = N(1/f_c) = N/(2\Delta B) \quad (8)$$

where N is the number of stages, f_c is the clock frequency, and ΔB is the bandwidth. The CCD delay line oper-

ates by sampling the input signal once every clock cycle. Therefore, it is capable of signal bandwidth, ΔB , of close to $f_c/2$. The electronically-variable delay is obtained by varying the clock frequency. The maximum time delay, τ_{dmax} , for a CCD delay line is independent of the number of stages and is limited by the dark current generation rate. The practical upper limit for τ_{dmax} at room temperature is 0.1 to 1.0 s. For example, audio delay of 10 to 20 ms with ΔB of 20 kHz (hi-fidelity delay for quadrasonic speaker synchronization) would require $f_c = 4$ kHz and $N = 400$ to 800 stages.

Since CCD's can store and transfer analog signals under the control of externally applied clock pulses, they can be used as basic components for sorting, switching, and processing of analog information. Examples of such applications are serial-to-parallel and parallel-to-serial conversion, time synchronization and time conversion (compression or expansion), and transversal filters. For example, parallel-to-serial conversion of N elements can be obtained by simultaneous parallel loading of a CCD shift-register by N input circuits. Once the shift-register is loaded, the clock is actuated and the N elements are readout serially at the CCD output. Time conversion can be achieved using a CCD shift register by reading in data at one clock rate and reading out at another higher (compression) or lower (expansion) clock rate. The transversal filters can be used to implement a large class of transfer functions, for example, matched filters. The operation of the transversal filter consists of weighting and summing of parallel signals tapped from various points along the analog delay line.

Charge-coupled image sensor applications

The CCD concept has introduced a revolutionary new approach to the design of self-scanned solid-state image sensors. We will refer to such a device as a charge-coupled imager (CCI). One can think of the CCD as the semiconductor equivalent of an electron-beam tube in which the charge signal can be moved (transferred) and stored under the control of the clock voltage pulses free of pick-up and switching transient. The only limitations on the charge-coupling process comes about because the charge transfer is not

100% complete. The finite transfer loss (inefficiency) results in some distortion of the signal, and introduces transfer noise. As will become apparent from the following description of known cci arrays, the pick-up from the clock voltages is limited to a single output stage.

Two ways by which the optical signal can be introduced into the cci are illustrated in Fig. 9. The optical input can be introduced from the top of the substrate through the spaces between non-transparent metal gates (Fig. 9a). Top illumination of the cci is also possible by transmitting the optical input through transparent gates such as thin polysilicon. An alternate approach (Fig. 9b) consists of thinning the substrate in the optically-sensitive area and applying the optical input from the back side of the substrate. Fig. 9 also illustrates two ways by which the output can be removed from the cci array. Output-1 is the current output derived from the drain diffusion *D*. The low impedance output-2 samples the voltage of the floating diffusion *F* and is proportional to the charge signal. Let us assume now that an optical input is applied to such a CCD register while the clock voltages are adjusted so that one potential well is created at each stage along the CCD channel. As suggested in Fig. 9a, the photogenerated charge will collect in these wells during the optical integration time. At the end of the integration time, the accumulated charge packets representing the integrated optical input are shifted down the cci register and detected by a single output amplifier. To prevent smearing of the image, the optical integration time should be much larger than the total time required to transfer the detected image from the CCD line sensor. Since all charge elements are amplified by the same amplifier, non-uniformities—usually a problem in optical arrays in which each sensor element uses a separate amplifier—are avoided. Since there is no direct coupling of the clock voltages to the charge signal in the CCD channel, the clock pick-up is limited only to a single output stage. In addition, since only the clock frequency, which is outside of the video bandpass, is used in CCD transfer, clock pick-up is not the problem as it is in x-y scanned arrays where one of the

clocks occurs at the horizontal line frequency and cannot be removed by appropriate filtering.

A more effective CCD line sensor (or cci line array) is shown schematically in Fig. 10a. Here, the optical input can be continuously integrated by the linear array of photodiodes. During the operation, the detected line image is periodically transferred in parallel to the CCD register from where it is read-out serially. It is essentially an analog parallel-to-series converter, with time-integrated optical input and electrical output. A dual CCD-channel line-sensor is shown in Fig. 10b. The operation of this cci is the same as for the line sensor described above except that the detected image is transferred into two parallel CCD registers and then combined into a single output line. The advantage of the dual CCD-channel line-sensor over the line-sensor shown in Fig. 10a is double resolution.

One way of implementing an area cci is illustrated in Fig. 11. This array can be visualized as a parallel array of the previously described linear arrays whose outputs are transferred in parallel into a single output register. The operation of this cci is as follows. Once every frame time the charge signal detected by the photodiode array is transferred into the vertical CCD channels, which are not photosensitive. Then, the entire detected image is shifted down in unison by clock A and transferred into the output register one (horizontal) line at a time. The horizontal lines are then transferred out from the output register by the high frequency clock B before the next horizontal line is shifted in.

Another frame transfer cci that does not require separate photosensors is shown in Fig. 12.¹⁵⁻¹⁶ In this cci, the photosensor function is performed by an additional photosensitive CCD array. This system is composed of three functional parts: the photosensitive array, temporary storage array, and the output register. The optical image is detected by the photosensitive array. Then assuming a tv format with 1/60-s frame time, the detected image is transferred into the temporary storage array by clocks A and B, during the vertical blanking time, (900 μ s). From there, it is shifted down one horizon-

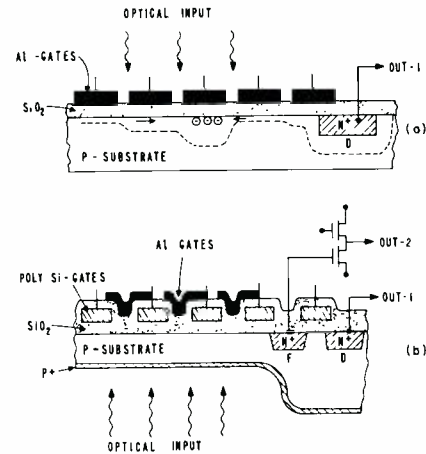


Fig. 9—Cross-sectional view of (a) top (front) illuminated CCI; (b) back illuminated CCI

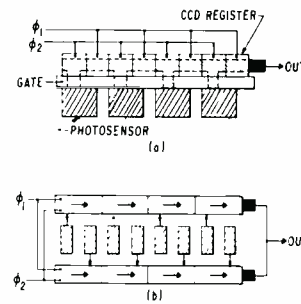


Fig. 10—Charge-coupled line sensors: (a) with single CCD channel; (b) with two parallel CCD channels.

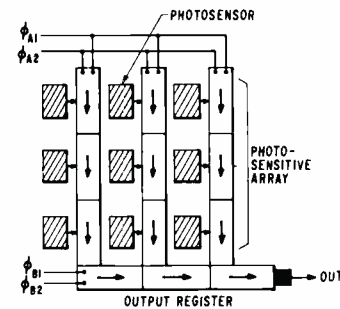


Fig. 11—Frame transfer with separated photosensors.

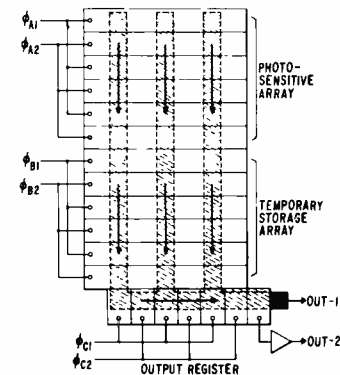


Fig. 12—Frame transfer CCI with a temporary storage array.

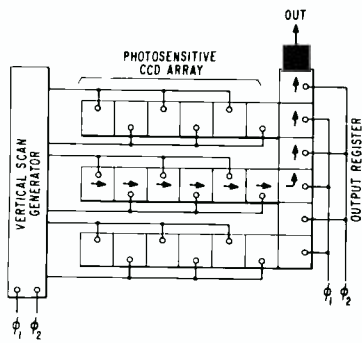


Fig. 13—Horizontal line-by-line transfer CCI.

tal line at a time into the output register and transferred out by the high speed clock C. The time available for parallel loading of the output register corresponds to the horizontal line retrace time of $10 \mu\text{s}$, which leaves $50 \mu\text{s}$ for the read-out of the horizontal line from the output register.

A third type of CCD area array (Fig. 13) was made originally at RCA Laboratories using bucket-brigade shift registers.¹⁷⁻¹⁹ This system consists of parallel array of photosensitive, horizontal, CCD channels, all leading into a single output register. This CCI operates by transferring, under the control of the vertical clock generator, one horizontal line at a time, from the photosensitive CCD array to the output register and out.

The frame-transfer system with temporary storage array has been chosen for the development of a two-phase CCI TV camera. Although this system requires somewhat larger area of silicon than the other two systems, it can be designed with known CCD techniques. Using design rules applied to our existing two-phase CCD, this system can be implemented with optical resolution elements on 1.2-mil centers. A device with blooming control and an electronically variable exposure time can be constructed more easily with the frame transfer system. However, unlike the charge-transfer system with separate photodiode arrays, it requires back-side illumination for efficient operation.

In addition to the advantages of solid-state construction offering small size, rugged construction, long life, and low power dissipation, CCI TV cameras should be relatively low-noise sensors—about an order of magnitude more sensitive than the silicon vidicon. While the sensitivity of the silicon vidicon is limited by the output capaci-

tance (10 to 20pF), the output capacitance of a CCI can be about two orders of magnitude smaller, 0.1 pF. Analysis shows²⁰ that the sensitivity of the CCI designed with the output amplifier integrated on the same chip should be limited by the transfer noise associated with the charge trapped by the fast interface states in the surface channel CCD, and the shot noise due to the background charge either thermally generated as the dark current, or introduced as a "fat zero" to eliminate the interface state losses.

Digital storage applications

One of the potentially attractive digital applications of the CCD is an inexpensive bulk digital storage. However, unlike the case of analog processing and image sensing devices where the CCD offers a new technology previously not available, the CCD must now compete in price and performance with other storage devices. Using comparable layout rules, the CCD offers packing density advantages only about 2 to 4 over the dynamic MOS memories.²¹ However, except for the signal regeneration and input/output stages, the CCD memories can be made without diffusions and contact openings. This implies that eventually CCD memories can be made with much higher packing density as well as higher yield and larger chip sizes than will be possible using MOS circuits.

Charge-coupled shift registers are basically analog devices with no signal gain mechanisms. To use these devices for storage of digital signals, it is necessary to periodically refresh or to regenerate the charge signal. Simple charge regeneration, such as shown in Fig. 14, can be laid-out in an area no larger than the area required for 2 to 4 stages of shift register.⁷

Various system organizations can be considered for the construction of charge-coupled memories. The choice of the system organization depends on the desired system performance. Two types of systems in the form of a single large-storage loop per chip are illustrated in Fig. 15. As is shown, the signal flow in system A follows a serpentine pattern and has signal refreshing stages at each corner. The system B on the other hand is in the form of two serial and one large parallel shift register as well as a single signal re-

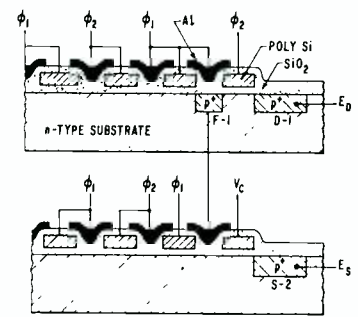


Fig. 14—Schematic cross-section of two CCD shift registers with simple charge regeneration scheme using a floating diffusion.

generation, similar to the frame transfer CCI shown in Fig. 12. Two-phase charge-coupled structures are needed for an efficient design of system A. The system B on the other hand could be constructed with either two-phase or three-phase structures. At this point, it should also be noted that the frame-transfer CCI with a separate store can be designed so that it can also be operated as a digital store, or as an electronic camera for digital images.

The system organizations for obtaining more parallel operation, smaller storage loops, and shorter access time are shown in Fig. 16. The addressing of the individual storage loops in system C is accomplished by a decoder. Still more parallel organization with smaller storage loops addressable by an x-y matrix switch is illustrated by system D. As in the case of system A, two-phase or uniphase charge-coupled devices will also lead to a more efficient design of systems C and D.

Finally, the most parallel memory is system E, shown in Fig. 17. This system represents the charge-coupled version of one transistor-per-bit refreshable memory. The signal is stored in single charge-coupled elements that are periodically gated by the word lines into the digit-line diffusions. Each digit-line drives a signal-regeneration or sense amplifier whose output regenerates the information in the selected bit location and also may be gated-out. The main difference is that, in systems A through D, the signal-regeneration amplifiers are driven by high impedance charge-coupled storage loops. Thus, high packing density can be accomplished since relatively high voltage (on the order of several volts) is available at the low capacitance input of the signal regeneration for small charge signals representing the information. However, system E

has a large number of individual charge-storage elements connected in parallel to a single regeneration amplifier. Therefore, the input voltage available to the sense amplifier is attenuated by the capacitance divider corresponding to a relatively small storage capacitance and a considerably larger capacitance associated with digit-line amplifier input.

Our analysis of the transfer of the free charge indicates that the maximum bit rate for such serial memories may be in excess of 10^7 bits/s. The chip selection and other signal switching may, however, impose a practical upper limit on the bit rate in the range between 10^6 to 10^7 bits/s. Assuming a packing density of about 1 square mil of silicon per bit of storage, the charge-coupled serial memories may be constructed with about 40 kilobits on a single chip of silicon having dimensions of about 200×200 mils. The above packing density involves more or less state-of-the-art circuit layout rules. Therefore, considerably higher packing density may be achieved by employing high resolution processing.

Another attractive feature for a large-capacity charge-coupled serial memory is a rather low power requirement if the high-frequency phase-voltage pulses are applied only to the selected shift registers while the unselected storage loops are idling at a much lower clock rate. Assuming a channel oxide of 2000 \AA and an area of one charge-coupled electrode of 10^{-6} cm^2 , the corresponding capacitance of each phase electrode is about $1.76 \times 10^{-14} \text{ F}$. For the phase voltage of 10V, the reactive energy per phase for one bit storage is about $2 \times 10^{-12} \text{ J}$. For a clock rate of 10^7 bit/s, the reactive power is

estimated as $20 \mu\text{W}$ per bit. If we assume that for a 10^8 -bit memory no more than 10^5 bits are operating at any time at the rate of 10^7 bits/s, the clock power required for the selected chips will be 2W. The total standby power for the 10^8 -bit memory will also be 2W if the idling clock rate for the unselected chips is chosen as 10^4 bits/s.

Conclusions

Although the CCD concept is not quite three years old, the operation of these devices is quite well understood, and has been experimentally verified. Charge transfer efficiencies of 99.99% have been achieved. A number of applications in the area of analog signal processing, image sensors, and digital memories are in the process of development. Some examples of CCD products that may soon become commercially available using present LSI technology are electronically-variable analog delay lines and low-resolution image sensors (100×100 elements). It is expected that the development of a full resolution CCI TV camera (500×500 elements) should provide the impetus for the achievement of a "giant" chip LSI technology.

References

- Boyle, W. S. and Smith, G. E., "Charge-Coupled Semiconductor Devices," *Bell System Tech. J.* (1970) p. 587.
- Amelio, G. F.; Tompsett, M. F.; and Smith, G. E., "Experimental Verification of the Charge-Coupled Device Concept," *Bell System Tech. J., Briefs* (April 1970) p. 593.
- Tompsett, M. F., and Zimany, E. J., "Use of Charge-Coupled Devices for Analog Delay," *Digest of Technical Papers, 1972 IEEE International Solid-State Circuits Conference*, Philadelphia (Feb. 1972) p. 136.
- Kosonocky, W. F. and Carnes, J. E., "Two-Phase Charge-Coupled Shift Registers," *Digest of Technical Papers, IEEE International Solid State Circuits Conference*, Philadelphia, Pa. (Feb. 1972) p. 132.
- Kosonocky, W. F. and Carnes, J. E., "Two-Phase Charge-Coupled Device," *Final Report PRRL-72-CR-6*, Langley Research Cen-

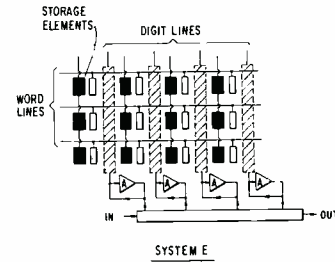


Fig. 17—Charge-coupled version of one transistor-per-bit refreshable random access memory.

- ter, Hampton, Virginia. NASA, Contract No. NAS 1-10983, (Feb. 1972).
- Heiman, F. P., "On the Determination of Minority Carrier Lifetime from The Transient Response of an MOS Capacitor," *IEEE Trans. Elect. Dev.* Vol. ED-14, No. 11, (1967) p. 781-786.
- Kosonocky, W. F. and Carnes, J. E., "Charge-Coupled Digital Circuits," *IEEE J. Solid-State Circuits* Vol. SC-6, (1971) p. 314.
- Carnes, J. E.; Kosonocky, W. F.; and Ramberg, E. G., "Free Charge Transfer in Charge-Coupled Devices," *IEEE Trans. on Electron Devices*, Vol. ED-19, No. 6, (1972) pp. 798-808.
- Carnes, J. E. and Kosonocky, W. F., "Fast Interface State Losses in Charge-Coupled Devices," *Appl. Phys. Ltrs.* Vol. 20, No. 7 (April 1, 1972) p. 261.
- Engeler, W. E.; Tiemann, J. J.; and Baertsch, R. D., "Surface Charge Transport in Silicon," *Appl. Phys. Letters* 17, (1970) p. 469.
- Kim, C. K., and Lenzlinger, M., "Charge Transfer in Charge-Coupled Devices," *J. Appl. Phys.* 42, (1971) p. 3586.
- Carnes, J. E.; Kosonocky, W. F.; and Ramberg, E. G., "Drift-Aiding Fringing Fields in Charge-Coupled Devices," *IEEE J. Solid State Circuits* SC-6, (1971) p. 322.
- Bertram, W. J., "Application of Charge-Coupled Device Concept to Solid State Image Sensors," *Digest of Technical Papers, 1971 IEEE International Convention*, New York (March 22-25, 1971) p. 250.
- Tompsett, M. F.; Amelio, G. F.; Bertram, W. J.; Buckley, R. R.; McNamara, W. J.; Mikkelsen, J. C.; and Sealer, D. A., "Charge Coupled Imaging Devices: Experimental Results," *IEEE Trans. Electron Devices*, ED-18, (Nov. 1971) p. 992.
- Bertram, W. J.; Sealer, D. A.; Sequin, C. H.; Tompsett, M. F.; Buckley, R. R., "Recent Advances in Charge-Coupled Imaging Devices," *Digest of Technical Papers, 1972 IEEE International Convention*, New York (March 20-23, 1972) p. 292.
- Weimer, P. K.; Kovac, M. G.; Pike, W. S.; Shallcross, I. V., "Charge-Coupled Imager," *Final Report*, Sept. 1972, Contract Number 0014-71-C-0415.
- Kovac, M. G.; Weimer, P. K.; Shallcross, F. V.; and Pike, W. S., "Self-Scanned Image Sensors Based Upon Bucket-Brigade Scanning," abstract of paper presented at the IEEE Electron Devices Meeting, Washington, D. C., (Oct. 1972).
- Kovac, M. G.; Shallcross, F. V.; Pike, W. S.; and Weimer, P. K., "Image Sensors Based on Charge Transfer by Integrated Bucket Brigades," *International Electron Devices Meeting*, Washington, D. C., (Oct. 11-13, 1971).
- Kovac, M. G.; Pike, W. S.; Shallcross, F. V.; and Weimer, P. K., "Solid State Imaging Emerges from Charge Transport," *Electronics*, (Feb. 28, 1972) p. 72.
- Carnes, J. E. and Kosonocky, W. F., "Noise Sources in Charge-Coupled Devices," *RCA Review*, Vol. 33, No. 2, (June 1972) pp. 327-343.
- Karp, J. A., Reitz, W. M.; and Chou, S., "A 4096-Bit Dynamic MOS RAM," *JSSCC Digest of Tech. Papers*, (Feb. 1972) pp. 10-11.

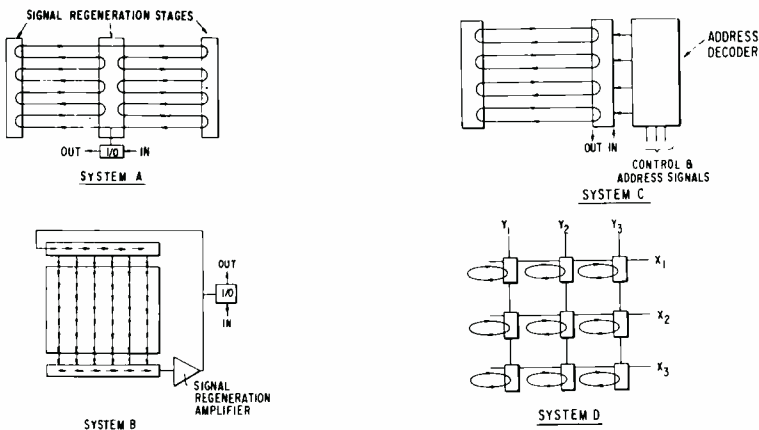
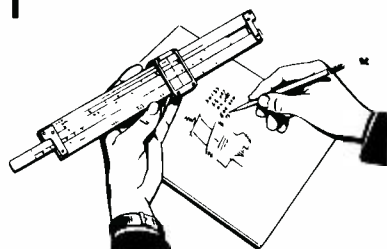


Fig. 15—Two types of memory systems using single storage loop.

Fig. 16—Two memory system organizations for obtaining more parallel operation, smaller storage loops, and shorter access times.

Engineering and Research Notes



Analog-to-digital (rolling sample) correlator

Hunter C. Goodrich
Missile and Surface Radar Division
Moorestown, New Jersey



H. C. Goodrich

Edward C. Farnett
Missile and Surface Radar Division
Moorestown, New Jersey



E. C. Farnett

A solid-state (rolling-sample) correlator provides for spatial correlation of an analog radar signal with a digitally coded waveform reference. Although the correlator retains analog signal levels, all transistor stages are operated either as *on/off* switches or as highly degenerative emitter-followers. The plan allows the substitution of simple sample-and-hold circuits for the usual tapped analog delay line by means of a unique "rolling sample" and circulating reference synchronization method. Thus the correlator is freed from the usual delay-line constraints of limited bandwidth and limited time-bandwidth product.

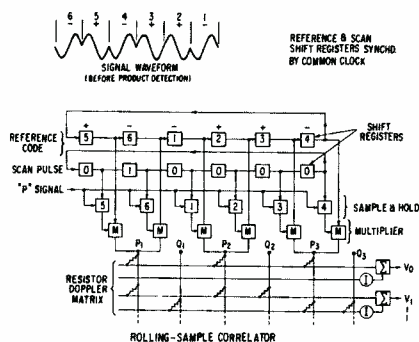


Fig. 1—Six-stage, biphasic, analog-to-digital correlator.

In the block diagram (Fig. 1), a small number of stages is shown for illustration. Correlators of up to 1000 or more stages will become practical with integration. The reference waveform code is stored in the upper shift register while a scan (or sample) pulse is stored on the lower shift register. Both shift registers are continuously recirculated by a clock. The timing is such that the scan pulse is in synchronism with the last element of the reference waveform. The shift rate of the registers is made equal to the waveform code bit rate. A correlator stage is provided for each element in the waveform code.

When the radar signal returns, each element of the signal is sampled by the scan pulse and stored on a sample-and-hold circuit. Each sample is held until the scan pulse has made full circulation of the register and returned to that particular correlator stage. For example, in a 100-bit waveform where each bit has a duration of $0.1 \mu\text{s}$, the signal sample would be taken within a period less than $0.1 \mu\text{s}$ and would be held for $10 \mu\text{s}$. Multiplication between data stored on the sample-and-hold circuits and the reference waveform stored on the upper shift register occurs on a continuous basis. When the final element (bit) of a given radar target signal arrives, it is sampled by the scan pulse and stored in the last (unloaded) sample-and-hold circuit. The full signal will be contained within the bank of sample-and-hold circuits for this one-bit period. Because of the synchronism between the scan pulse and the last element of the reference waveform, a one-to-one correlation will now occur between each element of the reference waveform and the corresponding element of the return radar signal. The output of the summing bus will now be at a maximum. Fig. 1 illustrates the case where the first element of the signal arrived as the third stage from the left was being sampled and the last element arrived when the sample pulse had circulated around and reached the second stage from the left. Because of the synchronization plan, the reference code is in the correlating position at this instant. If the target range time had been $0.1 \mu\text{s}$ longer, the stored position of each signal element would be shifted one position to the right from that shown, but the reference code would also have shifted one position to the right. Thus, full correlation would also occur from the second case, but would happen $0.1 \mu\text{s}$ later than in the first case.

For waveforms that are relatively short, so that no significant doppler phase shifts occur during the waveform interval, all the correlator stage outputs can be directly summed. If the waveform is long, so that phase shifts do occur for moving targets, the outputs can be summed in groups and applied to a resistor matrix as shown in Fig. 2. The horizontal summing lines of this matrix are coupled to the input lines with a coded pattern of coupling resistors so that a different output line is matched for each doppler resolution channel. The correlator now becomes two-dimensional, indicating both the range and velocity of each target.

The correlator configuration has been described for a contiguous element bi-phase. However, it can be adapted to multiple burst signals, to quadrature coding, and to stretch systems.

Self-contained impact detector and reporter

Anton J. Lisicky
Government Plans and Systems Development
Moorestown, New Jersey



Earl D. Grim
Mgr., Space Systems
Government Plans and Systems Development
Moorestown, New Jersey



Maurice G. Staton
Div. V.P., Advanced Space Programs
Astro-Electronics Division
Hightstown, New Jersey



A compact self-contained unit easily attachable to a missile or satellite provides a means for detecting and reporting on impact by a foreign object. The device is easily contained in a volume of one cubic inch utilizing integrated circuitry and miniaturized components. The device, as illustrated in Fig. 1, is provided with the piezoelectric transducer, a power supply such as a battery, a module of microwave integrated circuits arranged to provide the functions of a modulator and a transmitter, a solar cell, and a printed cross-dipole antenna.

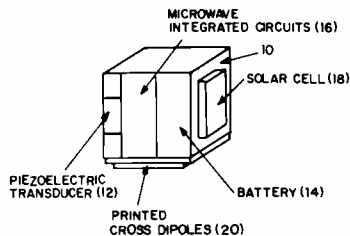


Fig. 1—Impact detector and reporter.

As shown in the system block diagram (Fig. 2), the transducer is coupled to a filter and threshold device, the output of which is coupled to a modulator, suitably a one-shot device for activating a transmitter. The transmitter output is coupled through the antenna to a ground station. The solar cell recharges the battery, which provides the power for the various circuits as indicated.

When an object strikes the vehicle, the piezoelectric transducer (*e.g.*, a barium titanate crystal) senses the vibrations caused by the object striking it. The transducer output is coupled directly or fed through electrical filtering to eliminate responses to vehicle operating noises. A bias adjustment provides a means for calibrating the level of threshold. Selectivity of the desired responses can be further enhanced by an adjustable threshold operating on the filter output. The threshold triggers the one-shot multivibrator which applies DC voltage to the transmitter.

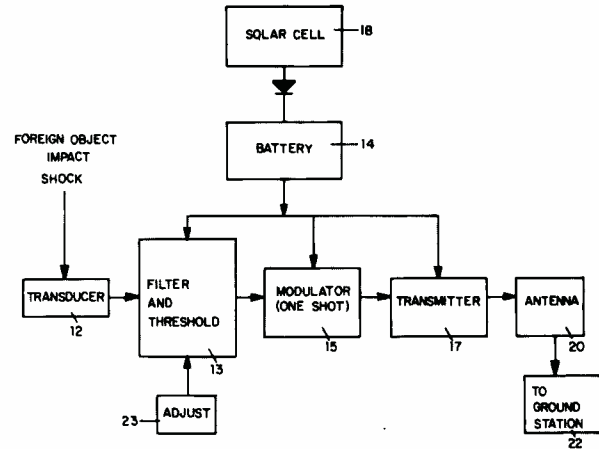


Fig. 2—System block diagram.

The RF energy output is radiated through a printed cross dipole or equivalent, antenna to a receiver at the ground station 22.

The transmitter can be an L- or S-band unit. It may be a loaded oscillator such as an RCA L-band Radiosonde. In the alternative, the transmitter may be an oscillator-power amplifier, RCA-TA-7785. A 500 mW output at a frequency of 2.2 to 2.3 GHz for a duration of 10 s is adequate to provide a signal to a ground facility from a satellite at synchronous altitude.

The power supply is typically a nickel-cadmium storage battery with a capacity of 280 W-s. If desired, at launch, the battery is in a discharged state, thereby preventing the unit from inadvertently responding to the vibrations of the vehicle that occur during the launch phase. A suitable solar cell provides 24 V at 1 mA and is adequate for the requirements of the system. It develops sufficient power after one hour exposure to the sun. Suitable controls, such as a back-biased diode prevents the battery from discharging through the solar cell.

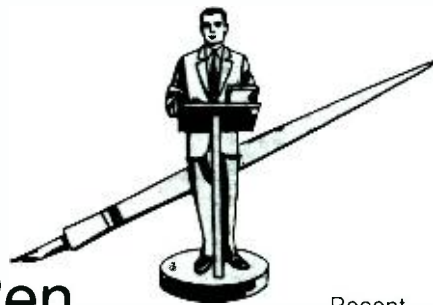
This arrangement eliminates the need for external control of the unit and thus the need for any sort of time and command receiver. Simplicity of design for a fully self-contained impact sensor unit is accordingly available with a simple design form.

The compact form of the unit *e.g.* one cubic inch, allows for it to be adhered to the vehicle at one or more positions which are best for sensing and reporting impact by foreign objects. In satellite systems, three axis vehicle rebalancing is minimized because of the light weight and the placement ease at suitable locations. Furthermore, the small size reduces the probability of it being hit either directly or by secondary impact. Also, the need for "hardening" from radiation contamination effects is minimized.

Other sensing applications

The basic configuration of this impact sensor is suitable for system applications other than spacecraft. For example, impact sensing on target drones and remotely piloted vehicles in test or under operational conditions is an obvious application. Perhaps less obvious, but also very possible, is application to burglar alarms, or personnel or vehicle detection with an RF link to a central station. Although these new applications could require changes in the layout of the sensor, the basic components and concept would remain the same. The device is also suited to other similar applications where there is emphasis on sensing impact or shock remotely with a small, cheap device whose reliability and survivability can be assured through redundancy.

Reprinted RE-18-5-1 | Final manuscript received August 24, 1972.



Pen and Podium

Recent RCA technical papers and presentations

Both published papers and verbal presentations are indexed. To obtain a published paper, borrow the journal in which it appears from your library, or write or call the author for a reprint. For information on unpublished verbal presentations, write or call the author. (The author's RCA Division appears parenthetically after his name in the subject-index entry.) For additional assistance in locating RCA technical literature, contact: **RCA Staff Technical Publications, Bldg. 2-8, RCA, Camden, N.J. (Ext. PC-4018).**

This index is prepared from listings provided bimonthly by RCA Division Technical Publications Administrators and Editorial Representatives—who should be contacted concerning errors or omissions (see inside back cover).

Subject index categories are based upon standard announcement categories used by Technical Information Systems, Corporate Engineering Services, Bldg. 2-8, Camden, N.J.

Subject Index

Titles of papers are permuted where necessary to bring significant keyword(s) to the left for easier scanning. Authors' division appears parenthetically after his name.

SERIES 100 BASIC THEORY & METHODOLOGY

105 Chemistry

... organic, inorganic, & physical.

TIN SENSITIZING SOLUTIONS. Some Aspects of the Chemistry of—N. Feldstein, J.A. Winer, G.L. Schnable (Labs,Pr) *J. of the Electrochem. Soc.*, Vol. 119, No. 11, pp. 1486-1490; 11/72

125 Physics

... electromagnetic field theory, quantum mechanics, basic particles, plasmas, solid state, optics thermodynamics, solid mechanics, fluid mechanics, acoustics.

INTERNAL PHOTOEMISSION in Insulator Systems—R. Williams (Labs,Pr) American Vacuum Soc. Symp., Yorktown Heights, N.Y.; 12/7/72

OPTICAL SCINTILLATION Through Turbulent Air (Part II), Strong—D.A. deWolf (Labs,Pr) 1972 Fall URSI Mtg., Williamsburg, Va.; 12/12/72

TURBULENT PLASMA, Direct and Cross Polarized Back Scatter from—I.P. Shkarofsky, A.K. Ghosh, E.N. Almey (RCA LTD.,Mont) *Plasma Physics*, Vol. 14, No. 10; 10/72

160 Laboratory Techniques & Equipment

... experimental methods & equipment, lab facilities, testing, data measurement, spectroscopy, electron microscopy, dosimeters.

INTEGRATING SPHERE for Use with a Spectroradiometer—L.J. Nicastro, A.L. Lea (ATL, Camden) *Applied Optics*, Vol. 11, No. 10, pp. 2379; 10/72

PHOTOEMISSION Measurements of the Silicon/Silicon Dioxide Interface. Laser Scanning—R. Williams, M. Woods (Labs,Pr) *J. of Applied Physics*, Vol. 43, No. 10, pp. 4142-4123; 10/73

SHEET-RESISTIVITY Measurements with Two-Point Probes. Non-Destructive—J.L. Vossen (Labs,Pr) *RCA Review*, Vol. 33, No. 3, pp. 537-542; 7/72

ELECTROLESS PLATING, The Mechanism of—N. Feldstein (Labs,Pr) Seminar - Dept. of Physics, Univ. of Windsor, Windsor, Ont.; 12/14/72

CONNECTOR SYSTEMS, Basic Selection of—B.R. Schwartz (M&SR) *Handbook of Wiring, Cabling and Interconnecting for Electronics*; 11/72

QUALITY-COST EQUATION, The Solid State, Its Impact on the Specifier, Buyer, and Supplier—D.P. Del Frate (SSD, Som) Western Electronic Show and Convention (WESCON), Los Angeles, Calif.; Conf. Proc.; 9/72

PLASTIC PACKAGE for Integrated Circuits, High-Reliability—H. Khajezadeh (SSD, Som) 1973 Reliability Physics Symp., Las Vegas, Nevada; 4/73

PRODUCIBILITY: the Critical Engineering/Manufacturing Interface (Session Chairman and Panel Moderator)—A. Levy (EASD, Van Nuys) '72 WESCON Professional Panel, Los Angeles, Calif.; 9/72

YIELD ANALYSIS FOR Hybrid Microelectronics Circuits—A. Levy (EASD, Van Nuys) 1972 Int'l Microelectronics Symp., Washington, D.C.; 10/30/72

180 Management & Business Operations

... organization, scheduling, marketing, personnel.

BETTER PRODUCTS at Lower Costs—E. Shecter (M&SR, Mrstin) Joint Engineering Management Conf., Atlanta, Ga.; 10/30/72

CANADIAN SCIENCE POLICY, Perspectives in—M.P. Bachynski (RCA LTD., Mont) Scitec Forum on Science Policy, Ottawa; 10/72

TECHNOLOGY on Management and the Work Force, Effect of—E.B. Galton (ASD, Burl) N.E. Aeronautical Institute Mtg., Daniel Webster Junior College, Nashua, N.H.; 11/8/72

SERIES 200 MATERIALS, DEVICES, & COMPONENTS

205 MATERIALS (ELECTRONIC)

... preparation & properties of conductors, semiconductors, dielectrics, magnetic, electrophysical, recording, & electromagnetic materials

AsP EMITTERS from Doped Glasses—F. Lee (Labs,Pr) 1972 IEEE Int'l Electron Devices Mtg., Washington, D.C.; 12/4-6/72

Bi-Sb ALLOYS for Magneto-Thermoelectric and Thermomagnetic Cooling—W.M. Yim, A. Amith (Labs,Pr) *Solid-State Electronics*, Vol. 15, pp. 1141-1165; 1972

CdS Single-Crystal Optical Cavities, High-Intensity Injection Luminescence in—F.H. Nicoll (Labs,Pr) *J. of Applied Physics*, Vol. 43, No. 10, pp. 4119-4123; 10/72

INSULATING GaN, Electroluminescence in—J.I. Pankove (Labs,Pr) American Physical Society Mtg., Los Angeles, Calif.; 12/27-29/72

LIQUID CRYSTAL, Materials and Display Devices—J.A. Castellano (Labs,Pr) Liquid Crystal Inst., Kent State Univ., Kent, Ohio; 11/29/72

p-TYPE PbTe-PbSe ALLOYS, Thermoelectric Properties of—I. Kudman (Labs,Pr) *J. of Materials Science*, Vol. 7, pp. 1027-1029; 1972

PYRACYLOQUINONE, The Photochemistry of—J.A. Castellano, F.J.M. Beringer, R.E.K. Winter (Labs,Pr) *J. of Organic Chemistry*, Vol. 37, No. 20, pp. 3151-3160; 10/6/72

SCHIFF-BASE LIQUID-CRYSTAL Mixtures, Equilibrium Properties of—H. Sorkin (SSD, Som) Symp. on Liquid Crystals, Kent State Univ.; 8/72, Kent, Ohio

SrTiO₃, Fundamental Absorption Edge of—D. Redfield, W.J. Burke (Labs,Pr) *Physical Rev. B*, Vol. 6, No. 8, pp. 3104-3109; 10/15/72

ZnSe and CdTe, Miscibility Between—W.M. Yim, J.P. Dismukes, E.J. Stofko, R.J. Ulmer (Labs,Pr) *Physica Status Solidi (a)*, Short Notes, Vol. 13, pp. K57-K61; 1972

210 Circuit Devices & Microcircuits

... electron tubes & solid-state devices (active & passive), integrated, array, & hybrid microcircuits, field-effect devices, resistors & capacitors, modular & printed circuits, circuit interconnection, waveguides & transmission lines.

CHANNEL CONCENTRATION in MOS Transistors by Statistical Analysis of the Substrate Bias Effect on Threshold Voltage—W.A. Bosenberg (Labs,Pr) 1972 Electron Devices Mtg., Washington, D.C.; 12/4-6/72

CHARGE-COUPLED DEVICES, Experimental Measurement of Noise in—J.E. Carnes, W.F. Kosonocky, P.A. Levine (Labs,Pr) 1972 IEEE Electron Devices Mtg., Washington, D.C.; 12/4-6/72

COS/MOS - The Pervasive Technology—V.E. Hills (SSD, Som) NY IEEE Subsection on Circuit Theory, Nutley, N.J.; 9/72

GaAs MILLIMETER-WAVE IMPATTIS, Fabrication and Performance of—K.P. Weller, A.B. Dreeben, S.T. Jolly (Labs,Pr) 1972 IEEE Int'l Electron Devices Mtg., Washington, D.C.; 12/4-6/72

GREEN ELECTROLUMINESCENT DIODES by "Double-Bin" Liquid-Phase Epitaxy, Efficient—I. Ladany, H. Kressel (Labs,Pr) *Proc. of the IEEE*, Vol. 60, No. 9; 9/72

GREEN-LIGHT-EMITTING DIODES, An Experimental Study of High-Efficiency GaP:N—I. Ladany, H. Kressel (Labs,Pr) *RCA Review*, Vol. 33, No. 3; pp. 517-536; 9/72

INTEGRATED CIRCUITS, Diagnostics of UHF and L-Band Applications—H.S. Veloric, S. Lazar, R. Minton, H. Meisel, P. Schnitzler, C. Kamnitsis (SSD, Som) First Regional Seminar on High-Frequency Applications of Hybrid Microelectronics, Technical Applications and Possibilities; Cambridge, Mass.; 6/72; Seminar Notes

LUMPED-ELEMENT Integrated Circuits for UHF and L-Band Applications—H.S. Veloric, S. Lazar, R. Minton, H. Meisel, P. Schnitzler, C. Kamnitsis (SSD, Som) First Regional Seminar on High-Frequency Applications of Hybrid Microelectronics, Technical Applications and Possibilities; Cambridge, Mass.; 6/72; Seminar Notes

MINIATURE TWT Design Suitable for High Output Power—New—M.J. Schindler (CE, Har) 1972 IEEE Int'l Electron Devices Mtg., Washington, D.C.; 12/4-6/72

MONOLITHIC DRIVERS, High Power—R.N. Guadagnolo (EASD, Van Nuys) Government Microcircuit Applications Conf. (GOMAC) Digest; San Diego, Calif.; 10/11/72

PHOTOMULTIPLIER with GaP (Cs) Dynodes, Fast Five-State—D.E. Persyk (CE, Har) 1972 IEEE Int'l Electron Devices Mtg., Washington, D.C.; 12/4-6/72

POWER TUBE for Mobile Communications at 900 MHz, New—F.W. Peterson (CE, Har) 1972 IEEE Int'l Electron Devices Mtg., Washington, D.C.; 12/4-6/72

TaTa²O⁵-Au Thin Film Shotky/Poole-Frankel Effect Devices—G.D. O'Clock (EASD, Van Nuys) *J. of Applied Physics*; 9/72

THRESHOLD CONTROL in COS/MOS Circuits, Ion Implantation for—A.G.F. Dingwall, E.C. Douglas (Labs,Pr) 1972 IEEE Int'l Electron Devices Mtg., Washington, D.C.; 12/4-6/72

TRANSISTOR CURRENT DISTRIBUTION, The Quasi-Saturation Regime, Infrared Observation of—R.A. Sunshine (Labs,Pr) 1972 IEEE Int'l Electron Devices Mtg., Washington, D.C.; 12/4-6/72

215 Circuit & Network Designs

... analog & digital functions in electronic equipment: amplifiers, filters, modulators, microwave circuits, A-D converters, encoders, oscillators, switches, masers, logic networks, timing & control functions, fluidic circuits.

ACOUSTIC SURFACE WAVE Signal Processing Devices in Communications Systems, Performance of—G.D. O'Clock, D.A. Gandolfo (EASD, Van Nuys) 1972 Ultrasonics Symp., Conf. Digest, Boston, Ma.; 10/7-7/72

A to D CONVERSION, Advances in High Speed—D. Benima (ATL, Camden) Government Microcircuit Applications San Diego, Calif.; 10/11/72

AMPLIFIER, 5W, Low Distortion, High Sensitivity—A.J. Leidich, L. Teslenko, C.F. Wheatley, Jr. (SSD, Som) IEEE Solid-State Circuits Conf., Philadelphia, Pa.; 2/72

COS/MOS Fuzer Timer Combines SCR and Analog Voltage Detector in Single IC—R. Fillmore (SSD, Som) 1972 Government Microcircuit Applications Conf., San Diego, Calif.; 10/72

DIGITAL INTEGRATED CIRCUITS for Consumer Applications. An Engineering Assessment of—D.R. Carley (SSD.Som) Western Electronic Show and Convention(WESCON), Los Angeles, Calif.: Coif. Proc.

DUAL-TRACKING VOLTAGE REGULATOR for Less than \$8—A.Sheng (SSD.Som) *Electronic Products*: 9/72

FREQUENCY MODULATOR, Serrasoid—B. Zuk, J.P.Keller (SSD.Som) IEEE Solid-State Circuits Conf., Philadelphia, Pa.: 2/72

FUNCTION GENERATOR, Super-Sweep—H.A. Wittlinger, A.J. Visoli (SSD.Som) *Electronic Products*: 8/72

MICROWAVE POWER TRANSISTOR Structures, Comparison of—D.S. Jacobson (SSD.Som) *Microwaves*: 7/72

MIS INPUT/OUTPUT SUBSYSTEM Development. Radiation Hardened—L. Dillon (ATL. Camden) Hardened Guidance & Weapon Delivery Technology Mtg., Princeton,N.J.: 10/18/72

OSCILLATORS, High-Power Microwave Transistor—G. Hodowanec (SSD.Som) *Microwave J.*: 10/72

PHASE-LOCKED LOOP, The RCA COS/MOS (CD4046A)—A Versatile Building Block for Micro-Power Digital and Analog Applications—D.M. Morgan, G. Steudel(SSD.Som) Mid America Electronics Conf., Kansas City, Missouri.: 10/72

PHASE-LOCKED LOOP, The RCA COS/MOS CD4046A Micro-Power—D. Morgan (SSD.Som) *Electronics*: 9/25/72

POWER SWITCH/AMPLIFIER IC for Industrial Applications, Programmable—G.J. Granieri (SSD.Som) Mid-America Electronics Conf., Kansas City, Missouri: 10/72

SAMPLE-AND-HOLD CIRCUIT, Simple, Low-Cost—H.A. Wittlinger (SSD.Som) *Electronic Design*: 10/12/72

THYRISTOR REGULATOR Circuit for SCR Deflection—W. Dietz (SSD.Som) *Fernseh Technische Tagung* (TV Bdcst. Recvr. Seminar), Braunschweig, Germany; 10/72

VOLTAGE REFERENCE SOURCES, Stable—D.Hampel (GCS. Camden) *IEEE J. of Solid State Circuits*, Vol. SC-7, Issue No. 3, pp. 267-269: 7/72

225 Antennas & Propagation

... antenna design & performance, feeds & couplers, phased arrays, radomes & antenna structures, electromagnetic wave propagation, scatter, effects of noise & interference.

ANTENNAS in Plasma as a Function of the Frequency of Excitation, The Behavior of—M.P. Bachynski (RCA LTD., Mont) *Radio Science*, Vol. 7, No. 8-9: 8/9/72

EARTH STATION ANTENNA for Domestic Satellite Communications, New—P. Foldes (RCA Ltd., Mont) Canadian Communications and EHV Conf., Montreal; 11/8-9/72

PHASED ARRAYS, Non-Classified Applications of—W.T. Patton (M&SR, Mrstn) Int'l IEEE/G-AP Symp., Williamsburg, Va.: 12/13/72

RADIATIVE-TRANSFER METHODS Applied to Electromagnetic Reflection from Turbulent Plasma, Discussion of—D.A. deWolf (Labs.Pr) *IEEE Trans. on Antennas and Propagation*, pp. 805-807, Vol. AP-20 No. 6: 11/72

240 Lasers, Electro-optical & Optical Devices ... design & characteristics of lasers, components used with lasers, electro-optical systems, lenses, etc. (excludes:masers).

ACOUSTO-OPTIC DEFLECTORS Using Sonic Gratings for First-Order Beam Steering, Broad-Band—G.A. Alphonse (Labs.Pr) *RCA Review*, Vol. 33, No. 3, pp. 543-594: 9/72

FAFEXAT—C.R. Horton, L.W. Dobbins (GCS, Camden) *Laser Focus* p. 46: 10/72

HOLOGRAPHIC MOVIES, Embossed—W.J. Hannan (Labs.Pr) Optical Soc. of America, Rochester, N.Y.: 12/5/72

HOLOTAPE—M.J. Lurie (Labs.Pr) Optical Soc. of America, Rochester Section, Rochester, N.Y.: 12/5/72

HOLOTAPE, Holographic Motion Pictures for TV Playback, RCA—R.A. Bartolini (Labs.Pr) Presentation to IEEE Student Chapter CCNY: 12/21/72

IMAGE SCANNER/RECORDER, LR 71 Laser—L.W. Dobbins (GCS, Camden) SPIE 16th Annual Tech. Mtg., San Francisco, Calif.: 10/16-18/72: *Proc. of 16th Annual Tech. Mtg. & Equip. Display*

INJECTION LASER Applications—W. Barratt, L. O'Hara, F. Shashoua (ATL, Camden) 1st European Electro-Optic Markets & Technology Conf., Geneva, Switzerland:9/12-15/72

INJECTION LASERS; Experimental Studies of Spontaneous Spectrum at Room Temperature—H.S. Sommers, Jr. (Labs.Pr) *J. of Applied Physics* Vol. 43, No. 10, pp. 4067-4123; 10/72

MODULATORS, Simple Acoustic Grating—J.M. Hammer, D.J. Channin (Labs.Pr) *Applied Optics*, Vol. 11, No. 10, pp. 2203-2209; 10/72

OPTICAL DETECTORS for High-Data-Rate Optical Communication, Factors Affecting the Ultimate Detectivities of—R.J. McIntyre (RCA Ltd., Mont) Canadian Communications and EHV Conf., Montreal: 11/8-9/72

Q-SWITCHED CO² LASER, Experimental Analysis of the Vibrational-Rotational Line Content of a—S. Sizgoric, A. Waksberg (RCA Ltd., Mont) *Canadian J. of Physics*, Vol. 50, No. 13; 7/1/72

RETURN-BEAM VIDICON A High-Resolution Camera Tube, Silicon—R. W. Engstrom, J.H. Sternberg (AED, Pr) *RCA Review*: 9/72

245 Displays

... equipment for the display of graphic, alphanumeric, & other data in communications, computer, military, & other systems, CRT devices, solid state displays, holographic displays, etc.

DIGITAL DISPLAY Systems, Liquid Crystal Driven by CMOS Offers Minimal Power—R.C. Heuner (SSD.Som) Northeast Electronics Research and Engineering Mtg.(NEREM), Boston, Mass.: 11/72

LIQUID CRYSTAL READOUT Display for Use in Watches, Calculators, and General Instrumentation—H.C. Schindler (SSD.Som) Mid-America Electronics Conf., Kansas City, Missouri; 10/72

280 Thermal Components & Equipment

... heating & cooling components & equipment, thermal measurement devices, heat sinks & thermal protection design, etc.

HEAT PIPES, Liquid Metal—W.E. Harbaugh (CE, Har) Heat Pipe Course at George Washington University, Univ. of Tennessee 12/8/72

PELLIER COOLING A Review, Compound Tellurides and Their Alloys for—W.M. Yim, F.D. Rosi (Labs.Pr) Solid-State Electronics, Vol. 15, pp. 1121-1140: 1972

SERIES 300 SYSTEMS, EQUIPMENT, & APPLICATIONS

305 Aircraft & Ground Support

... airborne instruments, flight control systems, air traffic control, etc.

SECANT—J. Browder (EASD, Van Nuys) San Fernando Valley, Chapter, IEEE 11/14/72

310 Spacecraft & Ground Support

... spacecraft & satellite design, launch vehicles, payloads, space missions, space navigation.

ORBIT-ADJUST PROPULSION SUBSYSTEM Aboard Atmosphere Explorer—Y. Brill, J. Mavrogenis (AED, Pr) JANNAF, Propulsion Specialists' Session, New Orleans, La.:11/27-30/72

315 Military Weapons & Logistics

... missiles, command & control.

AEGIS System and Its Technology—W.V. Goodwin (M&SR, Mrstn) AIAA Evening Technical Mtg., RCA Moorestown 12/13/72

INTEGRATED Logistics—J. Hurley (M&SR, Mrstn) Adult Educational Program at Willingboro High School: 12/72

320 Radar, Sonar, & Tracking Systems

... microwave, optical, & other systems for detection, acquisition, tracking, & position indication.

MULTIPATH-ANGLE ERROR REDUCTION Using Multiple-Target Methods—P.Z. Peebles (M&SR, Mrstn) *IEEE Trans. on Aerospace and Electronic Systems*, pp. 1123-1130: 11/71

325 Checkout, Maintenance, & User Support

... automatic test equipment, maintenance & repair methods, installation & user support.

AUTOMATIC TESTING, EQUATE, New Concepts in—P.M. Toscano, J. Kelly (ASD,Burl) IEEE Automatic Support Systems Symp., Philadelphia, Pa.: 11/14/72

HIGHER ORDER TEST LANGUAGE REQUIREMENT, A Fortran Solution to a—A. Vallance, H.L. Fischer (ASD,Burl) IEEE Automatic Support Systems Symp., Philadelphia,Pa.: 11/15/72

VEHICLE READINESS TESTING, Go/No-Go Indicator System for—H.E. Fineman (ASD,Burl) IEEE Automatic Support Systems Symp., Philadelphia,Pa.: 11/14/72

340 Communications Equipment & Systems

... industrial, military, commercial systems, telephony, telegraphy, & telemetry, (excludes: television & broadcast radio).

ANALOG MICROWAVE SYSTEMS as Digital Carriers, Simulation of—K. Feher, R. Williamson (RCA Ltd.,Mont) Canadian Communications and EHV Conf., Montreal; 11/8-9/72

COMMERCIAL SATELLITE EARTH STATIONS for Operation with Intelsat Global Network and its Influence on Maintenance Costs, Five-Phase Evaluation in Design of—J.A. Collins (RCA Ltd.,Mont) Canadian Communications and EHV CONF., Montreal; 11/8-9/72

DIGITAL SWITCH MATRIX Technique Evaluation, Time Division—A. Mack, B. Patrusky, F. Koziem (GCS, Camden) IEEE Int'l Conf. on Communications, Phila., Pa.:ICC 72 Conf. Proc., 7/19-21/72

MOBILE TECHNOLOGY Update, RCA—M.O. O'Molesky (SSD.Som) Pye Telecommunications Seminar, Cambridge, England: 9/72

PHASE LOCK LOOP RECEIVERS, Phase Detector Data Distortion in—G.D. O'Clock (EASD, Van Nuys) *IEEE Trans. on AES*: 5/72

345 Television & Broadcast Systems

... television & radio broadcasting, receivers, transmitters, & systems, televisions cameras, recorders, studio equipment, closed-circuit, spacecraft, & special purpose television.

FM SIGNAL PROCESSING in a Broadcast Magnetic Tape Equipment, Design Criteria for—K. Sadashige (CSD, Camden) 22nd IEEE Broadcast Symp., Washington, D.C.

TCR-100 - A Fundamental Innovation for the Broadcaster—R.N. Hurst (CSD, Camden) IREE Australia

380 Graphic Arts & Documentation

... printing, photography, & typesetting; writing, editing, & publishing; information storage, retrieval, & library science; reprography & microforms.

How Coherent My Light, How Good My Print—H.O. Hook (Labs.Pr) Eastman Kodak Seminar, San Diego, Calif.: 12/11-13/72

Author Index

Subject listed opposite each author's name indicates where complete citation to his paper may be found in the subject index. An author may have more than one paper for each subject category.

Advanced Technology Laboratories

Barratt, W., 240
Benima, D., 215
Dillon, L., 215
Lea, A.L., 160
Nicastro, L.J., 160
O'Hara, L., 240
Shashoua, F., 240

Aerospace Systems Division

Fineman, H.E., 325
Fischer, H.L., 325
Galton, E.B., 180
Kelly, J., 325
Toscano, P.M., 325
Vallance, A., 325

Astro-Electronics Division

Brill, Y., 310
Engstrom, R. W., 240
Mavrogenis, J., 310
Sternberg, J.H., 240

Commercial Electronics

Harbaugh, W.E., 280
Perysk, D.E., 210
Peterson, F.W., 210
Schindler, M.J., 210

Communications Systems Division

Hurst, R.N., 345
Sadashige, K., 345

Electromagnetic and Aviation Systems Division

Browder, J., 305
Gandolfo, D.A., 215
Guadagnolo, R.N., 210
Levy, A., 170
O'Clock, G.D., 210, 215, 340

Government Communications Systems

Dobbins, L.W., 240
Hampel, D., 215
Horton, C.R., 240
Kozien, F., 340
Mack, A., 340
Patrusky, B., 340

Missile and Radar Division

Goodwin, W.V., 315
Patton, W.T., 225
Peebles, P.Z., 320
Schwarz, B.R., 175
Shecter, E., 180

RCA Limited

Almey, E.N., 125
Bachynski, M.P., 180, 225
Collins, J.A., 340
Fetter, K., 340
Foldes, P., 225
Ghosh, A.K., 125
McIntyre, R.J., 240
Shkarotsky, I.P., 240
Sizgoric, S., 240
Waksberg, A., 240
Williamson, R., 340

Solid State Division

Carley, D.R., 215
DeFrate, D.P., 175
Dietz, W., 215
Fillmore, R., 215

Granieri, G.J., 215
Heuner, R.C., 245
Hills, V.E., 210
Hodowanec, G., 215
Jacobson, D.S., 215
Kamnitsis, C., 210
Keller, J.P., 215
Khajezadeh, H., 175
Lazar, S., 210
Leidich, A.J., 215
Meisel, H., 210
Minton, R., 210
Morgan, D., 215
O'Molesky, M., 340
Schindler, H.C., 245
Schnitzler, P., 210
Sheng, A., 215
Steudel, G., 215
Teslenko, L., 215
Veloric, H.S., 210
Visioli, A.J., 215
Wheatley, C.F., 215
Wittlinger, H.A., 215
Zuk, B., 215

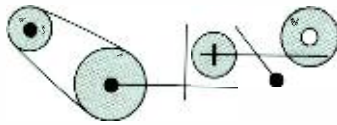
RCA Laboratories

Alphonse, G.A., 240
Amith, A., 205
Bartolini, R.A., 240
Beringer, F.M., 205
Burke, W.J., 205
Carnes, J.E., 210
Castellano, J.A., 205
Channin, D.J., 240
deWolf, D.A., 125, 225

Dingwall, A.G.F., 210
Dismukes, J.P., 205
Douglas, E.C., 210
Dreeben, A.B., 210
Feldstein, N., 170
Hammer, J.M., 240
Hannan, W.J., 240
Hook, H.O., 380
Jolly, S.T., 210
Kosonocky, W.F., 210
Kovac, M.G., 345
Kressel, H., 210
Kudman, I., 205
Ladany, I., 210
Lee, F., 205
Levin, E.E., 210
Levine, P.A., 210
Lurie, M.J., 240
Nicol, F.H., 205
Pankove, J.I., 205
Pike, W.S., 345
Redfield, D., 205
Rose, F.D., 280
Schnable, G.L., 105
Shallcross, F.V., 345
Sommers, H.S., 240
Stofko, E.J., 205
Sunshine, R.A., 210
Uimer, R.J., 205
Vossen, J.L., 160
Weimer, P.K., 345
Weller, K.P., 210
Williams, R., 125, 160
Winer, J.A., 105
Winter, R.E.K., 205
Woods, M., 160
Yim, W.M., 205, 280

Patents Granted

to RCA Engineers



Advanced Technology Laboratories

Aerial Photography — R.D. Scott (ATL, Cam.) U.S. Pat. 3707254, December 26, 1972

Light Beam Scanning — M. L. Levene (ATL, Cam.) U.S. Pat. 3707723, December 26, 1972

Article Identification Apparatus — J. F. Schanne (ATL, Cam.) U.S. Pat. 3708655, January 2, 1973

Aerospace Systems Division

High-Efficiency Capacitor Charging Circuit — E. E. Corey, R. A. Tuft, J. H. Woodward (ASD, Burl.) U.S. Pat. 3,706,022, December 12, 1972; Assigned to U. S. Government.

Communications Systems Division

Method of Making a Graded Photoprinting Master — J. A. Dodd, Jr., R. A. Geshner (GCS, Cam.) U.S. Pat. 3698903, October 17, 1972

Video Signal Noise-Limiting Apparatus — C. L. Olson, J. F. Monahan, R. A. Dischert (GCS, Cam.) U.S. Pat. 3715477, February 6, 1973

A Phase or Frequency Modulator Using PIN Diode — L. Schaeperkoetter (CSD, Mdwlids.) U.S. 3624559, November 30, 1971

Shuttering Apparatus for Television Cameras — H. G. Wright, R. A. Dischert (GCS, Cam.) U.S. Pat. 3715486, February 6, 1973

Consumer Electronics

Communication Among Computers — B. W. Beyers, L. L. Tretter (CE, Indpls.) U.S. Pat. 3699529, October 17, 1972

Safety Apparatus for Hot-Chassis Electronic Instruments — G. E. Kelly (CE, Indpls.) U.S. Pat. 3699562, October 17, 1972

Amplifier Circuits — L. A. Harwood, E. J. Wittmann (CE, Som.) U.S. Pat. 3699257, October 17, 1972

Phonograph Pickup with Self Formed Female Receptacles — M. E. Miller (CE, Indpls.) U.S. Pat. 3699268, October 17, 1972

Automatic Deguassing Apparatus for Minimizing Residual Current During Steady State Operation — J. C. Marsh, Jr. (CE, Indpls.) U.S. Pat. 3699400, October 17, 1972

Color Compensating Network with Range Limitation — L. R. Kirkwood, L. A. Cochran, R. D. Altmanshofer (CE, Indpls.) U.S. Pat. 3701842, October 31, 1972

Color Compensating Network for an Integrated Circuit Television — L. A. Cochran (CE, Indpls.) U.S. Pat. 3701844, October 31, 1972

Hue Control Circuit for a Color Television Receiver — J. Stark, Jr., D. H. Carpenter (CE, Indpls.) U.S. Pat. 3701845, October 31, 1972

Process for Forming a Conductive Coating on a Substrate — R. R. Russo (CE, Indpls.) U.S. Pat. 3704208, November 28, 1972

Motor Control Circuit — T. A. Bridgewater (CE, Indpls.) U.S. Pat. 3706016, December 12, 1972

Video Blanking and Audio Muting Circuit — L. M. Lunn (CE, Indpls.) U.S. Pat. 3707597

Gamma Correction Bandpass Amplifier Circuits — J. H. Wharton (CE, Indpls.) U.S. Pat. 3708615, January 2, 1973

High Voltage and Width Regulation Circuit — W. V. Fitzgerald, Jr., R. C. Lemmon (CCE, Indpls.) U.S. Pat. 3711738, January 16, 1973

Indpls.) U.S. Pat. 3711738, January 16, 1973

Alignment and Test Fixture Apparatus — J. W. Ham, J. M. Poplin (CE, Indpls.) U.S. Pat. 3714572, January 30, 1973

Method of Manufacturing Thick-Film Hybrid Integrated Circuits — W. H. Liederbach (CE, Indpls.) U.S. Pat. 3714709, February 6, 1973

High Voltage Hold-Down Circuit — G. K. Sendelweck (CE, Indpls.) U.S. Pat. 3715464, February 6, 1973

Service Switch Arrangement for Improved Interface Performance — J. K. Allen (CE, Indpls.) U.S. Pat. 3715493, February 6, 1973

Dual Mode Automatic Frequency Controlled Oscillator System — S. A. Steckler (CE, Som.) U.S. Pat. 3715489, February 6, 1973

Muting Circuit — J. Craft (CE, Som.) U.S. Pat. 3714585, January 30, 1973

Electromagnetic & Aviation Systems Division

Apparatus for Mounting and Spacing a Signal Transducer with Respect to a Recording Medium — G. J. Giel (Aviation Equip., Los Angeles) U. S. Pat. 3706861, December 19, 1972

Flip-flop and Hold Phase Detector — H. M. Volmerange (Aviation Equip., Los Angeles) U.S. Pat. 3710140, January 9, 1973

Mechanical Drive Mechanism with Programmable Output Function — A. Bernstein (EASD, Van Nuys) U.S. Pat. 3712147, January 23, 1973

Electronic Components

Negative Effective Electron Affinity Emitters with Drift Fields Using Deep Acceptor Doping — R. E. Simon, B. F. Williams (EC, Pr.) U.S. Pat. 3699404, October 17, 1972

Method of Assembling a Mask with a Frame Assembly for Mounting in a Cathode-Ray Tube Using a Remote Assembly Position — M. Van Renssen (EC, Lanc.) U.S. Pat. 3701185, October 31, 1972

Method of Assembling and Mounting an Aperture Mask in a Mask-Panel Assembly of a Cathode-Ray Tube Using a Full Surface Spacer — F. R. Ragland, Jr. (EC, Lanc.) U.S. Pat. 3701193, October 31, 1972

Apparatus and Method for Applying a Bead of Sealing Material to a Sealing Surface of a Cathode-Ray Tube — L. B. Kimbrough (EC, Lanc.) U.S. Pat. 3701674, October 31, 1972

Method for Preparing the Viewing-Screen Structure of a Cathode-Ray — S. B. Deal, D. W. Bartsch (EC, Lanc.) U.S. Pat. 3703401, November 21, 1972

Radio Frequency Window Assembly Having Shielded Solder Joints and Reweldable Replacement Flanges — W. A. Novajovsky, M. W. Heischer (EC, Lanc.) U.S. Pat. 3701061, October 24, 1972; Assigned to U.S. Government.

Photographic Method for Printing Viewing Screen Structure Including Treatment of Exposed Coating Before Development — H. R. Frey (EC, Lanc.) U.S. Pat. 3706558, December 19, 1972

Cathode-Ray Tube with Laminated Safety Panel and Separate Light-Attenuating Layer — G. J. Guille, Jr. (EC, Scranton) M. G. Brown, Jr., G. E. Long, III (EC, Lanc.) U.S. Pat. 3708622, January 2, 1973

Automatic Brightness Control for Image Intensifier Tube — P. A. Kryder (EC, Lanc.) U.S. Pat. 3711721, January 16, 1973

Method of Making an Electron Emitter Device — A. H. Sommer (EC, Pr.) U.S. Pat. 3712700, January 23, 1973

Method for Preparing a Conductive Coating on a Glass Surface — J. J. Malley (EC, Lanc.) January 30, 1973

Paired Nonlinear Active Elements in a Waveguide Cavity Adapted to Support Orthogonal TE₀ Mode Waves and TE₀ Mode Waves — B. S. Perlman (EC, Pr.) U.S. Pat. 3715686, February 6, 1973

Encapsulated Magnetic Memory Element — T. P. Fulton, H. Di Luca (EC, Needham Hgts) U.S. Pat. 3713886, January 30, 1973



As an industry leader, RCA must be well represented in major professional conferences . . . to display its skills and abilities to both commercial and government interests.

How can you and your manager, leader, or chief-engineer do this for RCA?

Plan ahead! Watch these columns every issue for advance notices of upcoming meetings and "calls for papers". Formulate plans at staff meetings—and select pertinent topics to represent you and your group professionally. Every engineer and scientist is urged to scan these columns; call attention of important meetings to your Technical Publications Administrator (TPA) or your manager. Always work closely with your TPA who can help with scheduling and supplement contacts between engineers and professional societies. Inform your TPA whenever you present or publish a paper. These professional accomplishments will be cited in the "Pen and Podium" section of the *RCA Engineer*, as reported by your TPA.

Calls for papers—be sure deadlines are met.

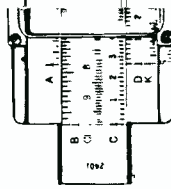
Date		Location	Sponsors	Deadline Date	Submit	To
AUG. 21-24, 1973	Int'l G-AP Symposium & USNC/URSI Meeting	Univ. of Colo. & Harvest House Hotel, Boulder, CO	G-AP, USNC/URSI	5/28/73	(a&s)	J. R. Wait, NOAA, Dept. of Commerce, Boulder, CO 80302
SEPT. 16-20, 1973	Jt. Power Generation Technical Conference	Marriott Hotel New Orleans, LA	S-PE, ASME	5/4/73	(ms)	L. C. Grundmann, Jr. New Orleans Public Svc. Inc. 317 Baronne St. New Orleans, LA 70160
SEPT. 17-19, 1973	Petroleum & Chemical Industry Technical Conference	Regency Hyatt Hotel Houston, TX	S-IA	5/15/73	(ms)	R. H. Cunningham Atlantic Richfield Co. POB 2451 Houston, TX 77001
SEPT. 25-28, 1973	Conference on Automatic Control in Glass Manufacturing	Purdue Univ. Lafayette, IN	S-IA, IFAC, AACC, ISA et al	7/15/73	(abst)	IEEE Office 345 East 47th St. New York, NY 10017
OCT. 30-NOV. 2, 1973	1973 Fall Meeting The American Ceramic Society	St. Francis Hotel San Francisco, CA	Nuclear Div., ACS	6/1/73	(abst)	J. M. Leitnaker Program Chairman Nuclear Div. Building 4500-S Room A-156 Oak Ridge Nat'l Laboratory Oak Ridge, TN 37830

Dates of upcoming meetings—plan ahead.

Date	Conference	Location	Sponsors	Program Chairman
APRIL 26-27, 1973	Trends in Naval Engineering	Shoreham Hotel Washington, DC	ASNE	Papers Chairman ASNE Day 1973 American Society of Naval Engineers, Inc. 1012 14th Street, NW Washington, DC 20005
APRIL 29-MAY 3, 1973	75th Annual Meeting and Exposition	Cincinnati Convention Center	ACS	The American Ceramic Society, Inc. 4055 North High St. Columbus, OH 43214
APRIL 30-MAY 2, 1973	Southeast-Con	Galt House Louisville, KY	Region 3	R. D. Shelton Univ. of Louisville EE Dept., Louisville, KY 40202
APRIL 30-MAY 2, 1973	Symposium on Computer Software Reliability	Americana Hotel New York, NY	S-C, G-R, Long Island Section, New York Section	Martin Shooman, PIB 333 Jay St. Brooklyn, NY 11201
MAY 1-2, 1973	Electron Device Tech. Conference	United Engrg. Ctr. New York, NY	G-ED	Hayden Gallagher Hughes Res. Labs. 3011 Malibu Canyon Rd. Malibu, CA 90265
MAY 2-4, 1973	Region Six "Mini-Computers and Their Applications"	Sheraton-Waikiki Honolulu, HI	Region 6 Hawaii Section	D. J. Grace Kentron Hawaii Ltd. 233 Keawe St. Honolulu, HI 96813
MAY 13-17, 1973	Industrial & Commercial Power Sys Conference	Regency Hyatt House Atlanta, GA	S-IA, Atlanta Section	R. G. Henderson Georgia Pwr. Co. Industrial Sales Dept. POB 4545, Atlanta, GA 30302

Dates of upcoming meetings—plan ahead.

Date	Conference	Location	Sponsors	Program Chairman
MAY 14-16, 1973	Aerospace Electronics Conference (NAECON)	Sheraton Dayton Hotel Washington, DC	G-AES, Dayton Section	Howard Steenbergen, AFAL/TEA, WPAFB, OH 45433
MAY 14-16, 1973	Electronic Components Conference	Statler Hilton Hotel, Washington, DC	G-PHP, EIA	W. E. Parker Aircoc Speed Elec. Packard Rd at 47th St. Niagara Falls, NY 14302
MAY 15-17, 1973	Electrical & Electronic Measurement & Test Instrument Conference (EEMTIC)	Skyline Hotel Ottawa, Ontario, Canada	G-IM, Ottawa Section, Comm. I	P. Cath, Kiethley Instr. Inc., 28775 Aurora Rd. Cleveland, OH 44131
MAY 17-19, 1973	Conf. on the Future of Scientific & Technical Journals	Commodore Hotel New York, NY	G-PC	John Phillips, Bldg. 2-8 RCA, Camden, NJ 08102
MAY 20-22, 1973	Ecology, Economics, and Energy	Stouffers Louisville, KY	ASME	P. Drummond, Mgr. Conferences & Divs. The American Society of Mechanical Engineers United Engineering Ctr. 345 E. 47th St. New York, NY 10017
MAY 21-23, 1973	Electron, Ion and Laser Beam Technology Conference	MIT, Cambridge, MA	G-ED, AS, MIT	IEEE Office 345 East 47th St. New York, NY 10017
MAY 30- JUNE 1, 1973	Conference on Laser Engineering & Applications		Quantum Elec. Council, OSA, Wash- ington, DC	D R. Whitehouse Raytheon Co. 130 Second Ave. Waltham, MA 02154
JUNE 4-6, 1973	Int'l Microwave Symposium	Univ. of Colorado Boulder, CO	G-MIT	R. W. Beatty, NBS, Boulder, CO 80302
JUNE 4-7, 1973	Power Industry Computer Applications Conference	Radisson Hotel Minneapolis, MN	S-PE	J. W. Skooglund Westinghouse Elec. Corp., 8L41, 700 Braddock Ave. Pittsburgh, PA 15112
JUNE 11-12, 1973	Chicago Spring Conf. on Broadcast & Television Receivers	Marriott Motor Hotel, Chicago, IL	G-BTR, Chicago Section	IEEE Office 345 East 47th St. New York NY 10017
JUNE 11-13, 1973	Int'l Communications Conference	Seattle Center Seattle, WA	S-Comm. Seattle Section	S. Tashiro, POB 648, Bellevue, WA 98009
JUNE 11-13, 1973	1973 IEEE Power Electronics Specialists Conference	California Inst. of Tech. Pasadena, CA	AES Group of IEEE	Dr. T. G. Wilson EE Dept., Duke Univ. Durham, NC 27706
JUNE 20-23, 1973	Electromagnetic Compatibility Symposium	New York Hilton Hotel, New York, NY	G-EMC, NY Section	R. Brook, AIL, EMC Section, Comac Rd. Deer Park, NY 11729
JUNE 20-23, 1973	Joint Automatic Control Conference	Ohio State Univ. Columbus, OH	S-CS, AIAA, ASME, ISA, TAPPI, SCI ITE	R. E. Larson, Sys. Control Inc., 260 Sherman Ave. Palo Alto, CA 94306
JUNE 25-27, 1973	Design Automaton Workshop	Sheraton-Portland Hotel Portland, OR	C-S, ACM, SHARE	J. M. Galey, Bldg 14 Dept. G90 Bldg 14 Monterey & Cottle Rds. San Jose, CA 94114
JUNE 25-29, 1973	Information Theory Symposium	Ashkelon, Israel	G-IT	N. J. A. Sloane, Bell Labs., Murray Hill, NJ 07974
JULY 9-27, 1973	Conference on the Science and the Unfolding of Technology	Mexico City, Mexico	IEEE Mexico Section, AAAS, CONACYT	Bruno DeVecchi Martin Mendale No. 1054 Mexico City 12
JULY 10-12, 1973	Conference on Video and Data Recording	Univ. of Birmingham Birmingham, England	IERE, IEEE UKRI Section et al	IERE, 8-9 Bedford Sq. London W.C. 1 B 3RG England
JULY 10-12, 1973	Joint Space Mission, Planning and Execution Meeting	Stauffer's Denver Inn, Denver, CO	AIAA, ASME, SAE	M. Jones, Mgr. Information Svcs., ASME United Engineering Ctr. 345 E. 47th St. New York, NY 10017
JULY 15-20, 1973	IEEE Power Engineering Society Summer Meeting & EHV/UHV Conference	Vancouver Hotel Vancouver, BC Canada	S-PE	D. G. McFarlane British Columbia Hydro & Pwr. Auth. 970 Burrard St. Van 1 BC Canada
JULY 16-19, 1973	Intersociety Conference on Environmental Systems	Hilton Inn San Diego, CA	SAE, ASME, AIAA, AICE, AMS	M. Jones, Mgr. Information Svcs., ASME United Engineering Ctr. 345 East 47th St. New York, 10017
JULY 18, 19, 20, 1973	1973 Fifth International Symposium on Acoustical Holography and Imaging	Rickey's Hyatt House, Palo Alto, CA	Sonics & Ultrasonics Group of IEEE, ASA, Stanford Res. Inst.	P. S. Green Bldg. 30, K1088 Stanford Res. Inst. Menlo Park, CA 94025



Vonderschmitt heads Solid State Division

William C. Hittinger, Executive Vice President, RCA Consumer and Solid State Electronics, recently announced that **Bernard V. Vonderschmitt** will become head of the RCA Solid State Division.

Mr. Vonderschmitt who is currently Division Vice President, Solid State Integrated Circuits, succeeds Mr. Hittinger as head of the RCA Solid State Division.

In his new post, Mr. Vonderschmitt will be responsible for the engineering, manufacturing and marketing of integrated circuits, power transistors, thyristors, liquid crystals and power hybrid modules for commercial, consumer, industrial and aerospace markets. He will be located at the Division's headquarters in Somerville, N.J. Other division locations are at Mountaintop, Pa.; Findlay, Ohio; Liege, Belgium; Sunbury-on-Thames, England and Taoyuan, Taiwan.

Mr. Vonderschmitt received the BSEE from Rose Polytechnic Institute in 1944 and the MSEE from the University of Pennsylvania in 1956. He joined RCA in 1944 as an engineer and was engaged in component design projects at Camden, N.J. After serving as a radar officer in the U.S. Navy, he returned to RCA and worked on deflection system development for monochrome and color TV receivers. He transferred to the Semiconductor Division in 1959 as Manager of Applications in the MicroElectronics Department and subsequently held engineering management positions of increasing responsibility. In 1971, Mr. Vonderschmitt was named Manager, Integrated Circuits and, later in the same year, became Division Vice President, Solid State Integrated Circuits

In January of 1971, Mr. Vonderschmitt was honored as a co-recipient of the David Sarnoff Outstanding Achievement Award in Engineering. This award cited his efforts and leadership in the timely development of superior integrated circuits for television receivers.



Stockton is Chief Engineer at ASD

Stanley S. Kolodkin, Division Vice President and General Manager, Aerospace Systems Division, Burlington, MA recently announced the appointment of **Eugene M. Stockton** as Chief Engineer.

In this capacity, Mr. Stockton has overall responsibility for the Engineering Department of the Division, a major developer of advanced systems for government, military, and commercial programs. He will report to Mr. Kolodkin. Prior to his promotion, he was Manager, Automatic Test Engineering.

Mr. Stockton received the BSEE from Michigan State College in 1955, and the MS from the Drexel Institute of Technology in 1959. He is a graduate of the University of Chicago's Advanced Management Program.

Mr. Stockton joined RCA in 1955 as an Associate Engineer. In 1959, he was assigned responsibility for the design and development of electronic automatic test equipment. He became Manager of Automatic Test Equipment Product Design in 1966, and a year later was promoted to the position he held prior to his new assignment.

Don Peterson retires

Donald W. Peterson retired on January 24, 1973, following a brilliant sendoff at the Woodbury Country Club. Approximately 150 of Don's friends and associates were on hand to add their best wishes to the occasion.

Don took early retirement at age 58, heading for Arizona where he will park his boat and mobile home. Don's career at RCA, after graduation from University of Wisconsin, started in 1937 with NBC, then in Princeton and Moorestown with Dr. Brown and associates, designing space antennas. His work at RCA-Deptford in latter years was highlighted by the design



Laschever is Manager of Planning at ASD

Stanley S. Kolodkin, Division Vice President and General Manager, Aerospace Systems Division, Burlington, Mass., recently announced the appointment of **Norman L. Laschever** as Manager, Planning.

In his new capacity, Mr. Laschever will be responsible for business development and investment planning. He will report to Mr. Kolodkin.

Mr. Laschever received the BSEE in 1940 from Massachusetts Institute of Technology. He received the MSEE from Northeastern University, Boston. He also has completed Pennsylvania State University's Executive Management Program.

Mr. Laschever joined the Aerospace Systems Division in 1962, as a Staff Engineering Scientist. He became Manager of Technical Planning and, later, Manager of Radio Frequency Engineering. Prior to his present assignment, he was Chief Engineer for the Division.

Following his discharge from the U. S. Air Force in 1946 with the rank of Captain, Mr. Laschever spent nine years as an Associate Engineer and Section Chief at Wright Patterson Air Force Base, Ohio. He joined the Laboratory for Electronics, Boston, in 1955 and was Manager, Technical Staff Office and Assistant Director, Research Engineering there when he was employed by RCA.

of a completely new line of all-RCA home receiving antennas, the first in RCA history and among the best in the industry. A number of patents and awards for other achievements through the years grace the study of his home and attest to a most brilliant and colorful career.

Mr. Peterson's later work is described in his article in this issue, p. 6.

Staff Announcements

RCA Corporation

Robert W. Sarnoff, Chairman and Chief Executive Officer has announced the election of **William J. Kennedy, III**, to the Board of Directors of RCA Corporation.

RCA Limited (Canada)

Frank J. O'Hara, Vice-President, RCA Electronic Components has announced the appointment of **Geoffrey Geduld** as Manager, RCA Solid State Division.

Marketing

James J. Johnson, Vice President, Marketing, has appointed **Joseph W. Curran**, Staff Vice President, Consumer Marketing and Marketing Services and **Edward J. Homes**, Director, Marketing Administration.

Richard W. Sonnenfeldt, Staff Vice President, Systems Marketing and Development has announced the following organization: **Holmes Bailey**, Director, Consumer Information Systems Development; **Henry Duszak**, Manager, Systems Planning; **Patrick S. Feely**, Manager, Business Planning; and **James D. Livingston**, Manager, Systems Marketing.

Laboratories

Donald S. McCoy, Director, Consumer Electronics Research Laboratory, has announced the following organization: **Jay J. Brandinger** continues as Head, TV Systems Research; **Paul K. Weimer** continues as Fellow, Technical Staff, **H. Nelson Crooks** continues as Manager, High-Density Recording Project; **Eugene O. Keizer** continues as Head, Video-Systems Research; **J. Guy Woodward** continues as Fellow, Technical Staff; **Charles B. Oakley** is appointed Head, Electro-Optic Systems Research; and **John A. van Raalte** continues as Head, Displays and Device Concepts Research.

Gerald B. Herzog, Director of RCA Laboratories Solid State Technology Center has announced the appointment of **John W. Gaylord** as Manager, Power Technology.

Parts and Accessories

John D. Callaghan, Manager, Engineering has announced the appointment of **Robert M. Wilson** as Manager, Product Development Engineering.

National Broadcasting Company, Inc.

Don Durgin, President, NBC Television Network has announced the appointment of **John R. Kennedy** as Vice President, Operations and Engineering.

Consumer and Solid State Electronics

William C. Hittinger, Executive Vice President, RCA Consumer and Solid State Electronics has appointed **Bernard V. Vonderschmitt**, Vice President and General Manager of the RCA Solid State Division.

Solid State Division

Bernard V. Vonderschmitt, Vice President and General Manager, Solid State Division has announced the following organization: **D. Joseph Donahue**, Division Vice President, Solid State Integrated Circuits, **Edward K. Garrett**, Director, Finance, and **Joseph W. Karoly**, Division Vice President, Solid State — Europe.

Richard A. Santilli, Manager, Linear Integrated Circuits, RCA Solid State Division has announced the following appointments in the Marketing organization: **Ralph S. Iovino**, Administrator, Consumer Electronics Linear IC Marketing; **Seymour Reich**, Administrator, Industrial Markets Linear IC Marketing; and **William K. West**, Price Analyst for Industrial Markets.

Ben A. Jacoby, Division Vice President, Power Devices has announced the appointment of **William A. Glaser** as Manager, Thyristors and Rectifiers.

Harry Weisberg, Manager, MOS Integrated Circuits and Liquid Crystal Products has announced the appointment of **Herbert B. Shannon** as Marketing Manager, MOS Integrated Circuits and Liquid Crystal Products.

Consumer Electronics

William H. Anderson, Division Vice President, Marketing for RCA Consumer Electronics has announced the appointment of **William S. Lowry** as Division Vice President, Color Television Product Management, and **William E. Boss** as Division Vice President, Product Management.

Electronic Components

Clifford H. Lane, Division Vice President, Technical Planning has announced the following organization: **Harold S. Basche**, Administrator, Facilities Services; **Wellesley J. Dodds**, Manager, Quality and Reliability Assurance; **Clifford H. Lane**, Acting, Staff Engineer; **Clifford H. Lane**, Acting Manager, Technical Aid and License Coordination; **Frederick C. Weisbach**, Manager, General Plant Engineering; and **John F. Wilhelm**, Manager, Commercial Engineering.

Executive Vice President and General Counsel

Stephen S. Barone, Vice President, Licensing has announced the following organization: **Jerold J. Benavie**, Staff Vice

President, Domestic Licensing; **Allan D. Gordon**, Staff Vice President, International Licensing; **H. Russell L. Lamont**, Director, European Technical Relations; **Norman E. Rosen**, Counsel, Licensing; and **Philip A. Roth**, Director, Finance—Licensing.

Philip A. Roth, Director, Finance—Licensing has announced the following organization: **Robert F. Amitrani**, Manager, Finance—Domestic Licensing and **Steven N. Morris**, Manager, Finance—International Licensing.

Government and Commercial Systems

I.K. Kessler, Executive Vice President, Government and Commercial Systems has announced the following appointments: **Nicholas J. Capello**, Division Vice President, Management Consulting Services and **George D. Black**, Division Vice President, Industrial Relations.

Electromagnetic and Aviation Systems Division

Frederick H. Krantz, Division Vice President and General Manager has announced the following appointments: **James H. Carbone, III**, as Manager, Business Planning; **George F. Fairhurst** as Manager, Product Assurance; and **O. Terry Hesellus** as Manager, Management Information Systems.

Carl J. Cassidy, Director, Government Marketing has announced the appointment of **Edward A. Elston** as Manager, Government Data Systems, Marketing.

John P. Mollema, Manager, Marketing has announced the appointment of **Dan Northrop** as Manager, Central Region Sales for RCA's Aviation Equipment Department.

Aerospace Systems Division

Stanley S. Kolodkin, Division Vice President and General Manager, has announced the appointment of **Eugene M. Stockton** as Chief Engineer and **Norman L. Laschever** as Manager of Planning; also he has announced the following organization: **John M. Nazak** as Manager, Tactical Systems Sales; **Malcolm M. Knopf** as Manager Navy Affairs; **Melvin E. Lowe** as Director, Building Management Systems.

Eugene B. Galton, Plant Manager has announced the appointment of **John W. Paxton** as Manager, Quality Assurance.

Electromagnetic and Aviation Systems Division

Frederick H. Krantz, Division Vice President and General Manager has announced the appointment of **George F. Fairhurst** as Manager, Product Assurance.

Promotions

Astro-Electronics Division

P.S. Abitanto from Assoc. Engr., Tiros Project Management, to Mgr., Specialty Engr. (A. Dusio, Hgtsn.)

Alaska Communication, Inc.

G.P. Roberts from Mgr., Special Proj. to Mgr., Engr. (F. D. Chie, Jr., Anchorage)

Consumer Electronics

F.C. Harvey from Mbr., Engr. Staff to Ldr., Engr. Staff (C.W. Hoyt, Indpls.)

E.E. Janson from Ldr., Engr. Staff to Mgr., Engr. Black-and-White TV (R.J. Lewis, Indpls.)

J.A. McDonald from Ldr., Engr. Staff to Mgr., Engr. Video Discs (R.K. Lockhart, Indpls.)

J.O. Simpkins from Sr. Mbr., Engr. Staff to Ldr., Engr. Staff (J.K. Kratz, Indpls.)

Electronic Components

D. Chemelewski from Engr., Equip. Dev. to Eng. Ldr., Equip. Dev. (K.D. Searce, Lanc.)

D.H. Headington from Engr. Mfg. to Mgr., Prod. Engr. (N. Meena, Marion)

S.T. Villany from Engr., Prod. Dev. to Sr. Engr., Prod. Dev. (A. Morrell, Lanc.)

J.P. Wolff from Engr. Ldr., Prod. Develop. to Mgr., Prod. Dev. (W.H. Warren, Hrsn.)

Global Communications

A. Longo from Engr. to Group Ldr., Leased Fac. & Engr. Dept. (D. Mandato, 60 Broad, New York)

M. Fruchter from Ldr., Tech. Control & Trans. Engr. to Mgr., Leased Channel Engr. (S. Schadoff, 60 Broad, New York)

Parts and Accessories

R.M. Wilson from Elec. Engr. to Mgr., Product Develop. Engr. (J.D. Callaghan, Deptford)

Solid State Division

E. Chabak from Engr. to Ldr., Tech. Staff (E. Czeck, Mountaintop)

W. Guerin from Engr. to Ldr., Tech. Staff (R. Satriano, Mountaintop)

E. Schmitt from Engr. to Ldr., Tech. Staff (R. Satriano, Mountaintop)

G. Diehl from Ind. Engr. to Mgr., Facilities & Equip. Standards (G. Reazer, Mountaintop)

A. Bianculli from Member, Tech. Staff to Mgr., Engr. Standards (R.M. Cohen, Somerville)

L. Gallace from Member, Tech. Staff to Mgr., Quality and Rel. Engr. (R.M. Cohen, Somerville)

J. Gaylord from Ldr., Tech. Staff to Mgr., Power Tech. (G. Herzog, Somerville)

F. Scheline from Member, Tech. Staff to Ldr., Tech. Staff (G. Herzog, Somerville)

R. Bailey from Member, Tech. Staff to Ldr., Tech. Staff (C.R. Turner, Somerville)

W. Bennett from Sr. Member, Tech. Staff to Ldr., Tech. Staff (C.R. Turner, Somerville)

Awards

Missile and Surface Radar Division

The following MSRD engineers received Technical Excellence Awards for the third quarter of 1972:

W. C. Blumenstein — for concept, design, and demonstration of a new high-density circuit packaging system with inherent low cost and high reliability.

W. L. Dvorak — for excellence in system design and implementation of the Automatic Antenna Pattern Data Acquisition System (AAPDAS).

J. Wonderlich — for outstanding accomplishments in the field of advanced computer-aided engineering design, on the basis of his mathematical analysis of the Viking High-Gain Antenna Control System.

The following MSRD received Technical Excellence Awards for the fourth quarter of 1972:

R. A. Baugh — for outstanding technical leadership in the successful development and test of the AN/SPY-1 radar control system programs for EDM-1.

C. C. Mathews — for his work in implementing two program modules of the overall AAPDAS program (TABOR and DISPLAY) which were used to display the certification data on the AN/SPY-1 Array and Beam Steering Control Cabinet at the AAPDAS Test Range.

J. W. Smiley — for outstanding achievements in initiating, proposing, and implementing new designs in circuits and interconnections for design automation based on AEWRAF.

In addition, **Richard A. Baugh** was selected as the Annual Technical Excellence Award for 1972. His selection represents recognition within MSRD of his outstanding contributions during the year.

Mr. Baugh was cited for outstanding technical leadership in the successful development and test of the AN/SPY-1 radar control system programs for EDM-1. As both lead engineer and working leader of the team during 1972, he directed to its completion the real-time computer control system programs for the most sophisticated radar ever built at MSRD. He developed the plans and test environment required to qualify the computer programs in formal performance tests, and then later in the year supervised the formal test and evaluation of these programs in accordance with a schedule developed at the beginning of 1972. These tests consisted of a full control system operating against a sophisticated real-time simulation of the AN/SPY-1 radar and other real-time control systems in AEGIS. The test setup included the radar control programs in two AN/UJK-7. Virtually all of the functional capabilities of the radar control system were demonstrated in an exhaustive series of tests.

Aerospace Systems Division

The team of **Frank J. Brown** (GCS), **Arthur L. Buchanan**, **Homer D. Eckhardt**, **Harvey Fichtelberg**, and **David Wellinger** was selected for the December 1972 Technical Excellence Team Award for its work on the Drone CCC study. Outstanding performance was demonstrated by the team during the seven-month study entitled "Command, Control and Communications of Tactical Unmanned Aerial Vehicles". The study was concerned primarily with how best to integrate drones into the AF Tactical Air Command System. It required a full technology assessment in the areas of communications, position location and reporting, and command and control. The customer (ESD) had also funded a competitor to conduct a second, parallel study.

Government Communications Systems

The Telex Engineering Team has been selected for the first Technical Excellence Award of 1973. This team consists of engineers — **Ed Tyndall**, **Neil Coleman**, and **Bernie Silverstein**; Programmer/Analysts — **Don Schaefer**, **Gale Ferris**, and **Gerry Moore**; and Material and Fabrication Specialists — **"Whitey" Coligan**, **Frank Baumierster**, and **Chester Kasian**. This team did an outstanding job in the development of a cost effective, computer controlled, time division Telex switch capable of interfacing with all known international Telex switching systems and flexible enough to permit future signaling changes to be included by program modification.



Dr. Mueller honored by IEEE group

Dr. Charles W. Mueller, a Fellow of RCA Laboratories, has been honored by the Electron Devices Group of the IEEE.

The J. J. Ebers Award was presented to Dr. Mueller "for outstanding technical contributions to electron devices, spanning the evolution of modern electronics from grid-controlled tubes through the alloy transistor, the thyristor, and MOS devices to silicon vidicons and silicon storage vidicons."

All of Dr. Mueller's significant research was done at RCA Laboratories, Princeton, N. J., where he has worked since since receiving the ScD from Massachusetts Institute of Technology in 1942.

Dr. Mueller received the B..Sc. (*magna cum laude*) from the University of Notre Dame in 1934 and the MS from MIT in 1936. He worked for the Raytheon Corporation for two years before returning to MIT for his doctorate.

Dr. Mueller is a Fellow of the IEEE, and a member of the American Physical Society and Sigma Xi. He has twice received RCA's highest technical honor, the David Sarnoff Award, as well as three RCA Laboratories Achievement Awards. He has published 17 technical papers and holds 18 U.S. Patents.

Professional activities

Government and Commercial Systems

Edwin S. Shecter, Manager, Product Assurance, was named Chairman of the newly-created Mandatory Standards Group of the Standards Committee of the American Society of Quality Control.

Astro-Electronics Division

Frank Papiano is a member of the Institute of Printed Circuits' Special Blue Ribbon Committee dealing with surface defects on printed-circuit boards. He recently supplied a set of color photographs and definitions of defects such as measing, blistering, haloing, and delamination for use in preparation of an Acceptability Standard to be issued by the IPC.

Corporate identification on engineering documentation

You can be helpful in overcoming a difficult problem in connection with the use of our corporate name and logotype on a variety of engineering and related documentation. Specifically, this includes, but is not necessarily restricted to, a great amount of engineering material such as drawings and specifications. There are literally millions of pieces of material such as this in existence, most of which were produced prior to the corporate name changeover.

Our corporate policy requires that the proper identification be used on material produced or issued either internally or externally. The following procedure is recommended in connection with engineering documentation:

- 1) Old documentation that is inactive need not be altered;
- 2) Old material that is still active and bears a last date prior to May, 1969 may be used without alteration;
- 3) Old material that is active and bears a date later than May, 1969 may not be published or distributed without correcting or updating the identification. This can be accomplished in a variety of ways, including stickers, decals or complete revisions to best meet the circumstances.
- 4) New or newly revised documents may not be issued unless these documents have the correct logotype or corporate name, RCA Corporation or RCA.

If you need any assistance in achieving our corporate objective of using correct corporate identification on engineering documentation, you can call either the Corporate Identification Department in New York or Corporate Standards Engineering in Cherry Hill.

Government Communication Systems

B. Tiger was Chairman of the Computer Applications Session of the 1973 Annual Reliability and Maintainability Symposium.

Missile and Surface Radar Division

Thomas G. Green, Leader, Design and Development Engineering, was appointed to the Membership Committee of the AIAA (American Institute of Aeronautics and Astronautics).

Merrill W. Buckley, Jr. was Moderator at IEEE Philadelphia Section Joint Meeting of the Engineering Management Group, Computer Society, Systems Man and Cybernetics Society, and Electron Devices Group on January 30, 1973. The subject was "Electronic Engineering — The Profession is Changing."



Winters is TPA for Patents

Milton S. Winters has been appointed Technical Publications Administrator for Patents and Licensing, Princeton, N. J. In this capacity, Mr. Winters is responsible for the review and approval of technical papers; for coordinating the technical reporting program; and for promoting the preparation of papers for the *RCA Engineer* and other journals, both internal and external.

Mr. Winters is presently Director of Patent Plans and Services. He has been with RCA since 1948. He received the BA in Mathematics (*cum laude*) from the University of Iowa in 1931; the MA in Mathematics from the University of Michigan in 1932; and the LL.B. from the Des Moines College of Law in 1938. After college, he entered general practice (1938-41), was a junior engineer with the Signal Corps. (1941-42), a Patent Officer (1943-45), and a Patent Attorney with Philips Laboratories (1945-48).

RCA Review, December 1972

Volume 33, Number 4

Contents

Sensitivity and resolution of charge-coupled imagers at low light levels.....
J. E. Carnes | W. F. Kosonocky

A television rate laser scanner—I. general considerations.....
I. Gorog | J. D. Knox | P. V. Goedertier

A television rate laser scanner—II. recent developments.....
I. Gorog | J. D. Knox | P. V. Goedertier | I. Shidlovsky

Thin-Film Lasers.....
J. P. Witke

A new earth-station antenna for domestic satellite communications.....
P. Folds

Wideband class-C Trapatt amplifiers.....
A. Rose | J. F. Reynolds | S. G. Liu | G. E. Theriault

1-2 GHz high-power linear transistor amplifier.....
A. Presser | E. F. Belohoubek

Integral heat sink transferred electron oscillators...
S. Yegna Narayan | J. P. Paczkowski

The *RCA Review* is published quarterly. Copies are available in all RCA libraries. Subscription rates are as follows (rates are discounted 20% for RCA employees)

	DOMESTIC	FOREIGN
1-year.....	\$6.00	\$6.40
2-year.....	10.50	11.30
3-year.....	13.50	14.70

Editorial Representatives

The Editorial Representative in your group is the one you should contact in scheduling technical papers and announcements of your professional activities.

Government and Commercial Systems
Aircraft and Systems Division

Electromagnetic and Aviation Systems Division

Astro-Electronics Division

Missile & Surface Radar Division

Government Engineering

Government Plans and Systems Development

Communications Systems Division

Broadcasts Systems

Commercial Systems

Government Communications Systems

Palm Beach Division

Research and Development

Laboratories

Fluorescent Tube Division

Entertainment Tube Division

Industrial Tube Division

Electronic Components

Consumer Products

Service

RCA Service Company

Parts and Accessories

RCA Global Communications, Inc.

North American Accounting Company Inc.
RCA Records
RCA International Corporation

RCA Ltd

Patent

ALAN EBBERTS Engineering, Burlington, Mass.
ALAN EBBERTS Industry Systems, Burlington, Mass.

ALAN EBBERTS Engineering, Van Nuys, Calif.
ALAN EBBERTS Engineering, Van Nuys, Calif.

ALAN EBBERTS Engineering, Princeton, N.J.
ALAN EBBERTS Advanced Development and Research, Princeton, N.J.

ALAN EBBERTS Engineering, Moorestown, N.J.

ALAN EBBERTS Advanced Technology Laboratories, Camden, N.J.
ALAN EBBERTS Advanced Technology Laboratories, Camden, N.J.
ALAN EBBERTS Central Engineering, Camden, N.J.

ALAN EBBERTS Engineering Information and Communications, Camden, N.J.

ALAN EBBERTS Studio, Recording, & Scientific Equip. Engineering, Camden, N.J.
ALAN EBBERTS Broadcast Transmitter & Antenna Eng., Gibbsboro, N.J.

ALAN EBBERTS Advanced Development, Meadow Lands, Pa.

ALAN EBBERTS Engineering, Camden, N.J.

ALAN EBBERTS Palm Beach Product Laboratory, Palm Beach Gardens, Fla.

ALAN EBBERTS Research, Princeton, N.J.

ALAN EBBERTS Solid State Technology Center, Somerville, N.J.

ALAN EBBERTS Solid State Technology Center, Somerville, N.J.

ALAN EBBERTS Chairman, Editorial Board, Harrison, N.J.

ALAN EBBERTS Receiving Tube Operations, Woodbridge, N.J.

ALAN EBBERTS Television Picture Tube Operations, Marion, Ind.

ALAN EBBERTS Television Picture Tube Operations, Lancaster, Pa.

ALAN EBBERTS Industrial Tube Operations, Lancaster, Pa.

ALAN EBBERTS Microwave Tube Operations, Harrison, N.J.

ALAN EBBERTS Chairman, Editorial Board, Somerville, N.J.

ALAN EBBERTS Solid State Division, Mountaintop, Pa.

ALAN EBBERTS Power Transistors, Somerville, N.J.

ALAN EBBERTS Integrated Circuits, Somerville, N.J.

ALAN EBBERTS Solid State Division, Findlay, Ohio

ALAN EBBERTS Chairman, Editorial Board, Indianapolis, Ind.
ALAN EBBERTS Engineering, Indianapolis, Ind.

ALAN EBBERTS Audio Products Engineering, Indianapolis, Ind.

ALAN EBBERTS Advanced Development, Indianapolis, Ind.

ALAN EBBERTS Black and White TV Engineering, Indianapolis, Ind.

ALAN EBBERTS Ceramic Circuits Engineering, Rockville, Ind.

ALAN EBBERTS Color TV Engineering, Indianapolis, Ind.

ALAN EBBERTS Engineering, RCA Taiwan Ltd., Taipei, Taiwan

ALAN EBBERTS Consumer Products Administration, Cherry Hill, N.J.

ALAN EBBERTS Consumer Products Service Dept., Cherry Hill, N.J.

ALAN EBBERTS Technical Support, Cherry Hill, N.J.

ALAN EBBERTS Missile Test Project, Cape Kennedy, Fla.

ALAN EBBERTS Product Development Engineering, Deptford, N.J.

ALAN EBBERTS RCA Global Communications, Inc., New York, N.Y.

ALAN EBBERTS (Acting) RCA Alaska Communications, Inc., Anchorage, Alaska

ALAN EBBERTS Staff Eng., New York, N.Y.

ALAN EBBERTS Record Eng., Indianapolis, Ind.

ALAN EBBERTS New York, N.Y.

ALAN EBBERTS Research & Eng., Montreal, Canada

ALAN EBBERTS Patent Plans and Services, Princeton, N.J.

Technical Publications Administrators (asterisked * above) are responsible for review and approval of papers and presentations. Photo at right was taken during a recent *RCA Engineer* Advisory Board meeting. At such meetings, Advisory Board members, Technical Publications Administrators, and Editorial Representatives lay out plans for future *RCA Engineer* issues.



RCA Engineer

A TECHNICAL JOURNAL PUBLISHED BY CORPORATE ENGINEERING SERVICES
"BY AND FOR THE RCA ENGINEER"

FORM NO. RE-18-5

Printed in U.S.A.